THE ROMANIAN ACADEMY

PROCEEDINGS

of The 14th CONSTRUCTAL LAW CONFERENCE

Design in Nature and Evolution

October 10–11, 2024, Bucharest, Romania

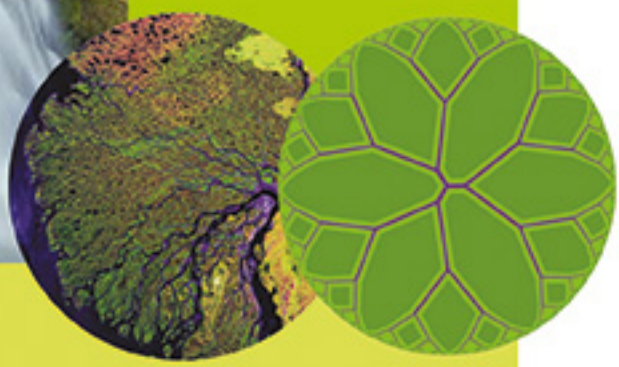

Editors:

ALEXANDRU-MIHAIL MOREGA

ÜMIT GUNEŞ

ADRIAN BEJAN

THE PUBLISHING HOUSE OF THE ROMANIAN ACADEMY

PROCEEDINGS OF THE 14th CONSTRUCTAL LAW CONFERENCE

DESIGN IN NATURE AND EVOLUTION

LUCRĂRILE CONFERINŢEI LEGII CONSTRUCTALE
Ediţia a XIV-a

DESIGN ÎN NATURĂ ŞI EVOLUȚIE

THE ROMANIAN ACADEMY

PROCEEDINGS OF THE 14th CONSTRUCTAL LAW CONFERENCE

DESIGN IN NATURE AND EVOLUTION

OCTOBER 10–11, 2024, BUCHAREST, ROMANIA

Editors: ALEXANDRU-MIHAIL MOREGA
ÜMIT GUNEŞ
ADRIAN BEJAN

THE PUBLISHING HOUSE OF THE ROMANIAN ACADEMY
Bucharest, 2024

Editorial assistant: Irina FILIP
Computer editing: Carmen MUNTEANU
Cover: Mariana ŞERBĂNESCU

EDITURA ACADEMIEI ROMÂNE
Address: Calea 13 Septembrie no 13, sector 5
050711, Bucureşti, România
Phone: + 40213188146, + 40213188106
Fax: + 40213182444
E-mail: edacad@ear.ro
Webb: www.ear.ro

Final proof: 17.12.2024 Format: A4

ISBN 978-973-27-3918-1
ISSN 3061-6239
ISSN-L 3601-6239

Contents

PREFACE

These are the presentations made at the 14th edition of the Constructal Law Conference at the Romanian Academy in Bucharest on 10–11 October 2024. The Constructal Law states: "For a finite-size flow system (not infinitesimal, one particle, or subparticle) to persist in time (to live), it must evolve with freedom to provide easier and greater access to what flows."

The flow designs we see in nature have shape, structure, and rhythm. They are macroscopic, finite in size, and familiar as images with names (river basins, blood vessels, trees), indicating that they have appearances that the observer recognizes. Constructal Law accounts for the dynamic, never-ending evolutionary design and nature. It is a law of nature, a self-standing universal tendency (phenomenon), not some artificial method of 'optimization'. By invoking the law, one predicts what and how something should be.

The presentations explored diverse instances that reveal the causal relationship between freedom, evolution, performance, and staying power (longevity) in all domains: bio, non-bio, engineered, and societal human design. Seemingly disconnected phenomena such as gravity, sound, turbulence, swimming, animal and human migrations, plants, and chemical processes are manifestations of Constructal Law in physics, biology, and engineering. The evolutionary design of artifacts (machines) led to the current era of human & machine evolution. When the time arrow of evolution is recognized, humans can predict their future and surroundings and improve their lives.

Constructal Law underpins predictive theories of evolution, bio, and non-bio. Its core concepts are interwoven: freedom with rules, organization, motion, shape, structure morphing, hierarchy, and arborescence. The articles in this volume illustrate perfection and diversity over space and time: the configurations and rhythms of moving and changing designs of people, animals, athletes, technologies, universities, and science itself: divergent evolution hand-in-glove with convergent evolution.

The Constructal law is the law of physics that covers all phenomena of design and organization evolution in nature. It unveils the universal tendency to evolve toward flow architectures that provide easier access to what flows.

In the decades since the first constructal publications (1996), we are witnessing the accelerated use of the Constructal Law to predict design and evolution in nature, from biology and geophysics to technology and social organization. This volume is a timely review of the field's current state and an open door to future advances.

Editors: ALEXANDRU-MIHAIL MOREGA
ÜMIT GUNEŞ
ADRIAN BEJAN

CONSTRUCTAL LAW CONFERENCE – CLC2024
Design in Nature and Evolution
Romanian Academy, Bucharest, 10–11 October 2024

Proceedings of CLC2024
pp. 9–12

DIVERSITY AND NATURE

ADRIAN BEJAN

Duke University, Durham, NC, USA
abejan@duke.edu

This article explores the causal relationship between freedom, the imagined (perfection), and the observed design in nature (diversity). The presentation is with familiar examples of perfection and diversity over space and in time: the configurations and rhythms of moving and changing designs of people, animals, athletes, technologies, universities, and science itself: divergent evolution hand-in-glove with convergent evolution.

Keywords: Nature; Design; Evolution; Perfection; Diversity; Freedom; Constructal.

Freedom is the cause of everything, from change and imagining to observing and describing, and from the inanimate to the animate diversity of flow designs in nature. Freedom is the collection of physical features that enable an object to change. Freedom is measurable in physics (*e.g.*, the number of degrees of freedom and the effect of more degrees on performance). Without freedom, nothing changes, nothing moves, and nothing is different from before.

Why does nature 'select' diverse forms from diverse media (water, land, air), not from one template, and not of one size? After all, in the struggle for 'survival of the fittest', clear winners must have been selected millions of years ago. Nature is quite different. Diversity is everywhere, around us, among us, and inside of each of us. Diversity is natural, a defining feature of nature.

What causes diversity?

When hearing words repeated in unison by the crowd, I reach immediately for my Webster's dictionary. Diverse comes from Latin: *diversus* is the past participle of the verb *divertere* (*dérouter* in French), to turn aside, as something different, dissimilar. Diversified means varied. Diversity is the quality of variety. Greater diversity (a distinct phenomenon in nature) comes from more degrees of freedom. This is the cause and direction of design evolution in the observable nature.

Diversity is a natural feature. Unnatural is the one category, such as the one size fits all, one color, brown shirt for fascism, red scarf for communism, one idea for an ideologue. Unnatural are the two categories, such as fascism and Marxism, oppressed and oppressor, proletarians and factory owners, healthy origin versus unhealthy origin, and under-represented and over-represented. Such policies are discrimination and *polarization*, not diversity.

Diversity is common sense because it happens naturally, not artificially. Diversity is not the result of dictate. Weeds appear among shrubs in the most carefully plated vineyard and apple orchard. Mutts are born every day. Mothers give birth to diverse children who grow up to have amazingly diverse ideas.

In science, features and phenomena tend to go unnoticed if they are present everywhere. They are noticed only when they are in contrast with a background filled with the usual stuff. They are noticed only if they are unusual.

Diversity is common, everywhere. It seems 'unusual' when we are forced to impose diversity on society, enterprise, university, competition in athletics, and the merit system. Whether this has a future is for the reader to conclude. To help the reader, I decided to question the *physics* origin of diversity – why diversity happens naturally, why it is a phenomenon that has a mind of its own, and why it successfully opposes any effort of being reduced to two or three categories by dictate.

DOI: https://doi.org/10.59277/CLC/2024.01

In resorting to physics to *predict* the natural origin of diversity, I continue on the path traced by my peer-refereed research, which is being condensed chronologically in books such as [1–5]. I chose physics because physics is not opinion. Everyone is entitled to his opinion, and so am I, because I am one of you. Physical facts and behavior are quite different They are observable, and an idea about them can be put to the test.

This, the questioning of the idea, has been going on forever in the evolution and emancipation of the *homo sapiens*, which is why today we have science, and why we will never have enough science. So, I invite the reader to question every new slogan and flavor of the day, to separate jargon from common sense, to detect coincidences, to question what caused them, and to draw conclusions that benefit the reader, the individual, and the next generation.

Coincidences are invitations to start digging in a new place. As we dig deeper, we uncover the natural origin of seemingly disparate phenomena such as divergent evolution hand-in-glove with convergent evolution, and rhythm in time hand-in-glove with diversity in space. In short, we discover why not everything should be big, small, or one size.

The presentation is a pictorial review of the physics principles that account for all the moving, changing, and predicting that go on in nature and science. It is a common-sense review because it is addressed to everyone. It is not jargon. It is about the directionality that unites the dynamic and changing behavior called nature. The single word for all such descriptors is *evolution*.

In Turin last year I showed how diversity happens naturally, and why 'perfection' does not, and will not happen. Perfection is a condition of complete excellence, faultless, and most excellent. Perfection (from *perfectus*, in Latin) means complete in all respects, without defect or omission, flawless. The demonstration was made in simple terms: the shape of an inhabited area affects the movement of people and their access to the area. The defining feature of life is movement with directionality (purpose, objective), not with perfect design or 'end design'. Movement requires *access* to the available space in the available time.

For example, the mathematical optimum (the best) shape and an identified class of diverse shapes differ little concerning performance. The difference between the best and the diversity is rooted in the difference between rigidity (fixed idea, ideology, arrogance) and the freedom to question the supposedly best idea, and the ability to say, 'enough of this' and move on.

Several phenomena of diversity are presented after this introduction. In every example, the same image (idea, mental viewing) jumps at you. Coincidences are precious. Their message is that a universal phenomenon is in play in seemingly disconnected domains: human movement, animal movement, athletics, rhythm, cost, construction, enterprise, and university. The challenge is to translate messages from many domains into one language and a design science with further reach and greater usefulness.

The simplest model can change because of a single degree of freedom, but it cannot capture nature completely. The moving animal is much more than a vehicle with speed and size. The animal is also an engine and a steadfast discoverer of fuel (food) for its engine. In the direction toward greater realism, the necessary degrees of freedom multiply, and so does the size of the diversity of designs that offer nearly the same performance as the perfect design. In aquatic movement, many features account for the diversity of *rhythm* during the moving cycle: arms, legs, body architecture, pulling oars (rowing), and so on. With animal and human examples from swimming and flying, we trace the path from multiple degrees of freedom to greater diversity in lifestyle, training, technique, performance, technology, and robotics.

Coincidental is the discovery of another source of natural diversity: Divergent evolution happens at the same time as convergent evolution. A lot is known about the convergent evolution of the body shapes of fish, swimming mammals, and birds (*e.g.*, whales, dolphins, penguins). Submarines look like orcas. But, the cross-sectional shapes of fish and mammals are quite different, oval versus round. Round is also the cross-section of the fuselage of

commercial jet airplanes. Although the evolution of airplanes converges with the evolution of birds, the evolution of helicopters diverges from airplanes and birds. Together, divergent with convergent evolution broaden the reach and impact of the diversity phenomenon.

How useful is it to know that being fixated on perfection (and overlooking the gathering clouds of diversity) is not the way to make progress? Well, the truly inventive and enterprising individuals know the answer instinctively. They do not waste time. They keep what works and devote their time to new challenges and ideas. Enterprising folks know that if they keep improving something to perfection nothing will happen, except waste of time, power, money, and zip.

In science and academia diversity happened naturally, over centuries, not because of the recent push for 'diversity, equity, and inclusion' (DEI). Seen from the outside, the diversity of academia is evident in the rankings of universities. From the inside, universities are diverse because of a huge variety of features: age, size, fame, ideas, and individuals (students, professors, alumni, culture, religion, country of origin, maternal language, parents, schooling, *etc*.).

Rankings lend artificial structure to the diversity that occurred naturally over the long history of the growth of the world university system. Yet, we hear constantly what a university must do to game the system, to increase its ranking by design: one must make the university bigger and more diverse. From high administrators on down, we keep hearing that size matters, and diversity matters. Well, a wise specimen of *homo sapiens* is known for not being too sure, and for the ability to question himself and others.

I knew that the size and diversity effect on rankings is false because I was raised as an athlete. In sports, it is common knowledge that to lift your team in the standings you must watch and learn from the better players and teams, and then try harder to become better yourself, you, the player. So, the solution is to study Harvard and strive to do better what Harvard does. During my eight years at MIT, I knew that Harvard was neither big nor diverse. The same was true about MIT. These two, along with a few other institutions, rank high in public opinion because of features other than size and diversity by design. What are those features?

Answers come from a bird's eye view of the facts. Effect betrays cause. This way we learn that the university ranks are correlated with the quality and number of precious ideas that come primarily from a few thinkers hosted by a few universities.

To think that one can game the system artificially to overtake Harvard in size and diversity is to go against nature. If one seeks to be ranked above Harvard, why not look at Harvard and do what Harvard does? If one believes that greater diversity leads to higher rankings, then why would one want a demographic composition that differs from that of Harvard?

Why is this useful to know? Because, by understanding the physics principles that underlie natural phenomena, people can position themselves and their society better in nature, can put the natural phenomena at their service, and can avoid fighting losing battles.

Useful to know is the origin and history of the thinking that by force one can 'sculpt' the diversity of an organization (or society) to make it achieve a predetermined performance.

Science is about us, for us to use to our advantage or to dismiss at our peril. Do not worry, you will always be saved by 'doers' who create quietly and often alone. This way, the advanced people keep advancing. Keep these thoughts in mind as you read my article.

Nature has a mind of its own.
Perfection: you may imagine it, but it never comes.
Diversity: you can't imagine it, but it always comes.

REFERENCES

1. Bejan A., *Shape and Structure, from Engineering to Nature*, Cambridge University Press, Cambridge UK, 2000.
2. Bejan A., Zane J.P., *Design in Nature: How the Constructal Law Governs Evolution in Biology, Physics, Technology, and Social Organization*, Doubleday, New York, 2012.
3. Bejan A., *The Physics of Life: The Evolution of Everything*, St. Martin's Press, New York, 2016.
4. Bejan A., *Freedom and Evolution: Hierarchy in Nature, Society and Science*, Springer Nature, New York, 2020.
5. Bejan A., *Time and Beauty: Why Time Flies and Beauty Never Dies*, World Scientific, Singapore, 2022.

13**CONSTRUCTAL LAW CONFERENCE – CLC2024**
Design in Nature and Evolution
Romanian Academy, Bucharest, 10–11 October 2024

Proceedings of CLC2024
pp. 13–16

CONSTRUCTAL LAW AND MEDICINE CRISES IN ROMANIA

MIRCEA SCURTU

NCSU
mitch.scurtu@optimalglobalpricing.com +1 336 380 3363

The document discusses the application of Constructal Law and Optimal Global Pricing technology to resolve the medicine crises in low and high-priced markets, focusing on the case of Romania.

Keywords: Global medicine crises; Low-priced markets; High-priced markets; Resistance to flow.

1. INTRODUCTION

The document discusses the application of Constructal Law and a new technology called Optimal Global Pricing (OGP) to address the global medicine crises, with a focus on Romania. The main points are:

Medicine Crises. There is a global issue with medicine prices being too high in some markets and too low in others, leading to shortages and unaffordability.

OGP Technology. This new technology uses a finitely converging algorithm to optimize medicine pricing and distribution globally, aiming to resolve these crises.

Romania's Situation. The medicine crises in Romania are highlighted through surveys, reports, and research, showing significant shortages.

Impact of OGP. Implementing OGP in Romania could increase medicine consumption by an average of 58%, potentially normalizing the market and adding about $2 billion in consumption. Economic Theory: The document links economics to physics through Constructal Law, suggesting that economic transactions can be optimized using principles from physical sciences.

Financial Plan. A detailed financial plan outlines the expenses and investments needed over seven years to implement OGP and resolve the medicine crises in Romania.

The document emphasizes that technology, rather than political or legal measures, is key to solving the global medicine crises.

2. MATERIALS AND METHODS

Optimal Global Pricing (OGP) resolves the medicine crises by using a finitely converging algorithm to optimize the pricing and distribution of medicines across different markets. Here's how it works:

Balancing Prices. OGP addresses the disparity between low-priced markets, where medicines are often missing, and high-priced markets, where medicines are unfordable. By optimizing prices, and trade flows it ensures that medicines are available and affordable in both types of markets.

Increasing Consumption. In low-priced markets, OGP helps increase the availability of medicines, leading to a significant rise in consumption. For example, in Romania, the consumption of medicines increased by an average of 58% after implementing OGP, normalizing medicine consumption.

Reducing Market Distortions. OGP reduces global market distortions contributing to the medicine crises. By optimizing the flow and distribution of medicines, it ensures a more efficient and equitable distribution, reducing shortages and making medicines more accessible.

DOI: https://doi.org/10.59277/CLC/2024.02

Financial Sustainability The technology also provides a financial plan to support the normalization of medicine consumption. Investments in the first few years help resolve the immediate crises, while subsequent years focus on maintaining normalized consumption and supporting the re-industrialization of the Romanian economy.

Overall, OGP leverages technology and the principles of Constructal Law to create a sustainable solution to the global medicine crises, ensuring that medicines are both available and affordable across different markets. Below is our study with five medicines reported by Bucharest as being in short supply. Resolving the global market distortions will increase medicine consumption by $2 billion normalizing the medicine consumption.

Table 1

From one of our studies on five medicines reported by Bucharest to the European Medicine Shortage List, Adalimumab (Humira), Levothyroxine Sodium, Enbrel (Etanercept), Infliximab (DRY INF VIAL 100MG 1), Hydroxychloroquine

Medicine	Consumption before solving parallel trade problem	Consumption after solving parallel trade problem	Net consumption gain after the parallel trade problem is solved
Adalimumab	$21,552,580.28	$31,368,347.78	45.54% OR $9,815,767.5
Levothyroxine Sodium	$1,995,759.0	$3,326,265.00	66% OR $1,330,506.0
Enbrel (Etanercept	$11,660,590.90	$18,488,808.0	58.5% OR $6,828,217.1
Infliximab (DRY INF VIAL 100MG 1)	$2,584,024.2	$5,311,134.13	48.65% OR $2,727,109.93
HYDROXYCHLOROQUINE	$287,864.82	$495,767.19	72.2% OR $207,902.37
Total consumption gains for medicines previously in short supply			$20,909,502.9
Average medicine consumption gain after parallel trade problems are solved			58.18%
Total consumption gains for the 494 medicines missing or in short supply as reported by Bucharest to the European Medicine Shortage List			$2.07 billion

3. **RESULTS**

I wanted to share a key takeaway from the recent document on the Constructal Law Conference. The new technology called Optimal Global Pricing (OGP) could significantly address the global medicine crises by optimizing medicine prices and availability.

Specifically, in Romania, implementing OGP could increase medicine consumption by 58%, potentially normalizing the market and adding about $2 billion in consumption. This approach highlights the importance of leveraging technology to solve complex global issues.

3.1. **ECONOMICS IS PHYSICS**

How does the Constructal Law apply to the medicine crises? The Constructal Law applies to the medicine crises by providing a framework for optimizing the flow and distribution of medicines in both low and high-priced markets. By using the principles of Constructal Law, the new technology called Optimal Global Pricing (OGP)aims to resolve the disparities in medicine availability and affordability. In low-priced markets, where medicines are often missing, and in high-priced markets, where patients cannot afford them, OGP can help normalize consumption and optimize prices and flows. This approach ensures a more efficient and equitable distribution of medicines, addressing the global medicine crises by reducing market distortions and improving access to essential drugs.

4. **DISCUSSION AND CONCLUSIONS**

The main causes of the medicine crises in Romania, as highlighted in the document, include: Price Disparities: There is a significant gap between high and low prices of medicines. In low-priced markets like Romania, medicines are often missing, while in high-priced markets, patients cannot afford them. Global Market

Distortions: These distortions fill the gap between high and low prices, sustaining the global medicine crises. The market inefficiencies and imbalances contribute to the unavailability and unaffordability of medicines. Parallel Trade Issues: Problems related to parallel trade exacerbate the shortage of medicines. Resolving these issues can significantly increase the consumption of medicines that are in short supply. Political, Administrative, and Legal Factors: The ongoing conversation around the medicine crises is often limited to political, administrative, and legal aspects, focusing primarily on prices rather than technological solutions.

By addressing these causes through the implementation of Optimal Global Pricing (OGP) and leveraging Constructal Law, the document suggests that the medicine crises in Romania can be effectively resolved.

Below financial projections resolving the medicine crises in Romania. First three years are dedicated to normalizing the medicine consumption, next 4 years are dedicated to earn Romania significant financial resources badly needed to re-industrialize the economy.

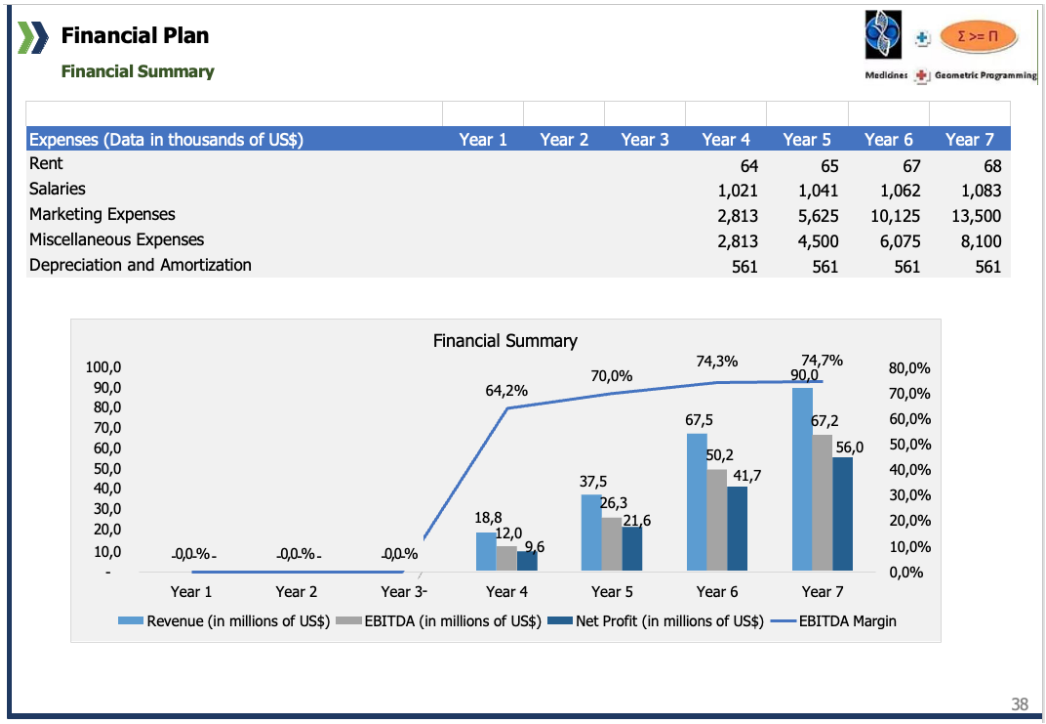

Expenses (Data in thousands of US$)	Year 1	Year 2	Year 3	Year 4	Year 5	Year 6	Year 7
Rent				64	65	67	68
Salaries				1,021	1,041	1,062	1,083
Marketing Expenses				2,813	5,625	10,125	13,500
Miscellaneous Expenses				2,813	4,500	6,075	8,100
Depreciation and Amortization				561	561	561	561

REFERENCES

1. Scurtu M., Aplicarea teoriei elasticității din fizică la studiul ciclurilor economice ale unei economii de piață la nivel macroeconomic, Academia de Studii Economice, Facultatea Relații Economice Internaționale, edițiile XIX, XX, Sesiunile Cercurilor Științifice Studențești, Aprilie 1975, 1976, Rector.
2. Scurtu M., *An Empirical Study of Spatial Economic Equilibria via Geometric Programming*, Doctoral Thesis, North Carolina University, Raleigh, USA, 1986.
3. Bejan A., *Freedom, and Evolution. Hierarchy in Nature, Society, and Science*, Basel, Springer, 2020.
4. Bejan A., *The Physics of Life: The Evolution of Everything*, New York, St. Martin's, 2016.
5. Fang S. C., Peterson E.L., Generalized Variational Inequalities, *Journal of Optimization Theory and Applications*, **38**, *3* 1982, 363–38.
6. General Network Equilibrium Analysis, *International Journal of Systems Science*, **14**, *11*, pp. 1249–1275 (1983).
7. An Economic Equilibrium Model on a Multi-commodity Network, *International Journal of Systems Science*, **16**, *4*, pp. 479–490 (1985).
8. Irwin C.L., Yang W.C., Iteration and Sensitivity for A Spatial Equilibrium Problem with Linear Supply and Demand Functions, *Operations Research*, **30**, *2* (1982).
9. King R.A., Gunn J., Reactive Programming User Manual: A Market Simulating Spatial Equilibrium Algorithm, Economic Research Report, No. 43, Dept. Of Ec. & Bus. NCSU Raleigh N.C., Dec 81.

10. McCarl B.A. *et al*., Sebend: A computer Algorithm for the Solution of Symmetric Multi-commodity spatial Equilibrium Problems Utilizing Benders Decomposition. Special Report 708, Agricultural Experiment Station Oregon State University, March 1984.
11. The Conical Duality and Complementarity of P and Quantity for Multi-commodity Spatial and Temporal Network Allocation Problems, Center For Math. Studies in Economics and Management Science: Disc, Paper #207, Northwestern University, Evanston, 111, March 1976.
12. Peterson E.L., Eaves B.C., Asmuth R., Computing Economic Equilibria on Affine Networks with Lemke's Algorithm, *Mathematics and Operations Research*, **4**, *3*, pp. 209–214 (1979).
13. O'Rourke A.D., Casavant K.L., Interregional and Intertemporal Competition in Fresh Sweet Cherries, College of Agriculture Research Center, Washington State University, Bulletin 803, November 1974.

ADDENDUM

SUBJECT – *Key Insights from the Constructal Law Conference Document*

I wanted to share some important points from the recent document on the Constructal Law Conference, which discusses the application of Constructal Law and Optimal Global Pricing (OGP) technology to address the global medicine crises, with a focus on Romania.

KEY POINTS

Global Medicine Crises: There is a significant issue with medicine prices being too high in some markets and too low in others, leading to shortages and unaffordability.

OGP Technology: This new technology uses a finitely converging algorithm to optimize medicine pricing and distribution globally. It aims to balance prices and trade flows, ensuring medicines are available and affordable in both low-priced and high-priced markets.

Impact on Romania: Implementing OGP in Romania could increase medicine consumption by an average of 58%, potentially normalizing the market and adding about $2 billion in consumption.

Economic Theory: The document links economics to physics through Constructal Law, suggesting that economic transactions can be optimized using principles from physical sciences.

Financial Plan: A detailed financial plan outlines the expenses and investments needed over seven years to implement OGP and resolve the medicine crises in Romania. The first three years focus on normalizing medicine consumption, while the next four years aim to support the re-industrialization of the Romanian economy.

Benefits of OGP: Balances medicine prices across different markets. Increases the availability and consumption of medicines in low-priced markets. Reduces global market distortions, ensuring efficient and equitable distribution. Provides a sustainable financial plan to support long-term solutions. This approach highlights the importance of leveraging technology to solve complex global issues rather than relying solely on political, legal and administrative measures.

CONSTRUCTAL LAW CONFERENCE – CLC2024
Design in Nature and Evolution
Romanian Academy, Bucharest, 10–11 October 2024

Proceedings of CLC2024
pp. 17–20

25 YEARS OF CONSTRUCTAL THINKING: HOW GLOBAL DISSEMINATION HAS GROWN FROM A SINGLE TREE TO A NETWORK OF TREES

DAN C. BACIU[ab*], SUNIT KAJAREKAR[a], MARCELO RISSO ERRERA[c], UMIT GUNES[d]

[a] Interpretation Laboratory, Architektur Studio Bellerive, Bern, Switzerland
[b] Münster School of Architecture, Münster, Germany
[c] Environmental Engineering Department, Universidade Federal do Paraná
[d] Yıldız Technical University, Istanbul, Turkey
*Correspondence: symposia@yahoo.com.

The Constructal Law has recently passed its 25th anniversary. At the 2023 Constructal Law Conference in Turin, we have looked back, presenting insights on how knowledge of the Constructal Law has spread globally. Here, we expand on our earlier article. Since our initial study, we have seen a daily average of three new publications that mention the term "constructal" in the Scopus database. In parallel, the number of laboratories affiliated with this research has grown from 10,956 to 12,787. Overall, we see a stable annual growth rate exceeding 25 % in our corpus, as well as a global coverage denser than ever. Studying old and new data, we expand on our earlier article not only with new statistics but also with a new insight: the dissemination paths of constructal thinking were initially tree-shaped, but they have presently become a network of overlapping trees. This insight seamlessly aligns with the predictions of the Constructal Law. According to the Constructal Law, trees grow and spread to become forests of trees, which eventually look like networks. This Constructal Law prediction is evidently confirmed in our corpus.

Keywords: Constructal law; Cultural life; Geography; Geographic information retrieval**.**

1. SUMMARY

The term "constructal" was coined by Adrian Bejan in the mid 1990s (Bejan, 1997). Since then, it has been used in phrases such as "constructal law", "constructal approach", "constructal design", "constructal evolution", "constructal tree", etc. All of these phrases are part of a larger body of constructal thinking that has kept growing over nearly three decades (Bejan 2000, 2016, 2020, Bejan & Merkx 2007, Bejan & Zane 2012, Bejan & Lorente S 2013, Bejan & Errera 2016). We call this larger body of thought "constructal thinking".

To quantitatively study constructal thinking, we have collected data through the Scopus database (details in section 2). Overall, the corpus we collected reveals that constructal thinking has exponentially grown since 1996. Specifically, we observe an annual growth rate exceeding 25% with a standard deviation of 0.43. The trend upwards has continued since our 2023 article. Since then, the number of articles has grown from 6,785 (spring 2023) to 7,789 (spring 2024). This averages three new publications every day. During the same period, the number of contributing laboratories affiliated with this research has grown from 10,956 to 12,787.

Next to studying growth, we evaluate how constructal thinking has spread geographically. In particular, we ask how constructal thinking has spread from Duke University to the rest of the world, connecting an increasing number of researchers. Our findings beautifully visualize that dissemination was initially tree-shaped, but the initial dissemination tree has grown into a network of overlapping trees.

DOI: https://doi.org/10.59277/CLC/2024.03

Our present study builds on our earlier research, presented at the 2023 CLC conference (Baciu *et al*. 2023), and it also reconfirms the results of earlier research by Razera *et al*. (2018) and Errera (2018). In the following section, we present updates based on our newly expanded corpus.

2. **NEW DATA, SPRING 2023 TO SPRING 2024**

Our initial dataset was collected through a search for the term "constructal" in the Scopus database. The corpus thus collected includes all documents that contain the term in title, text, references, or keywords. The discussion of our initial results is found in Baciu *et al*. [1].

In Spring 2024, we have collected new data, expanding our corpus with an additional year worth of publications that have been indexed by Scopus since 2023. The analysis of these new data with the methods and code from 2023 reconfirms the earlier findings.

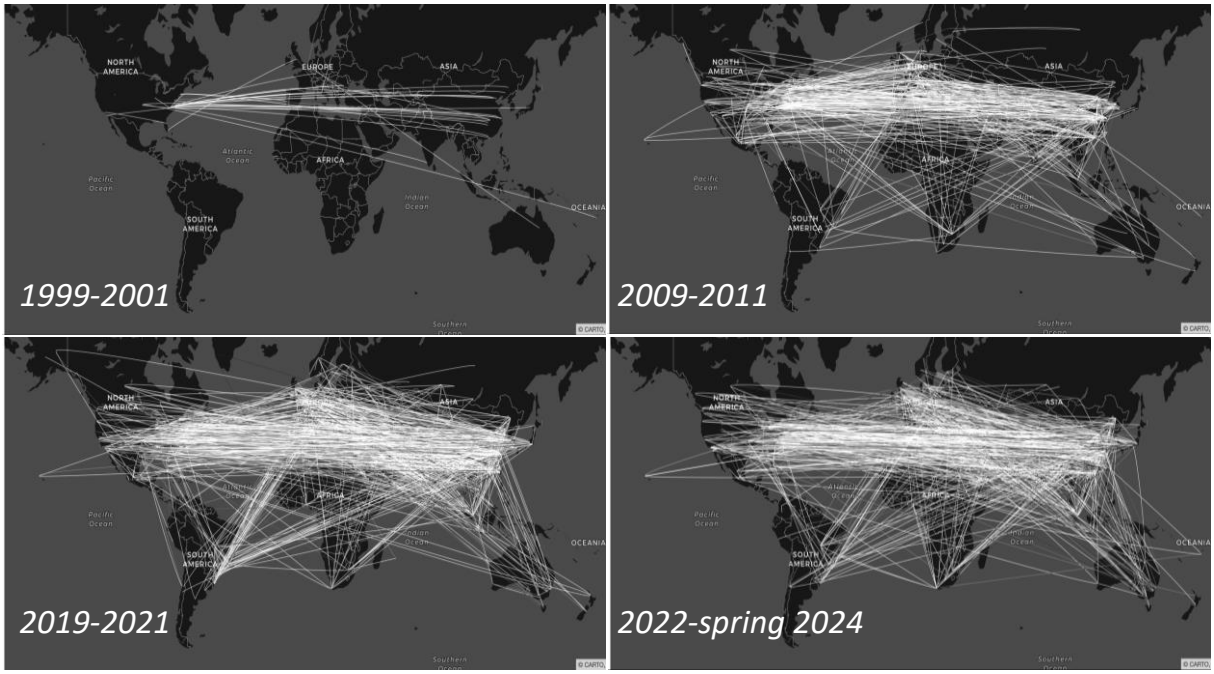

Fig. 1 – Geographical coverage of constructal thinking in four distinct periods of time. Clearly, the geographical distribution of constructal thinking is becoming wider and denser in an s-shaped manner, with the entire globe being the upper bound.

Evaluating the data, we have made an additional observation, visualized in Fig.1. In this visualization, each article is represented as a polygonal chain. The chain goes through the locations of the institutions where the co-authors are located, and it does so in the order in which the co-authors are listed in the publication. Furthermore, the visualization focused on four different time periods: 1999–2001, 2009–2011, 2019–2021, and 2022–Spring 2024. Comparing these four time periods, we punctually represent how constructal thinking has geographically grown, and we observe that it has grown from a tree-shaped configuration into a network. Evidently, the period 1999–2001 shows a system that is a topological tree. It is star-shaped without loops. In contrast, the periods after 2001 show systems that contain loops and are therefore considered to represent networks.

These networks that evolved out of the initial Duke-centered dissemination tree of constructal thinking can be broken back into individual trees. Figure 2 shows a network for the period 2018–2023, and it shows how this network can be broken down into trees. Three sample trees are shown. They are obtained by filtering for articles that have at least a co-author in a given area. Examples are shown for Bucharest, Cape Town, and Toulouse. Note how each of the present trees morphologically resembles the initial Duke-centered tree. As constructal thinking has spread around the world, it has created a forest of dissemination trees that resemble the initial one.

Fig. 2 – The present dissemination network of constructal thinking is a conglomerate of individual trees, which can be revealed by filtering for articles that have at least one author in a given geographical area. Examples are shown for Bucharest, Cape Town, and Toulouse.

Taken together, constructal thinking was initially disseminated from Duke University along divergent paths that followed a tree-shaped flow configuration, seen in Fig. 1, 1999–2001. These paths have kept diverging and converging, eventually becoming a network of overlapping trees, examples of which are shown in Fig. 2.
This insight aligns seamlessly with the predictions of the Constructal Law. According to the constructal law, trees grow and become forests of trees, which eventually look like networks [7].

Together, our earlier and present findings demonstrate that constructal thinking is very lively at present, flowing ever faster and further. While it is expected that the growth will follow an s-curve, it is presently still in its initial exponential growth phase, as evidenced by publication counts.

REFERENCES

1. Baciu D.C., Kajarekar S., Gunes U., Constructal flow of constructal thinking, *CLC2023* (2023).
2. Bejan A., Errera M.R., Complexity, organization, evolution, and constructal law, *Journal of Applied Physics*, **119**, 074901 (2016).

3. Bejan A., Lorente S., The Physics of Spreading Ideas, *International Journal of Heat and Mass Transfer*, **55**, pp. 802–807 (2012).
4. Bejan A., Merkx G.A., eds., *Constructal Theory of Social Dynamics*, New York, Springer, 2007.
5. Bejan A., Zane J.P., *Design in Nature: How the Constructal Law Governs Evolution in Biology, Physics, Technology, and Social Organization*, Random House LLC, New York, 2012.
6. Bejan A., *Freedom and evolution: hierarchy in nature, society and science*, Basel, Springer, 2020.
7. Bejan A., The evolving design of our life, *LA+ Interdisciplinary Journal of Landscape Architecture,* **9**, pp. 6–15 (2019).
8. Bejan A., *The Physics of Life: The Evolution of Everything*, New York, St. Martin's, 2016.
9. Bejan A., *Shape and Structure, from Engineering to Nature*, Cambridge, Cambridge University Press, 2000.
10. Bejan A., Constructal-theory network of conducting paths for cooling a heat generating volume, *International Journal of Heat and Mass Transfer*, **40**, pp. 799–816 (1997).
11. Errera MR, Constructal Law in light of philosophy of science, *Proceedings of the Romanian Academy, Series A-Mathematics Physics Technical Sciences Information Science*, **19**, 111–116 (2018).
12. Razera A.L., Errera M.R., Dos Santos E.D., Isolai L.A., Rocha L.A.O., Constructal Network of Scientific Publications Co-authorships and Citations, *Proceedings of the Romanian Academy Series A* – Special Issue, pp. 105–110 (2018).

CONSTRUCTAL LAW CONFERENCE – CLC2024
Design in Nature and Evolution
Romanian Academy, Bucharest, 10–11 October 2024

Proceedings of CLC2024
pp. 21–24

ANALYSIS OF HEAT TRANSFER TO A SHEET-TYPE HEAT EXCHANGER PLACED IN RUNNING WATER-THERMAL ENERGY EXTRACTION FROM IRRIGATION WATER

SHIGEO KIMURA*, YOICHI UTANOHARA

[a] Komatsu University, Japan
shigeo.kimura@komatsu-u.ac.jp and yoichi.utanohara@komatsu-u.ac.jp
*Correspondence: shigeo.kimura@komatsu-u.ac.jp;Tel. +81-761-48-3105

A sheet-type heat exchanger has been extensively used as a device for extracting heat from the ground soil. This heat exchanger consists of polyethylene capillary tubes bundled together in a sheet, positioned between two header pipes that serve as the inlet and outlet for circulating brine. The bundled thin tubes, with an outer diameter of 6 mm and an inner diameter of 5mm, are highly flexible, allowing for easy winding and bending. This flexibility provides significant freedom in configuring the device within the soil. This paper examines the possibility of using the same heat exchanger to collect heat from water flowing in irrigation channels and rivers.

We discuss an analytical method capable of predicting the performance of the heat exchanger when it is positioned parallel to the water flow. In this analysis, we employ the concept of overall heat transfer coefficient to evaluate a single polyethylene tube. Specifically, we determine the dimensionless inner convective heat transfer coefficient, known as the inner Nusselt number, for laminar flow conditions. Meanwhile, the outer convection heat transfer coefficient is derived from forced convection correlation obtained from an isothermal flat plate. Additionally, numerical simulations are conducted to account for the influence of header pipes on the flow field and to relax the assumption of a constant outer wall temperature. We find that the analytical and numerical results generally agree.

Furthermore, we compare the analytically predicted results with available experimental data, revealing agreement between the predicted and experimentally obtained heat transfer rates.

Keywords: Heat transfer; Convection; Heat exchanger; Irrigation water; Energy tapping; Agricultural use.

1. INTRODUCTION

In many agricultural areas, additional thermal energy is often required to cultivate a variety of fruits, vegetables, and flowers in greenhouses during the winter. Typically, this heat is provided by oil heaters and air-to-air heat pumps. However, in scenarios where irrigation water is available near the greenhouses, it becomes feasible to either extract heat from or dissipate heat into the water. Due to water's significantly higher thermal conductivity compared to air, utilizing water for heat exchange can reduce the energy consumption of heat pumps compared to air-to-air systems.

In this study, we focus on a specific type of heat exchanger and demonstrate how we can predict its performance when placed in an irrigation water channel. The heat exchanger consists of approximately 120 polyethylene capillary tubes, each with outer and inner diameters of 6mm and 5mm respectively, and a length of about 6 m. These tubes are tightly bundled together to form a single sheet, with a spacing of approximately 0.5 mm between them. Heat transfer occurs between the circulating brine within the capillary tubes and the surrounding irrigation water.

DOI: https://doi.org/10.59277/CLC/2024.04

Initially, we conduct an approximate analysis based on overall heat transfer coefficients. Subsequently, we compare these approximate heat transfer results with more accurate numerical simulations. Finally, we compare the experimentally measured heat transfer rates with those obtained from the approximate method.

2. APPROXIMATE AND NUMERICAL METHODS TO PREDICT HEAT TRANSFER RATES

A simplified approach was suggested using the overall heat transfer coefficient and assuming a constant convection heat transfer coefficient over the outer surface of the tube. The method utilizes convective heat transfer principles from a flat plate with a constant temperature to derive a straightforward expression for the brine temperature [1–6]. Additionally, a numerical method is employed, considering the influence of header pipes on flow fields and relaxing the assumption of a constant heat transfer coefficient over the outer pipe wall, as assumed in the simplified analysis [7–10]. Figure 1 illustrates a numerical result showing the development of brine temperature in a sheet-type heat exchanger. The simulation assumes the brine enters at an initial temperature of 0°C with a flow rate of 15 L/min, while the water in the channel is at 10°C and flows at a velocity of 10 m/min. The brine is introduced at the downstream inlet position to ensure the heat exchange process aligns with a counter-flow arrangement. As shown in the figure, the brine temperature increases rapidly near the inlet region and slows as it approaches the exit region, validating the constant heat transfer coefficient assumption used in the simplified analysis. Overall, the two approaches yield consistent results, as demonstrated in Table 1.

Table 1

Analytically predicted outlet brine temperatures compared to numerically obtained values

Water Flow Velocity U_∞[m / min]	4		10	
Water Temperature T_∞[°C]	8.2		7.4	
Refrigerant flow rate Q[L / min]	15	30	15	30
Inlet Temperature [°C]	–0.4	1.6	-0.8	1.5
Outlet Temperature [°C] (Analytical)	7.48	5.10	6.80	5.10
Outlet Temperature [°C] (Numerical)	7.57	6.42	6.80	5.82

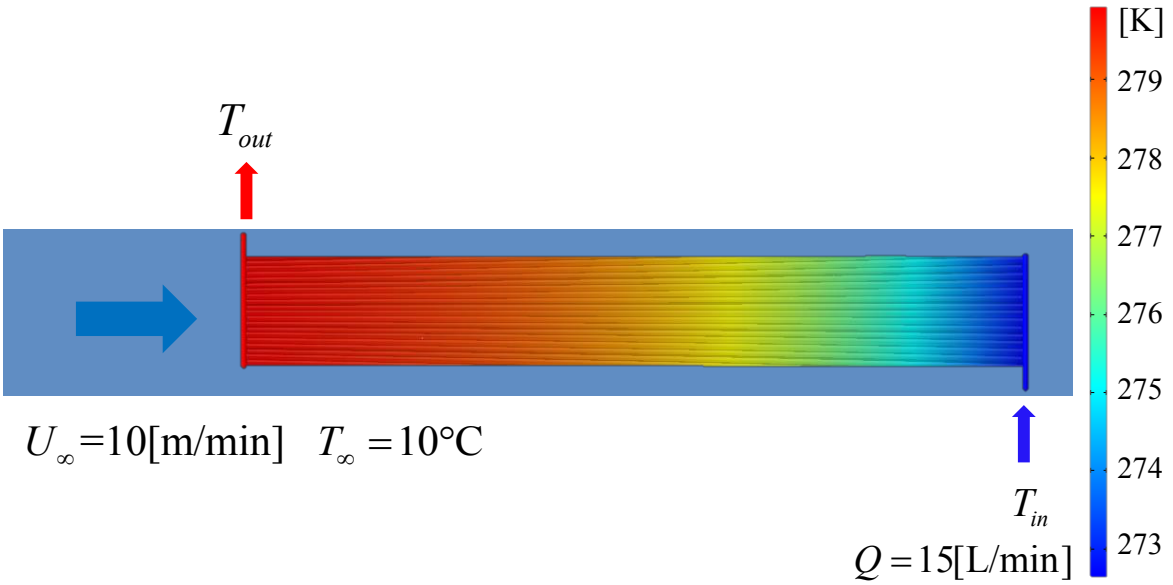

Fig. 1 – The brine temperature development in the sheet type heat exchanger when it is installed vertically in the water channel.

3. APPROXIMATE ANALYTICAL RESULTS COMPARED WITH EXPERIMENTAL ONES

Goto *et al.* [11] reported experimental results obtained from a real-size water channel as seen in Fig. 2. A comparison was made between the analytical predictions and the experimental findings. As indicated in Table 2, while the analytical predictions are generally underestimated, both methods agree within a margin of 15%.

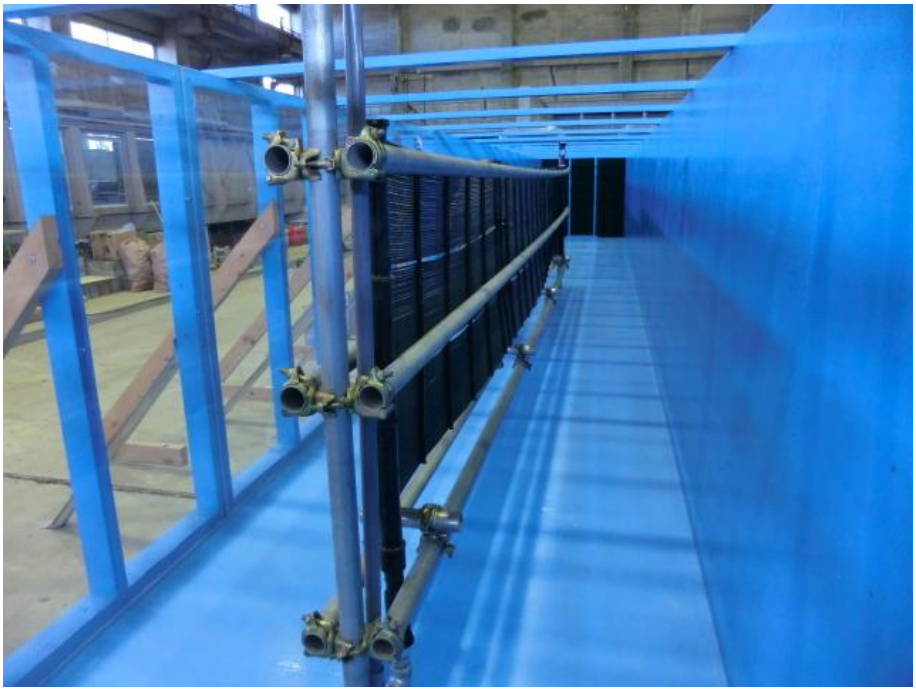

Fig. 2 – A sheet type heat exchanger installed vertically in the real scale water channel whose cross section is 1.6 m × 1.6 m.

Table 2

Analytically predicted outlet brine temperatures compared to experimentally measured values

	Heating		Cooling	
Water Flow Velocity U_∞[m / min]	10		10	
Water Temperature T_∞[°C]	6.75		12.3	
Refrigerant flow rate Q[L / min]	15	30	15	30
Inlet Temperature [°C]	-1.5	0.8	24.4	20.1
Outlet Temperature [℃] (Analytical)	5.0	4.04	14.8	15.9
Outlet Temperature [°C] (Experimental)	5.3	4.5	13.7	15

4. **DISCUSSION AND CONCLUSIONS**

A straightforward approximate method was introduced to predict the heat exchange performance of a sheet-type heat exchanger when placed parallel to water flows. This method was validated against numerical simulations and real-size experimental results, demonstrating its effectiveness in predicting the heat exchange performance of such heat exchangers.

REFERENCES

1. Bejan A., *Convection Heat Transfer*, 4th ed., Wiley, Hoboken, New Jersey, US, 2013, pp. 338–346.
2. Cengel Y.A., Ghajar A.J., *Heat and Mass Transfer – Fundamentals and Applications*, 6th ed., McGraw-Hill Education, New York, US, 2020, pp. 439–622.
3. Dang T.T., Teng, J.T., Chu J.C., A study on the simulation and experiment of a microchannel counter-flow heat exchanger, *Applied Thermal Engineering*, **30**, pp. 2163–2172 (2010).
4. Gnielinski V., New Equation for Heat and Mass Transfer in Turbulent Pipe and Channel Flow, *Int. Chem. Eng.*, **16**, pp. 359–368 (1976).
5. Krishne G.Y.T., Patnaik B.S.V.P., Aswatha N.P.A., Seetharamu K.N., Finite element simulation of transient laminar flow and heat transfer past an in-line tube bank, *International Journal of Heat and Fluid Flow*, **19**, pp. 49–55 (1998).
6. Lankford K.E., Bejan A., Natural convection in a vertical enclosure filled with water near 4˚C, *Journal of Heat Transfer*, **108**, pp. 755–763 (1986).
7. Marcotte D., Pasquier P., On the estimation of thermal resistance in borehole thermal conductivity test, *Renewable Energy*, **33**, pp. 2407–2415 (2008).
8. Ozudogru T.Y., Olgun C.G., Senol A., 3D numerical modeling of vertical geothermal heat exchangers, *Geothermics*, **51**, pp. 312–324 (2014).
9. Rahimi M., Shabanian S.R., Alsairafi A.A., Experimental and CFD studies on heat transfer and friction factor characteristics of a tube equipped with modified twisted tape inserts, *Chemical Engineering and Processing*, **48**, pp. 762–770 (2009).
10. Zeng, H.Y., Diao, N.R., Fang, Z.H., A Finite Line-Source Model for Boreholes in Geothermal Heat Exchangers, *Heat Transfer-Asian Research*, **31**, pp. 558–567 (2002).
11. Goto M., Okushima L., Miki T., Takasugi S., Tateno M., Koma N., Kimura S., Komatsu N., Heat exchange performances of sheet type heat exchanger submerged in water flow and installation method to an agriculture irrigation canal (in Japanese), *Bulletin of the NARO. Rural Engineering*, **3**, pp. 29–41 (2019).

CONSTRUCTAL LAW CONFERENCE – CLC2024
Design in Nature and Evolution
Romanian Academy, Bucharest, 10–11 October 2024

Proceedings of CLC2024
pp. 25–28

COMPLETE FORMULAS DEVELOPED TO CALCULATE THE ENTROPY CHANGES OF IDEAL GASES

YONGJIAN GU

The United States Merchant Marine Academy, 300 Steamboat Road, Kings Point, New York, 11024. USA
Guy@usmma.edu; Tel +1 516 726 5719

The entropy change of a system in a process is a key criterion to distinguish if the process is actual or ideal. The process without the entropy change is a perfect process called an isentropic process. Typical cycles involving the isentropic processes are the Otto, Ranking, and Brayton cycles. Two kinds of thermodynamic systems in the cycles are commonly encountered in engineering practices: closed and open. The equations calculating the entropy changes of ideal gases in processes are derived from the first Tds relation, the Gibbs equation, and the second Tds relation. Generally, the first Tds relation is applied to the closed systems, and the second Tds relation is applied to the open systems. There are two approaches used to analyze the entropy changes of ideal gases. They are the approximate analysis and the exact analysis, respectively. Equations relating to the Gibbs equation for the closed system in the precise analysis needed to be included in thermodynamics. This paper presents the development of the missing equations. The author describes the derivation of the complete equations to calculate the entropy changes of ideal gases and the correlated properties in the isentropic processes from the Tds relations for approximate and exact analysis. Examples illustrate the calculation using the equations for the entropy changes of air and the correlated properties in the isentropic processes.

Keywords: Entropy; Entropy change; Isentropic process; Ideal gases.

1. INTRODUCTION

Entropy is a property of a thermodynamic system. S is denoted as a total entropy, and *s* as a specific entropy. The entropy change of the system Δs in a process is a key criterion to distinguish if the process is actual or ideal. The process without the entropy change is an ideal process called an isentropic process. Otherwise, the process is an actual process. In engineering practice, the Otto, Ranking cycle, and Brayton cycles involving isentropic processes are presented in Figure 1.

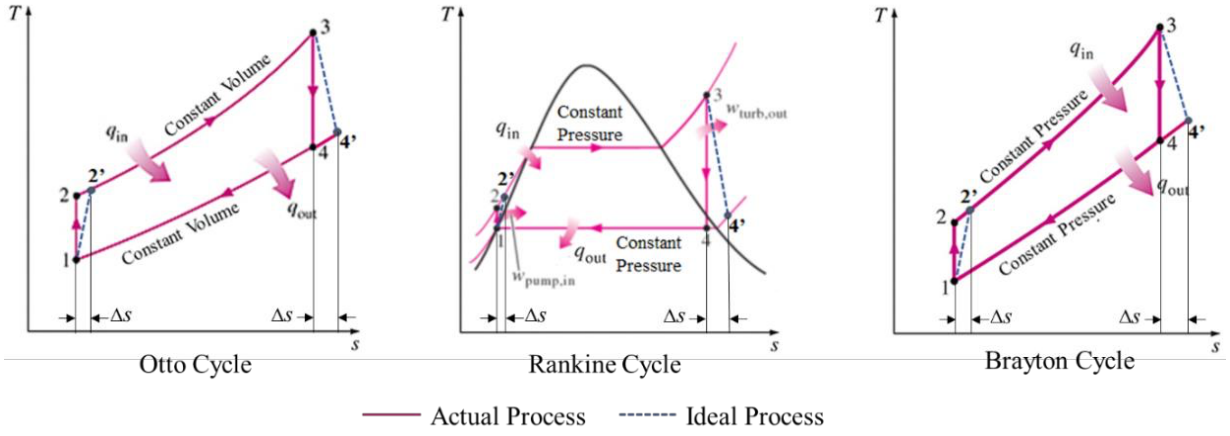

Fig. 1 – *T-s* Diagrams of Otto cycle, Ranking cycle, and Brayton cycle.

From the equipment view, the Otto cycle is a closed system, while the Rankine and Brayton cycles are open systems. In the figure, the isentropic processes are vertical, such as lines 1–2 (isentropic compression

DOI: https://doi.org/10.59277/CLC/2024.05

process) and 3–4 (isentropic expansion). Meanwhile, lines 1–2' and 3–4' are the actual processes. Entropy change in the processes can be described as

$$dS = \frac{\delta Q}{T} \qquad \text{(kJ/K)}. \tag{1}$$

For the Rankine cycle, the working fluid is steam. Detailed and well-organized tables of steam is available in which entropies based on temperature or pressure are entirely identified. The equations to calculate the entropy changes need to be developed for the Otto and the Brayton cycles.

2. ENTROPY CHANGE IN A PROCESS

Recalling the differential form of the conservation of energy equation for a closed stationary thermodynamic system containing a single compressible substance and undergoing an internally reversible process, $\delta Q_{\text{int rev}} - \delta W_{\text{int rev,out}} = dU$ ($W_{\text{int rev,out}}$ and U are the internally reversible work output and the internal energy), also considering $\delta Q_{\text{int rev}} = TdS$ and $\delta W_{\text{int rev,out}} = PdV$, Equation (1) can be expressed as

$$Tds = du + Pdv \qquad \text{(kJ/kg)}. \tag{2}$$

Equation (2) is called the first *Tds* equation, the Gibbs equation. If *du* is replaced by $dh = du + Pdv + vdP$ from the definition of enthalpy $h = u + Pv$, Equation (2) becomes

$$Tds = dh - vdP \qquad \text{(kJ/kg)}. \tag{3}$$

Equation (3) is known as the second *Tds* equation. These two *Tds* equations are developed with an internally reversible process. However, the results obtained are valid for both reversible and irreversible processes since entropy is a property, and the change of a property between two states is independent of the process type that the system undergoes.

Equations (2) and (3) are extremely valuable since they relate the entropy changes of a system and the changes in other properties. In general, the first *Tds* equation is applied to the processes of the closed systems, and the second *Tds* equation is applied to the processes of the open systems. Applying the relations of ideal gases, the relationship of *du* and *dh* with temperature $Pv = RT$, $du = c_v dT$, $dh = c_p dT$, and substituting them into Equation (2) and Equation (3), the differential entropy changes of an ideal gas are obtained,

$$\mathrm{d}s = c_v \frac{dT}{T} + R\,\frac{dV}{V} \qquad \mathrm{d}s = c_p \frac{dT}{T} - R\,\frac{dP}{P}.$$

Taking integration for the above two equations, the entropy changes for a closed system and an open system are,

$$s_2 - s_1 = \int_1^2 c_v\,\frac{dT}{T} + R\,\ln\frac{V_2}{V_1} \qquad \text{(kJ/kg·K)}, \tag{4}$$

$$s_2 - s_1 = \int_1^2 c_p\,\frac{dT}{T} - R\,\ln\frac{P_2}{P_1} \qquad \text{(kJ/kg·K)}. \tag{5}$$

2.1. Approximate Analysis (Constant Specific Heats)

The approximate analysis is also called a constant specific heat method. The analysis assumes constant specific heats, averages between the temperature ranges for ideal gases in Equations (4) and (5). The entropy change under the constant $c_{v,\text{avg}}$ and $c_{p,\text{avg}}$ can be determined,

$$s_1 - s_2 = c_{v,\text{avg}}\,\ln\frac{T_2}{T_1} + R\,\ln\frac{V_2}{V_1} \qquad \text{(kJ/kg·K)}, \tag{6}$$

$$s_1 - s_2 = c_{p,\text{avg}} \ln\frac{T_2}{T_1} - R \ln\frac{P_2}{P_1} \qquad \text{(kJ/kg·K)}. \tag{7}$$

2.2. **Exact Analysis (Variable Specific Heats)**

The exact analysis is also called a variable-specific heat method. The entropy change during a process is decided by substituting the $c_v(T)$ and $c_p(T)$ relations into equations (4) and (5) and performing integrations. In practice, instead of conducting the laborious integrals each time, the entropy change from a temperature range from 0 to T is applied, which is defined as

$$s^{\text{o}} = \int_0^T c_p \frac{dT}{T}.$$

The values of s^{o} are calculated at various temperatures and tabulated with temperature for ideal gases. Given this definition, the integral in equation (7) becomes $\int_1^2 c_p \frac{dT}{T} = s_2^0 - s_1^0$ where s_2^0 and s_1^0 are determined at the corresponding temperatures T_2 and T_1 in the thermodynamics property tables. Therefore,

$$s_2 - s_1 = s_2^0 - s_1^0 - R \ln\frac{P_2}{P_1}. \tag{8}$$

Using $c_v = c_p - R$,

$$\int_1^2 c_v \frac{dT}{T} = \int_1^2 (c_p - R)\frac{dT}{T} = \int_1^2 c_p \frac{dT}{T} - \int_1^2 R \frac{dT}{T} = s_2^0 - s_1^0 - \text{R}\int_1^2 \frac{dT}{T}.$$

Applying the above expression to equation (4),

$$s_2 - s_1 = s_2^0 - s_1^0 + R\ln[(\frac{V}{T})_2(\frac{T}{V})_1] \qquad \text{(kJ/kg·K)}. \tag{9}$$

The author develops equation (9) to calculate the entropy change in the exact analysis of a closed system with a volume change.

3. **ISENTROPIC PROCESS**

3.1 **Approximate Analysis (Constant Specific Heats)**

An isentropic process means no entropy change in the process. By setting the entropy change to zero in equations (6) and (7),

$$0 = c_{v,\text{avg}} \ln\frac{T_2}{T_1} + R \ln\frac{V_2}{V_1}, \quad 0 = c_{p,\text{avg}} \ln\frac{T_2}{T_1} - R \ln\frac{P_2}{P_1},$$

and rearranging above equations, following relations are obtained,

$$(\frac{T_2}{T_1})_{s=\text{const.}} = (\frac{V_1}{V_2})^{k-1}, \tag{10}$$

$$(\frac{T_2}{T_1})_{s=\text{const.}} = (\frac{P_1}{P_2})^{(k-1)/k}, \tag{11}$$

$$(\frac{P_2}{P_1})_{s=\text{const.}} = (\frac{V_1}{V_2})^{k}. \tag{12}$$

Equations (10), (11), and (12) are called the first, the second, and the third isentropic relations of ideal gases under the constant specific heats.

3.2. **Exact Analysis (Variable Specific Heats)**

Equations (8) and (9) developed in Section 2.2 should be used when the approximate analysis is inappropriate for the entropy change in the isentropic process. By setting the entropy change to zero in these two equations,

$$0 = s_2^0 - s_1^0 - R\ln\frac{P_2}{P_1}, \qquad 0 = s_2^0 - s_1^0 + R\ln[(\frac{V}{T})_2(\frac{T}{V})_1],$$

and rearranging the first equation above,

$$s_2^0 - s_1^0 = R\ln\frac{P_2}{P_1} \rightarrow \frac{P_2}{P_1} = \exp\frac{s_2^0 - s_1^0}{R} \rightarrow \frac{P_2}{P_1} = \frac{\exp(s_2^0/R)}{\exp(s_1^0/R)},$$

The quantity $\exp(s^0/R)$ is defined as the relative pressure P_r. Therefore,

$$(\frac{P_2}{P_1})_{s=\text{const.}} = \frac{P_{r2}}{P_{r1}}. \tag{13}$$

P_r is a dimensionless quantity and a function of temperature only. The value of P_r is tabulated in the property tables of thermodynamics. Likewise, rearranging the second equation above, the following equations are developed:

$$s_2^0 - s_1^0 = -R\ln[(\frac{V}{T})_2(\frac{T}{V})_1] \rightarrow (\frac{T}{V})_2(\frac{V}{T})_1 = \exp\frac{s_2^0 - s_1^0}{R} \rightarrow (\frac{T}{V})_2(\frac{V}{T})_1 = \frac{\exp(s_2^0/R)}{\exp(s_1^0/R)}.$$

Then, $\frac{V_2}{V_1} = \frac{T_2}{T_1}\frac{P_{r1}}{P_{r2}} \rightarrow \frac{V_2}{V_1} = \frac{T_2/P_{r2}}{T_1/P_{r1}}$.

The quantity T/P_r is only a function of temperature. It is defined as the relative specific volume V_r. So,

$$(\frac{V_2}{V_1})_{s=\text{const.}} = \frac{V_{r2}}{V_{r1}}, \tag{14}$$

the value of V_r is tabulated in the property tables in thermodynamics.

4. **SUMMARY**

The author systematically describes the entropy changes of ideal gases and develops the missing equations for the closed system in the exact analysis. Complete Equations (6) – (14) in the approximate and exact analyses to calculate the entropy changes and the correlated properties in the isentropic processes for both the closed and opened systems are presented in the paper.

REFERENCES

1. Cengel Y.A., Cimbala J.M., *Thermodynamics – An Engineering Approach*, McGraw-Hill, 2018.
2. Jones J.B., *Engineering Thermodynamics – An Introductory Textbook*, Wiley, 1986.
3. Moran M.J., Shapiro H.N., Boettner Daisie D., Bailey M.B., *Fundamentals of Engineering Thermodynamics*, Wiley, 2018.
4. Bejan A., *Advanced Engineering Thermodynamics*, Wiley, 2016.

CONSTRUCTAL LAW CONFERENCE – CLC2024
Design in Nature and Evolution
Romanian Academy, Bucharest, 10–11 October 2024

Proceedings of CLC2024
pp. 29–32

CONSTRUCTAL COUPLINGS IN THE ELECTROPERMEABILIZATION OF THE CELL MEMBRANE

ALEXANDRU M. MOREGA*, MIHAELA MOREGA

The National University of Science and Technology "Politehnica" Bucharest, Romania,
*alexandru.morega@upb.ro and mihaela.morega@upb.ro

Through electromagnetic field analysis and numerical experiments, the paper aims to explore the influence of the applied electric field frequency on the electropermeabilization (EP) conditions. The physical quantity correlated to the EP triggering is the transmembrane voltage induced before the pore generation process starts. The Constructal Law is here perceived and operates through the intrinsic couplings of the associated electromagnetic field, which may be tuned by the experiment designer, who is empowered to promote EP by adjusting the working frequency of the setup.

Keywords: Constructal law (CL); Electropermeabilization (EP); Electromagnetic field (EMF); Electric currents; Design.

1. INTRODUCTION

Electropermeabilization (EP) aims at raising the permeability of lipid membranes of cells or chemical-containing capsules to various substances, facilitating their passage between the inside and outside environment by exposure to a variable electromagnetic field (EMF); the process is highly dependent on both the characteristics of the target (cell morphology (shape and structure) and electric properties of the membrane) and the EMF (amplitude, waveform, frequency, and space-distribution) [1]. Here, the concern is related to the EMF, which may be frequency-tuned to reach the threshold of the membrane's EP: two pending electric currents – the conduction current and the displacement current – may be adjusted to assist the EP. This analysis confirms the designer's ability to utilize the constructal intrinsic nature of the EMF, which "morphs" the coupling between the electric and magnetic fields (EF – MF), such that EP is enabled through tuning the working frequency in the experiment.

2. PHYSICAL AND MATHEMATICAL APPROACH TO THE NUMERICAL EXPERIMENTS

EMF penetration in the experimental setup (Fig. 1) is described by Maxwell laws, which in **A**–V form (**A** – magnetic vector potential; V– electric scalar potential) lead to the PDEs (Lorentz gauge condition is utilized),

$$\left(\frac{1}{\mu\varepsilon}\frac{\partial^2}{\partial t^2}-\nabla^2\right)\mathbf{A}=\mu\mathbf{J},\quad \left(\frac{1}{\mu\varepsilon}\frac{\partial^2}{\partial t^2}-\nabla^2\right)V=0,\quad \nabla\cdot\mathbf{A}+\frac{1}{\mu\varepsilon}\frac{\partial V}{\partial t}=0, \tag{1}$$

where **A** [m·T] is the magnetic vector potential, V [V] is the electric scalar potential, **J** [A/m^2] is the electric current density (conduction), μ [H/m] is the magnetic permeability, and ε [F/m] is the electric

DOI: https://doi.org/10.59277/CLC/2024.06

permittivity. In this 2D model, the cells are represented as disks, the distance L = 3 μm = 30% d between adjacent cells, under the 1 kV/cm, continuous wave (CW) applied electric field (V_0 = 6 V).

The electric properties of the cell parts are frequency-dependent, following a Debye model

$$\varepsilon_r(f) = \varepsilon_\infty + \frac{\varepsilon_s - \varepsilon_\infty}{1 + (f/f_r)^2}\,, \sigma(f) = \sigma_s + \frac{\omega\varepsilon_0(\varepsilon_s - \varepsilon_\infty)}{1 + (f/f_r)^2}(f/f_r) \tag{2}$$

where ε_r is the dielectric constant, ε_r, and ε_∞ are the respective residual and static values, ε_0 [F/m] is the dielectric permittivity of free space, f_r [Hz] is the relaxation frequency, f [Hz] is the incident EMF frequency, σ [S/m] is the electrical conductivity with its static value σ_s. Figure 2 shows the frequency dependence of the dielectric properties, and Table 1 gives the values used here.

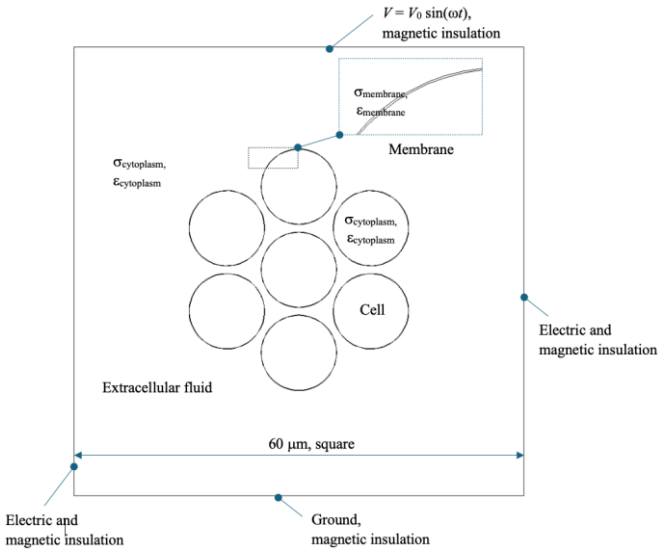

Fig. 1 – The 2D model – numerical experiment design and EMF constraints.

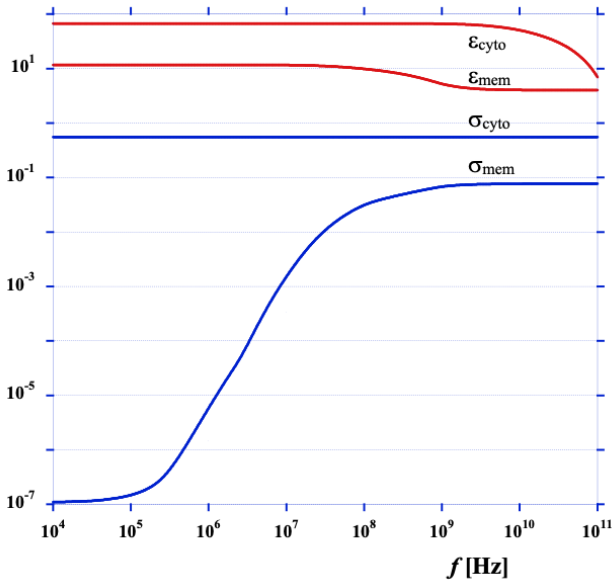

Fig. 2 – Frequency-dependent electric properties of cell parts (Deby models) [1].

Table 1

Electric properties of cell components (Debye model) [1]

Title 1	**Membrane**	**Cytoplasm & extracellular fluid**
Static electrical conductivity, σ_s [S/m]	$1.1 \cdot 10^{-7}$	0.55
Static dielectric permittivity, ε_s [S/m]	11.7	67
Residual dielectric constant, ε	4	5
Relaxation frequency, f_r [Hz]	$179.85 \cdot 10^6$	$17.9 \cdot 10^9$

3. **RESULTS**

In a lossy dielectric, the EMF intrinsic (EF - MF) coupling results in conduction ($\mathbf{J}_c = \sigma\mathbf{E}$) and displacement ($\mathbf{J}_d = \partial\mathbf{D}/\partial t$) currents. The cytoplasm conductivity here is higher than the membrane's; $\mathbf{J}_c$ cannot penetrate the membrane at lower frequencies, and its flow is mainly through the external cytoplasm (Fig. 3). At higher frequencies, the solenoidal part of $\mathbf{E} = -\text{grad}\, V - \partial\mathbf{A}/\partial t$ becomes significant (the amplitude of the applied electric field, Fig. 1, is constant), $\mathbf{J}_d$ increases and may flow through the membrane. EP may occur when the transmembrane voltage (the local $\mathbf{E}$) exceeds a threshold that may cause the membrane pores to "open", letting the substance flow through it. This simplistic explanation of EP is accompanied here by EMF spectra at some frequency values (medium and high frequencies of the Hertzian spectrum), which evidence the conduction–displacement currents flow.

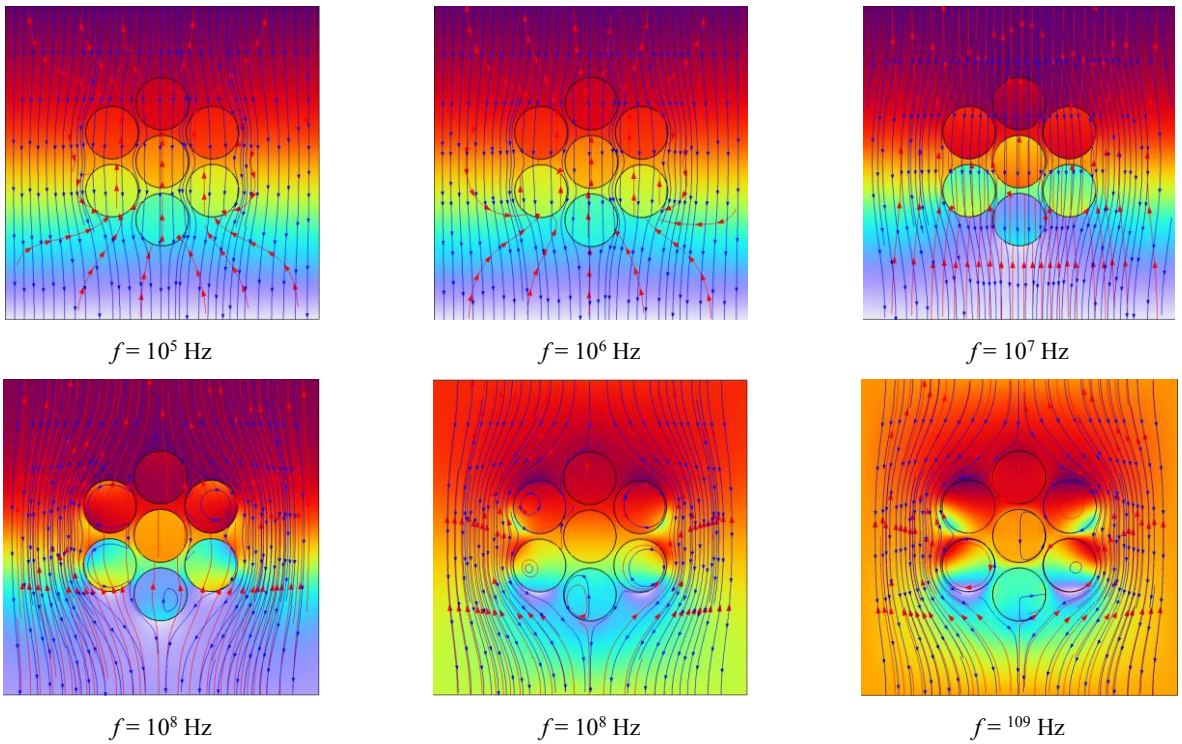

$f = 10^5$ Hz $f = 10^6$ Hz $f = 10^7$ Hz

$f = 10^8$ Hz $f = 10^8$ Hz $f = {}^{109}$ Hz

Fig. 3 – EMF spectra and current flow at different frequencies – conduction vs. displacement currents – $\mathbf{J}_c$ black streamlines and arrows; $\mathbf{J}_d$ red streamlines and arrows; V surface color map.

The electric power absorbed by the cell membrane, which may be related to EP success, differs at low vs. high frequencies, Fig. 4.

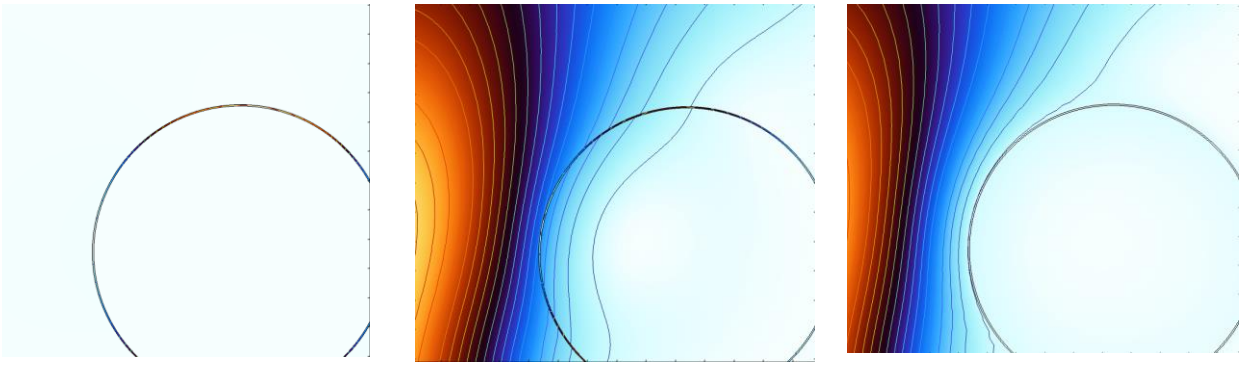

f = 10 kHz … 1 MHz f = 10 MHz f = 10 GHz

Fig. 4 – Electric power density (j/m^3) distribution. The membrane concentrates it at frequencies up to ~10 mhz.

4. **DISCUSSION AND CONCLUSIONS**

In this EP numerical experiment, the total electric current comprises the conduction current (which flows through highly conductive or higher-sigma media at any frequency) and the displacement current (which flows through highly polarizable or higher epsilon media at higher frequencies). The conduction current dominates the low-frequency range: it flows outside the cells (does not cross the membrane). The displacement current becomes more critical at higher frequencies. The role interplay between these currents accompanies the EP. Further research is devoted to drawing the limit.

The intrinsically coupled underlying EMFs here source each other. Evolution's constructal nature [2,3] applies to EMFs [4], and it governs their action-reaction morphing into propagation.

REFERENCES

1. Sandu A.M., Morega M., Electrical stress on membrane for cells in suspension under continuous wave electric field, *Proceedings of the 12th Int. Symposium on Advanced Topics in Electrical Engineering, IEEE*, March 25–27, 2021, Bucharest, Romania.
2. Bejan A., *Shape and Structure, from Engineering to Nature*, Cambridge Univ. Press, Cambridge, 2000.
3. Bejan A., *Freedom and Evolution Hierarchy in Nature, Society, and Science*, Springer Nature, 2020, p. 5.
4. Morega A.M., Morega, M., A constructal perception of the electromagnetic field, *International Communications in Heat and Mass Transfer*, **155**, *107531*, p. 10 (2024).

CONSTRUCTAL LAW CONFERENCE – CLC2024
Design in Nature and Evolution
Romanian Academy, Bucharest, 10–11 October 2024

Proceedings of CLC2024
pp. 33–36

PREVENTION OF EARTHQUAKES AND GLOBAL WARMING, DESIGNING IN THE NATURE, NEW STRUCTURAL MODELS, DESIGN METHODS AND SUSTAINABLE ARCHITECTURE AND ENGINEERING

AYDOGAN IBIS

Bogazici University Earthquake Engineering (Phd) and Yildiz Technical University Structural Engineering (Msc)-Civil Engineering (Bsc) and Architecture (Bsc), Saimekadın Hurel Mahallesi 4, Sokak 12/11, Sukru-Ercan Apartmanı, Mamak, Ankara, 06350, Turkey
aydogan_ibis@yahoo.com

Throughout history, humanity has passed through many periods, and new builds are designed in every step. The new construction builds and environments have changed their habits and habitats. Nowadays, nature requires explanations about old historic buildings and their structural systems. According to the study's latest design criteria, new structural and earthquake design models were implemented to provide the internal structures and contribute to constructional cost analysis. The regulations require natural designs, sustainable systems, and functionality, among other daily needs.

Humanity has recently lost and ruined all architectural designs, disciplines, laws, and engineering criteria. Thus, humanity has tried to provide balance, find a definite solution, and create natural designs. The study discovered new criteria, models, methods, calculation ways, and explanations about life in the world.

Furthermore, many ecological investments are made, and people try to support them, especially engineers, architects, and economists, who invest in natural energy. Therefore, the studies show a positive way that it can be applied in all regions worldwide, which is most effective. They contain the sustainable architecture and engineering criteria and assume the additional requirements. You can see more details below.

Keywords: Sustainability; Natural energy; New structural models; Calculation methods; Life in the world; intentions; Discoveries about the internal designs**.**

1. INTRODUCTION

In the beginning, most studies in the academy have proven climate change, so they produce new design methods and architectural designs that benefit from the sun and natural energy. In the survey, you will first find how many methods (my Ph.D. private or personal or individual conducts) can be used to take earthquakes under control? Secondly, how will the methods influence the structural design criteria? Thirdly, how can we design the structural projects and architectural designs according to new structural design criteria?

The first method is “the direct and indirect lights from the sun”. We can benefit from the expansion changes over the earthquake plates in terms of scale. As known, three types of expansion plates are famous because of their motions. Convergent boundaries move to or squeeze each other, divergent boundaries move away, and transform boundaries exhibit a parallel motion. In all boundaries, all motions can be taken under controlled by the expansions of the earth so we can easily benefit from the sunlight, and you can see the figures of the direct and indirect lights or wave distribution below.

DOI: https://doi.org/10.59277/CLC/2024.07

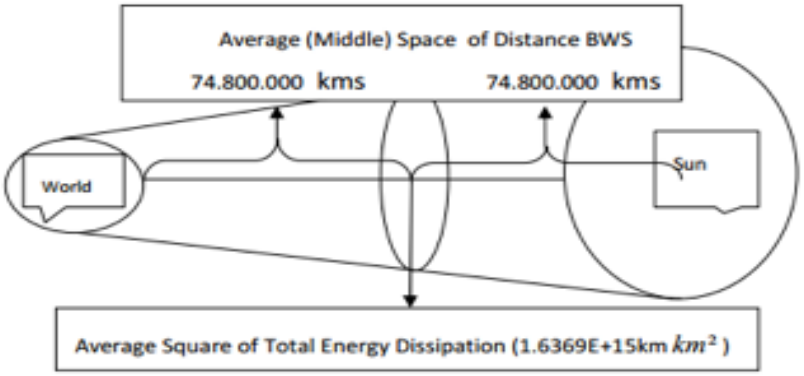

Fig. 1 – Energy integration scheme and indirect wave distribution.

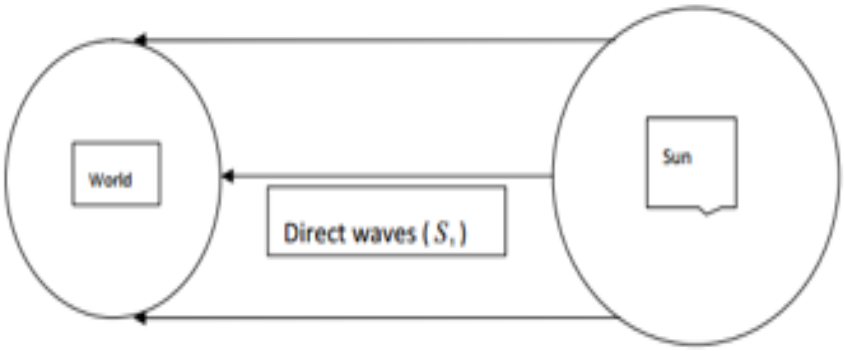

Fig. 2 – Energy integration scheme and direct wave distribution.

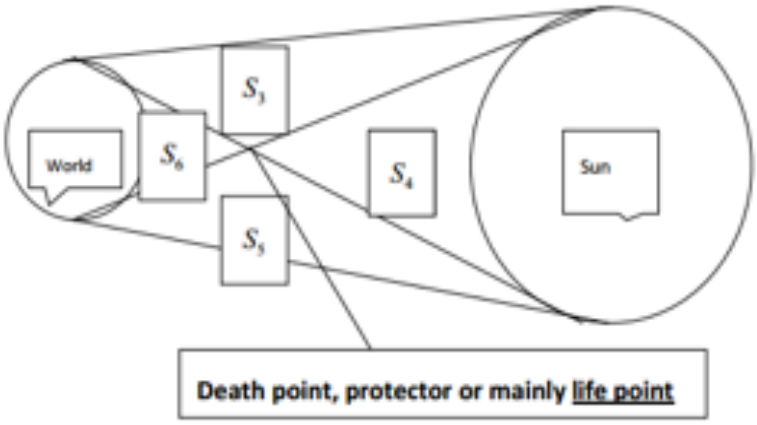

Fig. 3 – Energy integration scheme and energy dissipation region between shadow waves and direct and indirect waves.

The second method is "Liquefaction to soften the movable plates of the convergent, divergent, and transform boundaries." Thus, by drilling land surfaces and injecting the liquid material into a crust or outscoring all over the world, all zones can be easily monitored and controlled.

The third method is "the weight factor over plates." As known by a great audience, all underground resources have been consumed, and people have produced lots of cars and vehicles and designed plenty of devices. It can be solved using surface waves by weight and efficiently replacing raw money with people. We can change the weight over plates and provide a balance with a tiny weight factor. Do not forget that a micron-sized motion corresponds to 1000 years of energy dissipation (Integration) or the 7.2 magnitude size of an earthquake motion.

Secondly, all engineers and architects may design a softer build or structure and material. This will contribute to all economic advantages because earthquake factors or forces affect the cost analysis or budget of the state's economic conditions. It means tiny outforces or only death, live loads, and systematic designs according to functionality. This contains all engineering science fields. For an internal structural design, you can see the new structural scheme for the buildings under excitation and death loads.

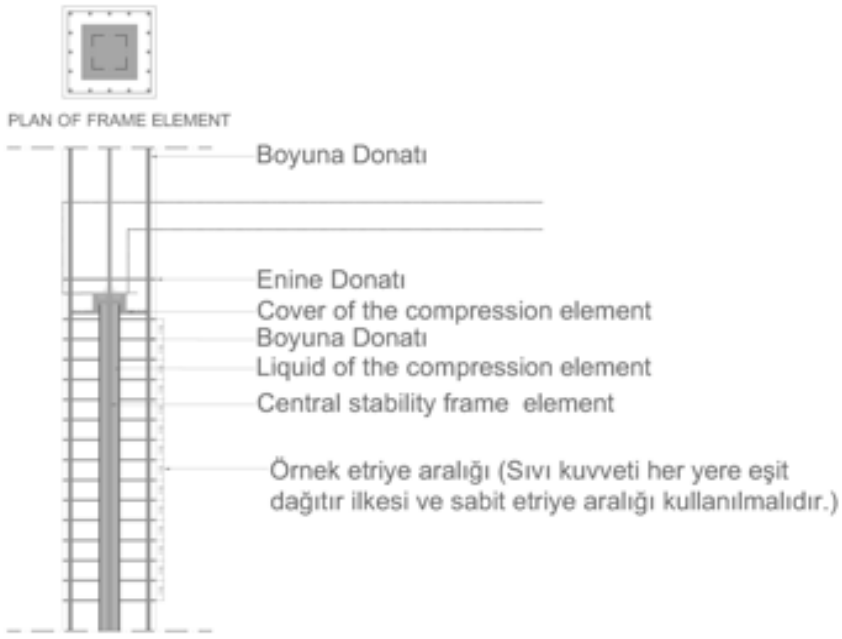

Fig. 4 – Integration scheme of the internal strength design for the columns and beams in reinforcement concrete systems.

In Fig. 4, the system requires a liquid column rod throughout the columns and compression regions in beams. Thus, the compression effects transmit to the foundation, and the incident prevents life losses on the column and beams because of the compression power. As well known, after casting the concrete in the compression elements, the strength is increased, but after death and live loads go up, it reduces to the improved conditions. Therefore, recycling systems damage the engineering principles (Safety, economy, and esthetics). The new design and calculation method are applicable all around the world. According to the criteria, earthquake methods first decrease the design dimension sizes under death and live loads, and the liquid column transmits the load direction to the foundation. During an earthquake or out effects, the system works as before. The liquid column rod conditions and resists. The combination will create a great advantage for all humanity.

Thirdly, while combining the new structure system or criteria with the engineering systems or architectural designs, we can derive ecological and sustainable designs, and after years and years, the structures

can be moved to new generations. Their materials have already depended on natural materials, predominantly liquid materials, so according to Archimed theory, liquids cannot squeeze by pressure because the strain amount is very close to zero. The hydraulic system is related to the same scientific law. The central rod can be designed as cylindric. Combining the different studies, all architectural designs are built efficiently and correctly.

2. **CONCLUSION**

First, most people know about architectural sustainable design. Still, they generally benefit from it in a tiny amount, so we have guaranteed the circular sustainable schemes in the study.

If the prevention of global warming and earthquakes is to be demanded, one of the three methods above should be applied. In this case, we can decrease global warming and create great energy for all buildings and all vehicles over the land surface. The design methods will provide significant advantages for human peace because people will have economic freedom, and we won't consume underground resources or raw materials. This will also offer groundwater and underground water level protection because humanity knows all underground resources are restricted, and people should discover or intend to return for natural balance.

Another Ph.D. study has proved that if we need to design environmentally sustainable structures or power, we should change the regulations because of the new structural models above. We can combine the steel material strains and liquid transmission power or target liquid displacements about compression.

As a result of the article, we can easily change the world so many times where the internal structure power or integrity can be constructed. It will provide it economically. All countries will profit or promote a great power, and in all international areas, people will be free.

ACKNOWLEDGMENTS

Aydogan IBIS owns all these studies, including his PhD studies at Bogazici University. His company, Akare Ahl&Akare Engineering, owns all copyrights for architecture, restoration, and project design.

REFERENCES

1. Ibis A., The life, protector or death point, energy dissipation for taking precautions against global warming, prevention and taking earthquakes and historical disasters under control, gaining underground resources and life needs, Bogazici University, PhD Studies, 2018, pp. 1–41.
2. Ibis A., Reducing the use of high strength concrete, preserving the life of concrete, and designing a new system to be applied against compression effects (in Turkish, *Yüksek mukavemetli beton kullanımının azaltılması, beton ömrünün korunması, compression etkilerine karşı uygulanacak yeni system tasarımı*), Bogazici University, PhD Studies, 2018, pp. 1–28.

CONSTRUCTAL LAW CONFERENCE – CLC2024
Design in Nature and Evolution
Romanian Academy, Bucharest, 10–11 October 2024

Proceedings of CLC2024
pp. 37–40

DEFINITION OF TIME: FROM THE SECOND TO CONSTRUCTAL LAW

UMBERTO LUCIA[a*], GIULIA GRISOLIA[b]

[a] Dipartimento Energia "Galileo Ferraris" Politecnico di Torino, Corso Duca degli Abruzzi 24, 10129 Torino, Italy, umberto.lucia@polito.it

[b] Dipartimento di Ingegneria dell'Ambiente, del Territorio e delle Infrastrutture, Politecnico di Torino, Corso Duca degli Abruzzi 24, 10129 Torino, Italy, giulia.grisolia@polito.it

*Correspondence: umberto.lucia@polito.it; Tel. +39 011 090 4558

One of the open problems in Physics is the analytical definition of time. This paper addresses a possible answer to this topic by proposing an analytical definition of time obtained by the Second Law of Thermodynamics and the Constructal Law approach.

Keywords: Constructal law; Quantum thermodynamics; Definition of time**.**

1. INTRODUCTION

The definition of time represents one of the open problems in physics. In Galilei's approach to motion, time represents an absolute and fundamental quantity [1], while Isaac Newton considers time as only a mathematical entity [2], without any real or physical essence; simultaneity and durations of phenomena are absolute [3]. On the contrary, Albert Einstein derived the concept of time from the postulate of invariance of the speed of light [4], with the consequence that duration becomes a quantity dependent on the observer (local quantity [5]). Moreover, Einstein introduced the concept of the isoentropic Universe [6], but understanding entropy in the context of the Universe is crucial for comprehending its evolution. Indeed, as the Universe expands, its energy and matter distributions undergo transformations that lead to changes in entropy. In all these approaches, time is used and defined in an operative way based on the concept of duration. Still, its analytical definition was not explicitly introduced until 2009, when an analytical mechanical approach was suggested [7], which, however, does not consider the energy conservation of all its components, particularly irreversibility.

In this paper, following Barbour's idea of an analytical approach, we propose a definition of time, not referring to Lagrangian mechanics as Barbour did, but starting from the Second Law of thermodynamics and evaluating each term by using the Constructal Law.

2. MATERIALS AND METHODS

We consider the Second Law of Thermodynamics:

DOI: https://doi.org/10.59277/CLC/2024.08

$$\frac{dS}{dt} = \frac{\dot{Q}}{T} + \dot{S}_g, ..., \tag{1}$$

where S is the entropy [J K^{-1}], Q is the heat power [W], T is the temperature [K], $\dot{S}_g = dS_g/dt$ is the entropy generation rate [W K^{-1}], and t is the time [s]. Considering our Universe in a stationary expansion [5] $dS/dt = 0$, so it follows:

Now, we consider a Hydrogen-like atom in interaction with an electromagnetic wave. The electromagnetic wave is a flow of photons. They income into the atoms and outcomes from them. At the atomic level, the photons can be absorbed by the atomic or molecule electrons, and an electronic energy transition occurs between energy levels of two atomic stationary states. Then, the photons can be also emitted by the excited electrons, when they jump down into the energy level of the original stationary state. Apparently, there are no changes in the atom energy, but only in the electronic transition. But, on the contrary, there exists a change in the kinetic energy of the centre of mass of the atom, but its amount is negligible in relation to the energy change in electronic transition, and its time of occurrence (10^{-13} s) is greater than the time of electronic transition (10^{-15} s). However, its contribution to the energy balance becomes relevant when we consider a great number of interactions as it happens in macroscopic systems, as shown by Condon [8]. In our analysis of a Hydrogen-like atom, of atomic number Z, in interaction with an external electromagnetic wave (a photon), we consider the apparent atomic radius, $s_1 r_n = 4\pi\varepsilon_0\hbar^2 n^2/m_e Z e^2$ where ε_0 is the electric permittivity, $\hbar$ is the reduced Plack constant, m_e is the mass of the electron, e is the elementary charge, n = 1, 2, 3, ..., is the principal quantum number, always integer, and the energy of the atomic level, $E_n = m_e Z^2 e^4/32\pi^2\varepsilon_0^2\hbar^2 n^2$. The atomic electron absorbs the incoming photon when its frequency, ν, is the resonant frequency, required by the transition between the initial E_i and final E_f energy levels, corresponding to the quantized energy $v = (E_f - E_i)/h$, where h is the Planck's constant. The emission of this photon results in the reverse process. In this approach, the atom has a *finite size,* and the interaction occurs in a *finite time*. Constructal Law evaluated the energy footprint of this process in Ref. [9–12]:

$$E_{ftp} = \Delta(h\nu) = -\frac{m_e}{M} h\nu. \tag{3}$$

The electromagnetic inflow power is well known from Electromagnetism:

$$\dot{Q} = \frac{A}{2}\varepsilon_0 c E_{el}^2 + \frac{A}{2\mu_0} c B_m^2, ... \tag{4}$$

where E_{el} is the electric field and B_m is the magnetic field, c is the velocity of light. Consequently, time results the mean value of the following relation:

$$\tau = \frac{T}{\frac{A}{2}\varepsilon_0 c E_{el}^2 + \frac{A}{2\mu_0} c B_m^2} \frac{m_e}{M} h\nu, ..., \tag{5}$$

with respect to all the local possible interactions.

3. **RESULTS**

We have introduced an analytical definition of time which emerges from the Second Law of Thermodynamics. Time results in the footprint of irreversibility from all the possible electromagnetic interactions, as Einstein conjectured. The footprint of atomic irreversibility has been evaluated by using a Constructal Law approach, considering the atom as a finite-size system.

4. **DISCUSSION AND CONCLUSIONS**

The result obtained satisfies all the requests from physics; indeed, time is a local quantity, it can be measured in any laboratory, and results strictly related to the evolution of the Universe, in agreement with the General Theory of Relativity [13–18]. Last, the analytical results allow us to obtain duration, $\tau = t - t_0$, and by setting $t_0 = 0$, we can obtain the definition of time.

REFERENCES

1. Galilei G., *Dialogo sopra i due massimi sistemi del mondo tolomaico e copernicano*, Ottavio Besomi and Mario Helbin (Eds.), Padova, Antenore, 1998.
2. Newton I., *Philosophiae Naturalis Principia Mathematica*, Editio tertia aucta & emendate, Londini, Guil. & Ioh. Innys, MDCCXXVI.
3. Borghi C., A critical analysis of the concept of time in physics, *Annales de la Fondation Louis de Broglie*, **2016**, *41*, pp. 99–130.
4. Einstein A., *Relativity: The Special and General Theory*, London, Routledge Classics, 1920.
5. Weinberg S., *Gravitation and Cosmology: Principles and Applications of the General Theory of Relativity*, Hoboken, John Wiley & Sons, 1971.
6. Madsen M.S., *The Dynamic Cosmos*, Boca Raton, Chapman and Hall, 1995.
7. Barbour J., *The Nature of Time*. arXiv:0903.3489v1 [gr-qc] 29 March 2009.
8. Condon E., Nuclear motion associated with electron transitions in diatomic molecules, *Physical Review*, **1928**, *32*, pp. 858–872.
9. Lucia U., Macroscopic irreversibility and microscopic paradox: A Constructal law analysis of atoms as open systems, *Scientific Reports*, **2016**, *6*, p. 35792.
10. Lucia U., Unreal perpetual motion machine, Rydberg constant and Carnot non-unitary efficiency as a consequence of the atomic irreversibility, *Physica A*, **2018**, *492*, pp. 962–968.
11. Lucia U., Electron-photon interaction and thermal disequilibrium irreversibility, *International Journal of Quantum Foundation*, **2017**, *3*, pp. 24–30.
12. Lucia U., Açikkalp U., Irreversible thermodynamic analysis and application for molecular heat engines, *Chemical Physics*, **2017**, *494*, pp. 47–55.
13. Lucia U., Grisolia G., Non-holonomic constraints: Considerations on the least action principle also from a thermodynamic viewpoint, *Results in Physics*, **2023**, *48*, p. 106429.
14. Lucia, U. Grisolia, G. Thermodynamic Definition of Time: Considerations on the EPR Paradox, *Mathematics*, **2022**, *10*, p. 2711.

15. Lucia U., Grisolia G., Kuzemsky A.L., Time, irreversibility and entropy production in nonequilibrium systems, *Entropy*, **2020**, *22*, p. 887.
16. Lucia U., Grisolia G., Time & Clocks: A thermodynamic approach, *Results in Physics*, **2020**, *16*, p. 102977.
17. Lucia U., Grisolia G., Time: A Constructal viewpoint & its consequences, *Scientific Reports*, **2019**, *9*, p. 10454.
18. Lucia U., Grisolia G., Time: A footprint of irreversibility, *Atti dell'Accademia Peloritana dei Pericolanti*, **2019**, *97*, SC1-SC4.

CONSTRUCTAL LAW CONFERENCE – CLC2024
Design in Nature and Evolution
Romanian Academy, Bucharest, 10–11 October 2024

Proceedings of CLC2024
pp. 41–44

CONSTRUCTAL LAW, BIOMIMICRY, AND TOPOLOGY OPTIMIZATION THROUGH THE LENS OF GENERATIVE AI

MATEI C. IGNUTA-CIUNCANU, PHILIP TABOR, RICARDO F. MARTINEZ-BOTAS

SETTL Lab, Imperial College, London, SW7 2AZ
mi3618@ic.ac.uk, philip.tabor2@imperial.ac.uk, r.botas@imperial.ac.uk

Efficient heat management in the context of semiconductor miniaturization demands unconventional solutions to navigate constrained design spaces. The emergence of unsupervised learning as a versatile design companion capable of processing multi-disciplinary datasets presents promising avenues for streamlined bio-inspired solutions for fundamental conduction problems. As a case study, we tackle the pivotal area-to-point problem that led to the formulation of the Constructal Law.

This study proposes a novel methodology harnessing *denoising diffusion probabilistic models* (DDPM) to seamlessly integrate features from topology optimization, constructal theory, and biomimetic structures. We use DDPM as a digital non-equilibrium complex system to generate geometric patterns for conductive heat sink design. These patterns are sampled to address the original formulation of the area-to-point problem.

This study emphasizes the significance of morphological freedom in addressing multi-objective problems, reinforcing arguments first formulated within the constructal paradigm. Our framework facilitates low-cost sampling of intricate shapes capable of serving multiple temperature objectives by synthesizing principles from different fields. We show the emergence of dendritic structures to solve distribution problems in an unsupervised learning scenario, drawing a parallel between information and energy flows.

This research underscores the transformative potential of Generative AI in blending design features across disparate disciplines, a potent tool for developing conductive heat sink solutions beyond deterministic optimization approaches.

Keywords: Generative AI; Morphological freedom; Thermal management; Nature-inspired design.

1. INTRODUCTION

The exponential increase in computing power as part of the digital transformation follows a direct consequence of a two-order of magnitude reduction in transistor scale. Formulated in 1965, Moore's Law accurately predicted doubling the number of transistors in an integrated circuit every two years. The more stringent requirements for heat dissipation capacity and the ever-smaller scale size progressively ruled out natural convection, fan, and liquid cooling. They ultimately limited the space available for high-conductivity material [1].

The cooling of electronic devices has become a hierarchical problem, considering the different objectives at each scale. At the chip level, the goal is to maintain a minimal temperature despite the high local fluxes. At the module level, where the heat loading becomes prominent, a minimal temperature gradient becomes relevant to reduce losses. Nonetheless, most consumer electronics operate under extensive variations in ambient conditions, making the ability to handle dynamic loads a priority at the system level.

Initially studied for electronics cooling applications, the area-to-point problem [2] contributed to formulating the Constructal Law as a general principle for resource allocation. This problem addresses bottlenecks in confined spaces and has seen a variety of alternative solutions, from gradient-based topology optimization through simulated bionic growth to particle swarm optimization [3–5].

The applicability of the Constructal Law as a design tool for challenges across various design spaces demonstrates that solutions developed for the ATP problem can be scaled seamlessly. Additionally, technologies like additive manufacturing open the design space, requiring new computational solutions to explore non-conventional avenues of inquiry.

2. COMPUTATIONAL METHODOLOGY

In this context, we propose a unifying generative approach to draw parallels between living and non-living systems to explore effective bi-material patterns. For this purpose, we use a diffusion algorithm developed to replicate non-equilibrium thermodynamics [6] for generating de novo structures. This method allows design feature blending and fast unsupervised sampling from a multi-modal heterogeneous dataset. We show that the

DOI: https://doi.org/10.59277/CLC/2024.09

AI agent can navigate a combinatorial design space and that the workflow enhances the morphological freedom of the samples, creating de novo candidates that visually display a high level of hybridity.

In the context of generative AI, diffusion models produce a Markov chain that gradually maps a known distribution (*e.g.*, a Gaussian) onto the underlying distribution of the dataset. Replicating statistical mechanics processes, the algorithm learns to estimate the steps for the inverse probability flow required to reach the smooth target distribution [7]. This strategy was motivated by the authors considering the Kolmogorov forward and backward equations, which showed that the two paths can be covered by respective small-perturbation diffusion processes that take the same functional form [6].

In the annealed importance sampling configuration, the algorithm estimates the multi-variate probability distribution from a single sample taken from the forward trajectory. Simulating a quasi-static physical process, the generative model assumes infinitesimally low diffusion rates and estimates the probability distributions of the intermediary steps using the Jarzynski equality [8].

In thermodynamics, this equality relates the exponential average of work done during non-equilibrium transformations to the free energy difference between two states. The denoising probabilistic model fundamentally resembles Langevin dynamics in discretizing the stochastic Fokker-Planck equation [7]. Hence, the amount of energy (here, information) lost along the path between the equilibrium distributions is proportional to the step size. This parallel provides a qualitative understanding of the diffusion rate as the critical parameter controlling sample quality [9].

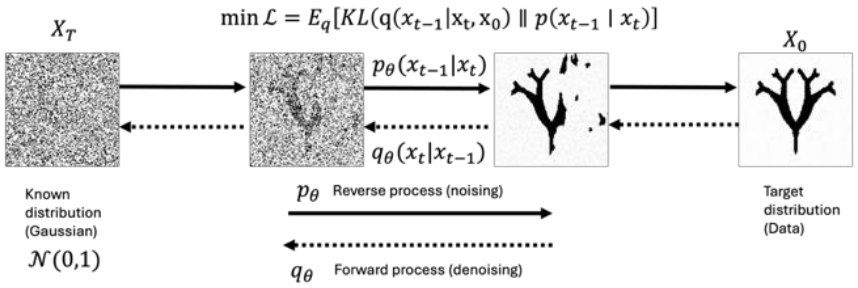

Fig. 1 – Diffusion probabilistic model that uses Markov chains that add (reverse process) and remove (forward process) noise and minimize local cross-entropy losses to establish computational and information efficient paths between the data and Gaussian equilibrium distributions.

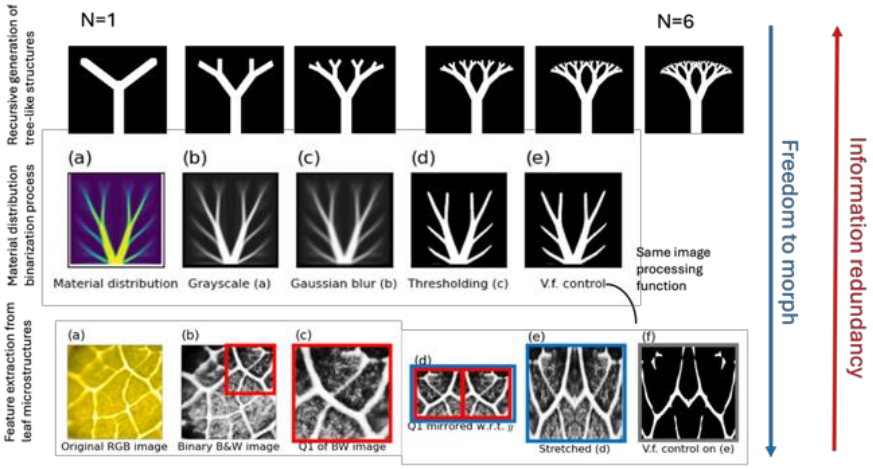

Fig. 2 – Three-modal dataset: hierarchical tree-like patterns with nested splitting, pre-optimized samples with boundary conditions and objectives to match the ATP problem, and bio-inspired leaf motifs with self-similarity. The freedom to morph and the degree of *orderliness* of the three families of samples are inversely correlated.

Given the method's unsupervised learning nature, the input data set will dominate the sampled structures. For the two-dimensional area-to-point (ATP) problem, we have curated a collection of microstructures: digital dendritic patterns with recursive scaling, output samples from an in-house topology optimizer following solid isotropic material with penalization, and processed close-up leaf pictures available online [10].

We reproduced the steps to normalize the three data modalities for brevity to compile a cohesive data set in Fig. 2. 11k bi-material samples represent each category. The recursive trees, which have a prescribed shape and an *orderly* appearance, carry the least amount of information. Conversely, the leaf structures contain self-similar and local symmetry-breaking features and require information-dense descriptions.

3. **RESULTS**

Figure 3 reproduces the results of unconditioned diffusion from the data set. They show that the solid inductive biases embedded in the three modalities can generate plausible candidates without an objective function feedback loop. Contrasting supervised learning aimed at ATP temperature objectives, the diffusion model's high-resolution synthesis improved feature interbreeding and produced some asymmetric samples through the open-ended generative process. The samples' diversity and the improved freedom to morph can be used for designing bi-material solutions for multi-objective problems with arbitrary boundary conditions.

From a constructal perspective, the non-equilibrium diffusion system improves the information flow access and enlarges the communication channels between the three categories in the input data set. Nonetheless, the form-function correlation is shown to be preserved in all the samples proposed having dendritic structures. The incremental changes caused by the noising/denoising processes, controlled by (information) entropy generation minimization, are thus well calibrated for configuration and evolution toward design freedom and, ultimately, better performance. Most importantly, the diffusion framework put forward provides the information flow architecture required to bridge disparate knowledge domains, growing novel branching forms that could quickly adapt for different physics and/or objectives rather than following prescriptions, targeting an *end design,* or mimicking nature [11–13].

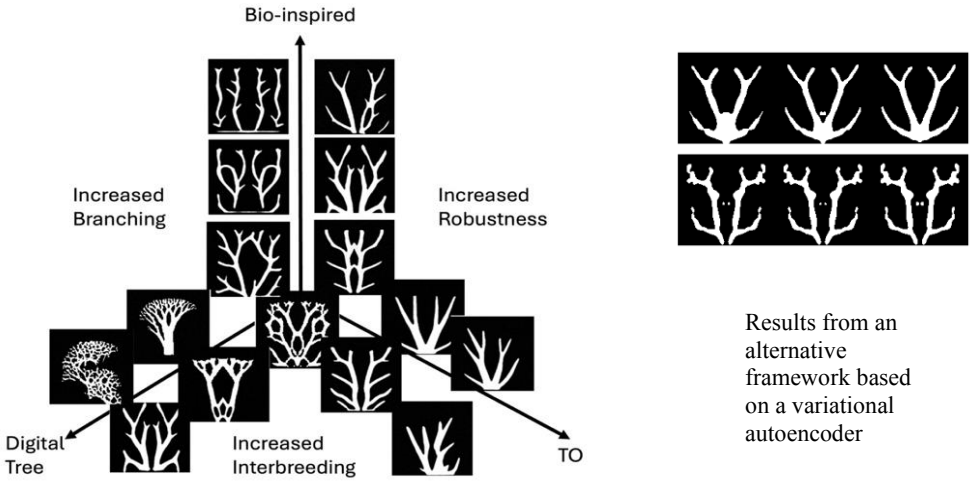

Fig. 3 – Unconditioned generation of *de novo* samples, ordered by origin and feature characteristics. The high resolution of the diffusion network yields improved mixing between design features from the three sources, showing enhanced freedom to morph compared to the samples obtained in a supervised learning setup (reproduced on the right [14]).

Moving forward from the original area-to-point problem, we have extended the capabilities of generative models beyond conductive heat sinks. The bio-inspired non-uniform structures are used to handle complex loading conditions, where temperature or heat flux varies across the surface. This adaptability is key in more advanced applications such as battery packs or high-performance computing systems where uniform cooling patterns would not be optimal. In this regard balancing thermal performance, material use, and manufacturing constraints with the hierarchical challenges posed at the beginning requires flexibility beyond conventional parametric design.

In Fig. 4, we show an example of a battery module assembly designed by the Formula Student Imperial Racing Green team. The temperature profile of the battery pack displays a clear temperature gradient. By morphing bio-inspired form to engineering function, the thermal solution adapts to the requirement of the system for enhanced performance and efficiency.

4. **CONCLUSIONS**

To conclude, we have presented a unifying generative design framework that improves the modelling resolution of thermal solutions beyond parametric design by enhancing the morphological freedom. This is made possible by the application of entropy generation minimization on the information flows to navigate complexity and produce dendritic structures from the border of chaos and order. This extends the application of constructal design to digital flow systems, demonstrating how natural flow architectures can be replicated probabilistically to optimize information and energy transfer, resulting in efficient, adaptive solutions for complex thermal and distribution challenges.

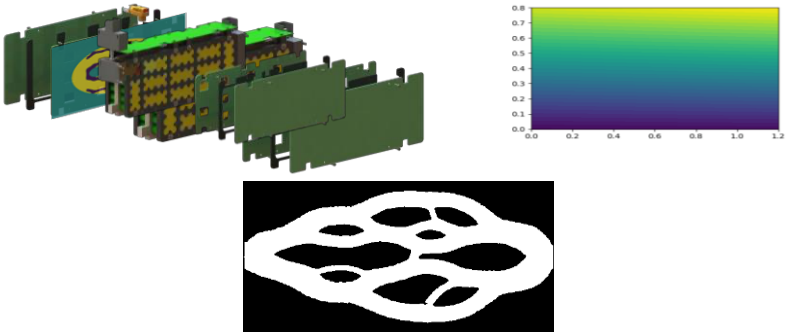

Fig. 4 – Solid model and temperature distribution of a generic battery pack (top).
Bio-inspired cooling channel topology generated from diffusion sample matching (bottom).

ACKNOWLEDGMENTS

MIC would like to thank Hannes Stark for the technical conversations on generative AI methods.

REFERENCES

1. Bejan A., Evolution in thermodynamics, *Appl. Phys. Rev.*, **4**, *1* (2017).
2. Bejan A., Constructal-theory network of conducting paths for cooling a heat generating volume, *Int. J. Heat Mass Transf.*, **40**, *4*, pp. 799–816 (1995).
3. Marck G., Nemer M., Harion J.L., Russeil S., Bougeard D., Topology optimization using the SIMP method for multiobjective conductive problems, *Numerical Heat Transfer, Part B: Fundamentals*, **61**, *6*, pp. 439–470 (2012).
4. Li B., Hong J., Yan S., Liu H., Ge L., Generating optimal heat conduction paths based on bionic growth simulation, *International Communications in Heat and Mass Transfer*, **83**, pp. 55–63 (2017).
5. Cai H., Guo K., Liu H., Xiang W., Liu C., Multiobjective optimization of area-to-point heat conduction structure using binary quantum-behaved PSO and Tchebycheff decomposition method, *Canadian Journal of Chemical Engineering*, **99**, *5*, pp. 1211–1227 (2021).
6. Sohl-Dickstein J., Weiss E.A., Maheswaranathan N., Ganguli S., Edu S., Deep Unsupervised Learning using Nonequilibrium Thermodynamics, *Forty-Second International Conference on Machine Learning, Vancouver Convention Center* (ICML), 13th – July 19th, 2025.
7. Ho J., Jain A., Abbeel P., Denoising Diffusion Probabilistic Models, *Adv. Neural Inf. Process. Syst.*, 2020, Jun.–Dec.
8. Jarzynski C., Equilibrium free energy differences from nonequilibrium measurements: a master equation approach, *Phys. Rev. E. Stat. Phys. Plasmas Fluids Relat. Interdiscip. Topics*, **56**, *5*, pp. 5018–5035 (1997).
9. Song J., Meng C., Ermon S., Denoising Diffusion Implicit Models, Cornell University, arXiv: 2010.02502.
10. Shen S.C., Buehler M.J., Nature-inspired architected materials using unsupervised deep learning, *Communications Engineering*, **1**, *1*, pp. 1–15 (2022).
11. Bejan A., Vascular flow design and predicting evolution, *International Communications in Heat and Mass Transfer*, **155**, p. 107517 (2024).
12. Bejan A., Constructal design evolution versus topology optimization, *International Communications in Heat and Mass Transfer*, **141** (2023).
13. Bejan A., Evolutionary design: Heat and fluid flow together, *International Communications in Heat and Mass Transfer*, **132**, p. 105924 (2022).
14. Ignuta-Ciuncanu M.C., Stärk H., Martinez-Botas R., *Bio-Inspired Design of Conductive Heat Sinks Using a Generative Autoencoder Framework*, https://ssrn.com/abstract=4576761.

CONSTRUCTAL LAW CONFERENCE – CLC2024
Design in Nature and Evolution
Romanian Academy, Bucharest, 10–11 October 2024

Proceedings of CLC2024
pp. 45–46

SOLUTIONS OF NEWTONIAN GRAVITATIONAL WAVES AND GRAVITATIONAL POYNTING VECTOR

PETER VADASZ

Northern Arizona University, Peter.Vadasz@nau.edu
Peter.Vadasz@nau.edu

Solutions to equations producing Newtonian gravitational waves are being presented. The derivations of these equations emerging directly from the second Newton law and mass conservation applied to a continuous mass distribution, *e.g.*, a compressible fluid or equivalent, have already been shown to lead to a form identical to the Maxwell equations for electromagnetism subject to a specific condition. Consequently, Newtonian gravitational waves are Lorentz invariant when the speed of wave propagation equals the speed of light. The resulting equations can derive a gravitational Poynting vector in complete analogy to the electromagnetic Poynting vector. A stationary solution exists for a spherical mass, creating the gravitational field. The evolution of a gravitational wave emerges and is presented as a linear, neutrally stable solution around this stationary one.

Keywords: Gravitational waves; Continuous mass; Newtonian dynamics; Lorenz force; Poynting vector; Maxwell equations.

1. INTRODUCTION

Gravitational waves were shown by Vadasz [1] to derive directly from Newtonian dynamics for a continuous mass distribution, *e.g*. compressible fluids or equivalent. It was shown that the equations governing a continuous mass distribution, *i.e*. the inviscid Navier-Stokes equations for a general variable gravitational field $\mathbf{g}(t,\mathbf{x})$, are equivalent to a form identical to Maxwell equations from electromagnetism, subject to a specified condition. The consequence of this equivalence is the creation of gravity waves that propagate at finite speed.

The latter implies that Newtonian gravitation is not "spooky action at a distance" but is like electromagnetic waves propagating at finite speed despite the apparent form appearing in the integrated field formula. Since gravitational waves were so far derived only from Einstein's general relativity theory, it becomes appealing to check if there is a connection between the Newtonian waves presented in this paper and the general relativity type of waves, at least in a specific limit of overlapping validity, *i.e.*, as a flat-space approximation.

Two specific stationary solutions of the gravitational field and mass density distribution within the mass-creating field and the possible waves associated with these solutions are presented.

2. GOVERNING EQUATIONS FROM NAVIER-STOKES TO MAXWELL EQUATIONS

The equations governing the gravitational field effect and its dynamics for a distributed mass (compressible fluid or equivalent) are the inviscid and compressible Navier-Stokes equations

$$\frac{\partial \rho}{\partial t} + \nabla \cdot (\rho \mathbf{v}) = 0, \tag{1}$$

$$\frac{\partial \mathbf{v}}{\partial t} = -\nabla\left[v_o^2(\ln\rho) + \left(\frac{\mathbf{v}\cdot\mathbf{v}}{2}\right)\right] + \mathbf{v}\times(\nabla\times\mathbf{v}) + \mathbf{g}, \tag{2}$$

where $\rho(t,\boldsymbol{x})$ is the mass density, $\mathbf{v}(t,\boldsymbol{x})$ is the velocity, $\mathbf{g}(t,\boldsymbol{x})$ is the gravitational field, t is time and $\boldsymbol{x}$ is the position vector. The term $\rho\mathbf{g}$ represents the intrinsic gravitational forces impressed between differential mass elements due to the distributed mass within the domain occupied by this mass. By using a linear approximation for the constitutive relationship between pressure and density in the form $P = P_o + v_o^2(\rho - \rho_o)$ where P_o and ρ_o are reference values of pressure and mass density, respectively, and $v_o = \sqrt{\frac{\partial P}{\partial \rho}} = \frac{1}{\sqrt{\rho_o \beta_P}}$ is the constant speed of propagation of the pressure wave (speed of sound as a special case, but affecting the wave propagation of the gravitational field g beyond the region containing the mass). These equations convert into a form identical

DOI: https://doi.org/10.59277/CLC/2024.10

to Maxwell equations subject to an extended Beltrami condition namely $\nabla \times (\mathbf{v} \times \boldsymbol{\xi}) = 0$ where $\boldsymbol{\xi}$ is the counter-vorticity vector. The solutions to the Newtonian gravitational field equations can be obtained from equations (1), and (2) in a form like Maxwell's equations presented in the form

$$\frac{1}{4\pi G}\nabla \cdot \mathbf{g} = -\rho; \frac{\partial g}{\partial t} = v_o^2 \nabla \times \boldsymbol{\xi} + 4\pi G\rho \mathbf{v}; \quad \frac{\partial \boldsymbol{\xi}}{\partial t} = -\nabla \times \mathbf{g}; \quad \nabla \cdot \boldsymbol{\xi} = 0. \tag{3}$$

3. STATIONERY AND WAVE SOLUTIONS

The solution inside the spherical domain contains the distributed mass assuming spherical symmetry, *i.e.*, $r \in [0, r_o]$ is due to the intrinsic gravitational forces impressed between differential mass elements due to the distributed mass. For this case there is a possible equilibrium mass density distribution and the corresponding equilibrium gravitational field distribution that can be obtained from (3) and (2) subject to $\mathbf{v} = 0$. Substituting $\mathbf{v} = 0$ yields

$$v_o^2 \nabla(\nabla \cdot \mathbf{g}) - \mathbf{g}(\nabla \cdot \mathbf{g}) = 0. \tag{4}$$

Assuming spherical symmetry, this equation becomes

$$\frac{\mathrm{d}}{\mathrm{d}r}\left[\frac{1}{r^2}\frac{\mathrm{d}(r^2 g_r)}{\mathrm{d}r}\right] - \frac{g_r}{v_o^2 r^2}\frac{\mathrm{d}(r^2 g_r)}{\mathrm{d}r} = 0, \tag{5}$$

$$g_r = -\frac{2v_o^2}{r};\ \rho = \frac{v_o^2}{2\pi G}\frac{1}{r^2}, \tag{6}$$

$$\mathbf{g} = -\frac{m_o G}{r_o r}\hat{\mathbf{e}}_r;\ \rho = \frac{m_o}{4\pi r_o}\frac{1}{r^2}. \tag{7}$$

where $\int_0^{\tilde{V}_o} \rho\, \mathrm{d}\tilde{V} = m_o$.

This equilibrium solution might or might not be stable. To investigate the stability of this equilibrium, one needs to consider the equations when $\mathbf{v} \neq 0$. Preliminary results from a linear stability analysis of this equilibrium indicate that the basic equilibrium solution might be neutrally stable with oscillations subject to some conditions, *i.e.*, $\mathbf{g} = \mathbf{g}_o + \boldsymbol{\varepsilon}\mathbf{g}^{(l)}(t, r, \varphi)$ and $\mathbf{v} = \mathbf{v}_o + \varepsilon \mathbf{v}^{(I)} = v_\varphi(t, r, \varphi)\hat{\mathbf{e}}_\varphi$ with $\mathbf{v}_o = 0$ because of the existence of the stationary solution.

The wave equations for waves propagating in the radial direction and having azimuthal polarization, *i.e.*, $\mathbf{g} = \mathbf{g}_o + \varepsilon \mathbf{g}^{(l)}(t, r, \varphi) = -\left(\frac{Gm_o}{r_o r}\right)\hat{\mathbf{e}}_r + \varepsilon g^{(l)}(t, r, \varphi)\hat{\mathbf{e}}_r$, $\mathbf{v}^{(t)} = v_\varphi(t, r, \varphi)\hat{\mathbf{e}}_\varphi$ based on the equation (3) have the form

$$\left[\frac{\partial^2}{\partial t^2} - \nabla^2 - \frac{2}{r^2}\right]\nabla\psi^{(1)} - \frac{2}{r}\hat{\boldsymbol{e}}_r\left[\frac{\partial^2}{\partial t^2} - \nabla^2\right]\psi^{(1)} = 0, \tag{8}$$

$$\left[\frac{\partial^2}{\partial t^2} - \nabla^2 - \frac{2}{r^2}\right]\mathbf{v}^{(1)} = 0, \tag{9}$$

$$\rho^{(1)} = \frac{1}{8\pi M a_o^2}\left[\frac{\partial^2}{\partial t^2} - \nabla^2\right]\psi^{(1)}, \tag{10}$$

$$\mathbf{g}^{(1)} = \frac{\partial \boldsymbol{v}^{(1)}}{\partial t} + \nabla\psi^{(1)}, \tag{11}$$

where $Ma_o^2 = \frac{Gm_o}{2v_o^2 r_o}$ is the square of the gravitational Mach number and ψ is a potential. Waves solutions to these equations will be presented. In addition, a gravitational Poynting vector emerges and is defined in the form

$$\mathbf{S}_g = \frac{v_o^2}{4\pi G}\mathbf{g} \times \boldsymbol{\xi}, \tag{12}$$

representing the power due to the gravitational field per unit area.

REFERENCES

1. Vadasz P., Newtonian Gravitational Waves from a Continuum, *Proc. Royal Society A*, **480**, http://doi.org/10.1098/rspa.2023.0656(2024).

CONSTRUCTAL LAW CONFERENCE – CLC2024
Design in Nature and Evolution
Romanian Academy, Bucharest, 10–11 October 2024

Proceedings of CLC2024
pp. 47–50

CONSTRUCTAL EVOLUTION OF GENETIC CODING SYSTEMS

ALBERT T. MAGNELL

Department of Economics, University of Oxford
albert.magnell@new.ox.ac.uk

This paper is a theoretical exploration of how biological evolution may evolve itself according to the Constructal Law. The astonishing diversity of life on Earth reflects how effective evolution is at augmenting survivability within various ecological niches. Yet, the genetic coding system that drives evolution is remarkably conserved among virtually all organisms. This is perhaps indicative that the process of evolution on Earth has so far been powerful enough to meet the planet's ecological challenges. If these challenges become increasingly intense or unstable, then for life to survive, its evolvability must evolve. Such second-order evolution may occur via fundamental changes to the genetic coding system.

Keywords: Constructal Law; Econobiology; Evolution of evolvability; Xenobiology**.**

1. INTRODUCTION

Virtually all life on Earth uses a remarkably conserved format for encoding genetic information. Genomes consist of strings of DNA nucleotides organized as triplets (codons). Since there are four different types of DNA nucleobases (adenine, guanine, thymine, cytosine), there are $4^3 = 64$ possible types of codons, which map onto the 20 types of canonical amino acids that serve as the building blocks of proteins. From a theoretical perspective, the combinatorics at play are ostensibly arbitrary. Why not have codons that are quadruplets or additional types of nucleobases?

When comparing different coding formats, it becomes apparent that there are functional tradeoffs. A format with high combinatorial diversity can encode genetic information with greater density and potentially more resilience to read/write errors. However, such an elaborate system will pose a more significant energetic burden to the organism. These advantages and disadvantages consequently serve as countervailing forces that delineate a set of quasi-optimal genetic coding formats. Framing this puzzle in terms of tradeoffs extends it beyond the purview of theoretical biology into the realm of economic theory. Since economics is fundamentally about how to optimally deal with scarcity, it is central to the origins of life and evolution. Perhaps surprisingly, though, a detailed framework of economic biology, or econobiology, has yet to be constructed.

In the context of the evolution of life, the genetic coding system is the configuration of coding format and molecular machinery that, together, control evolvability. Evolvability is critical for survival because it gives life greater access to the genetic sequence space encoding fitness adaptations [1,2]. Treating evolution as if it were a problem-solving process used by life to expand into new ecological niches or resist ecological shocks means that we can judge the effectiveness of a genetic coding system in terms of its evolvability. A good system has high evolvability, allowing the life that uses the system to adapt both resiliently and quickly [3]. When considering how a genetic coding system might evolve, a bioevolutionary form of the Constructal Law becomes a guiding principle: For life to persist in time (to thrive), its genetic coding system must evolve in such a way that provides easier evolutionary access to pathways of adaptability [4].

DOI: https://doi.org/10.59277/CLC/2024.11

2. **CONCEPTUAL MODEL**

This model of the potential evolvability of a genetic coding system has two degrees of freedom: the number of nucleobase types (N) and the codon length (L). Although this simplification precludes modeling even mildly alien genetic coding systems, it preserves much-needed tractability. The capacity of evolvability (E) is undergirded by a tradeoff between the benefits (B) and costs (C) of having a more complex genetic coding system. The two main benefits of having a more complex genetic coding format are a higher capacity for diversity (D) and enhanced coding fidelity (F). These come at the cost of a more significant energetic burden (J) and a longer time (T) for the system to operate. We, thus, represent B as a function of D and F, and C as a function of J and T,

$$E \sim B(D,F) - C(J,T). \tag{1}$$

Moreover, both B and C can be thought of as production functions. D and F are inputs for producing benefits, while J and T are inputs for 'producing' costs. Since their inputs are neither perfect substitutes nor complements, both of these production functions can be represented in standard Cobb-Douglas form,

$$E \sim XD^{\alpha}F^{\beta} - YJ^{\gamma}T^{\delta}. \tag{2}$$

X and Y are the total factors of production for B and C, respectively; however, it may be more helpful to think of them as shadow prices. The four exponents are output elasticities and determine whether B and C exhibit increasing, decreasing, or constant returns to scale in regard to their inputs. D, F, J, and T are all functions of the model's degrees of freedom, N and L.

3. **QUALITATIVE SIMULATIONS**

The diminishing returns to F concerning N and L potentially translate into B exhibiting decreasing returns to scale. In contrast, J and T have increasing (negative) returns concerning N and L. Thus, C exhibits increasing (negative) returns to scale. The countervailing forces on B and C mean that a point of optimality and a range of viable diversity exist, as illustrated in Fig. 1, panel a). The exogenous shadow prices of B and C affect their spread, which we may alter when qualitatively simulating hypothetical scenarios of interest. Although this is not formally a dynamic system, the intrinsic survival bias of evolution may render the optimality point an apparent attractor over time. Let us consider how systemic perturbations might steer the evolution of a genetic coding system toward greater evolvability. A sudden and drastic shock, such as a large meteor strike, to an ecosystem can destabilize the dynamic equilibria of niches beyond their resiliency. In order for life to thrive in these new conditions, it needs to be able to test a wider variety of phenotypes. This is manifested through an enhanced capacity for the genetic coding system to explore the genetic sequence space. This essentially raises the shadow value of B and the weight of α. Alternatively, if a positive shock occurs to an ecosystem, then life might more easily tolerate the costs of a more complex genetic coding system, thus decreasing the shadow value of C. If γ and δ also decrease sufficiently, then C could even exhibit negative returns to scale. Our behavior bias toward loss aversion means that we tend to fixate on the upfront negative effects of ecological change; however, a critical feature of life is that some organisms can construct new niches for themselves. From their

perspective, the aftermath of a negative shock to the ecosystem is the beginning of a bull market of evolutionary opportunity.

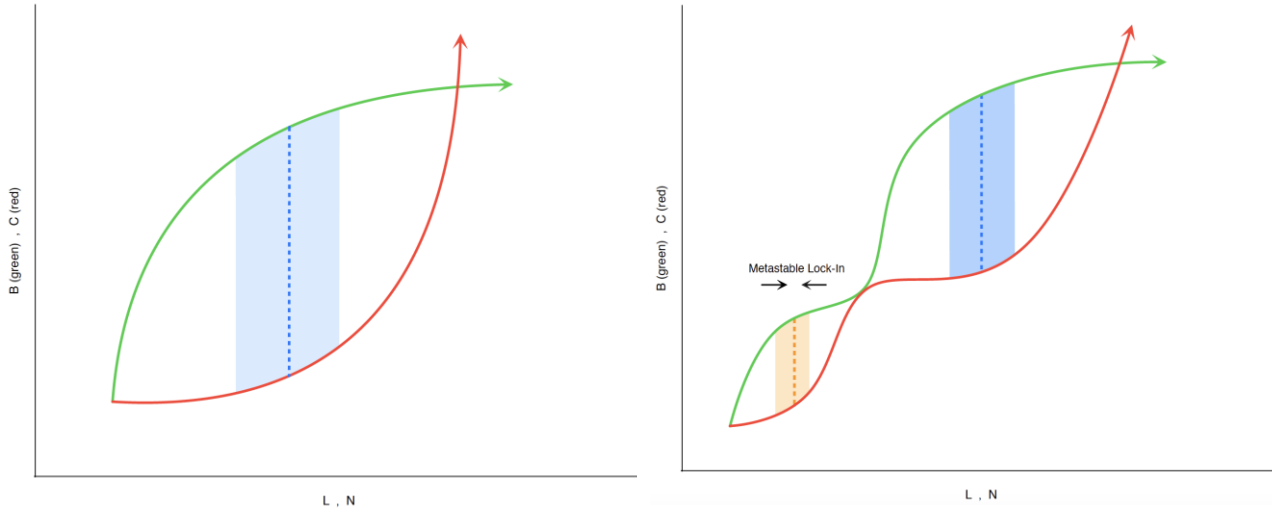

(a) (b)

Fig. 1 – (a) Countervailing returns to scale of B and C. The dashed blue line corresponds to the combination of *L* and *N* that yields optimal net benefits (the green curve minus the red curve) to evolvability. The lighter blue region represents a zone of viable diversity. (b) Pinched node prevents the genetic coding system from evolving out of the orange zone of locally viable diversity to the blue zone of absolutely viable diversity.

An important upshot of all of this is the interesting situation shown in Fig. 1, panel b), in which the generally decreasing returns to scale for *B* and the generally increasing returns to scale for *C* vacillate. If this happens, then two optimalities arise, one local and the other absolute. However, due to the node between them, the local optimality is locked in a state of metastability [5]. This lock-in may be escaped through a combination of stochastic ecological shocks that simultaneously smooth the dimples in the returns to scale of *B* and *C*. Given that there are not significantly different genetic coding systems on Earth, such an escape route may be extraordinarily rare via acts of nature. Bioengineering, in contrast, may feasibly open up such a path.

4. **DISCUSSION AND CONCLUSIONS**

As a proof-of-concept that economic theory and methods can yield new insights in theoretical biology, this paper should evoke a net surplus of questions directed not only at the origins and future of life on Earth but also toward other aspects of biological theory that implicitly involve economization, such as bioenergetics, intracellular trafficking, and intercellular communication. The formal cause of life is one of the most profound scientific problems because what we learn may alter our understanding of how we *Homo sapiens* see ourselves about our tree of life.

Indeed, we may find it to be just one small tree within an expansive forest. Our growing sophistication in synthetic biology has put us in the particular situation of being able to jailbreak our genetic coding system effectively [6]. With concerns on the rise that looming environmental disasters will harbinger the planet's next

mass extinction period, our newfound ‘unnatural’ powers may be what allow Earthly nature to flourish well beyond any expiration date.

REFERENCES

1. Maynard Smith J., Natural selection and the concept of a protein space, *Nature*, **225**, *5232*, pp. 563–564 (1970).
2. Kauffman S., Levin S., Towards a general theory of adaptive walks on rugged landscapes, *Journal of Theoretical Biology*, **128**, *1*, pp. 11–45 (1987).
3. Dawkins R., *The evolution of evolvability* in *Artificial Life*, Langton, C., Ed., Addison-Wesley Publishing Company: Reading, Massachusetts, United States, 1989, pp. 201–220.
4. Bejan A., Zane J.P, *Design in Nature: How the Constructal Law governs evolution in biology, physics, technology, and social organizations*, Doubleday, New York, United States, 2012.
5. Arthur W.B., Competing technologies, increasing returns, and lock-in by historical events, *The Economic Journal*, **99**, *394*, pp. 116–131 (1989).
6. de la Torre D., Chin J.W., Reprogramming the genetic code, *Nature Reviews Genetics*, **22**, *3*, pp. 169–184 (2021).

CONSTRUCTAL LAW CONFERENCE – CLC2024
Design in Nature and Evolution
Romanian Academy, Bucharest, 10–11 October 2024

Proceedings of CLC2024
pp. 51–52

FOUNTAIN OF LIGHT – CONSTRUCTAL CASCADES

KEENA GAO

Duke University, Durham, NC, USA
keena.gao@duke.edu

Constructal law governs how all flow systems, whether natural or man-made, exhibit a universal tendency to acquire configuration by facilitating easier and greater flow access over time and available space(Bejan). Applied to the dynamics of pedestrian flow, constructal law can facilitate urban designs for sustainability, accessibility, and efficiency. Inspired by these ideas, the sculpture is shaped like a fountain to symbolize the movement of people like a flowing fluid. The LED lights display the movement of people from a larger area through a bottleneck at the entrance to stairs or an escalator in the sculpture inspired by the dendritic structures anticipated with the constructal law. The sculpture visualizes the constant flux of people through urban environments where each individual contributes to the collective rhythm of society.

Though art and science may seem like distinct disciplines, interdisciplinary collaboration has significant value. For instance, visualization of scientific concepts and engineering designs can help create visual representations of scientific theories or communicate ideas to different audiences. Art can show beauty, efficiency, access, and freedom through constructal law.

Keywords: Pedestrian; Interdisciplinary; Sculpture; Urban; Constructal Law.

1. INTRODUCTION

Constructal law governs how all flow systems, whether natural or man-made, exhibit a universal tendency to acquire configuration by facilitating easier and greater flow access over time and available space(Bejan). Applied to the dynamics of pedestrian flow, constructal law can facilitate urban designs for sustainability, accessibility, and efficiency. My art installation seeks to show how constructal law can help envision innovative approaches towards the design of public places and invite contemplation onto the built environment and crowd movement.

2. RESULTS

I began the process of creating my installation with researching pedestrian flows in public spaces and visualizing crowd dynamics in large venues through sketches (Fig. 1). Through this research, I focused the scope of my project on showing the large-scale flows of crowds through physical space and wanted to create a sculpture that could demonstrate the power of crowd movement.

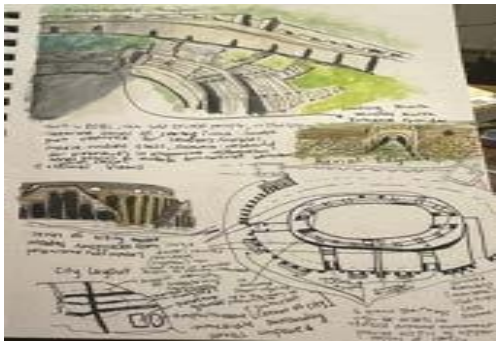

Fig. 1 – Illustrations/watercolors of the Pompeii Stadium and crowded subway stations.

My interest in the flux of people through urban environments led me to create a sculpture that could "move" through programmed LED lights using my engineering knowledge. I developed the concept of a fountain shape to symbolize the flow of people as "fluid" moving through the space of the physical sculpture. In addition, the shape of a fountain includes bottlenecks, which could be used to illustrate the bottlenecks at entrances to stairs or escalators, which I had observed in videos of large crowds moving through public spaces.

DOI: https://doi.org/10.59277/CLC/2024.12

Fig. 2 – A CNC machine to carve foam into bowl shapes and used paint-pouring techniques to create marbling textures. The final sculpture displays LED lights that repeat continuously in the Wilkinson building at Duke University.

The creation of the sculpture involved several processes and integration of physical sculpting and electrical engineering. First, I used a CNC machine to carve foam into large bowls and adhere them to a structural fountain centered around a metal lamp post. Then, using paint pouring techniques, I created a marbling effect on the sculpture to hide the texture/material of the foam. Then, using an Arduino microcontroller, I coded the dendritic shapes anticipated with constructal law into the LED lights placed on the structure. With consecutive lights flashing, the sculpture appears to flow upwards, creating an upward surge imagery that evokes power.

Through this process, I aim to help others visualize the flow of people through urban environments and spark conversation around the collective rhythms of society and the design of spaces where people live and move.

3. **CONCLUSION**

Art and science may seem like distinct disciplines, but interdisciplinary collaboration has significant value. For instance, visualization of scientific concepts and engineering designs can help create visual representations of scientific theories or communicate ideas to different audiences. Art can show beauty, efficiency, access, and freedom through the constructal law.

REFERENCES

1. Bejan A., *Freedom and Evolution: Hierarchy in Nature, Society and Science*, Springer, 2020.

CONSTRUCTAL LAW CONFERENCE – CLC2024
Design in Nature and Evolution
Romanian Academy, Bucharest, 10–11 October 2024

Proceedings of CLC2024
pp. 53–56

OPTIMAL DESIGN OF CONSTRUCTAL CONDUCTIVE PATHWAYS USING MACHINE LEARNING ALGORITHMS

MOHAMMAD REZA HAJMOHAMMADI[a]*, UMBERTO LUCIA[b], GIULIA GRISOLIA[c], MOHAMMAD GHAREKHANI[d]

[a] Amirkabir University of Technology (Tehran Polytechnic), Iran, Hajmohammadi@aut.ac.ir
[b] DENERG, Politecnico di Torino, Corso Duca degli Abruzzi 24, 10129 Torino, Italy, umberto.lucia@polito.it
[c] DIATI, Politecnico di Torino, Corso Duca degli Abruzzi 24, 10129 Torino, Italy, giulia.grisolia@polito.it
[d,a] Amirkabir University of Technology (Tehran Polytechnic), Iran, m.gharekhani@aut.ac.ir
*Correspondence: Hajmohammadi@aut.ac.ir;Tel. +9802164543427

Increasing the heat flux of future microchips requires implementing a reliable cooling system to reduce their operating temperatures. Researching better designs for high thermal conductivity pathways embedded into heat-generating components is also essential due to concerns about dimensions and costs. The present study investigates the Constructal design of highly conductive pathways embedded into a heat-generating piece using a numerical code based on finite element method (FEM) and an optimization process based on machine learning algorithms (MLAs). The inserted high thermal conductivity occupies a fixed volume fraction. Geometrical features of the highly conductive are considered the optimization variables, and minimization of the peak temperature is considered the optimization objective. To accomplish the optimization process, machine-learning algorithms are used and critically compared to determine the most efficient option among the considered ones. Finally, the optimal Constructal designs predicted by the machine-learning approach are compared with the optimal configurations generated by conventional methods.

Keywords: Constructal design; Machine learning; Optimization; Highly conductivity pathways; Electronic cooling.

1. INTRODUCTION

Microelectronic technology advances have enabled the miniaturization of dense electronic chip packages. However, miniaturization leads to increased heat generation and higher temperature, which can challenge microelectronic device operation. Conduction-based heat dissipation is among the prominent cooling methods for thermal management and efficient heat dissipation systems development. Bejan [1] proposed a new cooling method in 1997 using high thermal conductivity materials and tree-shaped channels, introducing the Constructal Theory fundamentals [2]. This led to further research by many researchers, including [3-5]. Combining machine learning (MLAs) with numerical analysis and data structures can accelerate analyzing and solving problems and save computational costs [6]. Many researchers have combined ML regression models and computational fluid dynamics (CFD) to conduct thermal analysis and optimize thermal systems [6]. Also, based on the Constructal Theory, researchers have applied ML methods to optimize the maximum temperature of studied cases [7]. The main objective of this study is to investigate the constructal design of highly conductive pathways embedded into a heat-generating piece using a numerical code based on finite element method (FEM) and an optimization process based on MLAs to reduce computational cost.

DOI: https://doi.org/10.59277/CLC/2024.13

2. MATERIALS AND METHODS

Figure 1(a) depicts the 2D heat-generating medium with $N = 4$ equal high thermal conductive branches (k_h) embedded in a low thermal conductive material (k_l). The medium generates heat at a uniform rate. The heat sink at a lower constant temperature (T_0) dissipates the heat, while the other outer surfaces are insulated. Figure 1(b) shows a brief flowchart of this study's machine learning algorithm-genetic algorithm (MLA-GA) method. A numerical simulation based on FEM is initially run on studied parameters to generate a dataset for training and testing the various MLAs. Different MLAs are analysed and compared using ML evaluation metrics, including regression coefficient R^2 and mean absolute error MAE, to determine the most suitable MLA for the dataset obtained from FEM. In the following, an optimization is implemented using the genetic algorithm GA to minimize the objective function ($\bar{T}_{max,min}$) based on the selected MLA. For various heights of the branch (H_j), the decision variables comprise the distance ratio of each branch from the origin ($\alpha_i = r_{i,j}/H_0$), and the length ratio of equal branches ($\beta = L_{1,j}/W_j$) with a fixed volume fraction ($\phi = A_h/(A_h + A_l)$).

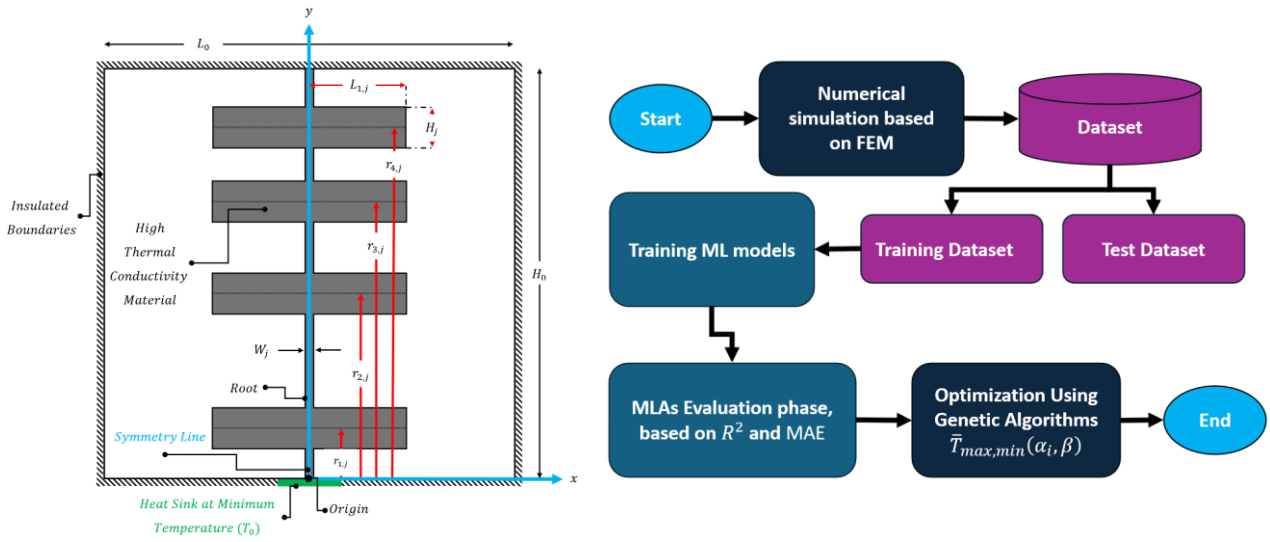

(a) (b)

Fig. 1 – (a) Schematic geometry of high conductivity pathways and coordinate system, (b) a flowchart of the methodology.

3. RESULTS

After comparing several ML models, it is found that for the present problem, the performances of Extra-trees regression model [8] are superior compared to other models. Therefore, the results in Fig. 2 and Tables 1 and 2, are based on the (complicated) function obtained by Extra-trees regression model and the GA optimization procedure that uses this function. Figure 2 illustrates (a) the effects of branch height at constant length ($L_{1,5}/L_0 = 0.46$) and (b) branch length at constant height ($H_5/H_0 = 0.05$) on $\bar{T}_{max,min}(\alpha_i, \beta)$ for various thermal conductivity ratios and, for $\phi = 0.2$.

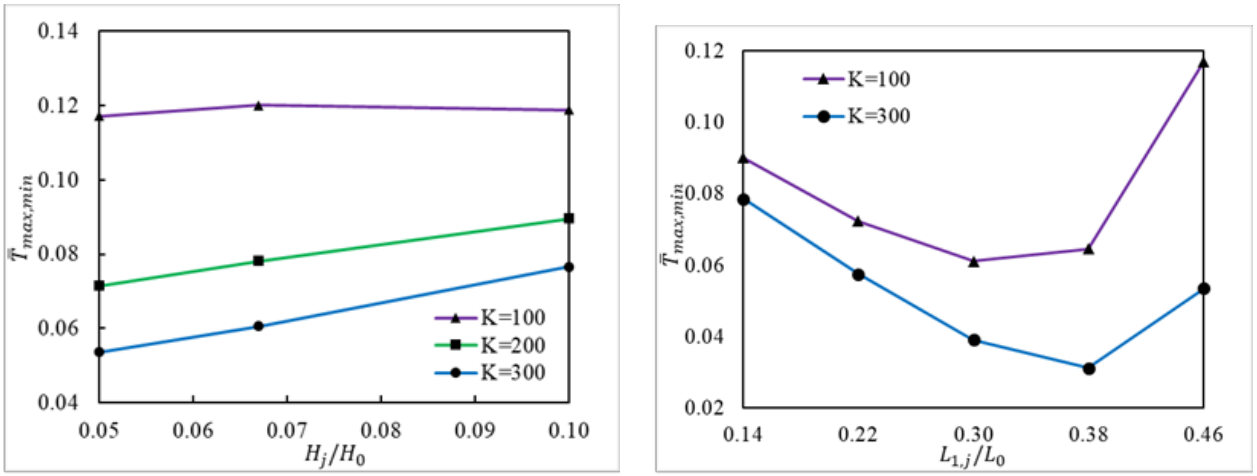

(a) (b)

Fig. 2 – The effects of (a) branch height at constant length and (b) branch length at constant height on $\bar{T}_{max,min}(\alpha,\beta)$.

Table 1 compares the predicted $\bar{T}_{max,min}(\alpha,\beta)$ values using the ML-GA method and those from previous studies for various thermal conductivity ratios at $\phi = 0.2$ and $H_5/H_0 = 0.05$.

Table 1

Comparison between the results of this study and previous works

K_h/k_l	Present Work	I-shaped [3]	Recursive Localization [4]	GA [5]
100	0.0612	–	0.0376	–
300	0.0312	0.0840	0.0222	0.0446

Table 2 presents the $\bar{T}_{max,min}$ values obtained using both the MLA and the FEM. The predicted results by the ML-GA method closely match the FEM results, for $K_h/K_l = 200$, $H_5/H_0 = 0.05$, and $L_{1,4}/L_0 = 0.38$.

Table 2

Comparing results predicted by ML-GA method and FEM

Parameter	**ML-GA**	**FEM**	**Deviation (%)**
$\bar{T}$	0.040512	0.040500	0.03

4. DISCUSSION AND CONCLUSIONS

The study utilized the MLAs-GA method to optimize the conductive pathways based on the Constructal Theory, aiming to reduce computational costs. The Extra-trees regression ML model shows good accuracy in predicting objective function values when compared with other MLAs using evaluation metrics on the dataset obtained from FEM. Also, the validity of the MLA-GA result based on the Extra-trees regression ML model is further confirmed with FEM.

REFERENCES

1. Bejan A., Constructal-theory network of conducting paths for cooling a heat generating volume, *International Journal of Heat and Mass Transfer*, **40**, pp. 799–816 (1997).
2. Bejan A., Lorente S., *Design with constructal theory*, John Wiley and Sons, Hoboken 2008.
3. Lui C.H.G., Fong N.K, Lorente S., Bejan A., Chow W.K., Constructal design for pedestrian movement in living spaces: Evacuation configurations, *Journal of Applied Physics*, **111**, *5*, p. 054903 (2012).
4. Hajmohammadi M.Reza, Rezaei E., Proposing a new algorithm for the optimization of conduction pathways based on a recursive localization, *Applied Thermal Engineering*, **151**, pp. 146–153 (2019).
5. Avendaño P.A., Souza J.A., Adamatti D.F., Construction of conductive pathways using Genetic Algorithms and Constructal Theory, *International Journal of Thermal Sciences*, **134**, pp. 200–207 (2018).
6. Mohammadpour J., Husain S., Salehi F., Lee A., Machine learning regression-CFD models for the nanofluid heat transfer of a microchannel heat sink with double synthetic jets, *International Communications in Heat and Mass Transfer*, **130**, p. 105808 (2022).
7. Liu X., Huijun F., Chen L., Ge Y., Design of a multi-scale cylindrical porous fin based on constructal theory, *International Communications in Heat and Mass Transfer*, **153**, p. 107352 (2024).
8. Simm J., de Abril I.M. Sugiyama M., Tree-Based Ensemble Multi-Task Learning Method for Classification and Regression, *IEICE Transactions on Information and Systems*, **E97.D**, *6*, pp. 1677–1681 (2014**)**.

CONSTRUCTAL LAW CONFERENCE – CLC2024
Design in Nature and Evolution
Romanian Academy, Bucharest, 10–11 October 2024

Proceedings of CLC2024
pp. 57–60

OPTIMIZING FORMATION FLIGHT *VIA* THE CONSTRUCTAL LAW

SAMUEL SAVITT

Duke University Dept. of Mechanical Engineering and Materials Science, 110 Science Dr, Durham NC, 27710
samuel.savitt@gmail.com

This paper explores 2 cases of flyers in formation: birds and aircraft, both seeking to save energy by flying in the wake of preceding flyers. The V-formation design occurs naturally with birds and is used in practice as a fundamental aircraft formation – aiming to boost lift/reduce induced drag felt by the flyers. The extent of the energy savings depends on the design configuration of the formation. The Constructal Law is applied to this formation flight problem to analyze how the distribution of drag among flyers in a V-formation is related to the optimal formation flight configuration. An analytical model that predicts this optimal configuration is developed and expressed regarding the fundamental formation parameters (velocity, number of aircraft, wingspan, weight, and air density).

Model results show that there is not a fixed optimal V-formation design for all formation systems. Instead, the optimal configuration adapts as parameters change. The optimal configuration becomes narrower as the flyers' speed and spacing increase. As the number of flyers increases, the optimal configuration approaches a finite maximum angle. Trends predicted by the model are substantiated by observations from nature, including those of birds, boats, and other wake-generating flow systems. In line with predictions of the Constructal Law, induced drag along the optimal V-formation is distributed as uniformly as possible among flyers (depending on the longitudinal spacing). The model suggests the formation flight system constantly evolves towards a state that maximizes collective access to energy savings by changing the formation design accordingly.

Keywords: Formation flight; Birds; Fighter jets; Aircraft; Constructal Law.

1. INTRODUCTION

Flyers rarely fly alone. Fighter jets have a "wingman" to assist in their mission and provide aerodynamic benefits. Birds have a natural advantage: they can "feel" what is most accessible as they fly. Thus, they will naturally fly in the optimal configuration (the configuration that uses the least energy). Birds naturally fly in a V-formation (figure 1a), and fighter jets use a nearly identical formation in practice called "fingertip" (Figure 1b) [1,2].

Fig. 1 – a) Flock of geese flying in a V-formation, credit: Birding World [3];
b) fighter jet aircraft flying in a V-formation, credit: 10th AF Public Site [4]

DOI: https://doi.org/10.59277/CLC/2024.14

The V-formation employs a concept known as "vortex surfing," trailing flyers benefit from the updraft of wingtip vortices trailing from the preceding flyers – boosting lift, reducing drag, and making flight easier [5,6]. Wieselsberger first suggested that the ideal V-formation among birds would provide an equal distribution of drag to maximize the collective energy savings of the flock [7]. For a fixed-wing flyer to maximize these benefits, it must be positioned at the ideal angle behind the leader. This paper models the V-formation design, defined by the V-angle α as shown in Fig. 2, to maximize energy savings and provide insight into predicting the natural optimal design for formation flyers.

This paper applies fundamental physics principles to this question, specifically the Constructal Law, which states that a flow system persists when it evolves to provide easier flow access to its currents [8]. The Constructal Law suits the formation flight problem well, as its application can lead to the prediction of nature and can be employed to predict the V-formation design at which birds fly. In this case, the formation flight configuration is a flow system of aerodynamic lift in which the induced drag is imperfection. The Constructal Law predicts that the optimal design is the configuration for which the imperfection is most evenly distributed across the system or the induced drag is equally partitioned among flyers in formation.

2. **THE OPTIMAL CONFIGURATION**

2.1. **Model Development**

The "optimal configuration" or "design" for formation flight maximizes energy savings by maximizing the boost in lift and corresponding reduction of induced drag. To determine the relationship between the formation flight configuration and the resulting energy savings, a theoretical model is developed for a flat-plane system of N fixed-wing flyers (in straight and level flight) with individual wingspan b, individual weight W, air density ρ, and formation velocity V_∞ in a V-formation configuration. The V-formation is parameterized with fixed lateral and longitudinal spacing coordinates x and y, respectively, as shown in Fig. 2 below.

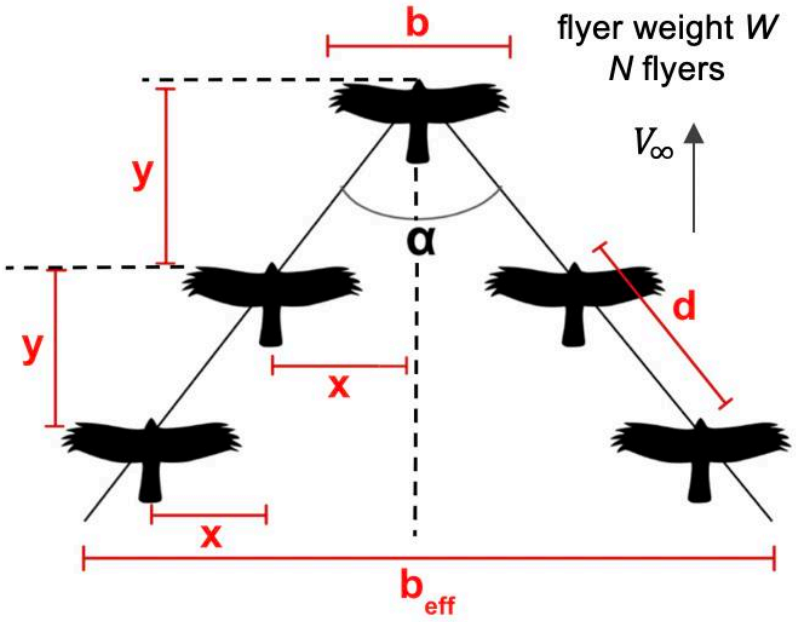

Fig. 2 – Fundamental V-formation design parameters.

Optimizing this design for maximal energy savings (minimal imperfection) yields the following model:

$$y_{opt} = \frac{2\pi\rho V_\infty^2}{NW}\left[(N-1)x_{opt}^3 + bx_{opt}^2\right]. \quad (1)$$

Since the relationship is nonlinear, no constant configuration optimizes the V-formation. Instead, the optimal configuration adapts to the variation of the formation system parameters, and the optimal flyers will evolve their formation to reflect this. To employ the model in equation 1 to find the optimal V-formation angle αopt, each (x_{opt}, y_{opt}) coordinate corresponds to a scenario-dependent nose-to-nose distance d, held constant in the V-formation. Given d, the corresponding (x_{opt}, y_{opt}) is determined from the model in equation 1, and then α_{opt} can be calculated geometrically.

2.2. **Analysis of the Optimal Design**

Analyzing the model in terms of the fundamental formation parameters provides greater insight into the model's accuracy and predictive applications to the real world. To determine trends between each parameter and the resulting optimal formation flight design, parameters d, V_∞, and N are computationally varied for an arbitrary aircraft and bird formation flight system. Beginning with nose-to-nose separation distance, the optimal V-formation becomes narrower as the flyers fly further apart. This trend aligns with experimental bird data from Williams, observing that Canada Geese fly narrower V-formations as the V-formation length increases [9]. This is likely due to an effort of the birds to distribute the induced drag as evenly as possible along the extended formation by remaining closer laterally, in line with the predictions of the Constructal Law.

Next, as V_∞ increases, the optimal configuration gets narrower. Therefore, the model suggests faster flyers fly narrower formations to maximize energy savings. Birds have also been observed to follow this trend, as bigger, faster birds tend to fly in narrower V-formations [9]. Boats display a similar phenomenon as their V-formation wakes become narrower with increasing speed.

Lastly, the optimal configuration model is evaluated for varying N flyers. This trend reveals an asymptotic relationship between optimal configuration and flyers. When there are few flyers ($N < 10$), the flyers should fly in a slightly wider formation as N increases to account for the broader divergence of the trailing wakes. However, for many flyers ($N > 10$), adding additional flyers has negligible impact on the wake geometry, leading to a constant optimal configuration angle.

3. **CONCLUSIONS**

To test the prediction of the Constructal Law of uniform distribution of drag (imperfection) in the optimal configuration, induced drag for each flyer in the formation is calculated. Results show that the induced drag force felt by the individual flyers varies very little (<6% body weight). Thus, in both cases, the flyers fly in the configuration that distributes the induced drag as evenly as possible among flyers – aligning with Constructal Law predictions. The effectiveness of this drag distribution is also primarily determined by the longitudinal spacing of flyers. However, in practice, the formation flight system can never achieve this perfect drag distribution because the induced drag consistently decreases along the V-formation, meaning the leading flyers will always work harder than the trailing flyers to maintain the V-formation. The Constructal Law also describes this inherent diversity in nature: No realistic optimal system can eliminate diversity and imperfection. Rather, its

design will constantly evolve to provide better access for its currents, as does the formation flight system seeking access to flight.

ACKNOWLEDGMENTS

I would like to thank my professor of Constructal Theory and Design in Nature, Adrian Bejan of the Duke University Mechanical Engineering and Materials Science Dept., for his mentorship and initial inspiration to pursue this project. I would also like to thank Dr. Kenneth Hall of the Duke Aeroelasticity Lab for his advice on aerodynamic theory. I would also like to acknowledge the people and funding that have made my travel and attendance at the Constructal Law Conference possible: Dean Carmen Rawls and Dr. Jessica Harrell with Duke's Undergraduate Research Support office, Dr. Linda Franzoni with Pi Tau Sigma, and Dr. Nico Hotz with the Duke MEMS department. Lastly, I am grateful to my family for making it possible to take on this project and encouraging me to pursue what I love.

REFERENCES

1. Heppner F. *et al*., Visual Angle and Formation Flight in Canada Geese (Branta canadensis), *The Auk: Ornithological Advances*, **102**, *1,* pp. 195–198 (1985).
2. T-34 Formation Knowledge Guide v1.2., *Fly Fast, Formation and Safety Team (FAST)* 2011, Available online: URL https://www.flyingsamaritans.net/Web/B2OSH/Pages/Training/T-34%20Formation%20Knowledge%20Guide%20v1.2.pdf (accessed on 20 March 2024).
3. *Why birds fly in a V-shaped formation (Image)*, Birding World 2024, Available online: URL https://birding-world.com/birds-fly-v-shaped-formation/ (accessed on 20 March 2024).
4. *10th AF Four Finger Formation (Image)*, Tenth Airforce Public Site 2007, Available online: https://commons.wikimedia.org/wiki/File:10th AF Four Finger Formation.PNG (accessed on 20 March 2024).
5. Lissaman P.B.S., Shollenberger C.A., Formation Flight of Birds, *Science*, **168** (3934), pp. 1003–1005 (1970).
6. Meng X. *et al*., Drag reduction analysis in close-formation flight, *International Council of Aeronautical Sciences*, 2021.
7. Wieselsberger C., Beitrag zur Erklärung des Winkelfluges einiger Zugvögel, *Zeitschrift für Flugtechnik und Motorluftschiffahrt*, **5**, pp. 225–229 (1914).
8. Bejan A., Constructal-theory network of conducting paths for cooling a heat generating volume, *Int J. Heat Mass Transfer*, **40**, pp. 799–816 (1996).
9. Williams T.C., Klonowski T. J., Berkeley, P., Angle of Canada Goose V flight formation measured by radar, *The Auk: Ornithological Advances*, **93**, *3*, pp. 554–559 (1976).

CONSTRUCTAL LAW CONFERENCE – CLC2024
Design in Nature and Evolution
Romanian Academy, Bucharest, 10–11 October 2024

Proceedings of CLC2024
pp. 61–64

QUANTUM MECHANICS – DETERMINISTIC *VS.* PROBABILISTIC

PETER VADASZ

Northern Arizona University, Peter.Vadasz@nau.edu
Peter.Vadasz@nau.edu

A deterministic quantum mechanics theory is presented. The proposed theory is shown to be consistent with the current mainstream statistical quantum theory as well as with classical physics. It produces solutions that demonstrate that causality, physical reality, and determinism are restored and can explain in simple form concerns raised by results from the current mainstream statistical quantum theory. The meaning of particle-wave duality and complementarity, the possibility of a particle, like an electron, crossing through the nucleus as it does when the angular momentum of the electron is zero at the ground state of the hydrogen atom, the possibility of a point-size particle to have an "intrinsic spin," the possibility of "quantum jumps" as the electron transitions instantaneously from one stable orbital to another without passing through the space in between the orbitals and does that at irregular time intervals. The natural collapse of the wave function as part of the solution is a result that emerges from the proposed deterministic quantum mechanics theory. The phenomenon of entanglement is also discussed in the context that information transfer between entangled "particles" does not occur in a superluminal fashion and is not a "spooky action at a distance" but rather the local measurement of global property. A linear stability method presents actual analytical solutions consistent with current mainstream quantum theory and classical physics. The Bohr-Schrödinger energy levels leading to the experimentally confirmed spectral lines and the fine structure constant emerge from an approximate solution to these equations.

Keywords: Deterministic quantum mechanics; Statistical quantum mechanics; Intrinsic spin; Quantum jumps.

1. INTRODUCTION

Bohr [1–3] in his planetary model of the atom introduced the postulate indicating that the electron radiates only as it moves from one stable orbit to another stable orbit but can never pass through the space between these orbits during these "jumps". This postulate was accepted and retained in the modern quantum theory represented by the Schrödinger [4] and Dirac [5] equations. Recent experimental evidence provided by Minev *et al.* [6] revealed that the electron does move in the space between the orbitals by "catching and reversing a quantum jump mid-flight". Vadasz [7,8] presents via a deterministic interpretation of quantum mechanics details that show how the equations governing a continuously distributed mass, such as an inviscid compressible fluid, convert into the Schrödinger equation subject to a certain condition. In addition, the Bohr-Schrödinger energy-levels leading to the experimentally confirmed spectral lines, as well as the fine structure constant emerge from an approximate solution to these equations[14]. The analysis of the properties of these governing equations reveals a realistic interpretation of quantum mechanics that is consistent with the current results from the probabilistic interpretation as well as with classical physics concepts and simple common sense.

2. RESOLVING CLASSICAL PHYSICS VIOLATIONS

The proposed interpretation of quantum mechanics here follows Vadasz [7,8], introducing only one postulate, which states that the electron and, most likely, other quantum (sub-atomic) particles consist of continuously distributed masses and behave like inviscid compressible fluids. They possess mass density

DOI: https://doi.org/10.59277/CLC/2024.15

$\rho(\boldsymbol{x},t)\left[\text{kg/m}^3\right]$, and if they are charged particles like electrons, they possess electric charge density, too $\rho_q(\boldsymbol{x},t)\left[\text{C/m}^3\right]$, which is allowed to vary in space and time. Then, one can define the center of mass of the electron-fluid $\boldsymbol{x}_{cm}$ in the form of the "quantum particle"

$$\boldsymbol{x}_{cm} = \int_{\tilde{V}_o} \rho(\boldsymbol{x},t)\boldsymbol{x}\,\mathrm{d}\tilde{V} \Big/ \int_{\tilde{V}_o} \rho(\boldsymbol{x},t)\,\mathrm{d}\tilde{V}, \tag{1}$$

where the electron-mass contained in the volume $\tilde{V}_o$ is the denominator in equation (1), and it is therefore constant. For one electron system this is $m_e = \int_{\tilde{V}_o} \rho(\boldsymbol{x},t)\,\mathrm{d}\tilde{V} = \text{const.}$, where m_e is the mass of the electron. Representing the wave function in the general form $\psi = \rho^{1/2}\,\mathrm{e}^{iS(x,t)/\hbar}$; $\psi^* = \rho^{1/2}\,\mathrm{e}^{-iS(x,t)/\hbar}$ yields the probability density function $r(\boldsymbol{x},t)$, as $r(\boldsymbol{x},t) = |\psi(\boldsymbol{x},t)|^2 = \psi\psi^*$. The expectation of finding the electron (or a subatomic particle) at a position $\boldsymbol{x}$ within a volume $\tilde{V}_o$ (e.g. in Cartesian coordinates $\boldsymbol{x} = x\hat{\boldsymbol{e}}_x + y\hat{\boldsymbol{e}}_y + z\hat{\boldsymbol{e}}_z$, where $\hat{\boldsymbol{e}}_x, \hat{\boldsymbol{e}}_y, \hat{\boldsymbol{e}}_z$ are unit vectors in the x, y, z directions, respectively) is

$$\langle \boldsymbol{x} \rangle = \int_{\tilde{V}_o} \psi\,\boldsymbol{x}\,\psi^*\,d\tilde{V} \Big/ \int_{\tilde{V}_o} \rho(\boldsymbol{x},t)d\tilde{V} = \int_{\tilde{V}_o} \rho(\boldsymbol{x},t)\boldsymbol{x}\,d\tilde{V} \Big/ \int_{\tilde{V}_o} \rho(\boldsymbol{x},t)d\tilde{V}, \tag{2}$$

where $\tilde{V}$ represents the volume. From comparing equations (1) and (2) it becomes evident that the expectation of finding the electron (or any subatomic particle) at a position $\boldsymbol{x}$ within a volume $\tilde{V}_o$ according to the probabilistic interpretation of quantum mechanics is identical to the position of the center of mass of the electron-fluid (subatomic-fluid) according to a deterministic interpretation, *i.e.*, $\boldsymbol{x}_{cm} = \langle \boldsymbol{x} \rangle$. Therefore we can decide to define the center of mass of the *"quantum-fluid"* as the *"quantum particle"*.

Wave-Particle Duality: With this definition it becomes clear how a wave associated with the "quantum-fluid" can be represented by a "quantum-particle" associated with the center of mass of the "quantum-fluid".

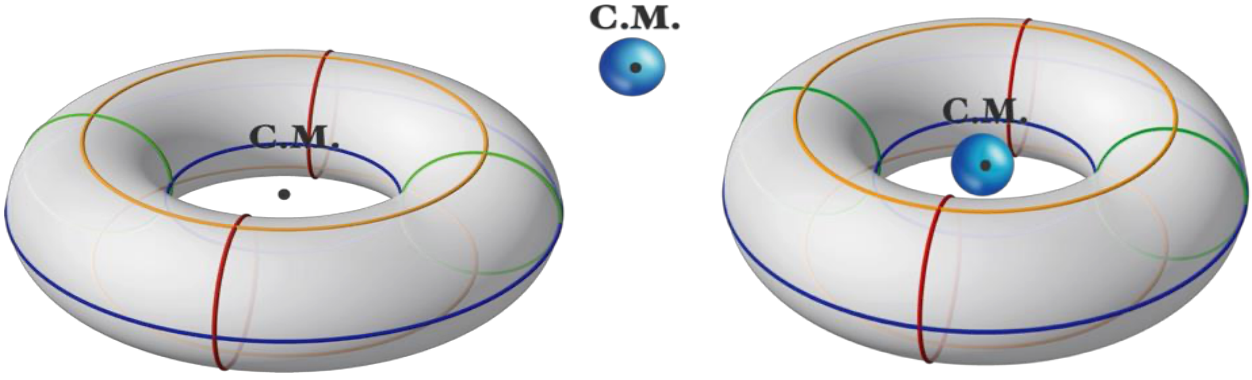

(a) (b)

Fig. 1 – (a) A torus and a sphere separated; (b) a torus and a sphere sharing the same center of mass, without touching each other.

Instantaneous Collocation: With this definition and interpretation of "quantum-particle" it becomes already clear how two particles can be found in the same region of space at the same time without having any parts of the matter (physical objects) even contacting each other. This is just the same as a small solid sphere concentrically located in the center of a larger solid torus as presented in Fig. 1b. No material from the sphere is touching the torus but their centers of mass are in the same location in space at all times.

An approximate solution of the equations governing the motion of the continuously distributed mass applicable to the hydrogen atom produced the following graphical representation [7,8], as presented in Fig. 2. The solution obtained for the azimuthal electron mass density distribution and its variation in time was integrated to evaluate the motion of its center of mass. The azimuthal electron mass density distribution and its variation in time are presented in Fig. 2. The electron-particle motion overlaps the electron-fluid motion presented as a density plot of the mass density solution on an annulus in the j direction. Figure 2 shows that the electron-fluid performs an "embracing" motion as its differential elements repel each other in the j same direction.

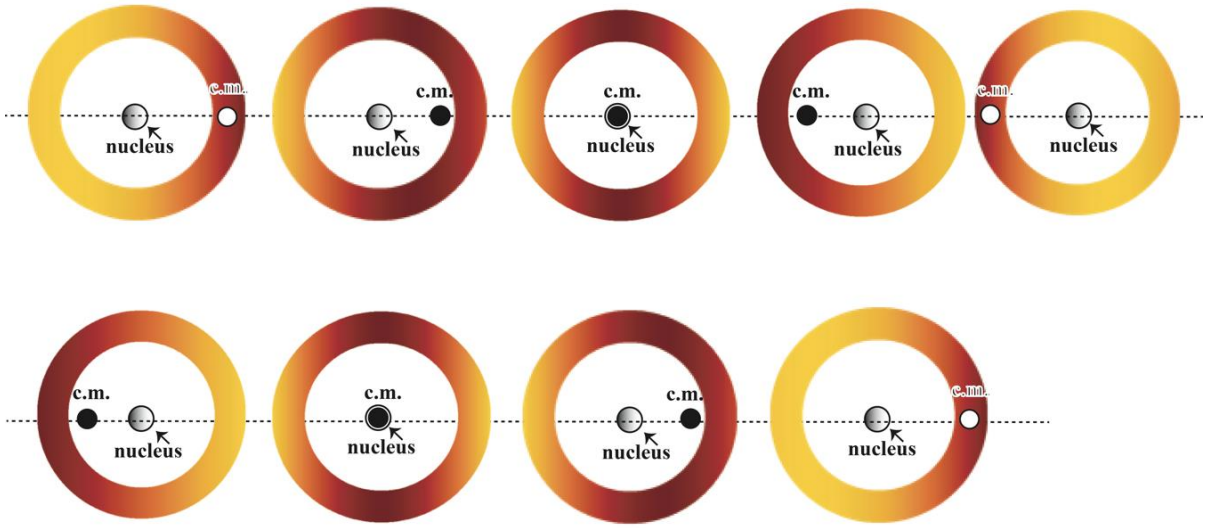

Fig. 2 – The electron-particle motion (center of mass) overlapping the electron-fluid motion presented as a density plot on an annulus in the j direction (Vadasz [7,8]).

At the same time, the electron-particle (center of mass) follows a horizontal motion from one side of the annulus to the other and back horizontally. The third and seventh of the annuli in Figure 3 show the electron-particle located at the center of the nucleus, while the electron-fluid is always outside the nucleus. Additional results related to quantum jumps that are identified as shock waves, intrinsic spin, wave function collapse, quantum tunneling, and quantum entanglement will be presented, too.

REFERENCES

1. Bohr N., On the constitution of atoms and molecules, Part I: Binding of electrons by positive nuclei, *Philosophical Magazine*, **26**, pp. 1–24 (1913).

2. Bohr N., On the constitution of atoms and molecules, Part II: Systems containing a single nucleus, *Philosophical Magazine*, **26**, pp. 476–502 (1913).
3. Bohr N., On the constitution of atoms and molecules, Part III: Systems containing several nuclei, *Philosophical Magazine*, **26**, pp. 857–875 (1913).
4. Schrödinger E., *21 Collected Papers on Wave Mechanics*, New York, Chelsea Publishing Company, 1982.
5. Dirac P.A.M., The quantum theory of the electron, *Proceedings of the Royal Society A: Mathematical, Physical, and Engineering Sciences*, **117** (778), pp. 610–624 (1928).
6. Minev Z.K., Mundhada S.O., Shankar S., Reinhold P., Gutiérrez-Jáuregui R., Schoelkopf R.J., Mirrahimi M., Carmichael H.J., Devoret M.H., To catch and reverse a quantum jump mid-flight, *Nature*, **570**, pp. 200–204 (2019).
7. Vadasz P., Deterministic Quantum Mechanics – Part I – Conceptual Framework, to be submitted for publication, 2024.
8. Vadasz P., Deterministic Quantum Mechanics – Part II – The Linearized Temporal-Azimuthal Wave Solution, to be submitted for publication, 2024.

CONSTRUCTAL LAW CONFERENCE – CLC2024
Design in Nature and Evolution
Romanian Academy, Bucharest, 10–11 October 2024

Proceedings of CLC2024
pp. 65–68

CONSTRUCTAL LAW AND THE OGP OPTIMAL GLOBAL PRICING TECHNOLOGY

SERAFIM GREGORY SCURTU[a], MIRCEA SCURTU[b]

[a]Johns Hopkins University, USA
[a]OGT – Optimal Global Technologies LLC, America
greg.scurtu@gmail.com, +1 919 323 5393, mitch.scurtu@optimalglobalpricing.com

The document discusses the integration of physics with economics through OGP technology and its application in resolving market arbitrage in various industries.

Keywords: Electrical circuits equilibrium; Economic systems equilibrium; Optimal solutions.

1. INTRODUCTION

The document discusses the integration of physics with economics through OGP (Optimal Globalization Prizing) technology, which aims to resolve market arbitrage and enhance economic equilibrium. Key points include: *OGP Technology:* A mathematical formulation for global economic transactions, incorporating transactional resistance to allow free evolution and increased access to transactions.

Components:

Economic equilibrium problem

Computational engine from Stanford University

Finitely converging algorithm developed through research at NCSU

Applications:

Resolving market arbitrage, particularly in the pharma industry, which faces $100-$200 billion in parallel trade annually. Addressing issues like optimal launch pricing, inter-regional and inter-temporal competition, trade and tariff arrangements, and market simulations.

Results: OGP technology can convert nonproductive capital from market arbitrage into productive capital for producers and consumers, addressing bottlenecks in global medicine launches and pricing.

Conclusion: OGP is a pioneering approach contributing to economic globalization by resolving market distortions and enhancing global trade efficiency.

The document also references various academic works that support the theoretical and empirical foundations of OGP technology.

2. MATERIALS AND METHODS

OGP (Optimal Globalization Prizing) technology integrates physics with economics by applying principles from physics, such as equilibrium and resistance, to economic systems. Specifically, it uses a

DOI: https://doi.org/10.59277/CLC/2024.16

mathematical formulation to model global economic transactions, incorporating the concept of transactional resistance to allow for free evolution and increased access to what flows. This approach helps resolve market arbitrage and enhance economic equilibrium.

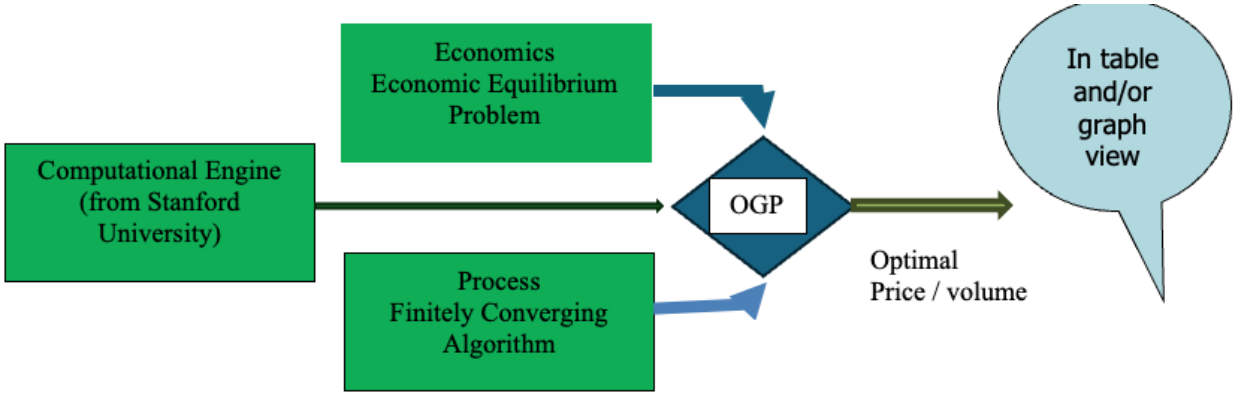

Fig. – Structure of the OGP technology with components 'Economic Equilibrium Problem' 'Computational Engine from Stanford University' 'Finitely Converging Algorithm'. Optimal Price / volume solutions is presented in graph and table format.

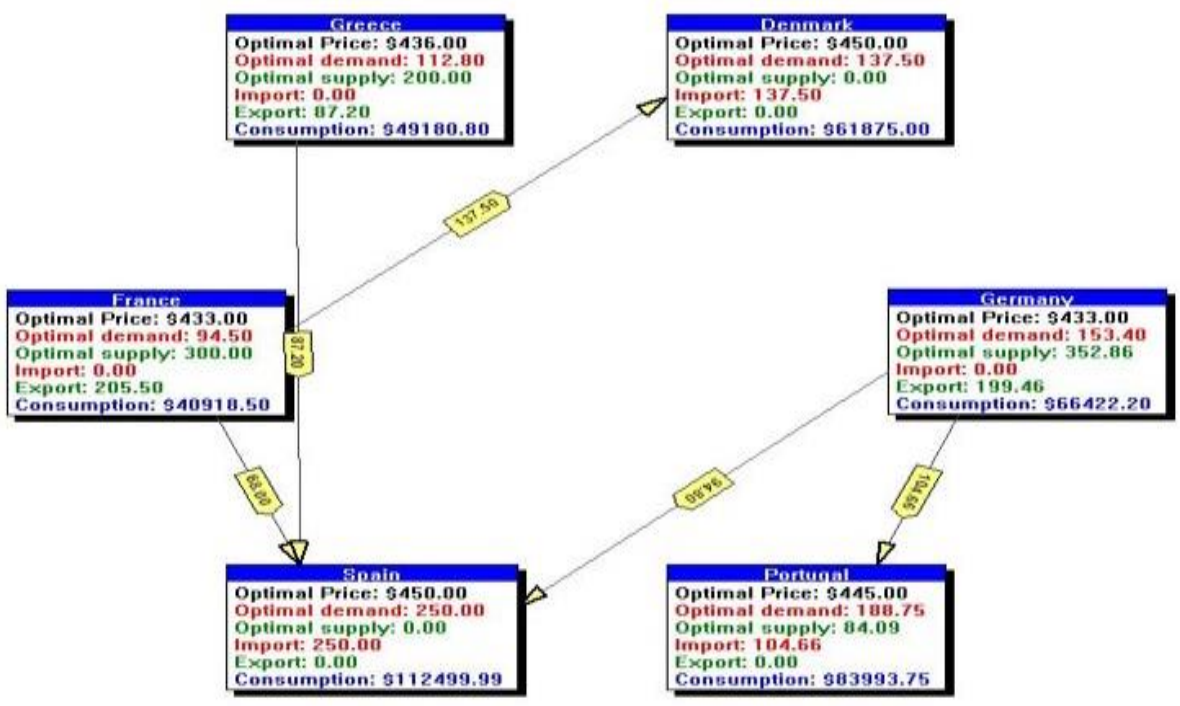

Fig. 2 – Example of an Optimal Solution in graph format: Optimal Price, Optimal Demand, Optimal Supply, Import, Export, Consumption, Trade Flows in directed arrows from-to and amounts traded in the yellow tags.

3. **RESULTS**

OGP technology addresses market arbitrage in the pharma industry by converting nonproductive capital, which exploits global price differentials, into productive capital for producers and consumers. It resolves issues such as parallel trade, which amounts to

$100–$200 billion annually, by containing transaction resistance and optimizing launch pricing, inter-regional and inter-temporal competition, and trade and tariff arrangements. This approach helps eliminate bottlenecks in global medicine launches and pricing, ultimately enhancing economic equilibrium and efficiency in the pharma industry.

OGP is resolving a host of marketing problems with presently inadequate solutions:

- containing resistance to flow (resolving the parallel trade problem)
- optimal launch pricing
- evaluating inter-regional and inter-temporal competition
- evaluating alternative trade and tariff arrangements
- evaluating policies combining different levels of quotas, tariffs, export taxes, exchange rates
- simulating producing and consuming markets with various levels of minimum reserve requirements, processing costs, retail markup margins, and minimum prices.
- supporting other pricing and trade-related activities

4. **DISCUSSION AND CONCLUSIONS**

OGP technology resolves market arbitrage by:

Converting Nonproductive Capital: It transforms capital that exploits global price differentials into productive capital for producers and consumers.

Containing Transactional Resistance: Incorporating the concept of transactional resistance allows for free evolution and increased access to transactions.

Optimizing Launch Pricing: It helps determine optimal pricing strategies for new product launches.

Evaluating Competition: It assesses inter-regional and inter-temporal competition to ensure fair pricing and distribution.

Optimizing Trade and Tariff Arrangements: It evaluates and optimizes trade policies, tariffs, quotas, export taxes, and exchange rates.

Simulating Markets: It simulates producing and consuming markets with various levels of minimum reserve requirements, processing costs, retail markup margins, and minimum prices. What are the applications of OGP technology in other industries? OGP technology has applications in various industries beyond pharma. In addition to the features above, other features *Inter-Regional and Inter-Temporal Competition, Which Evaluates* competition across different regions and time periods.

Supporting Pricing and Trade Flows: Facilitating activities related to pricing and trade flows in various industries.

These applications help resolve market arbitrage, enhance economic equilibrium, and improve efficiency in global trade.

REFERENCES

1. Scurtu M., Aplicarea teoriei elasticității din fizică la studiul ciclurilor economice ale unei economii de piață la nivel macroeconomic, Academia de Studii Economice, Facultatea Relații Economice Internaționale, edițiile XIX, XX, Sesiunile Cercurilor Științifice Studențești, Aprilie 1975, 1976, Rector.

2. Scurtu M., An Empirical Study of Spatial Economic Equilibria via Geometric Programming, Doctoral Thesis, North Carolina University, Raleigh, USA, 1986.
3. Bejan A., *Freedom and Evolution. Hierarchy in Nature, Society, and Science*, Springer, 2020.
4. Bejan A., *The Physics of Life: The Evolution of Everything*, St. Martin's Press, 2016.
5. Fang S.C., Peterson E.L., Generalized Variational Inequalities, *Journal of Optimization Theory and Applications*, **38**, *3*, pp. 363–383 (1982).
6. General Network Equilibrium Analysis, *International Journal of Systems Science*, **14**, *11*, pp. 1249–1275 (1983).
7. An Economic Equilibrium Model on a Multi-commodity Network, *International Journal of Systems Science*, **16**, *4*, pp. 479–490 (1985).
8. Irwin C.L., Yang W.C., Iteration and Sensitivity for A Spatial Equilibrium Problem with Linear Supply and Demand Functions, *Operations Research*, **30**, *2* (1982).
9. King R.A., Gunn J., Reactive Programming User Manual: A Market Simulating Spatial Equilibrium Algorithm, Economic Research Report, No. 43, Dept. Of Ec. & Bus. NCSU Raleigh N.C., Dec 81.
10. McCarl B.A. et al., Sebend: A computer Algorithm for the Solution of Symmetric Multi-commodity spatial Equilibrium Problems Utilizing Benders Decomposition, Special Report 708, Agricultural Experiment Station Oregon State University, March 1984.
11. The Conical Duality and Complementarity of P and Quantity for Multi-commodity Spatial and Temporal Network Allocation Problems, Center For Math. Studies in Economics and Management Science: Disc, Paper #207, Northwestern University, Evanston, 111, March 1976.
12. Peterson E.L., Eaves B.C., Asmuth R., Computing Economic Equilibria on Affine Networks with Lemke's Algorithm, *Mathematics and Operations Research*, **4**, *3*, pp. 209–214 (1979).
13. O'Rourke A.D., Casavant K.L., Interregional and Intertemporal Competition in Fresh Sweet Cherries, College of Agriculture Research Center, Washington State University, Bulletin 803, November 1974.

CONSTRUCTAL LAW CONFERENCE – CLC2024
Design in Nature and Evolution
Romanian Academy, Bucharest, 10–11 October 2024

Proceedings of CLC2024
pp. 69–72

INVESTIGATION OF PHASE CHANGE MATERIAL WITH/WITHOUT ALUMINIUM PLATE FOR BATTERY THERMAL MANAGEMENT

UMUT EGE SAMANCIOĞLU[a], ERDAL ÇETKIN[a*]

[a] Izmir Institude of Technology, Türkyie
umutsamancioglu@iyte.edu.tr and erdalcetkin@iyte.edu.tr
*Correspondence: erdalcetkin@iyte.edu.tr; Tel. +90 232 750 6713

Concerns about global warming related to carbon emissions increased interest in electric vehicles (EVs). The current EV technology requires development on fast charging and battery lifetime increment, which require strict temperature control. This study investigated the effectiveness of implementing phase change material (PCM) for battery thermal management with/without an aluminum plate. Initially, a 73 Ah NMC pouch cell was discharged in an insulated environment at a 1°C rate to record the behavior of the battery. Then, a PCM pack is inserted into the cell during discharge. Finally, an aluminum plate with 0.5 mm thickness is inserted between the battery and the PCM pack to uncover the effect on the thermal behavior.

To reveal the impact of the experiments, temperature measurements are taken from the upper surface (near positive and negative tabs) and bottom surface of the battery. Results show that the maximum temperature decreases, and temperature uniformity increases with PCM (with/without an aluminum plate) relative to the base case. The temperature difference between the two sides of the battery was measured as 4.3°C, 1.1°C, and 1.2°C for the base case, with the PCM pack and the PCM pack and aluminum plate, respectively. Even though the net temperature differences do not reflect the increased temperature homogeneity achieved with the added aluminum plate, the data set is helpful. In the end, the results of these experiments successfully demonstrated that using PCM is helpful in the thermal management of batteries and that using conductive layers can improve the battery's thermal uniformity.

Keywords: Battery thermal management; Phase change materials; Passive cooling.

1. INTRODUCTION

Electric vehicles (EVs) can reduce the greenhouse gasses produced by internal combustion engine (ICE) vehicles [1]. If electricity is generated from renewable sources, these emissions can be decreased to zero, increasing interest in EVs [2]. Li-ion batteries are preferred due to their high energy density, low self-discharge, and long life cycle [2,3].

Dis/charge of Li-ion batteries generates heat, which must be managed to keep the batteries in their optimal working range of 15°C – 35°C [4], which requires battery thermal management systems (BTMS). BTMSs can be categorized as active or passive systems. Active systems rely on pumps and compressors for convective cooling. Passive systems rely on natural convection or phase change [5,6]. PCMs gained interest because of their ability to keep the environment near isothermal conditions during phase change [7]. In this study, we aim to show the effectiveness of utilizing PCM for passive cooling and incorporating high thermal conductance materials with PCM.

2. MATERIALS AND METHODS

A 73 Ah NMC pouch cell was placed in an insulated container and discharged at 1C rate (73 Ah) using BK Precision 8614 programmable electronic load for three distinct setups as, without any PCM

DOI: https://doi.org/10.59277/CLC/2024.17

(base case), with PCM pack (265×103×2.5 mm) and with aluminum plate (Al) (265×103×0.5 mm) and PCM pack. A HIOKI-LR8431-20 datalogger was used for temperature (9 channels) and voltage (1 channel) measurements.

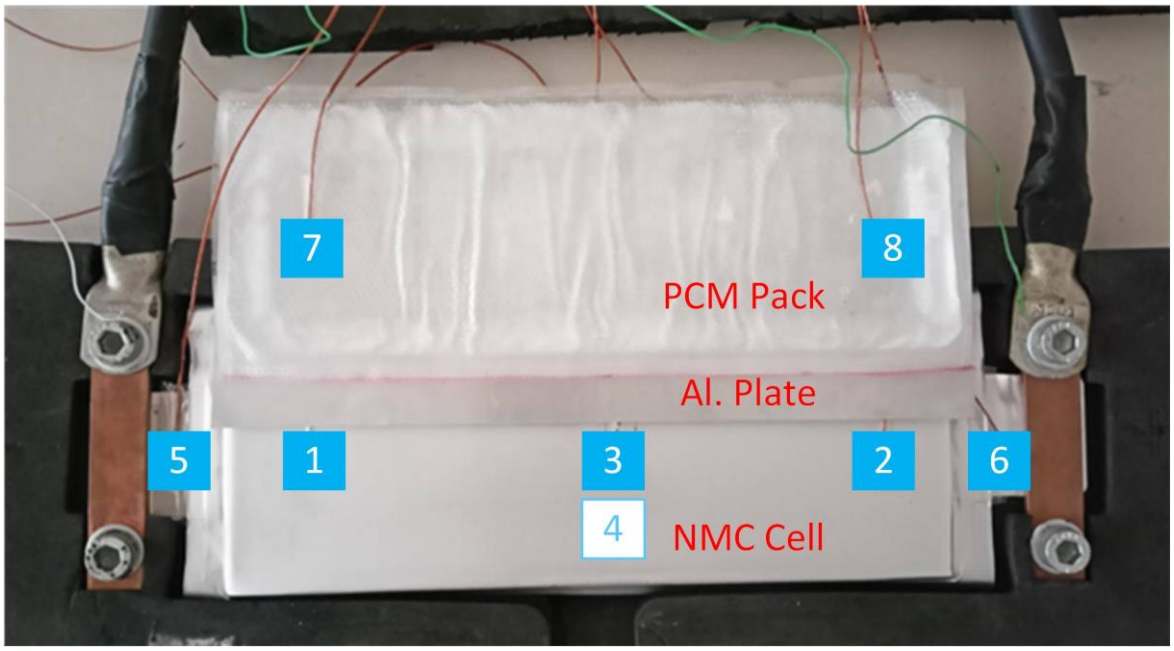

Fig. 1 – Experimental setup and thermocouple placement.

Figure 1 shows the location of thermocouples where temperatures are measured and documented for locations 1 (upper negative side), 2 (upper positive side), and 4 (bottom), which are plotted and used for uncovering the performance of the experimented methods.

3. **RESULTS**

Figure 2 shows temperature variation in time for locations 1 and 2.

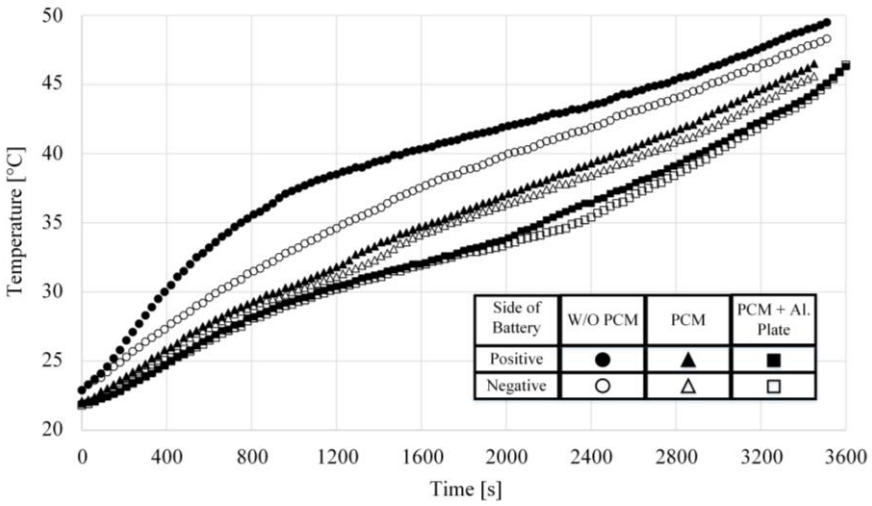

Fig. 2 – Temperature measurements from points 1 and 2.

The end-of-discharge temperatures for point 2 were recorded as 49.5°C, 46.5°C, and 46.3°C for the base case, with PCM, and with PCM + Al-plate, respectively. Differences between the two sides of the battery were measured as 4.3°C, 1.1°C, and 1.2°C in the same order.

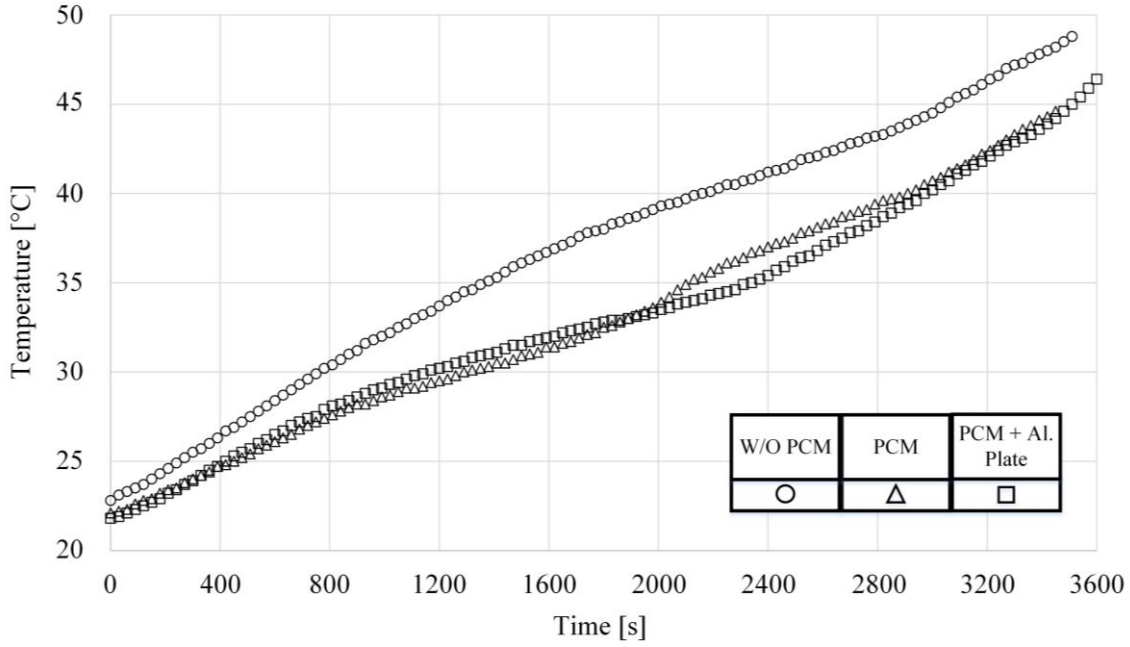

Fig. 3 – Temperature measurements from point 4.

Even though the temperature variation across the battery is in the same order for PCM pack cases, there is a more homogenous distribution for PCM + Al-plate case.

Figure 3 shows the temperature variation for point 4 (bottom/insulation side of the battery). It shows that the cell temperature decreases for PCM cases compared to the base case: 3.3°C decrease at the end of discharge.

4. **DISCUSSION AND CONCLUSIONS**

Figure 2 shows a clear decrease in temperature from the base case for both passive cooling methods, with a slight but distinct improvement in temperature uniformity benefitted from the Al plate. Figure 3 represents a similar improvement in cell temperature reduction with passive cooling methodologies compared to the base case, with a 3.8°C reduction in cell temperature.

The experiments conducted successfully present the possibility of improving battery thermal management with PCMs. A clear reduction in temperature increment is achieved, which proves that the improvement is not limited to the conditioned surface but affects the entire cell.

REFERENCES

1. Jouhara H., Olabi A.G., Editorial: Industrial Waste Heat Recovery, *Energy*, **160**, pp. 1–2 (2018).
2. Jaguemont J., Boulon L., Dubé Y., A Comprehensive Review of Lithium-Ion Batteries Used in Hybrid and Electric Vehicles at Cold Temperatures, *Appl. Energy*, **164**, pp. 99–114 (2016).

3. Wu W., Wang S., Wu W., Chen K., Hong S., Lai Y., A Critical Review of Battery Thermal Performance and Liquid Based Battery Thermal Management, *Energy Convers. Manag.*, **182**, pp. 262–281 (2019).
4. Bandhauer T.M., Garimella S., Fuller T.F., A Critical Review of Thermal Issues in Lithium-Ion Batteries, *J. Electrochem. Soc*., **158**, *3*, R1 (2011).
5. Iqbal U., Ali M., Khalid H.A., Waqas A., Mahmood M., Ahmed N., Shahzad N., Iqbal N., Mehboob K., Experimental Study to Optimize the Thermal Performance of Li-Ion Cell Using Active and Passive Cooling Techniques, *J. Energy Storage*, **70**, p. 108013 (2023).
6. Alaoui C., Passive/Active BTMS For EV Lithium-Ion Batteries, *IEEE Trans. Veh. Technol*., **67**, *5*, 3709–3719 (2018).
7. Khan M.M., Alkhedher M., Ramadan M., Ghazal M., Hybrid PCM-Based Thermal Management for Lithium-Ion Batteries: Trends and Challenges, *J. Energy Storage*, **73**, p. 108775 (2023).

CONSTRUCTAL LAW CONFERENCE – CLC2024
Design in Nature and Evolution
Romanian Academy, Bucharest, 10–11 October 2024

Proceedings of CLC2024
pp. 73–74

DISTINGUISHING MOTION AND WORK IN MECHANICS AND ENGINEERING THERMODYNAMICS

TERRY BRISTOL

Portland State University
1825 SW Broadway, Portland, OR 97201, USA
bristol@isepp.org

To fully appreciate Bejan's engineering thermodynamics, it is important to distinguish it from the Clausius, Boltzmann, Gibbs (CBG) mechanical rendering of thermodynamics. Concepts of motion and work occur in both formulations but have different meanings.

The aim here will be to distinguish Bejan's concepts from CBG's classical mechanical exposition. The latter reason is classical Newtonian mechanics. Focusing on motion and work also allows us to trace the historical antecedents of Bejan's thermodynamics, including the contributions of Lazare and Sadi Carnot.

1. INTRODUCTION

To fully appreciate Bejan's engineering thermodynamics, it is important to distinguish it from the Clausius, Boltzmann, Gibbs (CBG) mechanical rendering of thermodynamics. Concepts of motion and work occur in both formulations but have quite different meanings in each.

The aim here will be to distinguish Bejan's concepts from CBG's classical mechanical exposition. The latter reasons in terms of classical Newtonian mechanics. Focusing on motion and work also allows us to trace the historical antecedents of Bejan's thermodynamics, including the contributions of Lazare and Sadi Carnot.

That there were two versions of thermodynamics from nearly the beginning is evident from Clausius's comments. First noting that "[Carnot] says expressly that no heat is lost in the process [when work is produced], and [Carnot] adds, "This is a fact which has never been disputed; it is first assumed without investigation, and then confirmed by various calorimetric experiments. To deny it, would be to reject the entire theory of heat, of which it forms the principal foundation." Clausius then completely rejects Sadi's 'principal foundation' in favor of a mechanical interpretation: "I am not, however, sure that the assertion, that in the production of work a loss of heat never occurs, is sufficiently established by experiment. Perhaps the contrary might be asserted with greater justice."

It is not difficult to imagine that Clausius and Carnot might be speaking in two different conceptual languages. Clausius is talking about 'mechanical work' while Sadi is talking about 'engineering work'. Clausius sees the driving force as declining as mechanical work is produced. Carnot does not see heat as a mechanical driving force but as a 'living force' that is always conserved. Sadi's 'principal foundation' is the conservation of living force.

Clausius needed to resolve the difference between the conservation of mechanical energy and the decline in the potential to perform work. Mechanical energy is conserved as is required by the presuppositions of rational mechanics. And yet the 'potential to perform work', another common definition of energy, declines as work is performed. In his Second Law, Clausius introduces the novel term 'entropy' to represent 'the potential to perform work', a non-symmetric, non-conservative change. There is no Second Law in Carnot's engineering thermodynamics. One characteristic of Bejan's engineering thermodynamics is that entropy is eliminated. The non-symmetric, non-conservative irreversibility of change is newly understood as the constructive generation, the design evolution, of reality's dynamic structures and functions.

From a general overview the differences between CBG and Bejan's engineering thermodynamics can be seen in the nexus of concepts associated with each. The nexus of interconnected concepts in classical mechanics centers on force, mass, and motion, conservation of energy and time-reversibility. With the CBS mechanical thermodynamics entropy and the principle of least action are added. The concept of work is not a 'natural' concern in classical mechanics. Global change is simply a continual directionless re-arrangement of atoms. Even in CBG thermodynamics, at least since Boltzmann, the entropy of the universe can increase to its maximum without any work having been performed.

The nexus of interconnected concepts in Bejan's engineering thermodynamic centers on flow, design evolution (replacing entropy), the principle of optimality (replacing the principle of least action) and purposeful engineering work. Most distinct from the nexus of the mechanical framework are Bejan's concepts of freedom,

DOI: https://doi.org/10.59277/CLC/2024.18

choice, and purpose. Per hypothesis, in engineering thermodynamics work is understood to result in design evolution. Work embodies the generation of the recursively enabling dynamic structures and functions of reality.

In an earlier presentation at CLC23 I followed Bejan's 'clue' that in engineering thermodynamics ' is by finite-size steps that occur in finite-times. Bejan strongly rejects the reality of infinitesimals. Historically, there are two ways of reasoning about infinitesimals. Analytic calculus argues for completed infinitesimals. For instance, the area of a circle, or the area under a curve, can be found by taking the sum or integral of an infinity of infinitesimal linear constructions. The early Greeks shared Bejan's 'horror of infinitesimals'. Archimedes reasoned in terms of two opposite finite processes, inscribing and circumscribing the circle with polygons with an increasing number of sides. The steps in each process were always incomplete. He expressed the area of the circle as a ratio of these two converging but incomplete sequences.

The problem with the completed infinitesimal reasoning characteristic of analytic calculus is that it claims to express the area of a circle in terms of linear constructions. In effect this erases the real conceptual difference between lines and circles. In terms of motion, it erases the difference between translational and rotational motion. In Greek physics as in Bejan's engineering thermodynamics the conceptual difference of translational and rotational components of 'change' is preserved. Consequently, all 'real' motion has an irreducible component of both the translational and rotational. Erasure of the difference between conceptual 'opposites' is at the heart of the difference between mechanical and engineering thermodynamic conceptions of motion and work.

The paradigm of mechanical motion is Newton's straight-line motion that proceeds by infinitesimal linear steps. The rotational component is not even addressed in Newton's three laws. The experienced features of rotational motion, such as the force felt when turning a corner travelling in an automobile, has sometimes been referred to in classical mechanics as due to a 'fictional' force. This because such experiences of rotational forces, cannot be reduced to or made sense of in terms of linear forces. Force in mechanical is literally defined as linear in Newton's three laws.

In classical mechanics composite motion, where an object experiences two forces from different directions simultaneously, is reasoned in terms of the parallelogram of forces. The resultant motion is reasoned to be the diagonal of a parallelogram whose sides are the linear vectors of the two forces from the common point where they impact the object.

In the history of engineering thermodynamics, including the antecedents, from Huygens' compound pendulum and d'Alembert's vibrating strings, up through Bejan's 'two regimes', motion and work always incorporate two components. These are qualitative distinct and conceptually discontinuous opposites. From Leibniz through Planck the 'new' concept of 'change' with its dual components was referred to as an 'action'. All actions, all motions and work, properly understood, are composites. They are ratios with, for instance, both a linear (translational) and a curvilinear (rotational) component. These two components of motion and work are conceptual opposites undermine the parallelogram's reasoning in classical mechanics.

Per hypothesis, in engineering thermodynamics, the parallelogram takes on the more general form of a cycle. The two sides representing the opposite components have opposite curvature, reminding one of Sadi's 'indicator diagram'. Since the two phases of the cycle are not mechanically symmetric, the cycle forms a dynamic equilibrium and is net productive. The resultant is the area (or volume) between the cycle phases. The resultant has a direction perpendicular to the motion of the cycle and represents the thermodynamic work.

REFERENCES

1. Bejan A., *Entropy Generation Minimization: The Method of Thermodynamics Optimization of Finite-Size Systems and Finite-Time Processes*, Boca Raton, CRC Press, 1995.
2. D'Alembert J.R., *Treatise on Dynamics, in which the laws of equilibrium & of the motion of bodies are reduced to the smallest possible number, & demonstrated in a new way*, 2nd Edition, Gabay, Paris, 1743, 1990.
3. Leibniz G., *Preface to the Dynamics, Discourse on Metaphysics, in Leibniz: Philosophical Essays*, trans. Ariew R., Garber D., Hackett Publishing Co. (Indianapolis) & Cambridge, 1989.
4. Leibniz G.W., *Leibniz: Philosophical Essays*, Ariew and Garber (trans), Hackett Classics, 1989.
5. Carnot L. (1797), Browell W.R., trans. (1832), *Reflexions on the Metaphysical Principles of the Infinitesimal Analysis*, Andesite Press.
6. Carnot L., *Geometry of Position*, London, UK, Wentworth Press, 1803, 2018.
7. Carnot S., *Reflexions on the Motive Power of Fire*, Fox R. (editor and translator), Manchester U Press, Manchester, England, 1986.
8. Bristol T., *Give Space My Love: An Intellectual Odyssey with Dr. Stephen Hawking*, Institute for Sci, Eng and Public Policy, Portland Oregon, 2016.
9. Bristol T., Quantum Theory only makes sense in Lazare Carnot's participatory engineering thermodynamics, a development of Leibniz's dynamics, *Phil. Trans. R. Soc. A*, https://doi.org/10.1098/rsta.2022.0287.

CONSTRUCTAL LAW CONFERENCE – CLC2024
Design in Nature and Evolution
Romanian Academy, Bucharest, 10–11 October 2024

Proceedings of CLC2024
pp. 75–76

SEMI-EMPIRICAL CYCLING AGING MODELS WITH ENHANCED ACCURACY FOR A NICKEL MANGANESE COBALT CELL

GÜLŞAH YARIMCA[a], ERDAL ÇETKIN[a*]

[a] Izmir Institude of Technology, Türkyie
gulsahyarimca@iyte.edu.tr and erdalcetkin@iyte.edu.tr
*Correspondence: erdalcetkin@iyte.edu.tr; Tel. +90 232 750 6713

Batteries have recently garnered significant attention due to their numerous advantages across various applications, particularly in Electric Vehicles (EVs). However, one of the primary challenges limiting broader industry adoption is the aging of batteries over time. In this study, a semi-empirical aging modelling technique was used to predict battery degradation. Experimental data obtained from a 73 Ah NMC (Nickel Manganese Cobalt) cell to formulate three distinct models based on the Arrhenius Law to predict cyclic aging. Batteries underwent testing at two different temperatures and various depths of discharge (DoD) and C-rates up to approximately 800 cycles. Arrhenius' Law, which relates the rate of a chemical reaction to temperature, provided a solid framework for models. Between the three semi-empirical models developed, SEM-3 demonstrated satisfactory predictive accuracy when compared with the empirical data. Upon examining all data sets, SEM-3 exhibited the lowest Root Mean Square Error (RMSE) value of 0.95 in the model predictions, indicating a high degree of accuracy and reliability in its predictions.

Keywords: Electric vehicles; Battery aging; Cyclic aging.

1. INTRODUCTION

Recently, electric vehicle (EV) adoption has accelerated to reduce emissions associated with transportation and to enhance renewable energy use in transportation [1]. Among the various battery types used in EVs, Lithium-ion (Li-ion) batteries are preferred for their high energy density and technological benefits. Battery aging caused by chemical reactions results in decreased performance and lifetime. Environmental conditions and use characteristics (dis/charge) affect aging, which can be divided into calendar and cyclic aging. Methods for predicting Li-ion battery degradation include electrochemical, electrical, and semi-empirical models. Semi-empirical models (SEM), which merge theoretical principles with experimental data, are more versatile and widely applicable [2]. This research examines the capacity reduction of an NMC battery cell and analyses prediction models for cyclic aging, contributing to the literature on battery life prediction in EVs. The models were developed to enhance accuracy and reliability in predicting battery aging, thus contributing valuable insights to the literature on battery lifespan and performance prediction.

2. MATERIALS AND METHODS

The aging is affected by key factors such as time, temperature, depth of discharge (DoD), stage of charge (SoC), and current rate (C-rate). Equation (1) exemplifies the Q_{loss} aging model as a function of time (t), temperature (T), DoD, and C-rate, where the aging factors (T, DoD, C) are segregated from time:

$$Q_{loss}(T, DoD, C, t) = C_A(T, DoD, C) \times f(t). \quad (1)$$

In this study, semi-empirical approaches combining the temperature dependence of the Arrhenius equation with the power law relationship for the number of cycles were used in cyclic aging models [3,4], which is

$$Q_{loss} = A(DoD, C) \times e^{-\frac{E_a(SoC,C)}{RT}} \times n^z, \quad (2)$$

where E_a, R and n are activation energy, gas constant, and number of cycles (n), respectively. Table 1 presents a comprehensive overview of the model equations developed in this study.

Model parameters were determined using the Linear Regression and the Genetic Algorithm methods in MATLAB.

DOI: https://doi.org/10.59277/CLC/2024.19

Table 1

Model equations developed in HELIOS cyclic aging models

Model	Equation	Parameters
SEM-1	$a_1 \times \exp\left(\frac{a_2 \times \text{Crate}}{T}\right) \times \exp(a_3 \times DoD + a_4) \times t^{a_5}$	5
SEM-2	$c_1 \times \exp(c_3 \times DoD/T) \times \exp(c_3 \times Crate^2) \times n^{c_4}$	4
SEM-3	$c_1 \times \exp(c_3 \times DoD/T) \times \exp(c_3 \times Crate^2 + c_4 \times Crate) \times n^{c_5}$	5

3. RESULTS

Assessment of results obtained through the linear regression method shows that SEM-1 exhibited an error value of 18 RMSE, while SEM-2 and SEM-3 demonstrate an error value of 5 and 1.71 RMSE, respectively. Figure 1 shows the experimental data for 40°C and 5°C and the model results of SEM-3, which captures the best fit.

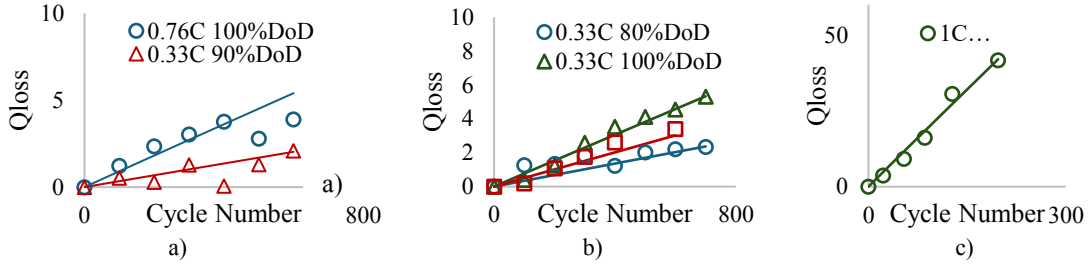

Fig. 1 – Experimental data and cyclic aging model:a) for 40°C and various DoD-Crate; b) for 5°C and different DoD-Crate; c) for 5°C 1C and 100% DoD.

Similarly, upon evaluating the models derived from the Genetic Algorithm method, SEM-3 once again displayed the most accurate fit with an RMSE of 0.95. The final version of the SEM-3 equation with the optimized parameters is as follows:

$$\boldsymbol{Q_{loss} = 0.003442 \times \exp(11,26341DoD/T) \times \exp\left(\frac{14.67921Crate^2 -}{14.562Crate}\right).n^{0.99}} \quad (2)$$

4. DISCUSSION AND CONCLUSIONS

A new semi-empirical model incorporating four distinct parameters has been developed, ensuring compatibility with experimental data. The results show that the numerical solution obtained using the Genetic Algorithm yields relatively better RMSE than the analytical solution derived from linear regression. The RMSE of the experimental results at 40°C is 0.64, indicating a high level of accuracy. In contrast, the RMSE for the results at 5°C is 1.15, which is still within acceptable limits. These findings highlight the robustness and sensitivity of the newly developed model under various temperature conditions.

REFERENCES

1. J. A. Sanguesa, V. Torres-Sanz, P. Garrido, F. J. Martinez, J. M. Marquez-Barja, A Review on Electric Vehicles: Technologies and Challenges, *Smart Cities 2021*, **4**, *1*, pp. 372–404 (2021).
2. A. Krupp *et al.*, Semi-empirical cyclic aging model for stationary storages based on graphite anode aging mechanisms, *J. Power Sources*, **561**, p. 232721 (2023).
3. J. de Hoog *et al.*, Combined cycling and calendar capacity fade modeling of a Nickel-Manganese-Cobalt Oxide Cell with real-life profile validation, *Appl. Energy*, **200**, pp. 47–61 (2017).
4. D. Werner, S. Paarmann, T. Wetzel, Calendar aging of Li-ion cells – experimental investigation and empirical correlation, *Batteries*, **7**, *2* (2021).

CONSTRUCTAL LAW CONFERENCE – CLC2024
Design in Nature and Evolution
Romanian Academy, Bucharest, 10–11 October 2024

Proceedings of CLC2024
pp. 77–80

ARCHITECTURAL INGENUITY AND THE CONSTRUCTAL LAW: UNLEASHING MAXWELL'S DEMONS

LAZAROS MAVROMATIDIS

ICube Laboratory, UMR 7357, Department of Mechanics, Civil Engineering and Energetics Team - GCE, CNRS, University of Strasbourg, INSA Strasbourg, Department of Architecture, 24 Boulevard de la Victoire, 67084 Strasbourg Cedex, France
lazaros.mavromatidis@insa-strasbourg.fr

Architectural ingenuity is a concept that epitomizes the fusion of design aesthetics and scientific principles, yielding spatial configurations that marry visual allure with science, functional resilience, sustainability, and energetic efficiency. Within this paradigm, the arrow of time, as dictated by the second law of thermodynamics, assumes significance. The evolution of architectural ingenuity unveils an alternative temporal narrative, often overlooked in architectural theory. This narrative finds resonance with the constructal law, propounded by Adrian Bejan, where architectural ingenuity mirrors the dynamic flow systems' fundamental principles. It is a contemporary manifestation of Maxwell's demon, driving spatial design's refinement and evolution. This interplay between human creativity and natural laws sculpts artificial living environments – flow configurations, enhancing human experience while mirroring the universal tendency of flow systems to improve accessibility over time. Architectural ingenuity, fluid and evolving, shapes spaces in synchrony with the essence of time.

Keywords: Architectural ingenuity; Maxwell's demons; Constructal law; Arrow of time; Living thermodynamics.

1. INTRODUCTION

Maxwell's Demon, a provocative thought experiment by physicist James Clerk Maxwell, challenges thermodynamic principles by suggesting entropy reduction without energy expenditure [1]. Though largely unexplored in architecture, its insights into architectural ingenuity transcend theoretical physics, informing sustainable spatial conception. Architecture, a multidisciplinary discipline, embodies philosophical currents, wherein architectural ingenuity manifests as a conduit for original thought, linking imagery and cognition [2]. Architects manipulate space and material to evoke sensory experiences and historical consciousness, reflecting societal currents and catalyzing contemporary discourse amidst the arrow of time.

2. MATERIALS AND METHODS: ARCHITECTURAL INGENUITY AND THE "MUSE OF ENTROPY"

Architecture, both in theory and practice, evolves dynamically under the influence of time, akin to thermodynamic flow systems governed by irreversibility. Maxwell's thought experiment, suggesting temperature differentials without energy expenditure, parallels the thermodynamic definition of temperature as a measure of kinetic energy and metaphorically represents pre-existing architectural knowledge. This analogy underscores architectural ingenuity's transformative potential, akin to Maxwell's demon, acting as a catalyst for profound changes in architectural discourse. As a "muse of entropy," architectural ingenuity navigates irreversibility to guide the evolution of sustainable, resilient, and energy-efficient spatial solutions.

DOI: https://doi.org/10.59277/CLC/2024.20

Architectural ingenuity embodies a complex interplay of irreversibility, energy flux, and conservation principles akin to thermodynamic systems, with fluid dynamics and equilibrium states signifying stability amidst change. The pursuit of efficiency in architectural design aligns with the constructal law, emphasizing the universal tendency of natural flow systems towards optimized configurations.

3. **RESULTS**

As is well established, architectural creativity often aligns with principles of disorder. This phenomenon parallels the process of spatial creation through architectural ingenuity, where space is conceptualized in two or three dimensions via the random interplay of lines, surfaces, or volumes. If we envision architectural ingenuity analogous to Maxwell's demon, it selectively navigates through all potential configurations. Consequently, it inevitably results in one of the myriad disordered spatial arrangements, underscoring the inherent complexity and variability in architectural design.

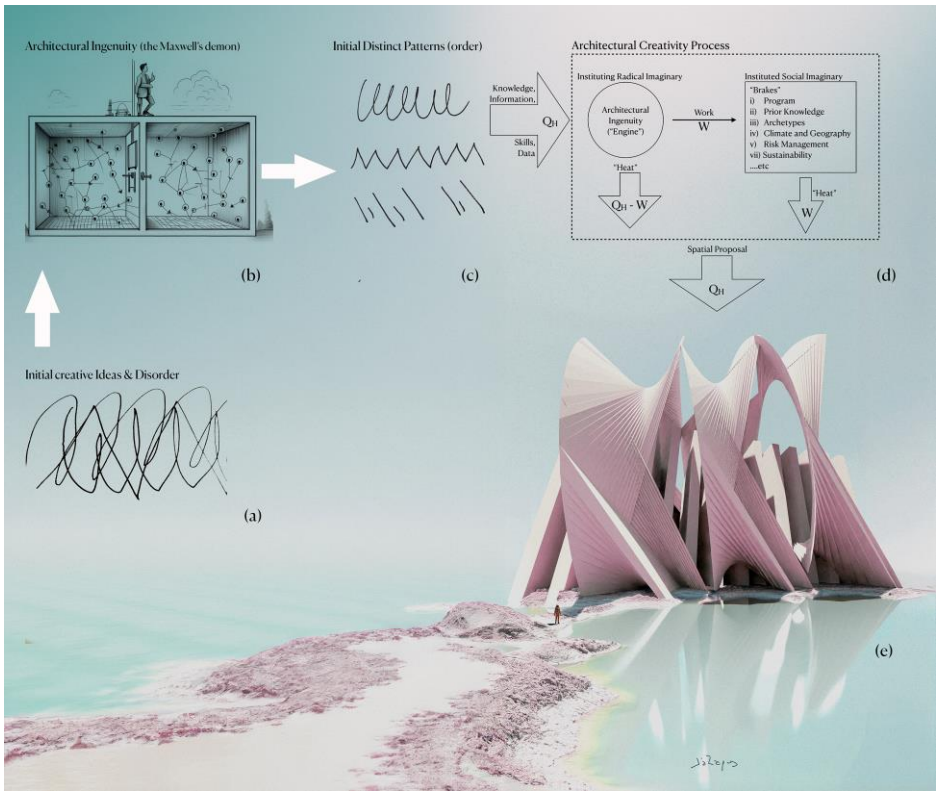

Fig. 1 – Architectural creativity process represented as a closed system in steady state, with heat flow in and out: (a) Initial complex idea and disorder; (b) Architectural Ingenuity as Maxwell's demon; (c) Initial patterns – ideas without flow organization (conceptual sketch); (d) Architectural conceptual process, is described as an engine (architectural ingenuity mobilizes the instituting radical imaginary [2]) that dissipates its power entirely into a brake (instituted social imaginary, see also [2]) during creation. The natural tendency of evolving design is the same as the tendency toward more power (the engine design, animal or machine), and toward more dissipation by mixing the archetypal schemes with imagination (Fig. 1d has been drawn based on a figure of Adrian Bejan [1,3,4]); (e) Final rendering of the initial idea presented in (a) © Lazaros Mavromatidis.

Figure 1 illustrates the creativity process as a closed system in a steady state, where thermodynamic theory offers a robust framework for understanding the transformation of nascent ideas into refined outputs.

In this context, creativity can be modeled as an energy-driven system, navigating entropy, energy flow, and equilibrium to sustain and refine its output. The process begins with nascent ideas (Fig. 1a), representing a high-entropy state. This is akin to the chaotic distribution of particles in a thermodynamic system, where potential energy is abundant but unstructured. These raw ideas embody creative energy in its least organized form, ripe with possibilities but requiring external input to catalyze meaningful order. Architectural ingenuity (Figs. 1b and 1c) functions as the system's engine, analogous to a heat engine in thermodynamics. In this stage, energy is applied to selectively organize and structure the raw material of ideas. Drawing parallels to the principles of energy transformation, this phase involves reducing entropy by imposing form and coherence. External inputs – whether cultural, experiential, or technological – act as sources of energy that the system metabolizes to create a lower-entropy, organized state. As the system moves toward equilibrium, the engine driving creative potential (Fig. 1d) operates at a steady state, maintaining a delicate balance between order and the introduction of new energy to prevent stagnation. This reflects the thermodynamic concept of a non-equilibrium system, where continuous energy input sustains a dynamic and creative steady state. The process mirrors Prigogine's idea of dissipative structures, where systems far from equilibrium self-organize into higher levels of complexity by dissipating energy into their environment. The final rendering (Fig. 1e) emerges as a refined and optimized low-entropy state, akin to the thermodynamic concept of achieving a more stable configuration. However, unlike closed systems in classical thermodynamics, the creative process is inherently open to feedback from the surrounding environment, allowing further refinement and evolution. This constant exchange ensures that the process does not devolve into stagnation or equilibrium but remains dynamic and responsive to new influences mirroring the idea of the constructal law. Creativity thrives on managing energy gradients, transforming high-potential, chaotic states (nascent ideas) into organized, coherent outputs (final renderings). This thermodynamic process relies on dissipating excess entropy into the environment to sustain flow. The depicted closed system, though conceptual, encapsulates the energy inputs, entropy reduction, and iterative refinement that drive innovation according to the constructal law as it is formulated by Adrian Bejan.

4. **DISCUSSION AND CONCLUSIONS**

The evolutionary trajectory of architectural design aligns with the constructal law, reflecting a universal tendency observed in natural flow systems. This progression, synonymous with self-organization and increasing complexity, is marked by directional movement towards optimization [1, 3, 4]. Within architectural discourse, the constructal law encompasses various contradictory intuitive statements regarding optimality, such as maximum entropy production or minimum flow resistance. This singular phenomenon represents the temporal evolution of design, propelled by the influx of new knowledge and currents. Architectural ingenuity orchestrates this transformative process, generating power through design while dissipating energy into the surrounding environment. The outcome is enhanced movement and accessibility, epitomizing the dynamic interplay between design evolution and environmental response governed by the arrow of time. Within this process lies the fertile domain of the radical imaginary – a space where human creativity transcends mere replication of functional forms to envision new modes of interaction and existence. Castoriadis' radical imaginary [2] invites us to see architecture not as a static response to predefined needs but as an ongoing act of creation that challenges and reshapes societal norms and possibilities. In this sense, architectural design becomes a living dialogue between the material and the conceptual, where time is not just a measure of

progression but a canvas for transformation. Through the radical imaginary, architecture ceases to be a mere tool for spatial organization [2]. It becomes a vessel for reimagining human connections to space, movement, and ecological processes.

The structures born of this imaginative impulse not only generate power and accessibility but also evoke alternative ways of inhabiting the world – ways that are adaptive, inclusive, and deeply attuned to the emergent realities of the environment. In this interplay, architecture is not only a response to the demands of the present but also a projection of a possible future. It harnesses the energy of the radical imaginary to disrupt entropy, allowing new forms of coherence to emerge from the interaction of human creativity and the unfolding universe. Through this lens, architecture becomes a testimony to the profound reciprocity between design and the ever-evolving interplay of natural and cultural forces and flows.

REFERENCES

1. Bejan A., Maxwell's Demons Everywhere: Evolving Design as the Arrow of Time, *Sci. Rep.*, **4**, p. 4017 (2014).
2. Mavromatidis L., A heterogeneous architectural theory inspired by living thermodynamics: Unveiling “architectural ingenuity” using the constructal law, *International Communications in Heat and Mass Transfer*, **155**, p. 107554 (2024).
3. Bejan A., Lorente S., The constructal law and the evolution of design in nature, *Phys. Life Rev.,* **8**, pp. 209–240 (2011).
4. Bejan A., Lorente S., Constructal law of design and evolution: Physics, biology, technology, and society, *J. Appl. Phys.*, **113**, p. 151301 (2013).

CONSTRUCTAL LAW CONFERENCE – CLC2024
Design in Nature and Evolution
Romanian Academy, Bucharest, 10–11 October 2024

Proceedings of CLC2024
pp. 81–84

LIBERATE HUMAN STRENGTH & LIFE

CHRISTINE BIZZELL

Canon Collaborative
christine@canoncollaborative.com

Keywords: Nature; Humans; Work; Wellbeing; Agency.

Humans are part of nature – its oneness includes all of us [1]. As our climate is greatly challenged to regulate itself, humans naturally follow suit. After all, we are subordinated to the motherly flows that created us. The same flow and flow architecture that generates life on earth moves through our bodies, minds, and consciousness. As freedom of thought goes hand-in-hand with access to power, space, and wealth [2], management designs that empower people more uniformly could enhance the flow of innovations to sustain life on our finite-sized planet. We could invest in workplace engagement as a holistic and generative strategy to support human and planetary health and wellbeing. As Adrian Bejan states, "the onus [is] on citizens, schools, businesses, and government to speed the process of creating designs to better serve society -- more effectively and with much greater confidence [3]."

According to the World Health Organization (WHO), mental health encompasses an individual's ability to cope with stress, realize and engage their abilities, and contribute to their community [4]. In 2019, 970 million people were living with a known mental health disorder – note these figures were presented before the Covid-19 pandemic and do not account for unknown conditions. Mental health is closely linked with productivity [5] and the WHO estimates that 12 billion working days are lost every year due to depression and anxiety, which costs an estimated 1 Trillion U.S. dollars in lost productivity. These mental health disorders impair the human spirit that drives innovation and economic energy [6]. These mental health disorders exist alongside the increasing prevalence of burnout, which is not categorized as a mental health disorder. Burnout is a syndrome resulting from chronic workplace stress that has not been successfully managed. However, stress management is a significant aspect of mental health. In 2024, many estimates show a minimum of half of the global workforce is at risk of burnout.

According to Gallup, wellbeing can be understood and measured in five interconnected domains: career, financial, physical, social, and community. With work claiming 20–50% of our waking hours, our experience in the career domain or "liking what you do everyday" is heavily weighted in connection with our holistic wellbeing and can be a tremendous stabilizing force in an individual's life [6]. Therefore, the positive transformation of work experience becomes a magnificent opportunity to support global wellbeing. Jim Harter, Chief Scientist at Gallup shares that the combination of strengths and wellbeing at work is "potentially the most transformational treatment yet" in the pursuit of mental health [6].

The human mind has an instinctive urge to recognize and understand the configuration required to promote ease, fulfillment, and happiness [7]. The CliftonStrengths assessment, written in 26 languages,

DOI: https://doi.org/10.59277/CLC/2024.21

identifies a person's most natural and prevalent currents of thinking, feeling, and behaving that can be consciously engaged and therefore productively called upon or utilized. For individuals, these currents of strength are dynamically interconnected and an extremely rare subset [8] often first appearing in childhood. The language associated with each strength, which can be likened to energy, is expressed in relatable terms for immediate utilization in any environment combined with knowledge of and access to the fuel enabling its contribution [9]. We know that "language speeds and strengthens connections in the brain when we are processing sensory information" [10] and that better utilizing language advances adaptations [11]. Our approach to strength empowerment illuminates significant aspects of an individual's tacit knowledge, which is understood as knowledge embedded in the human mind through subjective experience that is often very difficult to put into words, including personal wisdom, insight, and intuition. An individual may not be consciously aware of this embodied knowledge, yet it influences how we each perceive and interact with the world [12]. When understood, this embodied strength and tacit knowledge illuminates the path to individual genius – supporting an individual's ability to create situations and opportunities to release their strength with greater self-trust and confidence. Claiming this agency, we can map our instincts beyond survival and bring forth innovations that our mind, and only our mind, could create.

Our embodied strength naturally meets resistance in abundant and highly unique-to-us forms. This resistance or stress is often associated with work or the required activities that support the structure of our lives and niche environments. Gaining clarity of our unique environmental stressors, we can lead ourselves to success through the path of least resistance – conscious selection, claimed agency, and methodical self-directed movement. The Hungarian-American Psychologist Mihaly Csikszentmihalyi introduced the concept of a psychological flow state as empowered concentration on a consciously chosen goal and worthy challenge [13] – when our strengths and skills meet resistance with clarity and confidence [9]. These flow state experiences are represented in the mind as information, containing immensely invaluable data we can utilize to replicate past success and avoid past failure. A personal wellspring, this flow experience data can inform the best design for work. In Mihaly's view, this flow state arises when we claim control of our inner state of energy and experience, which can not only lead to success, but is also the closest that anyone can come to creating happiness in life [13]. As Mihaly states, "The steps we take to improve the quality of experience are very important to culture as a whole."

Organizational structures have evolved with the human species, as outlined by Frederic Laloux in his work "Reinventing Organizations." As our society grows more complex, so does our need for more complex structures to support our movement and empowerment. Scientific management was created during the Industrial Revolution and instrumental in building human connection or relationship to our new machine extensions. Eventually, some organizations realized this mechanistic approach diminished our humanity and pursued organizing as a family [14]. Today, Laloux believes organizations can be viewed as a living organism that would best flourish under holistic management practices that center higher purpose, distributed decision making, and self-management. Through viewing an organization as a living organism, we can gain powerful insight into pathways that can liberate human strength and ingenuity. This perspective not only gives us insight into individual pathways to flourishing, but also how the whole may be nourished through cultural practices and structures. Viewing an organization's

ecosystem of living human strength, we can analyze its design to understand dominant pathways to productivity, mitigate unique environmental stressors, and leverage outlying strength that might otherwise be overpowered. Through embracing a shared language, an organization can utilize strengths to connect on issues that greatly matter to the work – bolstering collaboration, innovation, and adaptation. Through this connection, leaders and managers can gain truly invaluable insight into what fuels their team to intrinsically pursue shared goals and collaborate toward realizing vision. Freedom to operate in strength at work is directly correlated with workplace engagement, which brings tremendous organizational benefits such as decreased safety incidents, lower turnover, higher productivity, and more [15].

With greater strength awareness, individuals can design for success, support their wellbeing, and be more confident in their quest for happiness. We can all learn to generate congruence in our lives by embracing our most natural strength and absorbing the timeless wisdom of the natural world in pursuit of balance and harmony that "form the golden thread of life [16]." Wellbeing and agency are critical components for an inclusive and sustainable path to global development [16]. The science of management should rapidly evolve to provide greater access to human strength for the sole purpose of benefiting global wellbeing – innovation and profit will naturally follow, which is why 90% of Fortune 500 companies have implemented a strength-based approach [15]. Viewing an organization as a living organism, we can gain insight into pathways that can liberate human strength and life [9]. The onus is on every one of us – we are empowered and it's time to revolutionize the way we work.

REFERENCES

1. Bejan A., Zane J.P., *Design in Nature: How the Constructal Law Governs Evolution in Biology, Physics, Technology, and Social Organization*, Doubleday, New York, USA, 2012.
2. Bejan A., *Freedom and Evolution*, Springer Nature, New York, USA, 2020.
3. American Institute of Physics (AIP), *Physics can predict wealth inequality*, ScienceDaily. ScienceDaily, 28 March 2017. <www.sciencedaily.com/releases/2017/03/170328120613.htm>.
4. World Health Organization (WHO), <www.who.int/health-topics/mental-health>
5. Psychology Today, Mental Health and Productivity <https://www.psychologytoday.com/us/basics/productivity/mental-health-and-productivity>
6. Clifton J., Harter J., *Wellbeing at Work: How to Build Resilient and Thriving Teams*, Gallup Press, 2021.
7. Bejan A., *Time and Beauty: Why Time Flies and Beauty Never Dies*, World Scientific, Singapore, 2023.
8. Science of CliftonStrengths, The Gallup Organization, 5 Aug. 2024, www.gallup.com/cliftonstrengths/en/253790/science-of-cliftonstrengths.aspx#
9. Bizzell C., *Grounding Journey*, Canon Collaborative Website, 2024. www.canoncollaborative.com/grounding-journey/.
10. Brown B., *Atlas of the Heart: Mapping Meaningful Connection and the Language of Human Experience*, First edition, New York, Random House, 2021.
11. Bejan A., *The Physics of Life: The Evolution of Everything*, St. Martin's Press, New York, USA, 2016.
12. Key Concepts in Information and Knowledge Management, Tacit and Explicit Knowledge. www.tlu.ee/~sirvir/Information%20and%20Knowledge%20Management/Key_Concepts_of_IKM/tacit_and_explicit_knowledge.html. Accessed 18 Nov. 2024.
13. Csikszentmihalyi M., *Flow: The classic work on how to achieve happiness*, Rider, Random House, 2002.

14. Laloux F., *Reinventing organizations: A guide to creating organizations inspired by the next stage of human consciousness*, Nelson Parker, Brussels, Belgium, 2014.
15. CliftonStrengths for Organizations, The Gallup Organization https://www.gallup.com/cliftonstrengths/en/253808/cliftonstrengths-for-organizations.aspx. Accessed 29 May 2024.
16. Global Wellbeing Initiative, Wellbeing for All: Incorporating Harmonic Principles of Wellbeing in Subjective Wellbeing Research and Policymaking, 2023.

CONSTRUCTAL LAW CONFERENCE – CLC2024
Design in Nature and Evolution
Romanian Academy, Bucharest, 10–11 October 2024

Proceedings of CLC2024
pp. 85–88

MAXIMUM BENEFITS FROM THE USE OF *T*-SHAPED TREE FLOW GEOMETRY WITH RECTANGULAR SHAPE OF THE CHANNELS: PERFORMANCE EVALUATION

VENTSISLAV D. ZIMPAROV, MILCHO S. ANGELOV, VALENTIN M. PETKOV

Technical University of Gabrovo, 4 Hadji Dimitar, Gabrovo 5300 Bulgaria
ventsi.zimparov@gmail.com

The study defines the conditions and constraints that must be obeyed to obtain the maximum benefit from the use of a heat exchanger with a *T*-shaped tree flow configuration and rectangular shape of the channels. The flow is laminar, and fully developed with constant physical properties. The boundary condition is the fixed temperature of the channel wall. The variations of the heat flow ratio q_t^+ and augmentation entropy generation number N_{sa} with the dimensionless mass flow rate M, shape factor χ, ratio B, and complexity n have been investigated. Comparisons of the thermal performance with other heat exchanger configurations like serpentine for two cases $q_t^+ = 1$ and $q_t^+ > 1$ have been made. The requirement for $N_{sa} \le 1$ has been implemented as a constraint instead of one of fixed pumping power. The performance evaluation criterion N_s^+ has been introduced as a general criterion to define the most beneficial complexity and working parameters.

Keywords: *T*-shaped tree; Rectangular shape; Maximum benefits; Performance evaluation criteria.

1. INTRODUCTION

Dendritic heat exchangers arose at the beginning of this century as a new direction for developing heat exchanger architectures [1]. They revealed a greater potential to reduce the pressure drop and improve the temperature distribution homogeneity and thermal efficiency than the traditional parallel channel network [2]. Since then, many experimental and numerical studies have been reported [3].

The results developed, and the optimization criteria applied reveal that the tree-shaped design heat exchangers are the following (fourth) generation heat exchangers using the natural heat transfer enhancement technique, pursuing the same objectives arising from the first and second laws of thermodynamics [4].

This paper demonstrates the usefulness of two criteria, like those used in [4]: augmentation entropy generation number N_{sa} and q_t^+. The objective of the first case is to evaluate the maximum reduction of the driving temperature difference, $\Delta T_m^* < 1$, whereas the objective of the second case is to assess the maximum increase of the heat duty, $q_t^+ > 1$.

2. ANALYSIS OF THE HEAT EXCHANGER CONFIGURATION

Figure 1 shows tree-shaped streams distributed over a rectangular area. The flow is laminar and fully developed with constant physical properties. The constraints are fixed heat transfer surface area of the channels A_w in the allocated area A. The boundary condition in the wall is $T_w = const$.

DOI: https://doi.org/10.59277/CLC/2024.22

The lengths are obeyed the rule $L_i = 2^{i/3} L_o$ and $D_{h,i} = 2^{i/3} D_{h,o}$. The total heat flow in dimensionless form is

$$\tilde{q}_n = \frac{\dot{q}_n}{k_f A^{1/2} T_{in}} = M\left(T^* - 1\right)\left\{\left[1 - \exp\left(-\chi Nu \frac{2^{(3n-7)/6}}{M}\right)\right] + S_1\right\}, \tag{1}$$

$$S_1 = \sum_{i=1}^{n}\left\{\exp\left(-\sum_{k=0}^{k=i-1} \chi Nu \frac{2^{(3n-4k-7)/6}}{M}\right)\left[1 - \exp\left(-\chi Nu \frac{2^{(3n-4i-7)/6}}{M}\right)\right]\right\}. \tag{2}$$

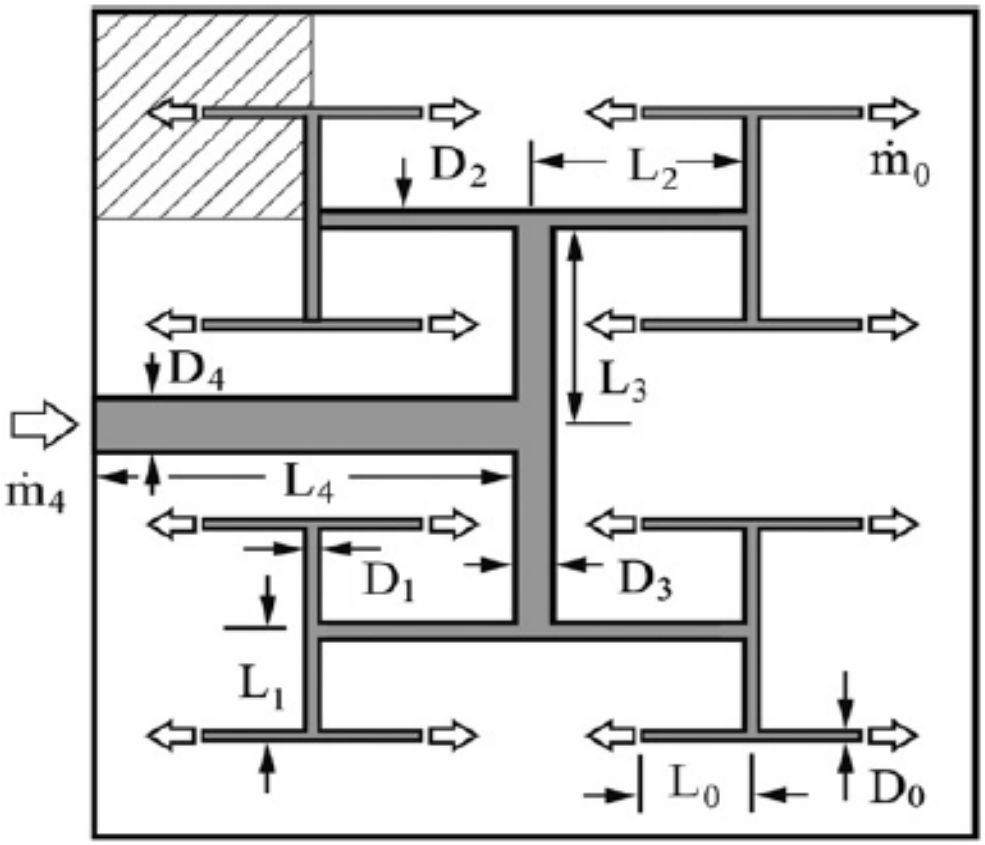

Fig. 1 – The flow of tree-shaped streams is distributed over a rectangular area.

The overall entropy generation for a tree-shaped heat exchanger in dimensionless form is

$$\tilde{S}_{gen} = M\left(T^* - 1\right)^2 \left\{\exp\left(-\chi Nu \frac{2^{(3n-7)/6}}{M}\right)\left[1 - \exp\left(-\chi Nu \frac{2^{(3n-7)/6}}{M}\right)\right] + S_2\right\} + \chi^3 \times B \times Po \times 2^{(3n-17)/6} \times \left[2^{-(n+1)/3} - 1\right]^4 M^2 \tag{3}$$

$$S_2 = \sum_{i=1}^{n}\left\{\begin{array}{l}\left[\exp\left(-\sum_{k=0}^{k=i-1} \chi Nu \frac{2^{(3n-4k-7)/6}}{M}\right)\right]^2 \exp\left(-\chi Nu \frac{2^{(3n-4i-7)/6}}{M}\right) \times \\ \times\left[1 - \exp\left(-\chi Nu \frac{2^{(3n-4i-7)/6}}{M}\right)\right]\end{array}\right\}, \tag{4}$$

$$B = \frac{A^3 \nu k_f}{A_w^4 T_w \rho c_p^2 \left(2^{-1/3} - 1\right)^4}. \tag{5}$$

3. **RESULTS AND DISCUSSION**

Figures 2 and 3 show the variation of the augmentation entropy generation number $N_{sa} = \tilde{S}_{gen,n} / \tilde{S}_{gen,n=0}$ and the ratio of heat flows $q_t^+ = \tilde{q}_{t,n} / q_{t,n=0}$ with the dimensionless mass flow rate M and the complex B for several levels $n = 1, 2, 4$ and $T^* = 1.4$. The results revealed several important characteristics: (i) N_{sa} strongly depends on shape factor $\chi = p / D_h$ and complexity n. As seen from Fig. 2, for $\chi = 6.25$ only for $n \le 4$, $N_{sa} \le 1$, whereas for $\chi = 10.125$, only for $n \le 2$ $N_{sa} \le 1$.

The parts of the curves N_{sa} vs. M where $N_{sa} > 1$ have been removed from Fig. 2. (ii) The variation of q_t^+ with M shows two regions with different behavior of q_t^+, namely $q_t^+ = 1$ for small values $M < 4$, and $q_t^+ > 1$ for $M > 4$. In the range $M < 4$, the benefit is the decrease in the driving temperature difference defined by the value of $N_{sa} < 1$. For instance, if $\chi = 6.25$, the most significant benefit is obtained for $M = 4$ and $n = 2$, whereas if $\chi = 10.125$, the most significant benefit is obtained for $M = 8$ and $n = 1$.

In the second range $M > 4$, the objective is the maximum increase in the heat flow that can be achieved, not a minimum entropy generation. The maximum q_t^+ is achieved for that value of M for which $N_{sa} = 1$. As seen from Fig. 3, the smaller χ, the more significant the benefit is.

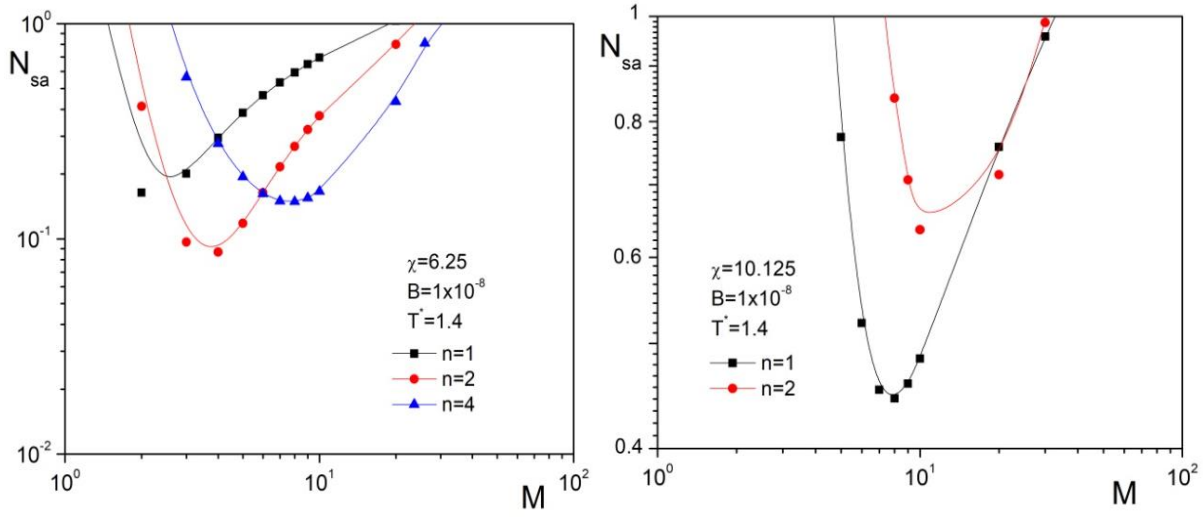

(a) (b)

Fig. 2 – The variation of N_{sa} with *M*; (a) $\chi = 6.25$, (b) $\chi = 10.125$.

With this study we try to encourage the use of these two criteria for assessing the benefits that tree-shaped heat exchangers can bring about in comparison with conventional heat exchangers with different structures like serpentine or banks of parallel tubes.

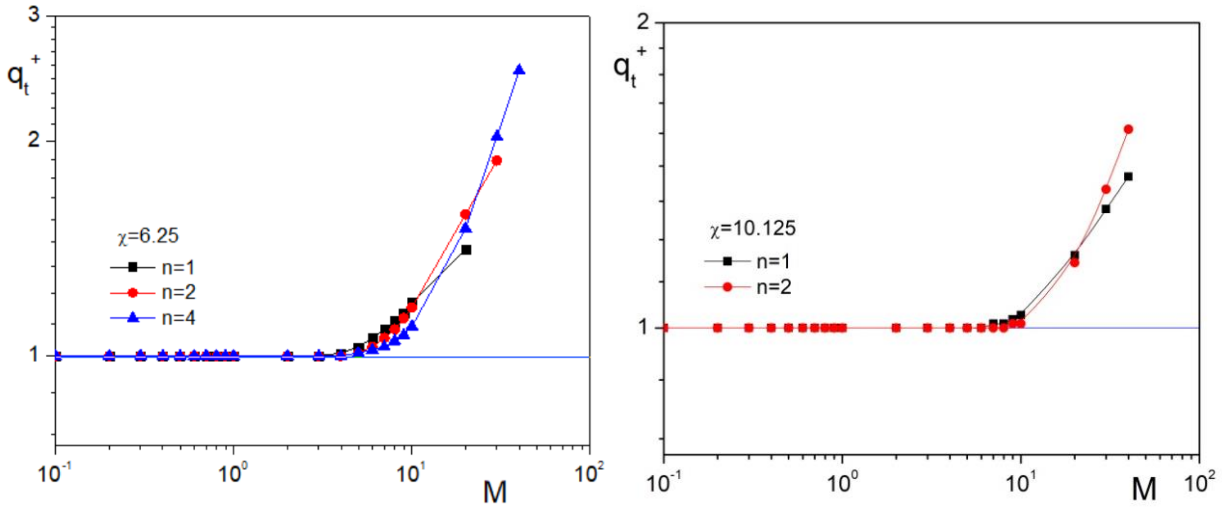

(a) (b)

Fig. 3 – The variation of q_t^+ with *M*; (a) $\chi = 6.25$, (b) $\chi = 10.125$.

ACKNOWLEDGEMENTS

This paper is dedicated to Adrian Bejan and A.K. da Silva as a reminiscence about our collaborative work at Duke University during 2005 (V.D. Zimparov).

The study has been supported by the Project 2211M/2024, Technical University of Gabrovo, BG.

REFERENCES

1. Bejan A., Lorente S., Dendritic Heat Exchangers, *Design with Constructal Theory*, John Wiley and Sons, New Jersey, 2008, pp. 274–294.
2. Pence D.V., Reduced Pumping Power and Wall Temperature in Microchannel Heat Sink with Fractal-Like Branching Channel Networks, *Macroscale Thermophysical Engineering*, **6**, pp. 319–330 (2002).
3. He Z.Y., Yunfei, Zhien Z., Thermal Management and Temperature Uniformity Enhancement of Electronic Devices by Micro Heat Sinks: A Review, *Energy*, **216**, p. 119223 (2021).
4. Zimparov V.D., Angelov M.S, Petkov V.M., Maximum Benefits from the use of Enhanced Heat Transfer Surfaces, *International Journal of Heat and Mass Transfer*, **134**, p. 105992 (2022).

CONSTRUCTAL LAW CONFERENCE – CLC2024
Design in Nature and Evolution
Romanian Academy, Bucharest, 10–11 October 2024

Proceedings of CLC2024
pp. 89–92

INFORMATIONAL PERSPECTIVE ON RAMIFICATIONS IN CONSTRUCTAL DESIGN

MIGUEL R. OLIVEIRA PANÃO

University of Coimbra, ADAI – Associação para o Desenvolvimento da Aerodinâmica Industrial, Portugal
miguel.panao@dem.uc.pt

What insights can informational analysis provide regarding the ramifications predicted by constructal design? The first step in answering this research question is to consider symmetric and asymmetric flow architectures. In the symmetric case, radial multi-branching shows diminishing returns of diversity (measured by the system's *informature*) in line with high thermofluid performance. In asymmetric flow architectures, assuming an evolution toward maximum complexity (as defined in information theory), patterns emerge like sap distribution in leaves.

Keywords: Diversity; Constructal design; Information theory; *Informature*; Complexity.

1. INTRODUCTION

In Bejan [1], the optimal solutions were converted to references. This conceptual change not only avoids the mistake of considering constructal design as an alternative optimization tool, but also emphasizes the freedom to change and evolve as a result of considering as much as 1% imperfection in the design goal of a physical system. Flow architectures that are free to change lead to diverse possible solutions, introducing a non-deterministic element in their design. In fact, Gosselin and Bejan [2] showed that even asymmetries in radial tree architectures can facilitate access to liquid flows, increasing the number of possible configurations and implying a higher diversity and complexity of flow architectures. This study sought insights retrieved by quantifying the information contained in ramified flow structures.

2. BASIC ELEMENTS OF INFORMATIONAL ANALYSIS

In 1948, Shannon [3] developed a formulation that quantifies the amount of information in any system containing several possible solutions. Although John von Neumann induced Shannon to name his formulation "entropy" due to its similarity to statistical mechanics [4], Denbigh [5] remarked it as a disservice to science because functions with the same formal structure do not necessarily represent the same. Instead, the Shannon's formulation in Eq. (1) is indeed a "measure of information" because it refers to the entire probability distribution, although some interpret it as average uncertainty or *indeterminacy*.

$$H = -K \sum_i p_i \log_2(p_i). \tag{1}$$

DOI: https://doi.org/10.59277/CLC/2024.23

To simplify and clarify the language of informational analysis, I introduce two new words: *informature* and *infotropy*.

Informature $H_{I,b}$ is only part of Shannon's formulation, which measures the amount of information obtained from the knowledge of the probability distribution:

$$H_{I,b} = -K_b \sum_i p_i \log_2(p_i), \tag{1}$$

where K_b is a constant that can change the logarithmic base and define the informature units. For example, $K_b = 1$ leads to $H_{I,2}$ measured in *bits*, whereas $K_b = \ln(2)$ leads to $H_{I,e}$ measured in *nats*. *Infotropy* is a neologism that synthesizes information (*info* -) and transformation (from the Greek *trope*) to signify an informature "contextualized" by a K_c scale parameter, as suggested by Tribus and McIrvine [4], corresponding to Shannon's formulation. Thus, $H_b = K_c \times H_{I,b}$ is an *infotropy*, *i.e.,* a "contextualized" *informature*. For example, in a gas where there are as many possible arrangements as *W* molecules, the probability of each configuration is $p_i = 1/W$, and if one defines $K_c = k_B$ with k_B as Boltzmann's constant and $K_b = \ln(2)$, the resulting *infotropy* is the well-known thermodynamic entropy at the microscopic level of reality $H_e = S = k_B \ln(W)$. If one considers the relative information, also known as the Kullback-Leibler information distance or information gain that measures the distance between the maximum informature, $H_{max,b} = K_b \cdot \log_2(N_k)$, where all possible configurations (N_k) are equally probable, and the actual informature, the result for the relative information becomes $D = H_{max,b} - H_{I,b}$. According to Feldman and Crutchfield [6], one can quantify the complexity of a finite-size system as the product of its informature and the relative information as $C = H_{I,b} \times D$, where is zero for systems without information ($H_{I,b} = 0$) or fully *indeterminate* systems ($D = 0$). For example, the dimensionless complexity $C_n = \frac{C}{H_{max,b}^2} = H_n(1 - H_n)$ with $H_n = H_{I,2}/H_{max,2}$ allows the comparison of different flow structures. In this study, an informational analysis of the informature of multi-branching radial symmetric and asymmetric flow structures provides insights into the evolutionary direction.

3. **RESULTS**

For ramifications with $b_p = 2$ and $b_p = 3$ branches, each branching level p implies the emergence of $n(p) = n_0 \cdot {b_p}^p$ channels in the flow structure. Therefore, the frequency of channels at each level p is $f(p) = n(p)/\sum_{i=0}^{p} n(i)$ with $\sum_{i=0}^{p} f(i) = 1$. The maximum informature in this simple reasoning method depends on the highest branching level: $H_{max,2} = \log_2(max\{p\})$. However, if one channel branches into several channels at the exit (n_{out}), then the flow rates at the exit $\dot{m}_i$ relative to the total flow $\dot{m}$ at the inlet provide proportions appropriate for informational analysis, $\sum_{i=1}^{n_{out}} (\dot{m}_i/\dot{m}) = 1$.

Figure 1(a) shows that 1) the informature develops toward diminishing returns with unfolding branching levels, and 2) lower informature values above bifurcations ($b_p > 2$) produce configurations

with lower diversity levels. Suppose one measures the informature based on the flow rates at the exit channels ($\dot{m}_{e,i} = f_i \dot{m}$) and selects the flow structures that maximize dimensionless complexity. In that case, the results depicted in Fig. 1(b) show the emergence of a consistent pattern, such as sap distribution in leaves.

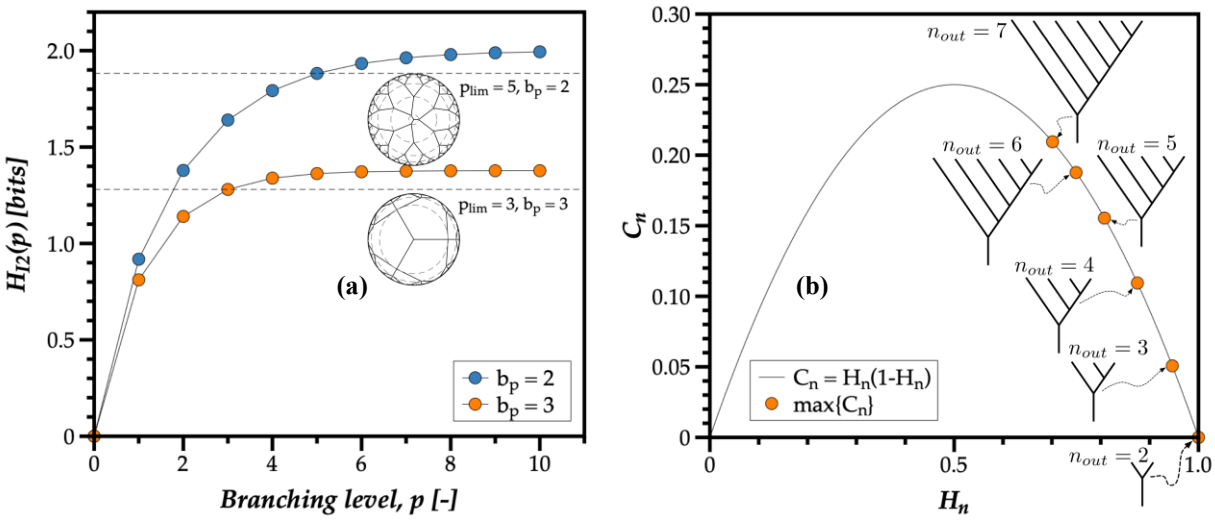

Fig. 1 – (a) *Informature* sensitivity with branching level p, (b) ramifications that maximize dimensionless complexity versus normalized *informature*.

4. DISCUSSION AND CONCLUSIONS

In Clemente and Panão [7, 8], the flow architectures with the highest performance considered a minimum number of $n_0 = 3$ initial channels and the miniaturization of vascularized multi-branching radial flow architectures pointed in the direction of p = 3 - 5 with bifurcations ($b_p = 2$). Without any consideration of the thermofluid performance, the informational insight based on the informature of the flow structure points in the same direction, considering diminishing returns. These results indicate that informature is directly proportional to the diversity of physical systems, including flow architectures, and that freedom-to-morph evolves toward higher complexity.

REFERENCES

1. Bejan A., Perfection is the enemy of evolution, *BioSystems, 104917*, pp. 1–6 (2023).
2. Gosselin L., Bejan A., Emergence of asymmetry in constructal tree flow networks, *Journal of Applied Physics*, *104903*, pp. 1–7 (2005).
3. Shannon C.E., A mathematical theory of communication, *The Bell system technical journal*, **27**, *3*, pp. 379–423 (1948).
4. Tribus M., McIrvine E.C., Energy and information, *Scientific American*, **225**, *3*, pp. 179–190 (1971).
5. Denbigh K., How subjective is entropy?, *Maxwell's demon: entropy, information, computing*, Leff HS, Rex AF, Eds., Princeton University Press, 1990, pp. 109–115.

6. Feldman D.P., Crutchfield J.P., Measures of statistical complexity: Why?, *Physics Letters A*, **238**, *4–5*, pp. 244–252 (1998).
7. Clemente M.R., Panão M.R.O., Generalizing multi-branching radial symmetric flow structures, *International Journal of Heat and Mass Transfer*, **216**, 124568 (2023).
8. Clemente M.R., Panão M.R.O., *Performance Scaled Svelteness Drives the Evolution of Multi-Branching Radial Symmetric Flow Structures*, Available at SSRN 4763680.

CONSTRUCTAL LAW CONFERENCE – CLC2024
Design in Nature and Evolution
Romanian Academy, Bucharest, 10–11 October 2024

Proceedings of CLC2024
pp. 93–96

ENHANCED ELECTRONIC COOLING USING FIN HEATSINK: A COMPARATIVE ANALYSIS

AHMED M. BUKAR[a], ABDULRAHMAN S. ALMERBATI[a,b]

[a] Mechanical Engineering Department, King Fahd University of Petroleum and Minerals (KFUPM), Dhahran 31261, Saudi Arabia
[b] Interdisciplinary Research Center for Sustainable Energy Systems (IRC-SES), King Fahd University of Petroleum and Minerals (KFUPM), Dhahran 31261, Saudi Arabia
*Correspondence: g202203340@kfupm.edu.sa ;Tel.+966503638505

Electronic devices consistently produce undesired thermal energy. The growing demand for these devices in various applications necessitates innovative cooling solutions to mitigate thermal losses. The main challenge in electronic cooling is the full development of the thermal boundary layer. This study aims to optimize the conventional rectangular plate-fin heatsink by redeveloping a new thermal boundary, which involves morphing the fin configuration and distribution while maintaining a constant fin volume. We used numerical simulation in COMSOL Multiphysics to analyze and compare conventional rectangular plate-fin heatsink performance with two optimized configurations: the bifurcated longitudinal split fin and hybrid plate-pin fin heatsinks. The methodology involves assessing the thermal and flow performance in the form of the average heatsink baseplate temperature and the average pressure drop across the heatsink. We investigated these under a constant heat flux of 5903 W/m^2 and varying air velocities between 4 and 12 m/s. The results showed that using five bifurcated plate fins and hybrid plate-pin fins lowers the temperature of the heatsink base plate by 25% and 47%, respectively, compared to conventional rectangular plate fins when the air velocity is 8 m/s. However, these optimized configurations increased the pressure drop across the heat sink.

Keywords: Constructal design; Fin heatsinks; Thermal management; Electronic cooling.

1. INTRODUCTION

Electronic devices consistently produce undesired thermal energy during their operation, and with electronic systems increasingly becoming more advanced, the challenge of providing an effective and dependable heat dissipation system has grown burdensome [1,2]. The proficient cooling of high-power electronic devices facilitates the downsizing and acceleration of electronic systems, making them more robust. One significant environmental factor that has an impact on built-in circuit performance is temperature. Overly elevated temperatures of operation typically interfere with the equipment's ability to function effectively [3]. Therefore, an innovative and effective cooling system is required to solve the overheating challenge and achieve efficient heat dissipation to prevent such failures. One of the main challenges in the thermal management of electronic chips is the full development of the thermal boundary layer, which greatly reduces the heat transfer coefficient along the flow channel. The existing research indicates that there is potential for increased heat transfer coefficients in a newly formed boundary layer along the flow channel by changing the fin shape and distribution [4,5].

Extensive research efforts over the years have been dedicated to the investigation of heat transfer within vertical [6] and horizontal [7], [8] channels containing heated obstructions, leading to a comprehensive body of literature on this subject. In this study, the performance of the rectangular plate fin (RPF) heat sink is optimized by changing the configuration and the distribution of the plate-fin heat sink. Two optimizations are proposed: bifurcated longitudinal split fins (BLSF) and hybrid plate-pin fins (HPPF).

DOI: https://doi.org/10.59277/CLC/2024.24

2. MODEL DESCRIPTION

The proposed approach enhances the efficiency of the traditional RPF heatsink by altering the type and distribution of the fins while maintaining constant fin volume. Figure 1(a) shows the heatsink with a BLSF. The main objective of this design is to control the thermal boundary layer by dividing the plate fin (n_2) at a specific length (L_1), splitting the remaining half into two (n_3), and then replanting it to the base plate. The primary design factor is the specific length (L_1) at which the plate fin divides, enabling it to morph in percentage of the overall fin length (L) represented by equation (1). Figure 1(b) illustrates the arrangement of the HPPF heatsink. The primary design concept entails decreasing the thickness (t_f) of the plate fin to embed a pin onto the plate fin's surface, thereby converting a specific proportion of the plate fin's volume into the pin. As the thickness of the plate fin (t_f) decreases, the height of the pin (H_p) increases while keeping the pin diameter (d_p) constant.

$$L^* = \frac{L_1}{L}, \tag{1}$$

$$T^* = \frac{T_b - T_{in}}{T_{in}}, \tag{2}$$

$$\Delta P = P_{out} - P_{in}. \tag{3}$$

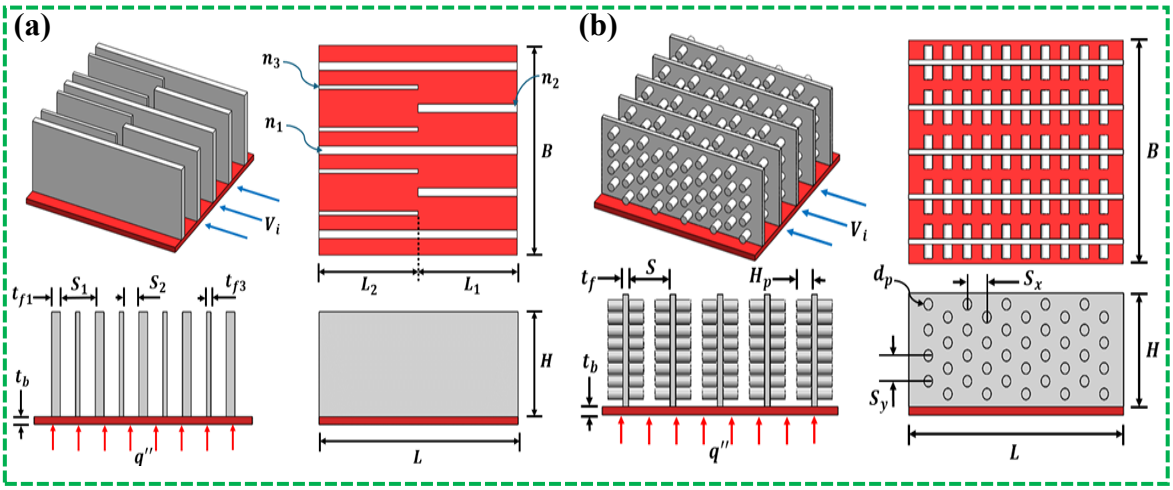

Fig. 1 – Model description of (a) BLSF heatsink, and (b) HPPF heat sink.

3. NUMERICAL METHOD

The numerical simulations were performed utilizing commercial CFD software, COMSOL Multiphysics. The simulations were conducted on a three-dimensional domain, considering both steady-state and turbulent flow conditions. The geometric model is constructed, boundary conditions are established, mesh independence tests are carried out, and the numerical model is validated with experimental work during the pre-processing phase. The processing stage involves solving the governing equations for fluid flow and heat transfer. The post-processing stage entails examining the simulation results to assess the hydraulic and thermal performance metrics of the heat sink configurations in terms of dimensionless baseplate temperature and pressure drop given by equations (2) and (3), respectively. Where subscript *b*, *in* and *out* represents baseplate, inlet and outlet.

4. **RESULTS AND DISCUSSION**

Figures 2(a) and 2(b) show the effect of bifurcation length (L^*) in BLSF. As the bifurcation length increases, both the plate temperature and the pressure drop increase. The optimum L^* is at the closest point to the inlet (0.1). Figures 2(c) and 2(d) show the effect of pin volume in HPPF. As the pin volume increases, the plate temperature decreases while the pressure drop increases. Hence, the optimum pin volume is 50% and 10% in terms of thermal, and hydraulic performance respectively. This is because as the pin volume increases, the flow obstruction increases, thus, increasing the pressure drop.

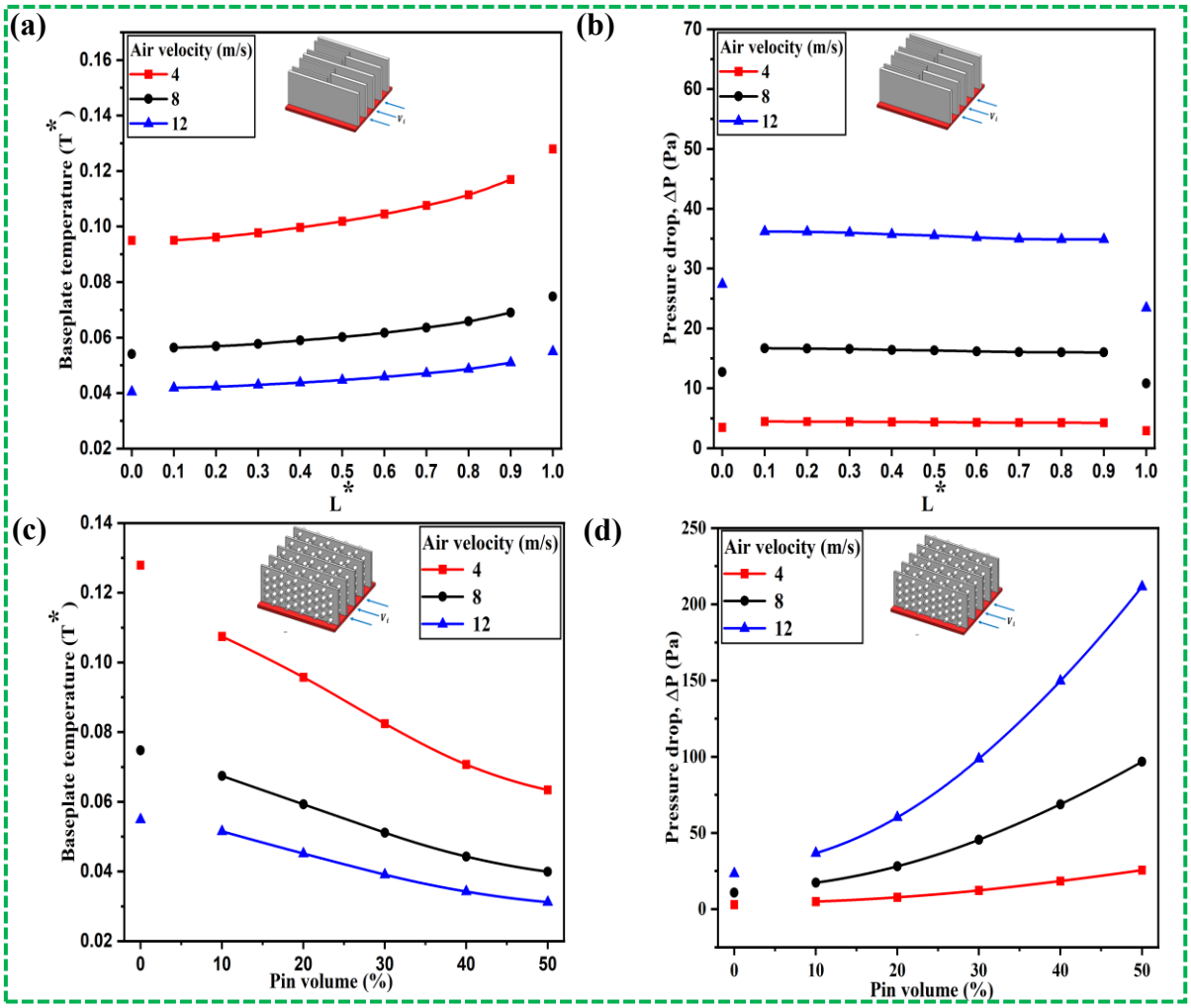

Fig. 2 – Effect of bifurcation length of BLSF on: (a) temperature, (b) pressure drop, and effect of HPPF pin volume on (c) temperature, (d) pressure drop.

5. **CONCLUSION**

In this study, we numerically showed the effect of optimizing the rectangular plate fin heatsink. The best configuration, which has a lower baseplate temperature, was found to be HPPF as shown in Figure 3(a). In contrast, the optimal configuration in terms of pressure drop is the conventional RPF heatsink, as shown in Figure 3(b). HPPF and BLSF resulted in a 47% and 25% reduction in baseplate temperature compared to the

RPF heatsink, respectively. The findings of this study are not limited to electronics cooling but also photovoltaic modules and similar applications.

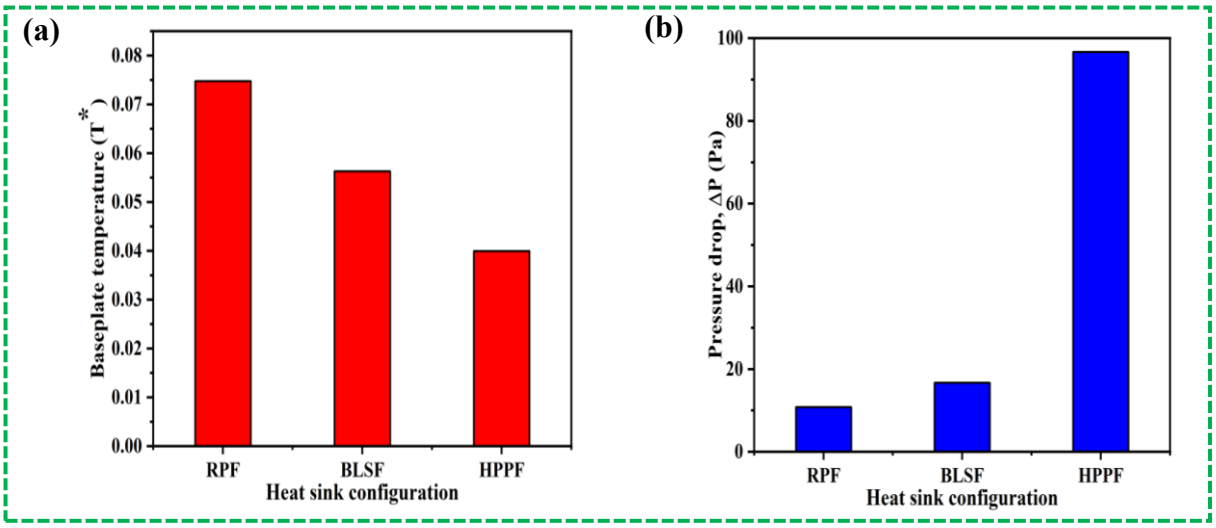

Fig. 3 – Comparison of (a) temperature and (b) pressure drop between RPF, BLSF, and HPPF.

REFERENCES

1. Almerbati A., Lorente S., Bejan A., The evolutionary design of cooling a plate with one stream, *Int. J. Heat Mass Transf.,* **116**, pp. 9–15, 2018.
2. T. Ambreen, Saleem A., Tanveer M., Shehzad A.K.S.A., Park C.W., Irreversibility and hydrothermal analysis of the MWCNTs/GNPs-based nanofluids for electronics cooling applications of the pin-fin heat sinks: Multiphase Eulerian-Lagrangian modeling, *Case Studies in Thermal Engineering*, **31** (2022).
3. Han X.H., Liu H.L., Xie G., Sang L., Zhou J., Topology optimization for spider web heat sinks for electronic cooling, *Appl. Therm. Eng.*, **195** (2021).
4. Xu J.L., Gan Y.H., Zhang D.C, Li X.H., Microscale heat transfer enhancement using thermal boundary layer redeveloping concept, *Int. J. Heat. Mass Transf.*, **48**, *9*, pp. 1662–1674 (2005).
5. Matsushima H., Almerbati A., Bejan A., Evolutionary design of conducting layers with fins and freedom, *Int. J. Heat Mass Transf.*, **126**, pp. 926–934 (2018).
6. Adhikari R.C., Pahlevani M., Characteristics of thermal plume from an array of rectangular straight fins with openings on the base in natural convection, *International Journal of Thermal Sciences*, **182**, p. 107798 (2022).
7. Almerbati A., Hexagonal and mixed arrays of flow channel design in counterflow heat exchanger, *International Communications in Heat and Mass Transfer*, **124** (2021).
8. Salim B. *et al*., Three-dimensional transient CFD modeling of multiple finned aluminum foam heat sinks in a horizontal channel, *Alexandria Engineering Journal*, **78**, pp. 426–437 (2023).

CONSTRUCTAL LAW CONFERENCE – CLC2024
Design in Nature and Evolution
Romanian Academy, Bucharest, 10–11 October 2024

Proceedings of CLC2024
pp. 97–100

FORGOTTEN PRINCIPLES: HOW THE DIGITAL AGE TRANSFORMED THE HUMAN CONNECTION TO PHOTOGRAPHY

ELSIE (M. GOTHMAN)

27 Raven Dr, Idaho Springs CO 80452, USA
elsiegothman@gmail.com

The goal of this paper is to explore the human connection to photography and examine the different principles that have been impacted by digital advancements in photography. This paper will investigate these principles and how they affect the perception of the beauty seen in photographs. The investigation of these principles builds upon Adrian Bejan's acclaimed book, 'Time and Beauty,' and the principles outlined in Constructal Law.

Keywords: Photography; Human Development; Perception; Scan; Light.

1. INTRODUCTION

Imagine human development as rivers flowing through time. The riverbed symbolizes accumulated knowledge, while the surrounding land represents the various opportunities and challenges human development has encountered. This land can be rugged, filled with rocks and obstacles that redirect the water's course, or it can be smooth clay, facilitating easy flow. The flow of the river signifies the energy invested in a chosen path. With enough flow, the water can cut deep, establishing historic roots, but without sufficient flow, a branch of the river can dry up and lose momentum. Technology functions like a pipeline, transporting our water more swiftly to desired destinations, and providing easier access. However, this comes at the cost of bypassing the natural riverbed, which holds the historical context and experiences of the land traversed. While the destination remains the same, the foundational knowledge imprinted in the riverbed is removed entirely when using a pipeline, altering our connection to the journey and the land left behind.

The pipeline of technology in the realm of digital photography has fundamentally changed the principles that make photography an art and changed the fundamental connection of photography with the human experience. Certain key elements of photography, namely how the light is captured, the aspect ratio of a photo, and the rate of perception of movement, have all been significantly impacted by this evolution. While digital photography has enhanced ease of use and photo quantity, it has also diminished the importance of these crucial factors which are deeply connected to our human appreciation of images. Through the understanding of these critical elements and their change over time, it is easy to see how the beauty and nostalgic feeling of film photography are more deeply connected to the human experience and represent a lost form of art that has yet to be replicated by digital means.

DOI: https://doi.org/10.59277/CLC/2024.25

2. METHODS AND FUNDAMENTALS

The beauty standards integral to Constructal Law as argued in “Time and Beauty” by Adrian Bejan are most closely supportive of this argument. The following methods described within this law are crucial to understanding the fundamental differences between digital and film photography:

- The medium in which light is captured
- Ratio aspects within film development and digital megapixels
- Perceived digital quantity

2.1. Medium for how light is captured

A film negative is created by casting shadows onto light-sensitive film which creates an inverted copy of the captured light. This process is raw and complete, avoiding the pixelation necessary for the coded structure of digital photos and identical to the method by which our own eyes interpret light. Since the negative is an exact shadow-casting of the moment, the quality remains consistent when enlarged through a light projector. In contrast, a digital camera focuses light onto a sensor (CCD or CMOS), converting it into an electrical signal. The sensor's pixels record this signal as a numerical value. These analog signals are then converted into digital data, which is used to recreate the captured light in separate pixels, forming a digital image. When enlarged these digital images lose their quality with size and turn into enlarged pixels. This causes a fractal look throughout the perceived image making it more difficult to discern change.

2.2. Ratio aspects

Film photography embodies the beauty standard of Constructal Law by maintaining the standard alignment of natural light as seen through human eyes. Film is shot in 24mm × 36mm dimensions, resulting in a more desirable 2×3 ratio, and offers a natural composition that is more easily and naturally scanned by human eyes attuned to this aspect ratio. In contrast, digital photography often reverts to the 3×4 ratio. This is most common in the digital photos taken by iPhones, which are encoded into dimensions of 3 024–4 032 pixels.

2.3. Perceived digital quantity

Saccades are small eye movements that occur within human eyes 3–5 times per second, allowing them to thoroughly scan our surroundings. Film photography requires more than a second to capture and rewind each photo, and allows for multiple saccades per photograph, making each one anatomically memorable. The limited quantity of film encourages thoughtful composition and intentionality. In contrast, digital photography captures images at shutter speeds faster than 1 millisecond, outpacing the 200–300 millisecond duration of

saccades. This rapid capture rate allows for more photos than our eyes can naturally process, making the act of taking photos effortless, less deliberate, and artificial.

3. **DISCUSSION AND CONCLUSIONS**

Contrast is defined as the change in time over the photo. The speed at which we perceive and understand an image depends on how quickly our eyes can discern the elements and actions within it. With film photography, this perception of scanning is a little more at ease since film isn't fractal. Negatives, in the context of film photography, don't have megapixels in the same sense as digital images. This gives a smooth transition from different changes in time of the photo just like in nature; Bejan himself even states that “Nature is not fractal. Every image is full, a continuum with distinct features distributed nonuniformly”[1]. Film, being a faithful replica of light, embodies this nonuniformity, enabling each photo to exude a natural and seamless aesthetic. The quality intentionality put into each photo allows for thoughtful shots that are remembered along with the moment. Furthermore, the preferred 2×3 aspect ratio of film facilitates swift comprehension of the perceived image, adding to its natural appeal.

The distinct principles underlying film photography contribute to the beauty and nostalgia associated with the art itself, which is deeply similar to our human interpretation of light and imagery. Digital photography, with its ease and lack of intentionality, can create a sense of time distortion. Many people feel they didn't fully "live" the moment because they were busy capturing it on their phones, experiencing the event through 2D megapixels rather than real reflections of light. This disconnects, along with a loss of understanding in how to take meaningful photos, has caused many to forget the fundamental purpose of photography: capturing each specific, beautiful, and intimite aspect of a moment.

ACKNOWLEDGEMENTS

I would like to extend my heartfelt gratitude to everyone who supported and guided me throughout this project. I am especially indebted to Professor Bejan, whose invaluable guidance and teachings enabled me to deve deeply into the application of Constructal Law.

Additionally, I am profoundly grateful to my family for their unwavering support and understanding throughout my studies.

REFERENCES

1. Bejan A., *Time and Beauty: Why Time Flies and Beauty Never Dies*, Harper, 2017.

[1] From Bejan, Adrian, *Time and Beauty: Why Time Flies and Beauty Never Dies*, Harper, 2017, p. 45.

2. Bejan A., Zane J.P., *Design in Nature: How the Constructal Law Governs Evolution in Biology, Physics, Technology, and Social Organization*, Anchor, 2013.
3. Camera Obscura, *Camera Obscura: What is a Camera Obscura?*, Camera Obscura, June 10, 2020, https://www.camera-obscura.co.uk/article/what-is-a-camera-obscura - :~:text=In fact, camera obscuras date,(or Mozi) in 400BC
4. Hofstätter M., *A Large Format Camera, Expired Film and Swans, What Else Do You Need for Wildlife Photography?*, YouTube, uploaded by Markus Hofstätter, 16 June 2021, https://www.youtube.com/watch?v=tS7Eb-vT-Fk.

CONSTRUCTAL LAW CONFERENCE – CLC2024
Design in Nature and Evolution
Romanian Academy, Bucharest, 10–11 October 2024

Proceedings of CLC2024
pp. 101–104

ENHANCING ENERGY ACCESS BY EARTH-AIR HEAT EXCHANGER FOR BUILDINGS' THERMAL COMFORT BY THE CONSTRUCTAL DESIGN

ALOÍSIO LEONI SCHMID[a], ALEXANDRE BESSA MARTINS ALVES[a,b], ALEXANDRE RUIZ DA ROSA[a], MARCELO RISSO ERRERA[c], GEORGE STANESCU[d,*]

[a]Construction Engineering Postgraduate Program, Federal University of Parana/ UFPR, Av. Cel. Francisco H. Dos Santos, 81530-000, Curitiba, Parana, Brazil, iso@ufpr.br, alexandre.bmalves@gmail.com, a.ruiz@saboiaruiz.com
[b]Postgraduate Program in Architecture and Urbanism, University of Vila Velha, Vila Velha, ES, 29102-920, Brazil
[c] Environmental Engineering Department, UFPR,81530-000, Curitiba, Parana, Brazil, errera@ufpr.br
[d]Graduate Program of Environmental Engineering, UFPR, 81530-000, Curitiba, Parana, Brazil, stanescu@ufpr.br
*Correspondence: stanescu@ufpr.br;Tel.+40-741-619-029

Harnessing soil low-depth thermal energy to support mechanical systems for buildings' thermal comfort has been considered one pathway for reducing the buildings' energy demand (avoid) and adding renewable energy to buildings. The literature addressed those issues in many ways. However, this work introduces two key novelties: (1) the optimization of the duct's configuration and (2) a strategy for the optimal use of the duct assembly to attend to the time-variable energy demand throughout the year. Both are based on the minimization of entropy generation. The irreversibility mechanisms relate to heat transfer and fluid flow in the EAHE and the coupled building-environment-soil-EAHE thermodynamic system.

This approach was carried out by numerically solving the mathematical model (3-D, transient, heat-conduction finite volume with an upwind scheme and heat convection inside the ducts by known convective correlations) developed considering a solid parallelepiped domain on the ground (W×L×H), crossed parallel to its central horizontal axis by several channels of rectangular section (w×L×h), positioned in arrangements of variable geometry.

The design degrees of freedom are the number of ducts, their dimensions, and the spacing among them while meeting prescribed thermal comfort temperatures for each season. Results show that if the energy access of the EAHE is enhanced or optimized for a date in the year, it may not be helpful in other seasons, thus showing that the greater access of the ground thermal energy throughout the year requires a compromise in the EAHE design.

Keywords: Built environment; Passive air conditioning; Entropy generation; Constructal design.

1. INTRODUCTION

Earth-Air Heat Exchangers (EAHE) have been addressed in the literature in many instances (*e.g.*, a review [1], modeling, simulation, and measurement [2, 3], and constructal design [4]). The metrics underlying those designs consider the potential thermal benefit for thermal comfort and the energy expenditure of blowing air through the ducts. Another design challenge is determining under which conditions a design shall be compared since the access of the thermal potential varies in space and time. Therefore, one shall understand the demand's thermal profile, the soil's thermal behavior, the soil-air heat transfer, and the design of duct geometry by minimizing the entropy generation [5].

2. PHYSICAL AND MATHEMATICAL MODELING

The gas-solid heat exchanger was modeled as a parallelepiped solid domain on the ground with dimensions $10\text{m}\times100\text{m}\times10\text{m}$ crossed parallel to its central horizontal axis by several channels of rectangular section

DOI: https://doi.org/10.59277/CLC/2024.26

($w \times 100m \times h$) positioned in variable geometry arrangements. The mathematical model considered mass and energy conservation and entropy balance. The degrees of freedom of the project are as shown in Fig. 1(a, b, c), the number of ducts, their dimensions, and the spacing between them. Meanwhile, the volumes of the solid parallelepiped domain (the gray color in Fig. 1) and all channels of the rectangular cross-section are kept constant (air flow occurs perpendicular to the paper sheet).

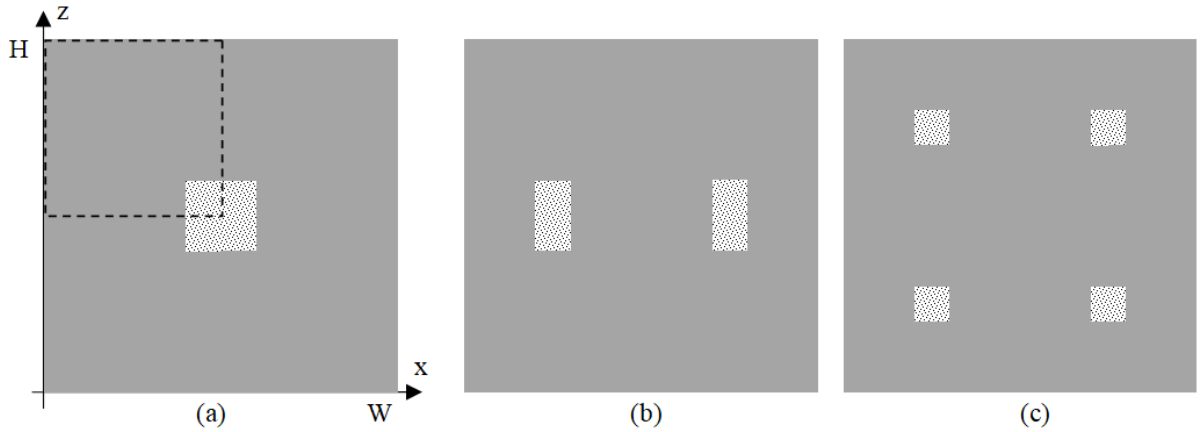

Fig. 1 – Arrangements of variable geometry are considered in the numerical simulations of the airflow passing throughout the parallelepiped solid domain (heat sink).

3. **RESULTS**

A particular demand for ambient air ($\dot{m} = 0.24$ kg) was initially considered, whose temperature must be reduced by 5°C, from 26°C to 21°C, for thermal conditioning purposes in a building when the ground temperature is approximately 18°C.The numerical results obtained based on the mathematical model $w = h = 2$ m indicate that, over long periods, the temperature of the soil at the contact surface with the air in the channels varies very little, while the air flows through the channels in a manner similar to a permanent process (see Fig. 2).

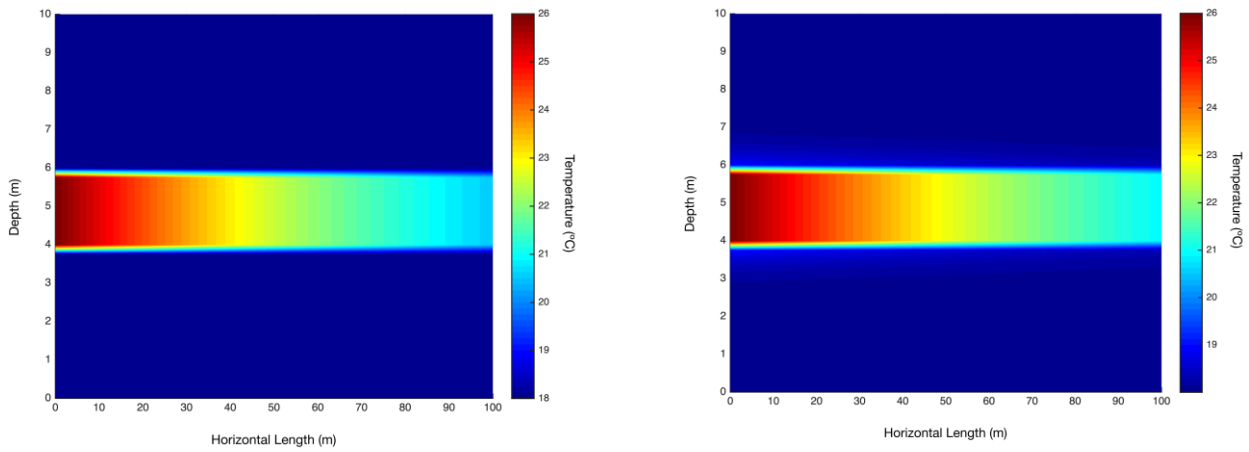

Fig. 2 – Temperature distribution in the middle of the solid domain and the flowing gas after 1 hour (a) of operation is very similar to that after 10 hours (b) of operation.

Based on these first results, for intermittent use for short periods of this type of gas-solid heat exchanger, the processes in the solid and gas are studied separately. Then, for minimal irreversibility, the optimal hydraulic diameter of the channels is determined based on the following formulae $D_{h,opt} = 4\dot{m}/(\pi\mu\rho\,Re_{opt})$, where μ and ρ are respectively the dynamic viscosity and air density, and $Re_{opt} = 2.023\,Pr^{-0.7}\,Be^{0.36}$ [5].

The number of channels to be implemented should be determined considering the thermal regimes that occur most frequently throughout the year and the possibility of meeting the demands for thermal conditioning purposes in a building using various combinations of one or more existing channels simultaneously. In this work, we seek the best of these combinations by minimizing entropy generation [5]:

$$\tilde{S} = \dot{S}'_{gen} / \dot{S}'_{gen,min} = 0.856 \times (Re/Re_{opt})^{-0.8} + 0.144 \times (Re/Re_{opt})^{4.8}. \quad (1)$$

4. **DISCUSSION AND CONCLUSIONS**

Although the problem is just optimizing the operation of the gas-solid heat exchanger when harnessing thermal energy from the ground, we are looking for its optimal functioning to satisfy the variable demand throughout the year. Once the channel geometry was optimized for a given regime, the question of how the already built channel systems would be operated in any other regime remains. In this work, the answer is given by minimizing the entropy generation.

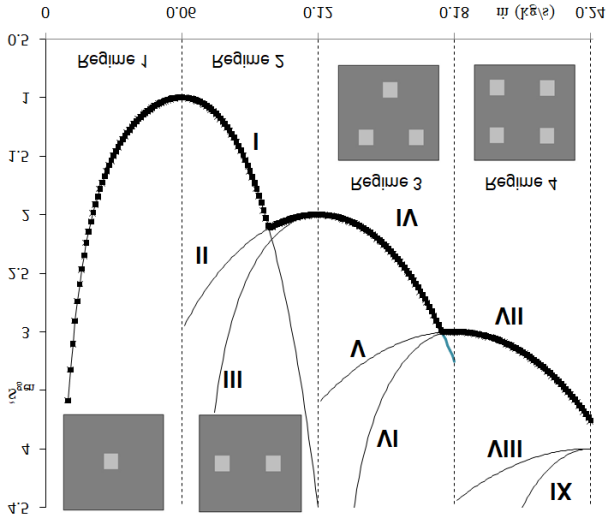

Fig. 3 – Dimensionless minimal entropy generation for different operating regimes that aim to reduce the variable air mass flow temperature by 5°C.

In Fig. 3, the black square markers indicate the sequence of operations leading to minimum entropy generation. For example, in Regime 2, where up to two of the channels initially optimized for airflow can be used, operation with minimum entropy generation occurs by initially passing all the airflow through a single channel (line **I**) while for $0.06 \le \dot{m} \le 0.098$ dividing the total airflow equally between the two operating channels (line **II**).

REFERENCES

1. Bordoloi N., Sharma A., Nautiyal H., Goel V., An intense review on the latest advancements of Earth Air Heat Exchangers, *Renewable and Sustainable Energy Reviews*, **89**, pp. 261–280 (2018).
2. Brum R. da S., Vaz J., Roch, L.A.O., dos Santos E.D., Isoldi L.A., A new computational modeling to predict the behavior of Earth-Air Heat Exchangers, *Energy and Buildings*, **64**, pp. 395–402 (2013).
3. Alves A.B.M., Schmid A.L., Cooling and heating potential of underground soil according to depth and soil surface treatment in the Brazilian climatic regions, *Energy and Buildings*, **90**, pp. 41–50 (2015).
4. Nunes B.R., Rodrigues M.K., Rocha L.A.O. *et al*., Numerical-analytical study of earth-air heat exchangers with complex geometries guided by constructal design, *Int. J. Energy Res*., **45**, *15*, pp. 20970–20987 (2021).
5. Bejan A., Sylvie L., Thermodynamic optimization of flow geometry in mechanical engineering and civil engineering, *J. Non-Equilib. Thermodyn*, **26**, pp. 305–354 (2001).

CONSTRUCTAL LAW CONFERENCE – CLC2024
Design in Nature and Evolution
Romanian Academy, Bucharest, 10–11 October 2024

Proceedings of CLC2024
pp. 105–108

COLD PLATE DESIGNS: A COMPARISON OF EVALUATION METRICS - CONSTRUCTAL SVELTENESS AND GLOBAL RESISTANCE

CHAIANAN SAILABADA[a], CRISTOFER HOOD MARQUES[b],
JOSE V.C. VARGAS[c], JUAN ORDOÑEZ[d,*]

[a] Department of Mechanical Engineering, FAMU-FSU College of Engineering, Energy and Sustainability Center, Center for Advanced Power Systems, Florida State University,
[b] School of Engineering, Federal University of Rio Grande -FURG, Rio Grande, RS 96203-900,
Department of Mechanical Engineering, FAMU-FSU College of Engineering, ESC, CAPS, Tallahassee, FL 32310, USA
[c] Department of Mechanical Engineering, Graduate Program in Mechanical Engineering, PGMEC, and Sustainable Energy Research & Development Center, NPDEAS, Federal University of Paraná, UFPR, CP 19011, 81531–980, Curitiba, PR, Brazil
[d] Department of Mechanical Engineering, FAMU-FSU College of Engineering, Energy and Sustainability Center, Center for Advanced Power Systems, Florida State University, Tallahassee, FL, 32310, jordonez@fsu.edu
cs22bc@fsu.edu, cristoferhood@furg.br, vargasjvcv3@gmail.com, (correspondence) jordonez@fsu.edu

Cold plates are heat transfer devices used in various industries such as aerospace, automotive, and telecommunications primarily to prevent overheating and ensure efficient operation of electronics and power electronics components. They are compact, flat heat exchangers designed mainly by dissipate heat to a liquid coolant. The present paper compares the thermal performance of three serpentine arrangements using a global resistance metric that accounts for thermal resistance and pumping power. Then, various Svelteness definitions that differ in the external length scale are investigated. All the designs hold the same five degrees of freedom: plate area, plate weight, pipe diameter, pipe bend radius ratio, and plate length ratio, but only the two latter ones are investigated here. Results show that the simple "S" shape performs better regarding the global resistance metric, mainly for configurations with low values of the ratio between the bend curvature radius and the pipe diameter (*R/d*). The three variants of Svelteness capture the general thermal performance very well, particularly the R/d effect and the impact of the plate aspect ratio (*W/d*). However, none of the Svelteness definitions considered could completely capture the performance differences among the different arrangements measured with the global resistance metric.

Keywords: Cold plates; Conduction; Convection; Internal flow; Svelteness.

1. INTRODUCTION

Power electronic components require an efficient thermal management system to maintain their performance and longevity [1]. Thermal management can be achieved through active or passive means. Active thermal management utilizes forced convection, employing fans or pumps to circulate a fluid coolant. In contrast, passive cooling methods rely on heat sinks and fins, utilizing free convection [2]. An example of indirect active cooling, whose design can benefit from results developed in relation with the Constructal Law, is the cold plate, which consists of a plate with attached or internal pipes for coolant flow.

Investigations considering various pipe shapes for heat-transferring devices were found in the literature [3-7] and motivated the present study. This work compares three internal pipe shapes for cold plates with the same degrees of freedom. The novelty here is in proposing two modified S-type serpentine shapes and investigating their performance according to a proposed non-dimensional global thermal resistance and three Svelteness definitions that differ in the external length [7].

DOI: https://doi.org/10.59277/CLC/2024.27

2. **METHODOLOGY**

Computational fluid dynamics simulations were performed in OpenFOAM considering steady-state solution and incompressible flow with constant thermophysical properties. Turbulence modeling was obtained with the Reynolds Average Navier-Stokes (RANS) method, and the $\kappa - \varepsilon$ model was used to close the system of equations. At the pipe inlet, the fluid temperature and speed were specified, while a heat transfer rate was prescribed on one of the plane surfaces of the cold plate, with the remaining surfaces being treated as adiabatic.

Figure 1 shows the three serpentine shapes and the variables that define the geometries. The geometrical relationships are determined by the expressions in Eq. 1 and the variable listed in Table 1.

$$R = R/d \cdot d,\ \ W = \left(A_p \cdot W/D\right)^{0.5},\ \ D = \frac{Ap}{W}, S_1 = 2R,\ \ S_2 = \frac{D-2S_1}{2} \tag{1}$$

Table 1

Variables

Parameters	Decision variables		Dependent variables
	R/d	***W/D***	
d = 0.004 m	2.0	1.2	H
A_p = 0.20 m²	6.0	1.6	$\dot{m}$
T_i = 298.15 K	10.0	2.0	T_o
Q = 1000 W			*T-field*
Δp = 0.25 bar			
m_p = 2.50 kg			

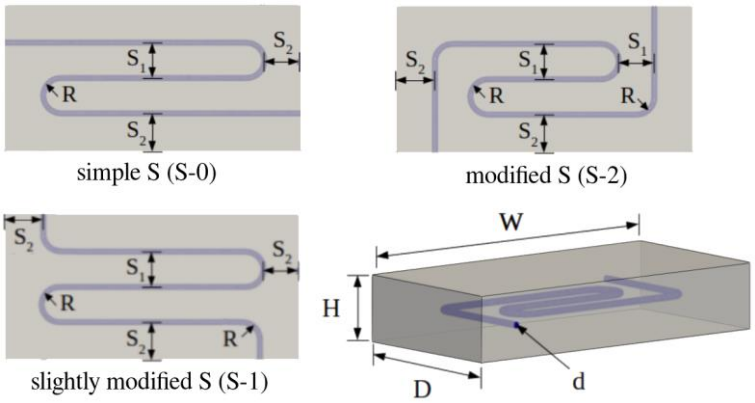

Fig. 1 – Serpentine shapes.

Three values are explored for each of the two degrees of freedom and for each of the three serpentine shapes, totaling 27 configurations.

3. **RESULTS AND DISCUSSION**

Results indicate that design S-0 provides a better temperature distribution, particularly for lower values of *R/d* and *W/D* (Fig. 2). When analyzing the non-dimensional global thermal resistance (defined here as the product of global thermal resistance and pumping power divided by fluid inlet temperature), S-0 exhibits significantly lower values, especially for lower *R/d* and *W/D* (Fig. 3).

To correlate the thermal performance with potential geometric shape advantages, three Svelteness definitions were examined in Figs. 4, 5 and 6. These definitions (see figures insets) differ in the external length scale (numerator of the equations), while the internal length scale consistently depends only on the serpentine volume (v).

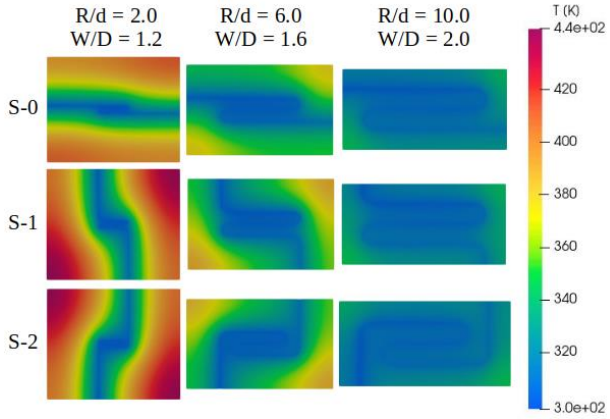

Fig. 2 – Temperature fields.

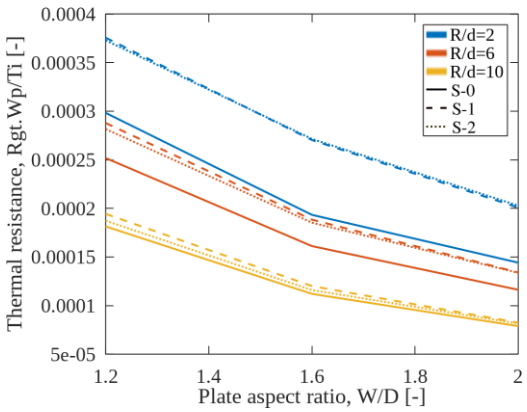

Fig. 3 – Non-dimensional global resistance.

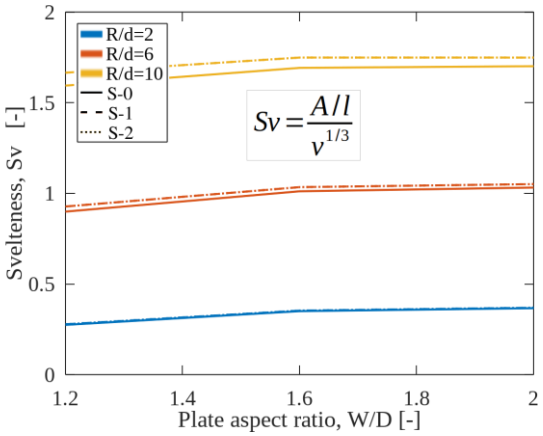

Fig. 4 – Svelteness by definition “a”.

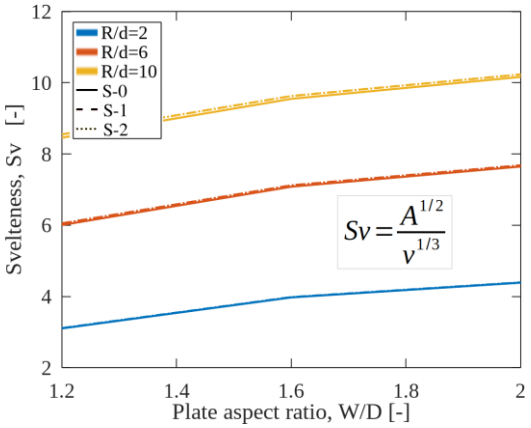

Fig. 5 – Svelteness by definition “b”.

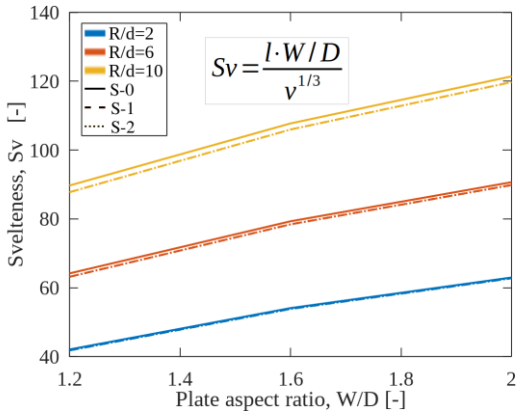

Fig. 6 – Svelteness by definition “c”.

Consider A as the area available to mount heat-dissipating devices and l as the serpentine length. Although the Svelteness definitions used do not capture the superiority of the S-0 design for R/d values of 2 and 6 (suggested by Fig.3), all the Svelteness definitions capture the general thermal performance, particularly concerning R/d. The impact of W/D is more strongly seen in Svelteness "c" (Fig. 6). Note that the current simulations assumed rough wall pipe and are for turbulent flow in all the cases.

REFERENCES

1. Ordonez J.C., Sailabada C., Chalfant J., Chryssostomidis C., Li C., Luo K., Santi E., Tian B., Biglo A., Rajagopal N., Stewart J., DiMarino C., Thermal Management for Ship Electrification-Approaches for Power Electronic Building Blocks and Power Corridors, *IEEE Transactions on Transportation Electrification*, 2024.
2. Yoon Y., Hyeon S., Kim D.R., Lee K.-S., Minimizing thermal interference effects of multiple heat sources for effective cooling of power conversion electronics, *Energy Conversion and Management*, **174**, pp. 218–226 (2018).
3. Kobayashi H., Lorente S., Anderson R., Bejan A., Serpentine thermal coupling between a stream and a conducting body, *Journal of Applied Physics*, **111**, *2*, p. 044911 (2012).
4. Almerbati A., Lorente S., Bejan A., The evolutionary design of cooling a plate with one stream, *International Journal of Heat and Mass Transfer*, **116**, pp. 9–15 (2018).
5. Mosa M., Labat M., Lorente S., Role of flow architectures on the design of radiant cooling panels, a constructal approach, *Applied Thermal Engineering*, **150**, pp. 1345–1352 (2019).
6. He L., Hu X., Zhang L., Xing T., Jin Z., Performance evaluation and optimization of series flow channel water-cooled plate for IGBT modules, *Energies*, **16**, *13* (2023).
7. Clemente M.R., Panão M.R.O., On the Svelteness as an Engineering Tool in Constructal Design: A Critical Review, *Applied Sciences*, **12**, *23*, p. 12053 (2022).

CONSTRUCTAL LAW CONFERENCE – CLC2024
Design in Nature and Evolution
Romanian Academy, Bucharest, 10–11 October 2024

Proceedings of CLC2024
pp. 109–112

ROBOTIC LEGS DESIGN – CONSTRUCTAL CONSIDERATIONS

JUAN ORDONEZ[a], CAMILO ORDONEZ[b]

[a] Department of Mechanical Engineering, FAMU-FSU College of Engineering, Energy and Sustainability Center, Center for Advanced Power Systems, Florida State University, Tallahassee, FL, 32310
[b] Department of Mechanical Engineering, FAMU-FSU College of Engineering, Energy and Sustainability Center, Center Intelligent Systems, Control, and Robotics, Florida State University, Tallahassee, FL, 32310
Correspondence: jordonez@fsu.edu, cordonez@eng.famu.fsu.edu

In robotic navigation, wheels are highly efficient for engineered surfaces. However, they need to be more efficient when navigating over rough terrains. Evolution has resulted in limbed creatures that are highly adapted to extreme terrains. This paper explores the design of robotic legs for sagittal motion in uneven terrains. The paper builds upon locomotion theories to identify geometrical features of the leg and groups of legs as a function of terrain features. The predictions of the analytical models are compared against observations in the animal kingdom. The study is focused on legs that can be represented with two degrees of freedom, connected via revolute joints. It uses simplified terrain features and reduced-order dynamic models to evaluate the cost of transport associated with the different legs and terrain configurations. Examples of animal and animal-inspired robots to which the model applies include crabs, horses, and some insects. The model is expected to help design more agile robots and be extensible to designing human prostheses and end effectors for robotic manipulators.

Keywords: Robotic locomotion; Animal design; Locomotion.

1. INTRODUCTION

The evolution of animal locomotion is a primary example of the constructal law in action. Locomotion modalities have evolved to support more efficient ocean, air, and land motion. Several features of the locomotion strategies and the geometry of the structures that support that locomotion have evolved to facilitate access to the flows of animal mass on the planet. This paper builds upon the constructal theory of animal locomotion [1] to explore features of legs that can guide the designs of mobile robots.

2. MATERIALS AND METHODS

In [1], Bejan shows how, by treating land animal locomotion as a rolling body, it is possible to predict inclination angles that favor forward motion, the benefit of two legs, and time scales for the swinging between them. The average forward speed, V_x, during the time interval t_1 while the body free falls in a rotational motion to the angle, θ, (see Fig. 1) is given by

$$V_x = \frac{R \sin(\theta)}{\left[2\left(\frac{R}{g}\right)(1-\cos(\theta))\right]^{1/2}}; V_y = \frac{R\,(1-\cos(\theta)}{\left[2\left(\frac{R}{g}\right)(1-\cos(\theta))\right]^{1/2}}, \quad (1)$$

where the duration of the time interval of free fall is the denominator in eq. (1). The variation of V_x and V_y with the angle of rotational motion is shown in Fig. 1.

DOI: https://doi.org/10.59277/CLC/2024.28

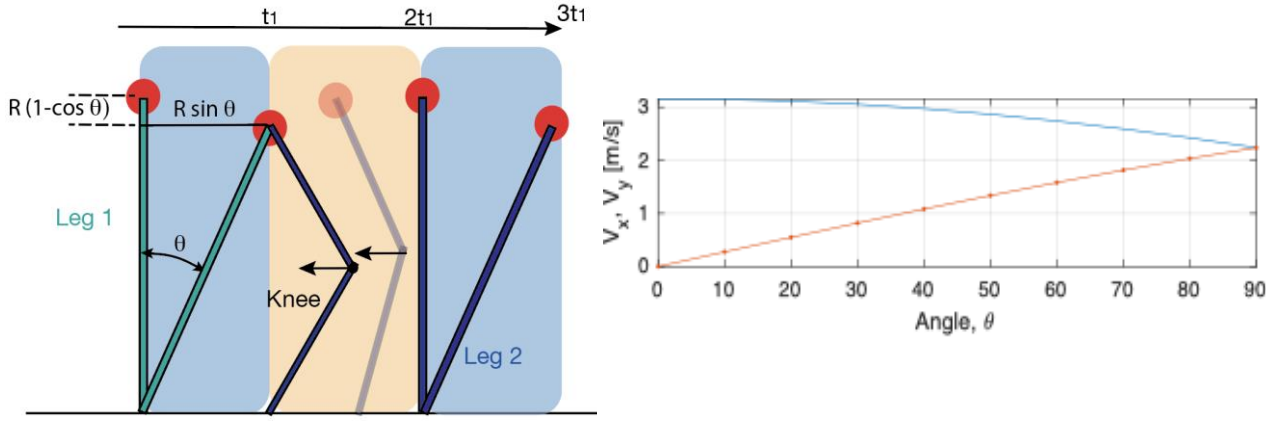

(a) (b)

Fig. 1 (a) Up to t_1, leg 1 supports rotational 'free-fall' motion, at that point leg 2 absorbs impact and provides the torque necessary to lift the body again. (b) Variation of vertical and horizontal speeds in the free-fall rotational model of locomotion. The horizontal speed is maintained near the maximum if $\theta \lesssim 30°$.

3. **EXPERIMENTAL RESULTS:**

A motion tracking system was used to monitor the angles during the sagittal walking stance of an individual with and without obstacles. Figure 2a illustrates the tracking of the angle under normal walking speed with no obstacles. It can be observed that the rotational angle 22º is close to that predicted by constructal theory (≲30º) [1]. Figure 2b shows schematically key variables involved in two-link multibody dynamic systems used to study stair climbing.

4. **CLIMBING UPSTAIRS:**

The model assumes that the stance leg is composed of two massive thin rods A, B with masses m_A and m_B. The remaining body mass is modelled as a particle H with mass m_H, and situated at the hip. Actuation is provided via ankle (τ_a) and knee (τ_b) torques. Additionally, we assume that each joint has linear viscous damping characterized by a damping coefficient b. The dynamic model is developed using a Newton/Euler formulation.

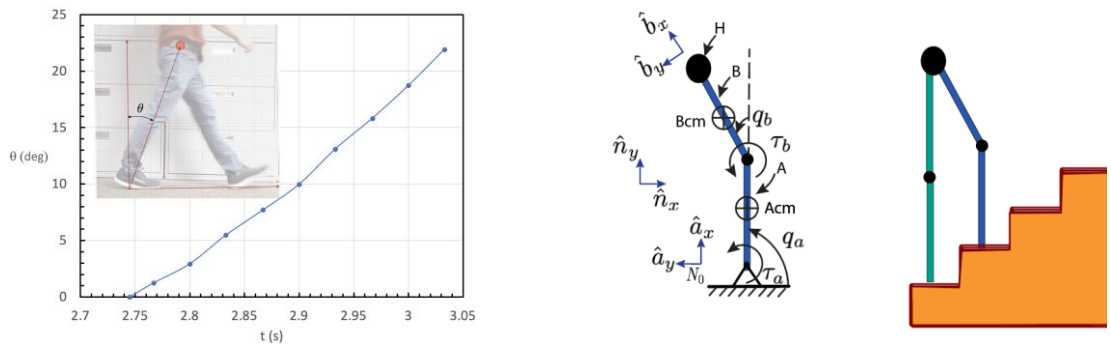

(a) (b)

Fig. 2 – (a) Measurement of rotational motion angle limit at which trigger to second leg occurs under normal walking stance. (b) Model schematic – stairs climbing.

Let the state of the system be $x = [q_a\ \dot{q}_a\ q_b\ \dot{q}_b]$, and its equations of motion in state space form, $\dot{x} = f(x,u)$. The system control input is $u = [\tau_a\ \tau_b]$. To determine the effort required to climb one step, we employ trajectory optimization:

$$\min_{x,u,T} \int_0^T \tau_a^2(t) + \tau_b^2(t)\,)dt,$$

$$s.t.\quad \dot{x} = f(x,u);\quad x(0) = x_0;\ x(T) = x_f,$$

$$q_{a,min} \le q_a \le q_{a,max};\ q_{b,min} \le q_b \le q_{b,max},$$

where the initial and final states are $x_0 = [q_{a,0}\ 0\ q_{b,0}\ 0]$ and $x_f = [\frac{\pi}{2}\ 0\ 0\ 0]$.

We formulate a nonlinear program (NLP) via direct collocation [2] using smooth and exact derivatives of the objective function and all constraints using the MATLAB COALESCE framework [3] and generate a solution using the large-scale NLP solver, IPOPT [4]. Figure 3 shows trajectory optimization results to climb one step of height of 12 cm. The ankle and knee torque magnitudes are consistent with torque values estimated via motion capture in [5]. Assuming that the overall objective is to climb upstairs for a total height of 3 m and that every step results in a horizontal displacement of 0.3 m, it is then possible to estimate the total effort to climb up as a function of step height. Table 1 presents the results and indicates that for this cost function and the model being used, the optimal step height is 12 cm.

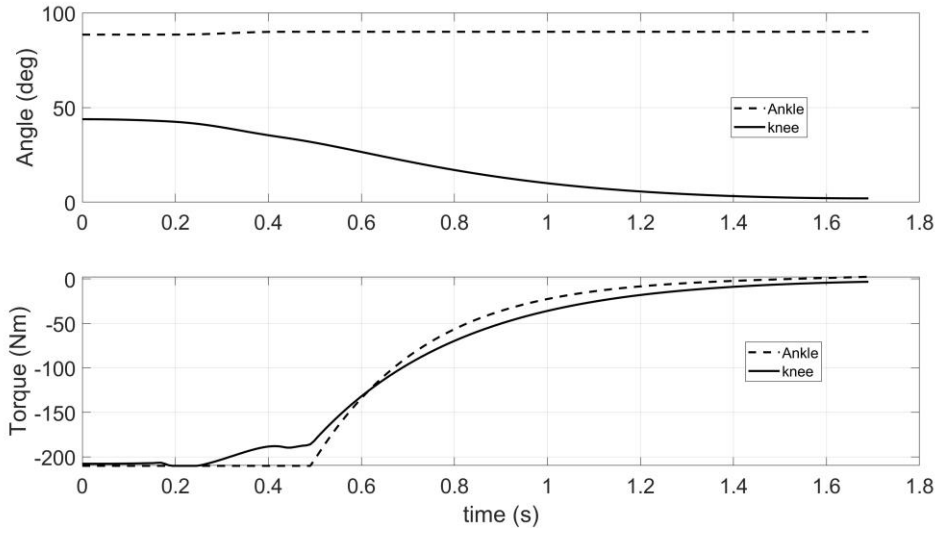

Fig. 3 – Angles and torque profiles to minimize climb effort (step height 12 cm).

Table 1

Effort required for climbing upstairs. The calculation assumes that with each step, the horizontal displacement is 30 cm

Step height (cm)	6	8	10	12	14	16
Effort per step ($\times 10^4$ Nm^2 s)	4.04	4.51	4.91	5.24	6.65	14.47
Number of steps needed to climb 3 m	50	37.5	30	25	21.42	18.75
Effort to climb 3m ($\times 10^4$ Nm^2 s)	202	169.12	147.3	131	142.44	271.31

5. **DISCUSSION AND CONCLUSIONS**

For walking on horizontal surfaces, the experimental value for the rotational angle 22^o (Fig. 2 (a)) is close to that predicted by constructal theory (~30^o) [1]. For obstacle climbing, the dynamic model optimization results suggest that the optimal step height for human-scale legs is close to 12 cm, which is reflected in modern staircases. This model and optimization approach can be used to size robot legs for robot navigation when there is information on the typical obstacle height.

REFERENCES

1. Bejan A., The constructal-law origin of the wheel, size, and skeleton in animal design, *American Journal of Physics*, **78**, *7*, pp. 692–699 (2010).
2. Kelly M., An introduction to trajectory optimization: How to do your own direct collocation, *SIAM Review*, **59**, *4*, pp. 849–904 (2017).
3. Jones M., Optimal control of an underactuated bipedal robot, Master Thesis, Oregon State University, 2014.
4. Wachter A., Biegler L., On the implementation of an interior-point filter line-search algorithm for large-scale nonlinear programming, *Math. Prog*., **106**, *1*, pp. 25–57 (2006).
5. Serbest K. Cilli M., Eldogan O., Biomechanical effects of daily physical activities on the lower limb, *Acta Orthopaedica et Traumatologica Turcica*, **49**, *1*, 85–90 (2015).

CONSTRUCTAL LAW CONFERENCE – CLC2024
Design in Nature and Evolution
Romanian Academy, Bucharest, 10–11 October 2024

Proceedings of CLC2024
pp. 113–116

UNIVERSAL DYNAMICS: A THEORY OF EVERYTHING WITHOUT INVENTING ANYTHING

JOHN MULLALY

Director, Global Strategic Alliances, Kyndryl; IBM Master Inventor, Emeritus
17 Wayne Drive, Coxsackie NY, 12051, USA
john.mullaly@gmail.com; 1-914-659-6209

This paper seeks to reconcile the constructal law with thermodynamics, quantum mechanics, and general relativity. Reconciling the constructal law with the more established laws of thermodynamics, we constitute a more complete and universal model of dynamics capable of explaining emergent and evolving design configurations observable throughout nature. Presented is a theory of universal dynamics, in which a core set of known universal laws can explain the universe's evolution through space, time, and all its emergent properties.

Keywords: Constructal; Quantum; Relativity; Complexity; Evolution; Emergence.

1. INTRODUCTION

Chemist P.W. Atkins wrote of the wonder that life is "not over in a flash" but rather "a slow unwinding of energy [1]." The same could be said for the rest of the universe, otherwise destined for a death state of maximum entropy [2]. But it's not over in a flash; the energy of the Big Bang continues to evolve, with a progressively complex structure that enhances access to flow and throughput of energy [3–5]. The constructal law explains how and why nature does this, despite the 2nd law of ever-increasing entropy. As its author Adrian Bejan explained, "The designs we see in nature are not the result of chance. They emerge to enhance access to flow in time [6]." Enhanced flow means flowing faster and further with less resistance and less energy sacrificed to entropy; this extends the world line of the flow system, increasing its proper time duration, or lifetime. It is thus a universal tendency of every flow system, with the freedom to do so, to structure itself in space-time to maximize its world line, thus forestalling entropy and death.

2. APPROACH

Physicist Neil Turok said earlier this year, "Maybe we don't need extra dimensions." "Maybe we do know the laws of physics….and what we have to do now is to understand how to use these laws to understand nature" [7].

As a thought experiment, assume only that the laws of each of the constructal laws, thermodynamics, general relativity, and quantum mechanics are all true and inviolable but incomplete to the extent they are not clearly reconciled with each other. Rather than invent theoretical constructs to fill the gaps, let's rethink how the four known pieces could logically and physically fit together. Consider a minimum viable universe at the time of the Big Bang, at which only universal law applied and only energy existed. From

DOI: https://doi.org/10.59277/CLC/2024.29

there, using only universal laws, can we explain how everything else in the universe emerged and evolved? Such a universal law, if one exists, must be absolutely universal and apply everywhere, at all times, at all scales of space-time. It must also explain how other laws are derived henceforth, and how such laws relate and apply to each other. This is the lens through which we consider each of the currently disparate models: How universal is it? How can it explain or be explained by each of the others? Finally, how predictive is it, and how is it supported by observational data?

3. **OBSERVATIONS**

• If universal means applicable at any place, any time, and any scale, that rules out quantum mechanics; scale symmetry being broken with the emergence of matter from energy; does not explain the other laws but can be explained by universal dynamics.

• The constructal law implies increasing efficiency (η) in a flow system, which proportionally increases energy rate density (Φ_m[erg/s/g]) over the lifetime or proper time (τ) of the system (see Fig. 1)

$$\Delta\eta \geq 0 \tag{1}$$

$$\eta \propto \Phi_m \tag{2}$$

$$\eta \propto \tau \tag{3}$$

• The constructal law and 2nd law of thermodynamics are closely interrelated [8]; a new insight is that both are monotonically positive and change in efficiency is inversely proportional to the change in entropy (see Fig. 2).

$$\Delta\eta = \frac{1}{\Delta S} \tag{4}$$

• For any system, at any point and any scale of spacetime, universal dynamics dictate that energy remain constant and entropy increases towards dynamic equilibrium or death and also that with the freedom to do so, the flow of energy structures itself to enhance access to flow, thus extending its world line in spacetime and forestalling entropy and death (see Fig. 3).

• The general relativity concept of proper time is integral to universal dynamics; the phenomena of spacetime curvature and gravity cannot explain the other laws but can be explained as manifestations of universal dynamics.

All figures are author's illustrations of the key concepts described.

Universal dynamics predicts directional evolution, towards higher levels of efficiency and energy throughput, through emergent hierarchical structure and complexity which extends the world line and proper time of the system.

To ground this theory in observation, we can look back across several distinct epochs in the evolution of the universe. From the Big Bang to the present, each epoch demonstrates increasing levels of emergent complexity and energy density. This initial analysis shows observations to be consistent with the predictions of the theory.

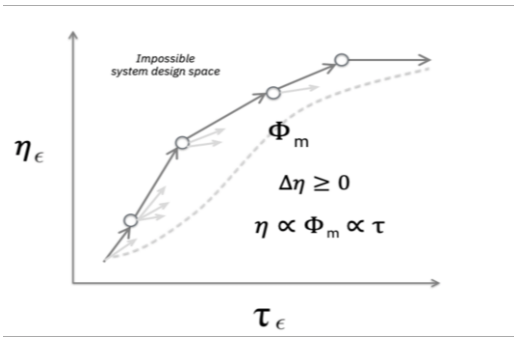

Fig. 1

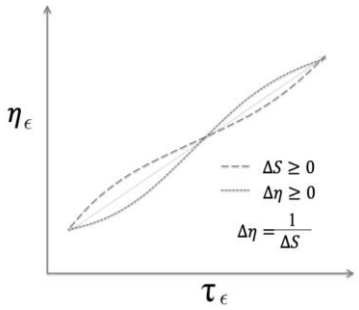

Fig. 2

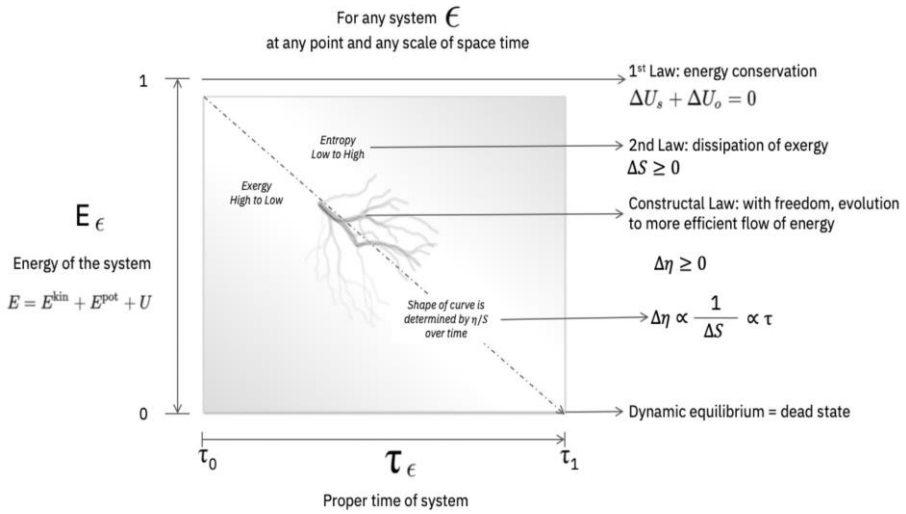

Fig. 3

Table 1

Predictions and observations across epochs of evolution in the universe

Predictions	**Fields and spacetime**	**Particles and matter**	**Stars and galaxies**	**Planets and plants**	**Animals and society**	**Technology**
Directional	yes	yes	yes	yes	yes	yes
Emergent structure	yes	yes	yes	yes	yes	yes
Hierarchical structure	yes	yes	yes	yes	yes	yes
Increasing energy rate density Φ_m [erg/s/g] (source: [3])	TBD	TBD	Milky Way, 12 Gya: 0.5 erg/s/g	Earth geosphere, 4 Gya: 4 erg/s/g Plants generally, 3 Gya: 900 erg/s/g	Animals, 0.5 Gya: 40,000 erg/s/g; Human society, 0 Gya: 500,000 erg/s/g; Hunter-gatherers, 300 Kya: 4×10^4 erg/s/g	Agriculturalists, 10 Kya: 10^5 erg/s/g Industrialists, 0.2 Kya: 5×10^5 erg/s/g Technologists 0 Kya:2×10^6 erg/s/g

4. **CONSIDERATIONS**

This view of universal dynamics is based entirely on a set of known laws that seem able to explain emergence and evolution, including emergent phenomena of spacetime curvature and quantum mechanics. A preliminary review of relevant data seems to correspond with its predictions. What one must believe is not the existence of unobserved phenomena but simply that the emergence and evolution of quantum mechanics is not the source but an early outcome of universal dynamics, consistent with all other emergence and evolution according to the constructal law and other laws of thermodynamics. Current alternative explanations are not as simple or satisfactory. Space here does not permit, but more analysis is called for. Validation through experimentation and data analysis is necessary. The good news is that the theory is predictive, and observational data that already exists is vast. More rigorous mathematical analysis is needed, and any observations that contradict the theory will dispel any illusions. If the theory does hold, it offers a reconciliation of known but otherwise disparate laws, thus advancing our understanding of nature and the evolution of the universe.

REFERENCES

1. Atkins P.W., *Periodic Kingdom*, BasicBooks, New York NY, USA, 1995, pp. 21–28.
2. Aaronson S., Carroll S.M., Ouellette L., *Quantifying the Rise and Fall of Complexity in Closed Systems*, arXiv:1405.6903 [cond-mat.stat-mech] (or arXiv:1405.6903v1 [cond-mat.stat-mech] for this version).
3. Chaisson E.J., Energy Rate Density as a Complexity Metric and Evolutionary Driver, *Complexity*, *Wiley Periodicals*, **16**, *3*, pp. 27–40 (2010).
4. Bejan A., Zane J.P., *Design in Nature: How the Constructal Law Governs Evolution in Biology, Physics, Technology, and Social Organization*, Doubleday, New York NY, USA, 2012.
5. Bejan A., *The Physics of Life: The Evolution of Everything*, St.Martin's Press, New York NY, USA, 2016.
6. Bejan A., *Freedom and Evolution: Hierarchy in Nature, Society and Science*, Springer Nature Switzerland AG, 2020.
7. Neil T., *On the simplicity of nature*, Perimeter Institute for Theoretical Physics, April 2024.
8. Bejan A., Tsatsaronis G., Purpose in Thermodynamics, *Energies*, **14**, *2*, p. 408 (2021).

CONSTRUCTAL LAW CONFERENCE – CLC2024
Design in Nature and Evolution
Romanian Academy, Bucharest, 10–11 October 2024

Proceedings of CLC2024
pp. 117–120

OPTIMIZING VOLUMETRIC SOLAR AIR RECEIVERS: NUMERICAL ANALYSIS OF POROSITY AND FLOW EFFECTS ON TEMPERATURE DISTRIBUTION

KAMAL NAYEL [a], ABDULRAHMAN ALMERBATI [a,b,*]

[a] Mechanical Engineering Department, King Fahd University of Petroleum and Minerals (KFUPM), Dhahran 31261, Saudi Arabia
[b] Interdisciplinary Research Center for Sustainable Energy Systems (IRC-SES), King Fahd University of Petroleum and Minerals (KFUPM), Dhahran 31261, Saudi Arabia
[*] Correspondence: almerbati@kfupm.edu.sa; Tel. +966-13-8604496

Ceramic foams are promising as absorber materials for volumetric solar receivers (VSR) in concentrated solar thermal power (CSP) systems. The temperature distribution of the VSR is very important to ensure that it operates efficiently and steadily. This study aims to simulate and analyze the temperature distribution within a VSR considering both the solid and fluid phases. The modelling of the open-cell volumetric receiver employs combined volume-averaged equations, assuming the ceramic foam to possess isotropic and homogeneous properties. To assess the pressure-drop in the VSR a non-Darcian model is adopted. A local thermal non-equilibrium (LTNE) model is implemented to describe the energy equations for both the solid and fluid phases.

Additionally, the study considers the influence of solar radiation as a heat source on the solid phase. The heat transfer between the surfaces of the volumetric solar air receiver's struts is calculated using the P1 model. At the same time, a macroscopic approach is utilized to evaluate the thermal profile of the ceramic foam. This study also aims to assess the impact of the VSR's porosity and cell size variation on the outlet air temperature. Moreover, the flow scheme of the flowing air, concerning the incident of concentrated radiation, is considered.

Keywords: Volumetric solar receiver; Ceramic foam; Local thermal non-equilibrium model; Macroscopic approach; Thermal analysis**.**

1. INTRODUCTION

Continuous developments to reduce the greenhouse gas emissions by replacing the fossil fuel generation with cleaner energy sources. This can help meet the increasing energy demand of modern society while mitigating the effects of climate change and global warming [1]. The growing attention placed on renewable energy sources such as wind and solar has led to the development of new technologies. One of these is concentrated solar power [2], in which the thermal efficiency reaches 40% [3]. The open-cell volumetric receiver is a vital component of solar power tower technology. It is composed of a porous material that is heated by concentrated solar radiation [4]. The stability of the porous material, high concentration, and optics of the solar receiver are some technological obstacles that still need to be overcome [5]. Most of the research on open-cell volumetric receivers focused on ceramics due to their ability to endure higher temperatures [6,7]. Studies on the design and parameters of the porous solar receivers have been carried out to improve their performance [8]. Wu *et al*. [9] have studied the temperature distribution of the fluid and solid phases in volumetric solar receivers using the Local Thermal Non-Equilibrium approach. The study analyzed the effects of velocity, porosity, mean cell size, and the thermal conductivity of the solid phase on the temperature fields.

DOI: https://doi.org/10.59277/CLC/2024.30

The aim of the presented study to simulate and analyze the distribution of temperature within a volumetric solar air receiver that encompasses both solid and fluid phases. The modelling of the open-cell volumetric receiver employed the averaged-volume equations. It assumes that the ceramic foam possesses isotropic and homogeneous properties. A non-Darcian model is adopted to evaluate the pressure drop within the volumetric solar receiver. A local thermal non-equilibrium model is implemented to accurately describe the energy equations for both the solid and fluid phases.

Additionally, the study considers the impact of solar radiation as a heat source on the solid phase. The heat transfer occurring between the surfaces of the struts in the volumetric solar air receiver is calculated using the P1 model. At the same time, a macroscopic approach is employed to assess the thermal profile of the volumetric receiver. The primary focus of this study is to evaluate how variations in the porosity and cell size of the volumetric solar receiver impact the outlet air temperature with different air flow schemes relative to the incident concentrated radiation within the open-cell ceramic foam.

2. MATERIALS AND METHODS

A real volumetric solar receiver absorber can have different shapes, such as rectangles, hexagons, or other configurations. Experimental studies typically utilize cylindrical absorber samples. In numerical studies, the shape of the absorber can be easily adjusted. This study employed a bulk of cylindrical-shaped ceramic foam to compare with experimental data. The dimensions of the foam material, the physical model, and the coordinate system are presented in Fig. 1.

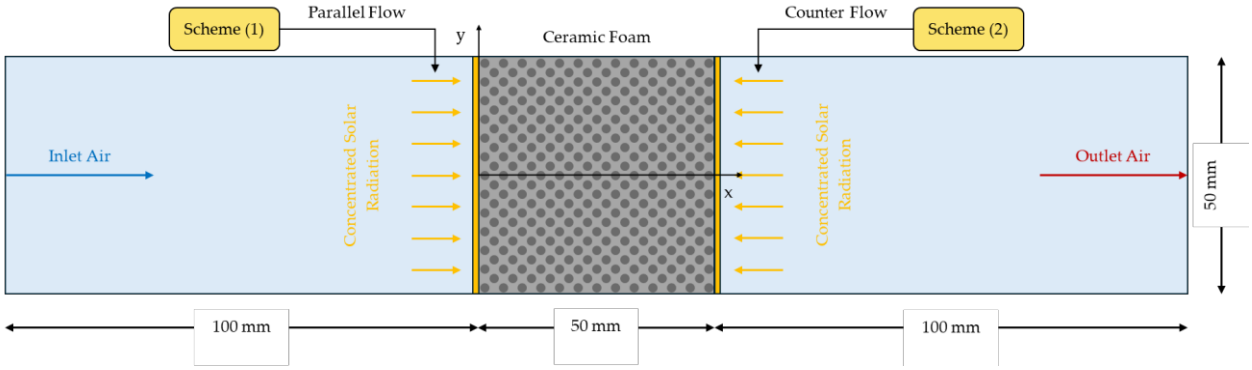

Fig. 1 – The sketch of the open-cell SiC volumetric solar receiver.

3. RESULTS AND DISCUSSION

Figure 2 illustrates the temperatures of the open-cell ceramic foam, both solid and fluid phases, along its axial line. The investigation reveals the thermal characteristics of the volumetric receiver under specific conditions. These include an inlet air velocity (u_d) of 1.08 m/s, a porosity (ϕ) of 0.8, and a mean cell size (d_c) of 1.5 mm. The preliminary findings were validated by comparing them to the findings of Wu *et al*. (T_s* and Tf*) [8]. The comparison demonstrated that any disparities between the temperatures predicted by the presented model and those of Wu *et al*.'s model can be ignored.

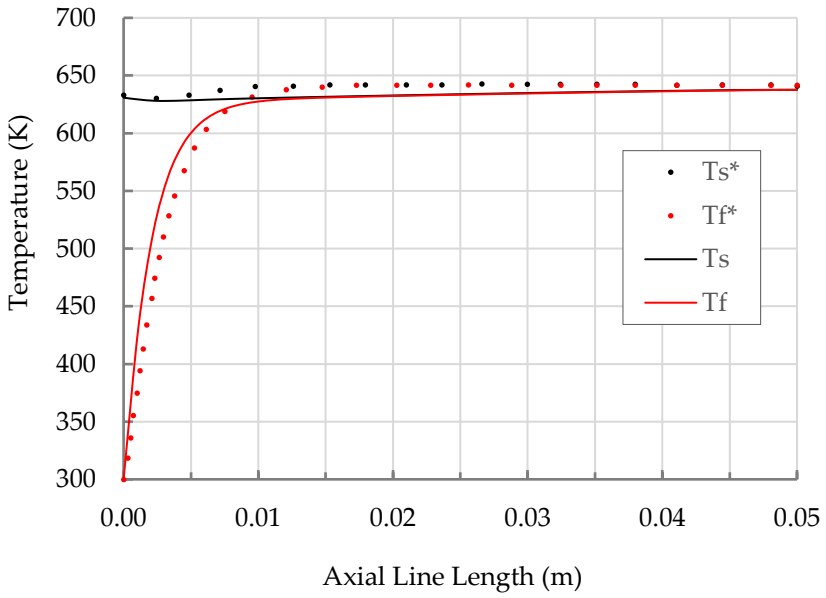

Fig. 2 – The solid and fluid temperatures along the axial line of the open-cell SiC volumetric solar receiver with u_d = 1.08 m/s, ϕ = 0.8 and d_c = 1.5 mm.

A parametric study on the arrangement of the ceramic foam's structure parameters has been evaluated. They consider parallel and counterflow schemes with different combinations of porosities and cell sizes to maximize the outlet air temperature. The porosity and cell size have varied from 0.70 to 0.90 and 1.0 mm to 3.0 mm, respectively. Figure 3 presents the outlet air temperature of (a) parallel and (b) counterflow schemes. The results reveal that the lower porosity and the higher cell size porous ceramic foam shows higher thermal performance within an outlet air temperature of 844 K for the parallel-flow scheme. However, the numerical results illustrate different tendencies for the counter-flow scheme where the lower porosity and the lower cell size porous ceramic foam show higher thermal performance within an outlet air temperature of 862 K.

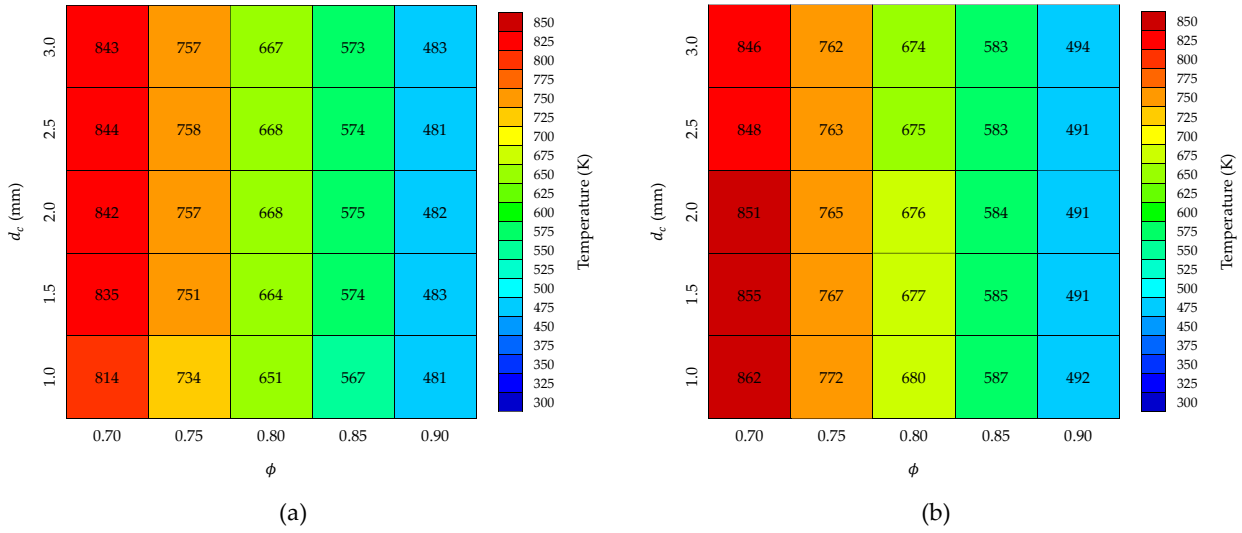

Fig. 3 – The outlet air temperature of **(a)** parallel and **(b)** counter flow schemes for one layer open-cell SiC volumetric solar receiver with different combinations of porosities and cell sizes.

4. **CONCLUSIONS**

- The counter-flow scheme exhibited higher thermal performance than the parallel-flow scheme at the same porosity and cell size values of the porous ceramic foam.
- For the parallel-flow scheme, the lower porosity and the higher cell size porous ceramic foam configuration exhibited higher thermal performance. In contrast, the lower porosity and the lower cell size porous ceramic foam configuration exhibited higher thermal performance for the counter-flow scheme.
- Additional future work may include a double-layered SiC volumetric solar receiver structure with different combinations of cell sizes and porosities within parallel and counterflow schemes to maximize the outlet air temperature at the lower pumping power needed.

ACKNOWLEDGMENTS

The authors express their profound gratitude to King Abdullah City for Atomic and Renewable Energy (K.A.CARE) for their financial support in accomplishing this work.

REFERENCES

1. Qudah A., Almerbati A., Mokheimer E.M.A., Novel approach for optimizing wind-PV hybrid system for RO desalination using differential evolution algorithm, *Energy Conversion and Management*, **300**, p. 117949 (2024).
2. Kauffman J., Lee K.-M., Eds., *Handbook of Sustainable Engineering*, Dordrecht, Springer Netherlands, 2013.
3. Al-Sulaiman F.A., Atif M., Performance comparison of different supercritical carbon dioxide Brayton cycles integrated with a solar power tower, *Energy*, **82**, pp. 61–71 (2015).
4. Ávila-Marín A.L., Volumetric receivers in Solar Thermal Power Plants with Central Receiver System technology: A review, *Solar Energy*, **85**, *5*, pp. 891–910 (2011).
5. Gomez-Garcia F., González-Aguilar J., Olalde G., Romero M., Thermal and hydrodynamic behavior of ceramic volumetric absorbers for central receiver solar power plants: A review, *Renewable and Sustainable Energy Reviews*, **57**, pp. 648–658 (2016).
6. Faizan M., Almerbati A., Yilbas B.S., A novel approach for volumetric solar receiver performance assessments, *Appl. Therm. Eng*., **211**, p. 118487 (2022).
7. Faizan M., Almerbati A., Yilbas B.S., Numerical investigation of turbulent flow across a SiC ceramic foam, *International Journal of Energy Research*, **46**, pp. 14436–14451 (2022).
8. Li, L. Xie, B. Zhao, W. Shen, Y. Liu, Analysis on the Effects of Different Receiver Structures and Porous Parameters on the Volumetric Effects and Heat Transfer Performance of Porous Volumetric Solar Receiver, *International Journal of Energy Research*, **2023**, pp. 1–13 (2023).
9. Wu Z., Caliot C., Flamant G., Wang Z., Coupled radiation and flow modeling in ceramic foam volumetric solar air receivers, *Solar Energy*, **85**, *9*, pp. 2374–2385 (2011).

CONSTRUCTAL LAW CONFERENCE – CLC2024
Design in Nature and Evolution
Romanian Academy, Bucharest, 10–11 October 2024

Proceedings of CLC2024
pp. 121–124

FINNED ELLIPTIC TUBES HEAT EXCHANGERS IN THE TURBULENT REGIME CONSTRUCTAL DESIGN

MARCUS PEREIRA[a], JEFERSON SOUZA[b], JOSÉ V.C. VARGAS[c,*], DIOGO PITZ[a], JUAN ORDONEZ[c], VANESSA KAVA[d]

[a] Department of Mechanical Engineering, Graduate Program in Materials Science Engineering (PIPE), and Sustainable Energy Research & Development Center (NPDEAS), UFPR – Federal University of Paraná, CP 19011, 81531–980, Curitiba, PR, Brazil, marcusvap15@gmail.com, diogopitz@gmail.com

[b] Graduate Program of Ocean Engineering, School of Engineering, Federal University of Rio Grande – FURG, Italy Avenue, km 8, CP. 474, Rio Grande, RS, Brazil, jasouza1974@gmail.com

[c] Department of Mechanical Engineering, Energy and Sustainability Center, and Center for Advanced Power Systems, Florida State University, Tallahassee, Florida 32310–6046, U.S.A., vargasjvcv@gmail.com, ordonez@eng.famu.fsu.edu

[d] Department of Genetics, Graduate Program in Genetics (PPG-GEN), and Sustainable Energy Research & Development Center (NPDEAS), UFPR – Federal University of Paraná, CP 19011, 81531–980, Curitiba, PR, Brazil, vanessagenetica@gmail.com

*Correspondence: vargasjvcv@gmail.com;Tel. + 55 41 99705-0766

This work seeks numerically the heat exchanger structure direction of evolution in time, i.e., the general optimal that maximizes the total heat transfer rate between a fixed volume arrangement of finned tubes and a turbulent external flow governed by a pressure difference, Δp_∞, both for circular and elliptic tube arrays. In this way, the dynamic, ever-changing heat exchanger design that provides easier access to the currents that flow through it is sought for any time reality (*e.g.*, geometry, materials, environment), according to Constructal law. The optimization procedure began by recognizing the limited availability of the design space as a fixed volume constraint. The three-way optimized (3wo) arrangement concerning tube-to-tube distance, eccentricity, and fin density was found as $(S/2b, e, \phi_f)_{3wo} \cong (0.5; 0.4; 0.094)$. A relative heat transfer gain of up to *38%* was noted with the elliptic compared to the 3wo circular arrangement, demonstrating that elliptical tube arrangements have potential for considerably better performance and lower cost than traditional circular arrangements.

Keywords: Heat transfer; Numerical simulation; Refrigeration; Tube banks.

1. INTRODUCTION

Human society depends heavily on the utilization of finned tube heat exchangers. For example, they are the main components of Heating, Ventilation, Air Conditioning, and Refrigeration (HVAC-R) systems that require 13.2%, 14.9%, and 3.7% (residential, commercial, and industrial sectors, respectively) of the US consumed electrical power, adding up to 31.8% of total US electricity consumption in 2019 [1]. Therefore, in recent decades, in this area, many studies have been carried out on modeling, simulation, design, and operating parameters optimization aimed at achieving the highest possible efficiency for reaching the minimum possible cost and resource waste [2].

This study broadens such optimization efforts with the Constructal law: “For a finite-size flow system to persist in time, it must evolve with freedom such that it provides greater and easier access to its flows” [3, 4]. So, the entropy generation minimization (EGM) method could predict the system’s optimal structural design and energy

DOI: https://doi.org/10.59277/CLC/2024.31

flow organization for minimum losses [5] for any time reality (*e.g.*, geometry, materials, environment). For that, a quasi-steady process [6] is assumed, *i.e.*, the dynamic design phenomenon is modeled by a succession of periods (time steps) where, in each of them, the optimal design remains practically unchanged, "…like the images in a movie at the cinema…" [3]. The quasi-steady assumption is justified because the duration of each time step is much shorter than the evolution timescale since evolution never ends. The changing rate of optimal designs points to the direction of heat exchangers evolution in time, *i.e.,* the constructal design.

2. MATERIALS AND METHODS

The mathematical model was developed for the turbulent flow regime external to elliptical finned tubes driven by a pressure difference Δp_∞. The finite volume method was used to discretize the governing equations. The model was written for the domain of the unit cell in Fig. 1a, considering all system symmetries.

Figure 1b shows the finned elliptical (or circular) tube arrangement. The comparison criterion was to use the same tube section in the flow direction [7], *i.e.*, the same free-flow obstruction area.

The adopted simplifying assumptions were forced convection, Newtonian fluid, incompressible flow, steady-state, and constant fluid properties. The fluid flow and heat transfer governing equations are based on the mass, momentum, and energy conservation principles and are listed as follows:

$$\nabla\cdot\vec{V}=0;\ \rho\frac{D\vec{V}}{Dt}=-\nabla p+\mu\nabla^2\vec{V}+\vec{F},\ \text{and}\ \rho c_p\frac{DT}{Dt}=k\nabla^2T+\mu\Phi, \tag{1}$$

where $\vec{V}=(u,v,w)^T$ is the velocity vector, $\vec{F}=(X,Y,Z)^T$ the body force vector per unit volume and Φ the viscous dissipation function.

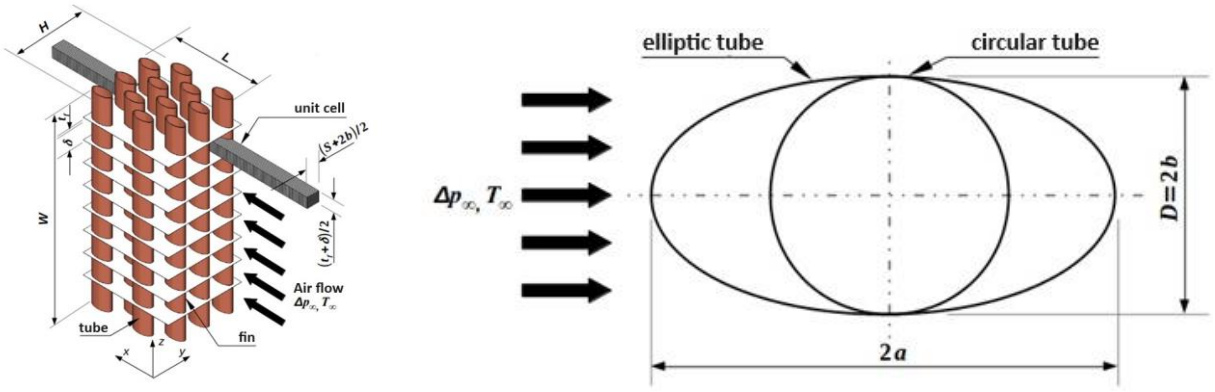

(a) (b)

Fig. 1 – (a) Finned tubes heat exchanger arrangement and
(b) Circular and elliptic tubes comparison criterion.

For brevity, the full description of all variables and the SST k-w (Shear Stress Transport) turbulence model used to solve the problem are not shown here but can be found in Pereira [7].

3. **RESULTS**

The results of Fig. 2 investigate the existence of optima concerning tube-to-tube distance, S/2b, eccentricity, e, and fin density, $\phi_f = t_f/(t_f+\delta)$. The airflow covered the range $1\,240 \leq Re_{2b} \leq 28\,180$, where Re_{2b} is the Reynolds number based on 2b. Numerical results were validated against published data for flow in tubes and bundles of tubes in the laminar and turbulent regime [7]. The Nusselt number, Nu, was calculated and validated with empirical correlations, in good agreement, with a 2.8% error for $Re_D = 5\,000$ and 18.3% for $Re_D = 30\,000$.

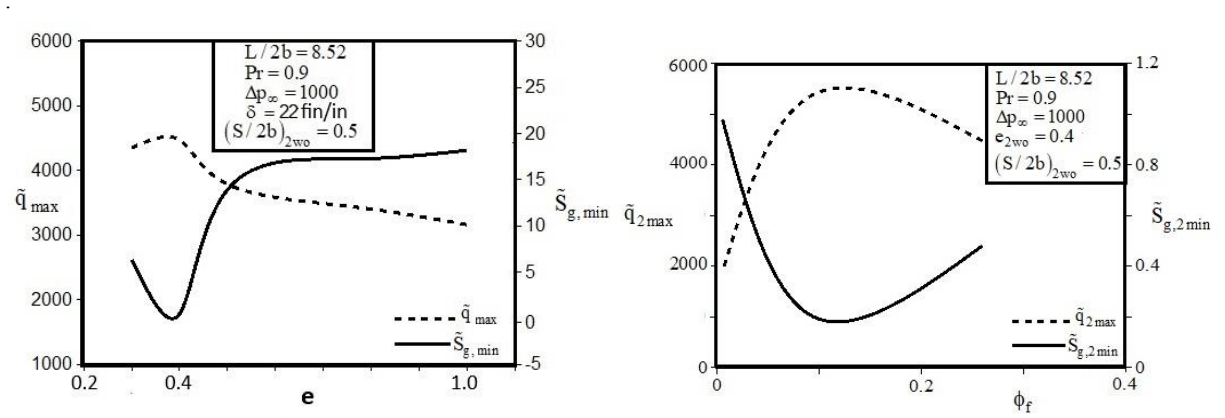

(a) (b)

Fig. 2 – The finned heat exchanger two- (a) and three-way (b) optimization.

The three-way optimized (3wo) arrangement was found as $(S/2b, e, \phi_f)_{3wo} \cong (0.5; 0.4; 0.094)$. The heat transfer gain was up to *38%* for the 3wo elliptic arrangement in comparison to 3wo circular one. The calculation of the system total entropy generation allowed for obtaining both 3-way maximized heat transfer and 3-way minimized entropy generation, $\tilde{q}_{3\max}$ and $\tilde{S}_{g,3\min}$, respectively, for $(S/2b, e, \phi_f)_{3wo} \cong (0.5; 0.4; 0.094)$ for the arrangement.

4. **DISCUSSION AND CONCLUSIONS**

In sum, it is reasonable to state that the heat exchanger constructal design has been achieved by minimizing the system's total entropy generation, which simultaneously minimizes the system's thermal and flow resistances.

REFERENCES

1. Matos R.S., Vargas J.V.C., Rossetim M.A., Pereira M.V.A., Pitz D.B., Ordonez J.C., Performance comparison of tube and plate-fin circular and elliptic heat exchangers for HVAC-R systems, *Applied Thermal Engineering*, **184**, p. 116288 (2021).
2. Macchitella S., Colangelo G., Starace G., Performance Prediction of Plate-Finned Tube Heat Exchangers for Refrigeration: A Review on Modeling and Optimization Methods, *Energies*, **16**, p. 1948 (2023).
3. Bejan A., Lorente S., Constructal law of design and evolution: Physics, biology, technology, and society, *J. Appl. Phys.*, **113**, p. 151301 (2013).

4. Bejan A., Tsatsaronis G., Purpose in thermodynamics, *Energies*, **14**, *2*, p. 408 (2021).
5. Bejan A., *Entropy Generation Minimization*, CRC Press, Boca Raton, Florida, USA, 1995.
6. Martinho L.C.S., Vargas, J.V.C., Balmant W., Ordonez J.C., A single stage absorption refrigeration system dynamic mathematical modeling, adjustment and experimental validation, *Int. J. Refrigeration*, **68**, pp. 130–144 (2016).
7. Pereira M.V.A., *Modeling, Simulation and Optimization of Finned Tubes Heat Exchangers in Turbulent Regime*, PhD Dissertation, Federal University of Parana, Curitiba, Brazil, 2018.

CONSTRUCTAL LAW CONFERENCE – CLC2024
Design in Nature and Evolution
Romanian Academy, Bucharest, 10–11 October 2024

Proceedings of CLC2024
pp. 125–128

CONSTRUCTAL DESIGN APPROACH FOR CARBON DIOXIDE ADSORPTION SYSTEMS

MARCELO RISSO ERRERA[a*], EMILIO GRACILIANO FERREIRA MERCURI[b], GEORGE STANESCU[c]

[a] Department of Environmental Engineering, Federal University of Parana, Brazil, errera@ufpr.br
[b] Department of Environmental Engineering, Federal University of Parana, Brazil, emilio@ufpr.br
[c] Graduate Program of Environmental Engineering, Federal University of Parana, Brazil, stanescu@ufpr.br
*Correspondence: errera@ufpr.br; Tel. +(55)41-3362-3012

Current carbon capture and storage (CCS) benchmark technologies and materials are both energy and economically costly. Therefore, it hopes to rely on uncovering combinations of designs or materials to provide the performance leap to scale up the CCS deployment to meet the most optimistic Intergovernmental Panel on Climate Change (IPCC) projections and socioeconomic shared pathways to mitigate global warming. While the search for advanced materials for carbon capture has drawn much of the efforts to enhance the so-called productivity (CCPr), *i.e.*, CO_2 mols per volume of CC material per cycle for high levels of purity for CO_2 recovery, there is an opportunity to investigate before-hand how those materials would fare energy wise (PE) (total energy expenditure by total amount of CO_2 mols captured) in the reactor. This work presents a formulation based on the Constructal Theory to explore how the features of the materials themselves (absorptivity, molecular diffusivity, density), the packing (pellets shape and size, effective diffusivity, specific capturing rate, porosity), and the configuration of a column packed-bed reactor affects the energy penalty (PE). The investigation is theoretical and numerical by modeling the CO_2 mass balance in a prescribed and constant mobile phase flow rate (initially CO2-rich exhaust gases) isothermal 1d tubular packed-bed reactor and the coupling with CO_2 mass balance at the pellet level with linear driving force model – both are saturated porous media. The simulations were performed using newly developed Python code and commercial software. The model was turned nondimensional, and the influence of the adapted Peclet and Damkhöler numbers was explored, which showed reverse trends in the indices CCPR and PE. It showed the trade-off between the resistances to adsorb CO_2 and the other features of the reactor's design, providing insights into how those systems may evolve.

Keywords: Carbon capture; Constructal design; Carbon capture and storage (CCS); Energy efficiency**.**

1. INTRODUCTION

According to the IPCC, the demand for carbon capture and storage (CCS) increases as the so-called energy transition from fossil hydrocarbons to low greenhouse gas energy pathways progresses slower than expected [1]. Current CCS benchmark technologies and materials are energy- and economically costly [2]. Recently, Gasparovic *et al.* [3] addressed the design of CCS reactors for mineral capture using Constructal Design approach to explore low-energy expenditure possibilities. In this work, we now explore the comparative influence of the macroscopic and the microscopic CO_2 transport and adsorption (capture) on the two metrics that drives the evolution of CCS systems, namely, the so-called productivity

DOI: https://doi.org/10.59277/CLC/2024.32

(*CCPr*) given in CO_2 mols per volume of carbon-capturing material per cycle and the energy penalty (*PE*) (total energy expenditure in kJ by the total amount of CO_2 mols captured) in a adsorption/desorption reactor.

2. MATERIALS AND METHODS

The investigation is theoretical and numerical by modelling the CO_2 mass balance in a prescribed and constant mobile phase flow rate (CO_2-rich exhaust emissions) isothermal 1D tubular plug-flow spheroidal-pellets-packed-bed reactor and the coupling with CO_2 mass balance at the pellet level for linear driving force (LDF) and Langmuir adsorption regime (*e.g.*, [5]):

$$\varepsilon_{\mathrm{b}} \frac{\partial C}{\partial t} + u \frac{\partial C}{\partial x} = \varepsilon_{\mathrm{b}} D_{\mathrm{b}} \frac{\partial^2 C}{\partial x^2} - (1 - \varepsilon_{\mathrm{b}}) \rho_{\mathrm{p}} \frac{\partial q}{\partial t}, \tag{1}$$

$$\frac{\partial q}{\partial t} = K_{\mathrm{L}}\left(q_{\mathrm{p}}^{*} - q\right),\ q_{\mathrm{p}}^{*} = \frac{q_{\mathrm{pm}} b C}{1 + bC}, \tag{2}$$

$$C(x,t) = C_0,\ x = 0, t = 0, \tag{3}$$

$$C(z,t) = 0 \text{ and } q(z,t) = 0,\ 0 < x \leq L, t = 0, \tag{4}$$

$$u \cdot C_0 = u \cdot C(x,t) - \varepsilon_b D_{\mathrm{b}} \frac{\partial C}{\partial x},\ x = 0,\ t > 0, \tag{5}$$

$$\frac{\partial C(x,t)}{\partial x} = 0,\ x = L,\ t > 0, \tag{6}$$

where, $C(x,t)$ is the concentration of the free CO_2 in the mobile phase (mol kg^{-1}) along the axial direction, x (m) in time, t (s); u is the given uniform surface velocity along the axial direction (m s^{-1}); $q(x, t)$ is the average concentration of CO_2 in the pellets of the capturing material (mol kg^{-1}); ε_b is the bed porosity (−); D_b is the uniform, constant, axial dispersion coefficient (m^2 s^{-1}), ρ_p is the adsorbent pellet density (kg m^{-3}); q_p^* is the amount adsorbed at equilibrium (mol kg^{-1}); K_L is the LDF overall mass transfer and adsorption coefficient (s^{-1}); q_{pm} is maximum adsorption capacity of the pellets ($kg_{adsorbed}$ $kg_{adsorbent}^{-1}$); and b is Langmuir isotherm constant (m^3 kg^{-1}).

The ratio between the macroscopic and the microscopic CO_2 transport and adsorption (capture) is seen by the Peclet number, $\mathrm{Pe} = uL/(\varepsilon_b D_b)$ and the Damköhler number, $\mathrm{Da} = K_L L \varepsilon_b / u$. The cycle time (s), t_{cycle}, was given when the rate of variation of $C(L, t)$ in time at the exit of the reactor ($x = L$) is negligible. The volume of adsorbent material (pellets) is given by the macroscopic non-void portion of the reactor, V_{ads}, and the CC in each cycle by the time-cumulated CO_2 by the balance between the known constant feed and the exit (mol). The energy expenditure is computed by constant feed flow rate, near constant pressure flow, and the pressure drop, calculated by the known Ergun formula (*e.g.*, [4]). The model was turned nondimensional, and the influence of the adapted Peclet and

Damkhöler numbers on *CCPr* and *PE* was explored. The simulations were performed in newly developed Python code and commercial software.

3. RESULTS

We explored 101 random consistent combinations of reasonable ranges for L, u, ε_b, D_b, and K_L, with fixed q_p^* and b, then expressed *CCPr* and *PE* concerning Peclet and Damköhler (Fig. 1).

4. DISCUSSION AND CONCLUSIONS

In this brief report, we showed that the two main design criteria for CCSs, namely, the Carbon Capture Productivity itself and the Energy Penalty (*PE*), respond in a reverse way concerning Peclet and Damköhler number, showing there is an opportunity to find a matching balance between the macroscopic transport of CO_2 and the microscopic, local, transport in the capturing pellets up to the adsorption of the CO_2. The most promising combinations are Pe ~ 10^3 and Da ~ 10.

Further investigations will show the sensitivity of the maximum adsorption material, the rate in which it reaches such plateau on the balance of transport and the internal structure of the adsorbents.

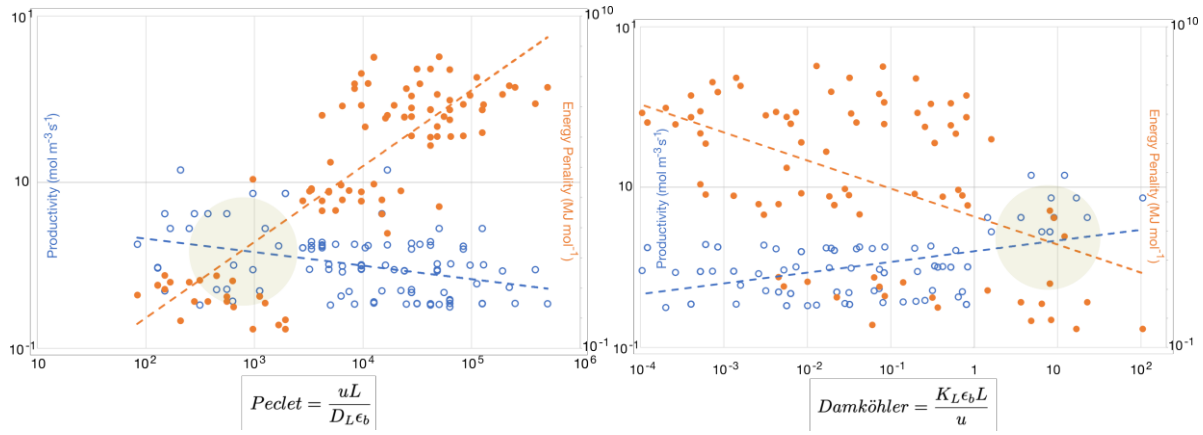

(a) (b)

Fig. 1 – Variation of the Carbon Capture productivity (*CCPr*) and the Energy Penalty (*PE*) *vs* the (a)Peclet and (b)Damköhler numbers of 101 random simulations (log-log).

REFERENCES

1. Intergovernmental Panel on Climate Change, Emissions Trends and Drivers (IPCC), Climate Change 2022 – Mitigation of Climate Change: Working Group III Contribution to the Sixth Assessment Report of the IPCC, Cambridge University Press, 2022, pp. 215–294.

2. Al-Sakkari E.G., Ragab A., Dagdougui H., Boffito D.C., Amazouz M., Carbon capture, utilization and sequestration systems design and operation optimization: Assessment and perspectives of artificial intelligence opportunities, *Science of The Total Environment*, **17**, p. 170085 (2024).
3. Gasparovic C.L.M., Stanescu G., Errera M.R., Constructal Design of a Mineral Carbonation System for Post-Combustion Carbon Capture, *International Communications in Heat and Mass Transfer*, **156**, p. 107657 (2024).
4. Kaczmarski K., Szukiewicz M.K., An efficient and robust method for numerical analysis of a dead zone in catalyst particle and packed bed reactor, *Engineering Reports*, **3**, *8*, p. e12370 (2021).
5. Dantas T.L., Luna F.M.T., Silva Jr. I.J., de Azevedo D.C., Grande C.A., Rodrigues A.E., Moreira R.F., Carbon dioxide–nitrogen separation through adsorption on activated carbon in a fixed bed, *Chemical Engineering Journal*, **169**, *1–3*, pp. 11–19 (2011).

8ONSTRUCTAL LAW CONFERENCE – CLC2024
Design in Nature and Evolution
Romanian Academy, Bucharest, 10–11 October 2024

Proceedings of CLC2024
pp. 129–132

THE EUKARYOTE ENDOSYMBIOTIC ORIGIN: A CONSTRUCTAL THEORY-BASED EXPLANATION

VANESSA KAVA[a], JOSÉ V.C. VARGAS[a,*], JUAN ORDONEZ[b], ANDRÉ MARIANO[a]

[a] Sustainable Energy Research & Development Center (NPDEAS), UFPR – Federal University of Paraná, CP 19011, 81531–980, Curitiba, PR, Brazil, vanessagenetica@gmail.com, andrebmariano@gmail.com

[b] Department of Mechanical Engineering, Energy and Sustainability Center, and Center for Advanced Power Systems, Florida State University, Tallahassee, Florida 32310–6046, U.S.A., ordonez@eng.famu.fsu.edu

*Correspondence: vargasjvcv@gmail.com;Tel. + 55 41 99705-0766

The origin of eukaryotes is understood as one of the most important issues in the history of living beings. There are several points of view to seek a broad understanding of the eukaryote origins, which encompass paleontological data, energetics, eukaryote-particular characteristics origins or the connections among dissimilar eukaryotic groups. Many proposals of endosymbiotic theory have been presented to explain the origin of eukaryotes and their mitochondria. Only recently, energy and the energetic constraints started to be considered by endosymbiotic theory to understand the contribution of prokaryotic cell organization to cell history, acknowledging that only cells that possessed mitochondria had the bioenergetic assets to achieve eukaryotic cell complexity, which explains why no in between beings existed in the prokaryote-to-eukaryote transition. This study attempts to approach the eukaryote origins from the standpoint of constructal theory, i.e., "For a flow system to persist in time (to survive), it must evolve in such a way that it provides easier and easier access to the currents that flow through it." Therefore, the explanation is based on the direction of evolution in time, in which it has been introduced the thought that system structure should morph freely towards the optimal architecture and flow organization that minimize resistances to the internal flows (exergy losses) that are required for the system existence, which is proposed as the origin of eukaryotes, mitochondria, chloroplasts, and for the origin of the eukaryotic nucleus.

Keywords: Exergy destruction; Nucleus; Archaebacterium; Evolutionary design.

1. INTRODUCTION

The formation process of the eukaryotic cell with all its contents (nucleus, membrane encapsulated organelles, cytoskeleton and endomembrane system) is still enigmatic. Most likely, the process started from a prokaryote cell, which are known to be the first living cells in the planet, to the first eukaryotic common ancestor (FECA). Such innovatory cellular structure and the symbiotically acquired mitochondria allowed for broader ecological participation, and eventually originated the last eukaryotic common ancestor (LECA), which evolved and diverged to form the successful origins of the current uni and multicellular eukaryotes' lineages [1, 2]. Figure 1 shows the main steps of cellular evolution on Earth [3].

There are several models that propose to explain the evolutionary path of the modern eukaryotic cell. The evolution of the nucleus is based: (i) on prokaryote plasma membrane invaginations or (ii) on archaeon endosymbiosis in a prokaryote host, or (iii) on a membrane system autogenous origin with the nuclear

DOI: https://doi.org/10.59277/CLC/2024.33

component in an archaeal host after mitochondria incorporation. The assumption that an endosymbiont (protomitochondria) entered an archaeal cell host through phagocytosis and united to form the first eukaryotic common ancestor (FECA) is the fundamental basis for the symbiogenic models, that are currently the most accepted theories [1, 2]. Recently, because of experimental evidence gathered from cultivation, genomics, and literature data interpretations, an alternative eukaryogenesis theory has been proposed, namely, the entangle–engulf–endogenize (E^3) model [4]. All such perspectives comprise the so-called *outside-in* models, which have been questioned by the fact that archaea are known to produce extracellular protrusions but typically do not carry out endocytosis or phagocytosis [5]. Hence, the *outside-in* perspective has been challenged by suggesting that a prokaryotic cell generated protrusions beyond its surrounding membrane, aggregating to form the endomembrane and cytoplasm system. According to this *inside-out* model, the nucleus would be the first and oldest part of the eukaryotic cell, which was kept unaltered. In contrast, the cell organization changed from prokaryotic to eukaryotic [5]. The natural question is: Which of these two models best represents what happened during the evolution of eukaryotic cells?

This study invokes the Constructal law to provide a possible answer: "For a finite-size flow system to persist in time, it must evolve with freedom such that it provides greater and easier access to its flows" [6,7]. One way to figure out which of the two unsteady processes led to the most negligible resistances to the flows required for the system to exist is to estimate the total entropy generated (or exergy destruction) in each process.

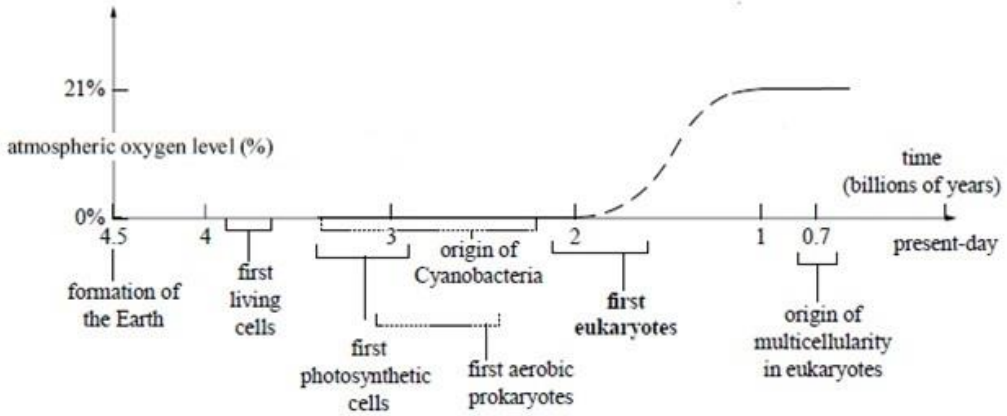

Fig. 1 – The currently accepted eukaryotic cellular evolution steps [3].

2. **MATERIALS AND METHODS**

The schematic diagram of the *inside-out* and *outside-in* models is shown in Fig. 2, where 1 and 2 are the start and finish of the process, respectively. Consider the resulting eukaryotic cell ancestor as an open system in Fig. 2 – right. The system has inlet and outlet ports through the permeable boundary, and the system's operation is unsteady. Mass conservation, the 1st and 2nd law of thermodynamics, and the *quasi*-steady assumption for crossflow pumping state at any instant that [7]:

$$\frac{dM}{dt} = \dot{m}_{in} - \dot{m}_{out}\ ; \quad \frac{dU}{dt} = \dot{Q} + \frac{dM}{dt} h_{in} + \underbrace{\dot{m}_{out}(h_{in} - h_{out})}_{=0} - \dot{W}, \tag{1}$$

$$\dot{S}_{gen} = \frac{dS}{dt} + \dot{m}_{out} s_{out} - \dot{m}_{in} s_{in} - \frac{\dot{Q}}{T_0} \geq 0, \tag{2}$$

where M is the mass, $\dot{m}$ the mass flow rate, U is the internal energy, $\dot{Q}$ the heat transfer rate, h is the specific enthalpy, $\dot{W}$ the work transfer rate, $\dot{S}$ the entropy rate, s is the specific entropy, T is the temperature, and subscripts in, out, 0, and gen the inlet, outlet, environment, and generation, respectively.

Next, the *quasi*-steady assumption will be adopted, and eqs. (1) and (2) will be integrated from states 1 to 2:

$$Q_{1-2} = -(M_2 - M_1)\, v_0 p_0 = -\Delta M\, v_0 p_0 = -p_0 \Delta V\ ;\ S_{gen,1-2} = p_0 \Delta M\, v_0 / T_0, \tag{3}$$

where v is the specific volume, p is the pressure, Δ the variation, and V is the volume.

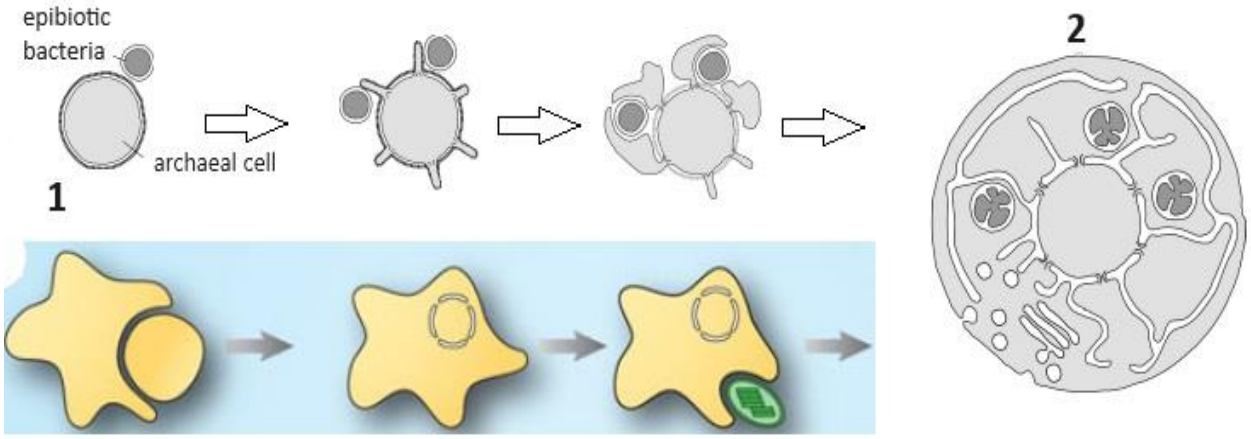

Fig. 2 – Top left: the *inside-out* model evolution path; Bottom left: the *outside-in* model evolution path, and Right: the resulting eukaryotic cell ancestor (adapted [1, 5]).

From Fig. 2 and Eq. (3), the archaeal cell is only the nucleus for the *inside-out* model, so $M_{1,oim} > M_{1,iom}$, $\Delta M_{oim} < \Delta M_{iom}$ and $S_{gen,1-2,iom} > S_{gen,1-2,oim}$, in which subscripts "oim" and "iom" refer to the outside-in and inside-out models, respectively.

3. **DISCUSSION AND CONCLUSIONS**

The total entropy generated with the *inside-out* process was more significant than that with the *outside-in* process. Hence, based on Constructal law, the *outside-in* process is expected to be the actual direction of eukaryotic cell evolution over time.

REFERENCES

1. Mast F.D., Barlow L.D., Rachubinski R.A., Dacks J.B., Evolutionary mechanisms for establishing eukaryotic cellular complexity, *Trends in Cell Biology*, **24**, pp. 435–442 (2014).
2. Koonin E.V., Origin of eukaryotes from within archaea, archaeal eukaryome and bursts of gene gain: eukaryogenesis just made easier?, *Phil. Trans. R. Soc. Lond*. *B*, **370**, p. 20140333 (2015).
3. Vellai T., Vida G., The origin of eukaryotes: the difference between prokaryotic and eukaryotic cells, *Proc. R. Soc. Lond*,, **266**, pp. 1571–1577 (1999).
4. Imachi H., Nobu M.K., Nakahara N., Morono Y., Ogawara M., Takaki Y., Takano Y., Uematsu K., Ikuta T., Ito M., Matsui Y., Miyazaki M., Murata K., Saito Y., Sakai S., Song C., Tasumi E., Yamanaka Y., Yamaguchi T., Kamagata Y., Tamaki H., Takai K., Isolation of an archaeon at the prokaryote-eukaryote interface, *Nature*, **577**, pp. 519–525 (2020).
5. Baum D.A., Baum B., An inside-out origin for the eukaryotic cell, *BMC Biology*, **12**, p. 76 (2014).
6. Bejan A., Lorente S., Constructal law of design and evolution: Physics, biology, technology, and society, *J. Appl. Phys.*, **113**, p. 151301 (2013).
7. Bejan A., Tsatsaronis G., Purpose in thermodynamics, *Energies*, **14**, *2*, p. 408 (2021).

CONSTRUCTAL LAW CONFERENCE – CLC2024
Design in Nature and Evolution
Romanian Academy, Bucharest, 10–11 October 2024

Proceedings of CLC2024
pp. 133–136

CONSTRUCTAL LAW APPLIED TO PROOF MAXIMUM WORK PRINCIPLE. CONSEQUENCES ON CONVEXITY AND NORMAL RULE OF BULKING PLASTICITY & SURFACE FRICTION POTENTIAL TOGETHER WITH ESTIMATION OF REAL THERMO-MECHANICAL POWER DURING CONTINUUM MEDIA FLOWS

ADINEL GAVRUS[a]

National Institute of Applied Sciences – INSA Rennes, 20 Av. des Buttes de Coesmes, 35700 Rennes, France
adinel.gavrus@insa-rennes.fr

Following the author's previous studies, this scientific article uses the proof of the "Principle" of Maximum Work (PMW), used in metals plasticity theory and surface tribology, through a more general mathematical framework starting from the fundamental Constructal Law. In this paper, the author focuses on the mathematical proof of convexity and normal rule properties of both plastic and friction flow criteria.

Keywords: Maximum Work "Principle" proof; Bulk plasticity; Surface friction; Potential convexity and normal rule; Thermo-mechanical power estimation.

1. INTRODUCTION

Starting from previous author studies, this research uses the proof of the "Principle" of Maximum Work (PMW) defined in metals plasticity theory and surface tribology [1] through a more general mathematical framework starting from the fundamental Constructal Law [2,3], and the Virtual Powers Principle (VPP) defined because of the momentum stresses equilibrium. The Constructal Law postulates the natural tendency of any finite-size system to evolve towards an optimal space-time configuration, minimizing losses and entropy generation.

Regarding a material deformation during a forming or flow process, under specified boundary/loadings conditions, the real mechanical variables defining the flow (velocities, stresses, strain, and strain rate) are those that minimize the sum of dissipated bulk deformation and contact surfaces friction powers written in terms of all other virtual and admissible states. It is then show that PMW becomes a Theorem [4-8] and can be applied to all continuous media (solid, fluid, mushy state, plasma) and any type of materials.

An equivalent form has also been defined for contact friction (isotropic and anisotropic). This paper focuses on the mathematical proof of convexity and normal rule laws of both plastic and friction potential.

DOI: https://doi.org/10.59277/CLC/2024.34

2. GENERAL THEORETICAL FRAMEWORK

Starting from the Constructal Law which postulate the tendency of all system to search a such configuration evolution or flow minimizing losses, as it has already been applied by authors in previous research works [4-8], in the case of continuum media flow, this one is obtained by minimizing the functional defining the virtual dissipated or lost power P^*_d, *i.e.*:

$$P_d = \mathrm{Min}\left(P^*_d\right) \text{ with } P^*_d = \iiint_{\Omega} \left[\sigma^*\right] : \left[\dot{\varepsilon}^*\right] dV + \iint_{\partial\Omega'} -\vec{\tau}^* \cdot \Delta\vec{v}^* \, dS' + \iint_{\partial\Omega''} -\vec{T}^d \cdot \vec{v}^* \, dS'' . \quad (1)$$

Here, ":" denotes the matrix contracted product equivalent to the vector's scalar product, where * represents all admissible virtual values corresponding to all kinematic and mechanical variables: $\vec{v}^*$ – virtual velocities vector, $\left[\dot{\varepsilon}^*\right]$ – virtual strain rate tensor (symmetric part of the velocity vector gradient matrix), $\left[\sigma^*\right]$ - virtual Cauchy stress tensor, $\vec{\tau}^*$ – virtual shear stress vector occuring on surfaces interfaces and $\vec{T}^d$ – imposed stress-force vector regarded also as constraint loading.

Then the real solution of the flow in terms of real stresses and flow velocities is obtained by minimizing P^*_d corresponding to the optimization problem (1).

Using the well known Virtual Power Principle, it has proven the First PMW Theorem:

$$\left(\left[\sigma^*\right] - [\sigma]\right) : \left[\dot{\varepsilon}^*\right] \geq 0, \forall \left[\sigma^*\right], \Phi_p\left(\left[\sigma^*\right]\right) - \sigma_0 = 0 \,; -\left(\vec{\tau}^* - \vec{\tau}\right) \cdot \Delta\vec{v}^* \geq 0, \forall \vec{\tau}^*, \Psi_f\left(\vec{\tau}^*\right) - \tau_f = 0 , \quad (2)$$

In a reverse form it can be written the First PMW Theorem using the equivalent form:

$$\left([\sigma] - [\sigma^*]\right) : \left[\dot{\varepsilon}\right] \geq 0, \forall \left[\sigma^*\right], \Phi_p\left(\left[\sigma^*\right]\right) - \sigma_0 = 0 \,; -\left(\vec{\tau} - \vec{\tau}^*\right) \cdot \Delta\vec{v} \geq 0, \forall \vec{\tau}^*, \Psi_f\left(\vec{\tau}^*\right) - \tau_f = 0 , \quad (3)$$

Here $\Phi_p\left(\left[\sigma^*\right]\right)$ it is the plastic criterion (as isotropic Von-Mises or anisotropic Hill one) and $\Psi_f\left(\vec{\tau}^*\right)$ represents the friction potential (circular for isotropic friction and elliptic for anisotropic friction where friction coefficient is function of sliding directions).

2.1. Proof of Plastic and Friction Potential Normal Rule

In conformity with the relationship (2) concerning the stress state, for any infinitesimal stress variation $\pm d[\sigma] = \left[\sigma^*\right] - [\sigma]$ with $\Phi_p\left([\sigma \pm d\sigma]\right) = \Phi_p\left([\sigma]\right) = \sigma_0$ it is obtained:

$$\mp\left[d[\sigma] / \left\|d[\sigma]\right\|\right] : [\dot{\varepsilon}] \geq 0 \Rightarrow \left[d[\sigma] / \left\|d[\sigma]\right\|\right] : [\dot{\varepsilon}] = 0 \quad (4)$$

A first Taylor development gives $\Phi_p\left(\left[\sigma \pm d\sigma\right]\right) = \Phi_p\left(\left[\sigma\right]\right) \pm d[\sigma] : \partial\Phi_p / \partial[\sigma]$, then:

$$\pm\left[d[\sigma] / \left\|d[\sigma]\right\|\right] : \partial\Phi_p / \partial[\sigma] = 0 \quad (5)$$

Using equations (4) and (5), it can be conclude on the proportionality of $\partial\Phi_p / \partial[\sigma]$ with $[\dot{\varepsilon}]$ and the named normal rule law of plastic potential it is obtained, *i.e.* :

$$d\varepsilon^p / dt = [\dot{\varepsilon}] = \lambda_p \partial\Phi_p / \partial[\sigma], \lambda_p \geq 0 \tag{6}$$

In a similar way, concerning the virtual friction shear stress can also be prove the friction normal rule law, *i.e.:*

$$\Delta\vec{v} = -\lambda_f \partial\Psi_f / \partial\vec{\tau}, \lambda_f \geq 0 \tag{7}$$

Figure 1 shows the potential shape, the plastic strain hyper-vector, and the stress states.

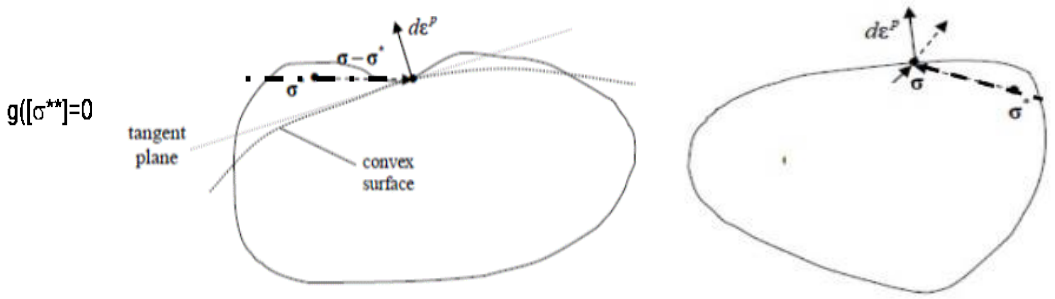

(a) (b)

Fig. 1 – Schema of real or virtual stress states and the plastic potential surface shape: (a) different positions of infinitesimal plastic deformation vector $d\varepsilon^p = [\dot{\varepsilon}]dt$; (b) plastic potential surface and tangent plane.

2.2. **Proof of Plastic and Friction Potential Convexity**

All tangent hyper-planes on the plastic potential curves can be defined by $g([\sigma^{**}]) = \Phi_p([\sigma]) - \Phi_p([\sigma^{**}]) + ([\sigma^{**}] - [\sigma]) : \partial\Phi_p / \partial[\sigma] = 0$, when applying inequality given by equation (3) written in the reversible form of the first PMW Theorem (2), for any real stress states situated on a potential curve, together with the corresponding normal rule law i.e. $([\sigma] - [\sigma^*]) : [\dot{\varepsilon}] \geq 0 \Rightarrow ([\sigma] - [\sigma^*]) : \partial\Phi_p / \partial[\sigma] \geq 0$, it is obtained $g([\sigma^*]) \leq 0$.

Consequently, the potential curve is located at any point inside the tangent plane's family. In conformity with one of the convexity definition form, the convex shape of stress criteria is then proven. Similar conclusion can be obtain concerning the convexity of friction potential.

Finally, using this convexity property, the two inequalities of equation (2) can be extended to all virtual stress or friction shear respecting $\Phi_p([\sigma^*]) - \sigma_0 \leq 0$ $\Psi_f(\vec{\tau}^*) - \tau_f \leq 0$ corresponding to the points inside the closed potential curve. It is then possible to define the final form of the PMW Theorem for both stress and friction state:

$$([\sigma] - [\sigma^*]) : [\dot{\varepsilon}] \geq 0, \forall [\sigma^*], \Phi_p([\sigma^*]) - \sigma_0 \leq 0 \tag{8}$$

$$-(\vec{\tau} - \vec{\tau}^*) \cdot \Delta\vec{v} \geq 0, \forall \vec{\tau}^*, \Psi_f(\vec{\tau}^*) - \tau_f \leq 0 \tag{9}$$

3. **RESULTS**

Previous author's works concerning computation applications for plane compression [4], cylindrical crushing [5], direct extrusion [8], and anisotropic contact surface friction [6] show the feasibility of the above PMW theorem and its consequences.

Accurate analytical predictions are obtain to estimate average forming process power P, with an error ε less than 5%, by formula:

$$P = \left(\tilde{P} + \tilde{\tilde{P}}\right)/2 \tag{10}$$

where $\varepsilon = 100*(\tilde{P} - \tilde{\tilde{P}})/2P$.

Here $\tilde{P}$ represents the Upper Bound Power estimation and $\tilde{\tilde{P}}$ the Lower Bound Power estimation, obtained from applying the PMW theorem to specific predefined subspaces of virtual stresses, kinematic velocities and boundaries-loadings conditions [4-8].

4. **DISCUSSION AND CONCLUSIONS**

This paper proves plastic and friction criteria convexity with customary rule laws corresponding to plastic flow of any continuum media. The performed theory has been valid by previous works of the author through comparisons of numerical results obtained from Finite Element Modelling (FEM) with analytical computations based on the PMW theorem and its consequences.

REFERENCES

1. Avitzur B., *Metal Forming: Processes and Analysis*, New-York, McGraw-Hill, 1968
2. Bejan A., *Shape and Structure: From Engineering to Nature*, UK, Cambridge Univ., 2000.
3. Bejan A., S. Lorente, *Design with Constructal Theory*, New Jersey, John Willey & Sons, 2008.
4. Gavrus A., The Maximum Work Principle Regarded as a Consequence of an Optimization Problem Based on Mechanical Virtual Power Principle and Application of Constructal Theory, *AIP Conf. Proc*., Vol. 1896, pp. 100009-1-6, 2017.
5. Gavrus A., Application of Constructal Theory to Write Mechanical Maximum Work Principle and Equilibrium State of Continuum Media Flow as a Solution of a Variational Optimization Problem, *Int. Revue IJMO*, **8**, *4*, pp. 227–231 (2018).
6. Pîrva E., Tudor A., Gavrus A., Stoica N., Cananau S., Some aspects regarding the influence of the anisotropy of an AA2021-T351 rolled thick plate on its tribological behaviour, *Mechanics & Industry*, **20**, *6* (2019).
7. Gavrus A., Computational Framework Concerning the Formulation of Maximum Work Principle used in Plasticity, Materials Forming and Tribology as a Consequence of a Variational Optimization Problem Defined From the Constructal Law, *IOP Conf. Series: Mat. Sci. and Eng*., Vol. 968, 2020.
8. Gavrus A., Use of the Constructal Law to Prove the Maximum Work "Principle" Defining Plasticity, Contact Friction and Continuum Media Flow Using a Variational Optimization Framework. Application to Extrusion Power Estimation, *Int. CLC 2023 Conf*., Turin, Italy, 21–22 September 2023.

CONSTRUCTAL LAW CONFERENCE – CLC2024
Design in Nature and Evolution
Romanian Academy, Bucharest, 10–11 October 2024

Proceedings of CLC2024
pp. 137–140

EVOLUTIONARY PATTERNS OF LEAVES: PALEOBOTANY AND CONSTRUCTAL LAW

ANTÓNIO HEITOR REIS

ICT Energy Group, Un. Évora, Portugal
ahrgoo@gmail.com; Tel. (0351)967324948

Paleobotany has been making the evolution of living structures that gave rise to present-day plants with thin planar leaves increasingly clear. And it tells us a fascinating story with many chapters to write and enigmas to decipher. The evolution of the structures that gave rise to present-day leaves with dense venation is one of those enigmas for which Constructal Law can offer a consistent, scientifically based, and beautiful explanation.
In this article, we show how it is possible to understand the evolution of the shape and venation of the structures that gave rise to present-day leaves. We aim to promote "easier and easier access" to all the energy and mass currents that allow photosynthesis and subsequent redistribution of products throughout the leaf system within a constraints framework (optimization of solar radiation capture and access to water and nutrients).

Keywords: Paleobotany; Leaf evolution; Venation patterns; Constructal Law**.**

1. INTRODUCTION

Bejan´s Constructal Law [1] is increasingly establishing itself as a reference paradigm in the evolution of animate and inanimate systems. Applications of Constructal Law to the evolution of natural systems is a hot topic that has been covered in multiple publications, some recent [2].

Paleobotany offers us a varied record of the evolution of plant leaves from microphylls, small and simple leaves, to megaphylls, larger and more complex leaves, over billions of years. Quoting Kenrick [3]: "The fossil record shows that megaphylls evolved from the photosynthetic branching systems of early vascular plants that became flattened and later webbed to produce a broad lamina in several groups by the end of the Devonian" (see. Fig 1). However, as noted by Tomescu [4]: "current understanding of plant phylogeny and leaf development fails to shed light on the origin of microphylls and supports several independent origins of megaphylls.".

This paper shows how Constructal Law can provide a convincing explanation for this question.

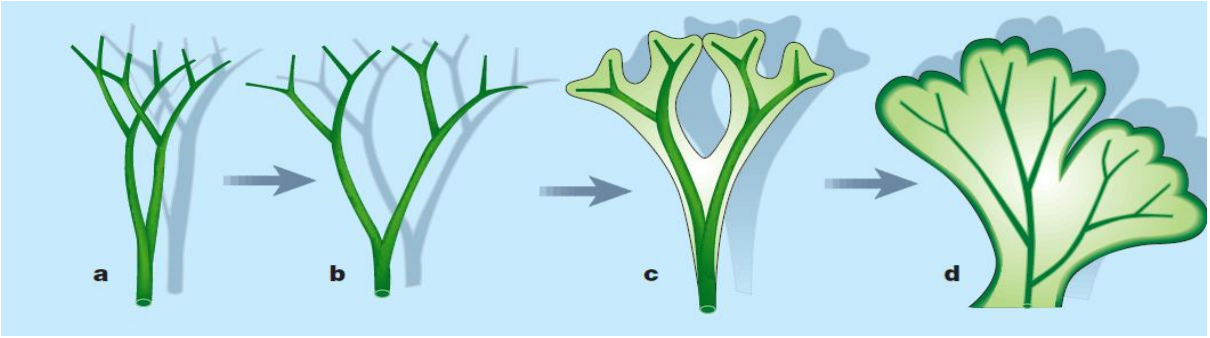

Fig. 1 – Evolution of leaves from microphylls: (a) Dichotomous branching; (b) Widening for maximum exposition to sunlight; (c) Transition to a planar leaf; (d) Fully developed planar leaf. (reprinted from ref. [3]).

DOI: https://doi.org/10.59277/CLC/2024.35

2. **FLOW ACCESS IN A DICHOTOMOUS BRANCHING MICROPHYLL**

Leaf is a plant construct that performs several functions: (i) it is the plant's powerhouse where molecules essential to the plant's life are manufactured through photosynthesis; (ii) it is the panel that collects the solar energy that powers photosynthesis; (iii) it is the reception center for raw products (minerals and water) necessary for the manufacture of complex molecules; (IV) is the distribution center of these molecules throughout the plant structure.

To fulfill its function as a receptor for solar energy, the shape of the leaf has evolved to improve its capacity for exposure to direct solar radiation. To fulfill the functions of receiving nutrients and distributing the products of photosynthesis, the leaf has evolutionarily developed a channel structure that can fulfill these objectives increasingly efficiently, within the framework of environmental restrictions.

The first stage of evolution consists of developing a channel structure where mineral salts and water can circulate. Nature's “intelligence” lies in its ability to develop structures that perform in the vicinity of the optimum point of operation [2]

Constructal theory has proven that such basic point-to-area structures are flow trees. Dichotomous branching flow trees have been shown to provide the best flow access to the fluids circulating in them [5].

In Fig. 1 (a), in fact, we can observe that this was the solution adopted by nature. Chloroplasts, i.e. the cells where photosynthesis takes place, cover the outside of the channels that transport mineral salts and water in a layer with the maximum thickness δ that allows the transmission of sunlight. The next stage of evolution (Fig. 1(b)) corresponds to the widening of the tree to maximize exposure to sunlight.

Fluids circulate in the leaf structure in bundles of microchannels driven by forces other than pressure gradients. Therefore, the total current is proportional to the cross-sectional area (d^2) of the bundle (leaf vein) of diameter *d*. Then, in this case, the general form of the flow resistance at the level *n* of a dichotomous branching tree of channel bundles of length l_n reads: $r_n = k2^{-n}d_n^{-2}l_n$ (where *k* is a constant) which gives rise to the following structural rule of the flow tree $(d_{n+1}/d_n) = 2^{-3/4}$ (see [5]). A general rule of symmetric trees is that the resistance is the same at all branching levels, i.e. $r_n = r_0, \forall n$ [5]. Therefore $r_n = kd_0^{-2}l_0$ and, $l_{n+1}/l_n = 2^{-1/2}$. Hence, the additional resistance R_N that comes from adding a *N*th branching level is $R_N = kd_0^{-2}l_0$. The *N*th branching level will accommodate a number of cells equal to $2^N\sigma\pi d_N l_N \delta$ where σ stands for cell density.

Therefore, the total resistance per unit cell reads:

$$(\rho_N)_{microphyll} = k\,2^{N/4}/(\sigma\pi d_0^3\,\delta). \tag{1}$$

3. **FLOW ACCESS IN A LEAF**

Microphylls evolved into megaphylls and present-day leaves, representing a new concept for organizing the distribution of fluids that enter and leave the chloroplasts. From a central vein (bundle of microchannels) lateral veins develop from each side that feed chloroplasts distributed in a layer of thickness δ (Fig. 2).

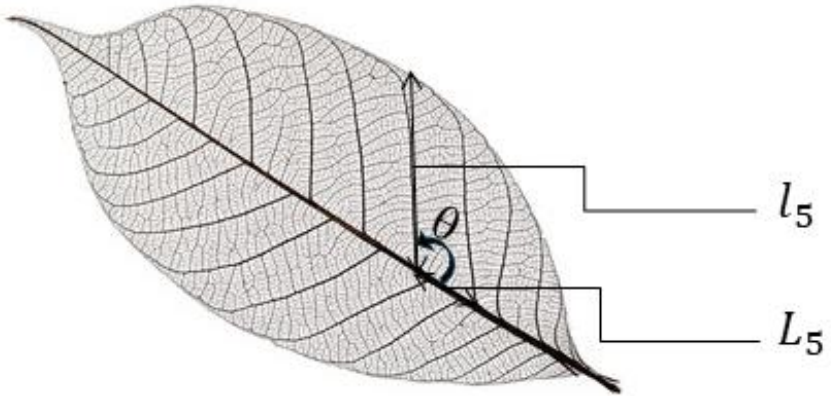

Fig. 2 – Present-day leaf, with a central vein and lateral second-order veins.

Let l_n be the length of the n^{th} lateral vein and L_n be the length of the adjacent segment of the central vein. So, the area served by these veins is $A_n = L_n l_n \sin\theta$. The total resistance to flow that fluids face to serve this area is made up of the resistance to moving fluids along the entire length of the microchannels that serve that area (proportional to total length $(\sum_{i=1}^{n} L_i + l_n)$ plus the resistance to delivering fluids to A_n from the adjacent veins (inversely proportional to the number of third-order veins and, therefore, to the length of the origin veins).

Therefore, it reads $R_{n(leaf)} = \alpha_n(\sum_{i=1}^{n} L_i + l_n) + \frac{\beta_n}{(L_n + l_n)}$, then the flow resistance per cell served in that area is:

$$(\rho_n)_{leaf} = (1/L_n^3)(\emptyset_n + \gamma_n)(\sigma\delta\sin\theta)^{-1}, \tag{2}$$

where $\emptyset_n = \alpha_n L_0^2 \lambda_n^2 \left[\psi_n^{-1} \sum_{i=1}^{n} \left(\frac{L_i}{L_n}\right) + 1\right]$, and $\gamma_n = \frac{\beta_n}{(\psi_n + \psi_n^2)}$, with $\lambda_n = \frac{L_n}{L_0}$ and $\psi_n = \frac{l_n}{L_n}$.

4. **MICROPHYLL EVOLUTION INTO LEAF**

As microphylls are free to morph, according to Constructal Law they will evolve to gain greater and greater access to flows. Therefore, microphylls would have evolved into leaves when $(\rho_n)_{leaf} < (\rho_N)_{microphyll}$, *i.e.*, in view of eqs. (1) and (2) once the following condition was verified:

$$2^{N/4} > (d_0/L_N)^3(\emptyset_n + \gamma_n)(\pi/(k\sin\theta)). \tag{3}$$

This condition is easily satisfied by the present-day leaves because $d_0/L_N \ll 1$ while microphyll resistance per cell grows with $2^{N/4}$, which constitutes a limiting factor for microphyll development.

Additionally, planar leaves offer better access to sunlight, which is essential to power photosynthesis. In this way, the evolutionary transition between microphylls and present-day leaves is explained based on Constructal Law.

5. **CONCLUSIONS**

The Constructal Law provides the theoretical framework for understanding the evolution of plant leaves from microphylls to present-day leaves. In this context, it is possible to perceive that the planar leaf structure

provides access to water and mineral salts and removes photosynthesis products from each chloroplast with lower resistance than that provided by microphylls, in addition to better access to sunlight. Evolution towards better design through easier and easier access to flows are the drivers of evolution (Constructal Law) [1].

REFERENCES

1. Bejan A., Constructal-theory network of conducting paths for cooling a heat generating volume, *Int. J. Heat Mass Transfer*, **40**, pp. 799–816 (1999).
2. Bejan A., *Freedom and Evolution: Hierarchy in Nature, Society, Science*, Springer, N. Y, USA, 2020.
3. Kenrick P., Turning over a new leaf, *Nature*, **410**, pp. 309–310 (2001).
4. Tomescu A.M.F., Megaphylls, microphylls and the evolution of leaf development, *Trends in Plant Science*, **14**, pp. 5–12 (2009).
5. Reis A.H., General formalism for symmetrically structured flows according to Constructal Law, *Int. Communic. Heat Mass Transfer*, **156**, p. 107593 (2004).

CONSTRUCTAL LAW CONFERENCE – CLC2024
Design in Nature and Evolution
Romanian Academy, Bucharest, 10–11 October 2024

Proceedings of CLC2024
pp. 141–144

TURBULENT MULTI-BRANCHING RADIAL SYMMETRIC FLOW STRUCTURES

MIGUEL R. CLEMENTE

University of Coimbra, ADAI, Department of Mechanical Engineering
Correspondence: miguel.clemente@dem.uc.pt

This study builds upon previous research that developed optimized tree-shaped flow networks within disc-shaped bodies for enhanced thermal management, extending these principles to explore turbulent flow regimes. Previously, a multi-branching approach combined with strategic hydraulic diameter settings was utilized to balance thermal and fluid performance in laminar flow conditions, successfully minimizing flow resistance. These efforts revealed that symmetric tree designs could significantly boost hydraulic and thermal efficiencies via a constrained minimization approach. In the current work, the focus shifts to examining the implications of transitioning these optimized designs from laminar to turbulent flow conditions. By comparing performance metrics between the two regimes, this study aims to elucidate the effects of flow regime transitions on network efficiency and effectiveness. The results enhance understanding of the fundamental dynamics governing flow networks and guide the development of more robust designs capable of operating across a broader range of flow conditions.

Keywords: Constructal Law; Radial branching; Bifurcation; Flow structure; Turbulent flow.

1. INTRODUCTION

Recent advancements in thermal management systems, particularly those incorporating disc-shaped bodies, have demonstrated the instrumental role of flow networks designed based on constructal theory. Previous investigations delineated an optimized framework for tree-shaped flow networks, predominantly focusing on laminar flow regimes. Expanding upon these foundational results, the current study delves into the dynamics of turbulent flow within these optimized tree-shaped networks. Turbulent flow, known for its enhanced mixing and heat transfer capabilities, is pivotal in scenarios where thermal loads surpass the handling capacity of laminar flows. The research aims to critically assess the adaptability of previously optimized geometric configurations under turbulent conditions, exploring the impact on fluid distribution and system efficacy. By comparing results from the laminar regime with the turbulent regime, a detailed examination of the interplay between flow regime transitions and network performance is provided.

2. METHODS

This study continues the exploration of tree-shaped flow networks, particularly extending the analysis to turbulent flow regimes by employing the foundational equations that defined the optimized network geometries in previous research. The objective is to evaluate how these geometric configurations perform under turbulent conditions. Following the Multi-Branching Generalization method found in Clemente and Pañao [1], and adapting it to turbulent regime conditions, the core geometric and flow equations are presented in Eqs. 1, providing the framework for this investigation.

DOI: https://doi.org/10.59277/CLC/2024.36

$$d_i = d_0 2^{-11i/27}, \tag{1a}$$

$$R_{G_t} = 2^6 n_0^{-\frac{7}{4}} \pi^{-\frac{7}{4}} d_0^{-\frac{19}{4}} g, \tag{1b}$$

$$g = \sum_{i=0}^{p} 2^{5i/27} L_i. \tag{1c}$$

Equations 1 correspond to Blasius flow, valid for a Reynolds number in the range of $4 \times 10^3 \leq \mathrm{Re} \leq 10^5$ [2,3], with the equations valid for scenarios involving smooth circular channels, in a dichotomous branching structure where $b = 2$. Equation (1a) presents the diameter of a channel d, at level i of the structure, as a function of the diameter of the first channel ($i = 0$). Equation (1b) defines the total flow geometric resistance, where n_0 is the number of initial channels, and g (Eq. 1c) is the objective function to minimize, with L_i representing the length of the channel. The volume of the structure is the same for all structures, maintained constant at 0.1 m^3.

The subsequent section provides a comparative analysis of the results obtained from turbulent versus laminar flow regimes. This comparison aims to highlight significant differences and insights into the performance and efficiency of tree-shaped flow networks under varied flow conditions.

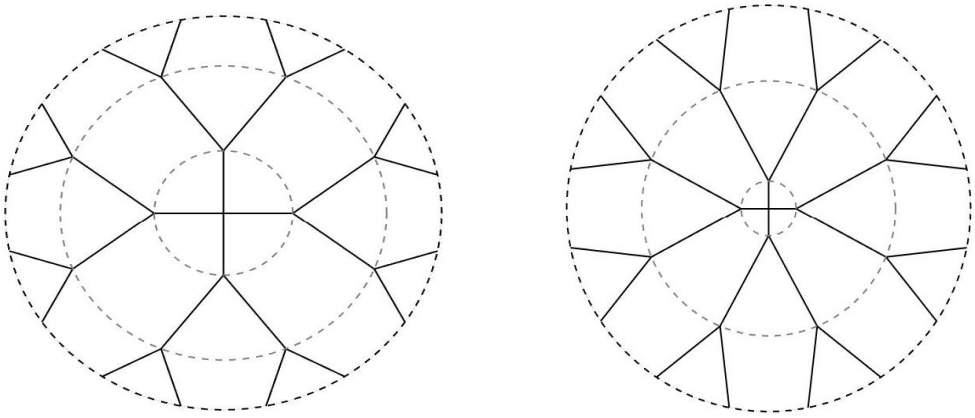

(a) Laminar regime - Hagen-Poiseuille flow. (b) Turbulent regime - Blasius flow.

Fig. 1 – Laminar and turbulent radial symmetric flow structures with $b = 2$, $p = 2$, and $n_0 = 4$.

3. **RESULTS AND DISCUSSION**

A significant distinction between turbulent and laminar flow structures is observed in the configuration of initial channels. Specifically, turbulent flow architectures do not incorporate three initial channels ($n_0 = 3$) due to the resultant negative length in the first channel. To facilitate an effective comparison, laminar structures configured with $n_0 = 3$ have been excluded from this analysis.

Turbulent structures exhibit lower Svelteness values than their laminar counterparts, yet they demonstrate marginally reduced geometric resistance. Figure 3 illustrates the evolution of Svelteness (Sv) and total geometric resistance (RGt), presenting results specifically at the lower boundary of the Blasius flow, where $\mathrm{Re} = 4 \times 10^3$. In the laminar regime, the evolution of Svelteness is consistent, whereas in the turbulent regime, it stabilizes starting from $p = 3$. This stabilization in the turbulent regime is attributed to much shorter initial channels possessing larger diameters. Like the laminar regime, an increase in p leads to a general decrease in Sv, indicating that deeper branching diminishes Svelteness. However, the differences in geometric resistance are minimal, with the turbulent regime exhibiting slightly more favorable outcomes.

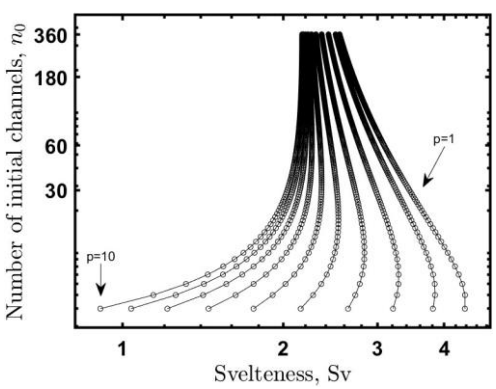

(a) Svelteness in Hagen-Poiseuille flow.

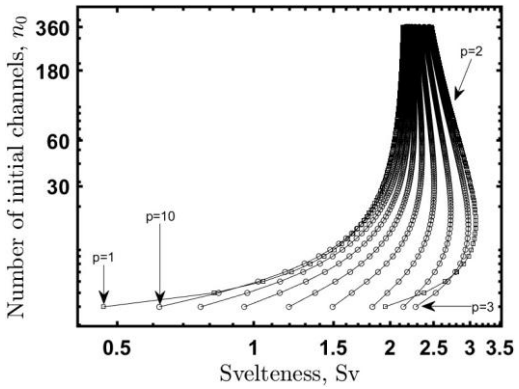

(b) Svelteness in Blasius flow.

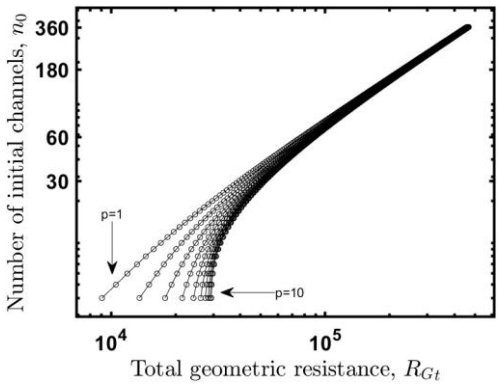

(c) Total geometric resistance in Hagen-Poiseuille flow.

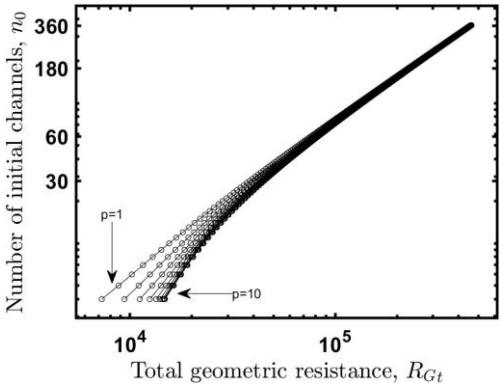

(d) Total geometric resistance in Blasius flow.

Fig. 3 – Evolution of Svelteness and total geometric resistance with branching level p, and several initial channels n_0 for laminar and turbulent regimes.

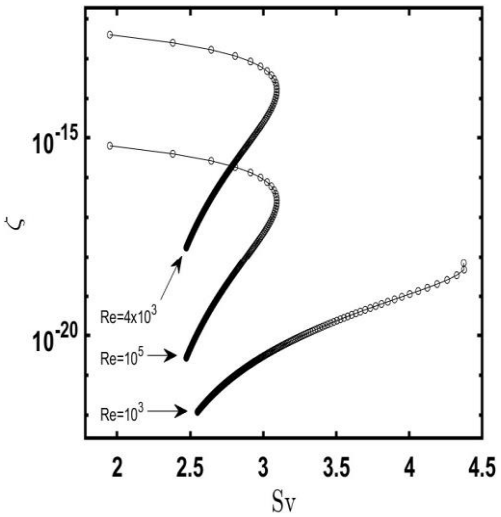

Fig. 4 – Evolution of Svelteness and performance with the Reynolds number, for configurations with $b = 2$ and $p = 2$.

Figure 4 illustrates the evolution of Svelteness (Sv) and its impact on thermal fluid performance (ζ) across different Reynolds numbers. It presents a compelling visualization of how geometric optimizations translate into performance enhancements in fluid flow systems. The figure showcases three distinct set of architectures by varying the Reynolds numbers, Re = 10^3, Re = 4×10^3, and Re = 10^5. Each set displays a unique trajectory

of performance as a function of Sv. In the laminar regime, performance increases proportionally with Sv in the direction of less initial channels. This behavior contrasts markedly with the turbulent regime, where thermal fluid performance starts at a higher baseline and maintains a gradual ascent until a maximum Sv, indicating a sustained benefit from increased Svelteness even at higher values. This discrepancy underscores the influence of flow characteristics – dictated by Reynolds numbers – on the effectiveness of geometric enhancements.

Transitioning from the laminar regime to the turbulent regime leads to notable performance improvements. However, there's a clear disadvantage in further increasing turbulence. In the turbulent regime, increasing the number of initial channels initially leads to a more prominent effect in increasing Sv, while performance decreases slightly until it reaches a plateau. This behavior is indicative of a moderate flow regime where geometric optimizations are effective but have limited benefits.

These insights are critical for the design of flow networks, emphasizing the need to tailor geometric configurations based on anticipated operational flow conditions to optimize thermal fluid performance effectively.

4. **CONCLUSION**

This investigation into the evolution of Svelteness and its impact on performance in tree-shaped flow networks across different regimes provides crucial insights into the interplay between flow characteristics and network geometry. These findings underscore the critical role of geometric design in enhancing flow efficiency and can significantly influence the development of more efficient thermal management systems. By emphasizing the need to consider the flow regime during the design phase, this study highlights how tailored design strategies can optimize performance.

Furthermore, the detailed comparison across various Reynolds numbers clearly shows that although increasing Svelteness generally boosts performance, the extent and nature of these improvements are profoundly influenced by the specific fluid dynamics of each flow regime. This nuanced understanding allows for the design of flow networks that are not only optimized for efficiency but also customized to the operational conditions expected in practical applications.

REFERENCES

1. Clemente M.R., Pañao, M.R.O., Generalizing multi-branching radial symmetric flow structures, *International Journal of Heat and Mass Transfer*, **216**, 124568 (2023).
2. Fox R.W., Mitchell J.W., McDonald A.T., *Fox and Mcdonald's Introduction to Fluid Mechanics*, Wiley & Sons, Incorporated, John, 2019.
3. Idelchik I.E., *Handbook of Hydraulic Resistance*, Begell House, 2008.

CONSTRUCTAL LAW CONFERENCE – CLC2024
Design in Nature and Evolution
Romanian Academy, Bucharest, 10–11 October 2024

Proceedings of CLC2024
pp. 145–148

A LOW-IMPACT HIGH-EFFICIENCY BRAYTON CYCLE CONCEPT WITH EVAPORATIVE COOLING DURING THE COMPRESSION PROCESS USING H_2/CH_4 FUEL BLENDS

GEORGE STANESCU[a,*], JENI VILAG[b], VALERIU VILAG[b], ENE BARBU[b],

[a]Graduate Program of Environmental Engineering, UFPR, 81530-000, Curitiba, Parana, Brazil, stanescu@ufpr.br
[b]INCDTurbomotoare COMOTI, Iuliu Maniu 220D, Bucharest, 061126, Romania, jeni.vilag@comoti.ro, valeriu.vilag@comoti.ro, barbu.ene@comoti.ro
*Correspondence: stanescu@ufpr.br;Tel. +40-741-619-029

Towards a low-impact high-efficiency Brayton cycle concept, a gas generator system including a compressor with evaporative cooling, a combustion chamber using H_2/CH_4 fuel blends and a gas turbine is being analyzed at this preliminary stage. The Constructal approach on the effectiveness of compressed air temperature control by evaporative cooling, previously carried out by the authors, shed some light on the potential growth of mechanical power provided by gas turbine power plants of 45.81% and a simultaneous reduction of 2.26% in specific fuel consumption.

The current study, carried out on the combustion chamber, reveals that increasing the H_2 fraction in the fuel blend results in a direct reduction in carbon dioxide production and in a decrease in CO and NO_x emissions when the temperature of the flue gas is maintained at 1450 K. Meanwhile, the exergy efficiency of the combustion chamber remains almost constant at 39.3%. Study of the two components already analyzed, the compressor and the combustion chamber, allows us to move towards a low-impact, high-efficiency Brayton cycle concept as close as possible to its technical implementation.

Keywords: Evaporative cooling; Hydrogen; Brayton cycle; Entropy generation; Constructal Law.

1. INTRODUCTION

A large body of work has been devoted during the last decade to studying evaporative cooling, one of the simplest and least expensive air cooling technologies applied in the gas turbine industry [1-3]. The authors have already developed, based on the Constructal Law, a complete assessment of the maximum potential of evaporative cooling to control the temperature of compressed air in gas turbine power plants (GTPP) [4]. In an attempt to develop a Brayton cycle concept not only aiming at high efficiency but also focusing on lower impact, this work considers evaporative cooling of the compressor and the use of methane and hydrogen blends in the combustion chamber. The thermodynamic optimization method based on the minimization of entropy generation is used to study the operation of a combustion chamber with H_2/CH_4 fuel blends, aiming at the direct reduction in carbon dioxide production and also the reduction of CO and NO_x emissions.

2. PHYSICAL AND MATHEMATICAL MODELING

The physical model of the gas turbine power plant considered in this study is represented by the compressor, the combustion chamber and the turbine assembly shown in Fig. 1. Details of the compressor design are presented conceptually in Fig. 1, where it can be observed how temperature control is physically

DOI: https://doi.org/10.59277/CLC/2024.37

performed during the compression process by means of the evaporative cooling due to the vaporization of liquid water continuously injected along the compressor [4].

The combustion chamber, which is the focus of this study, receives high-pressure saturated humid air in state 2 after its passage through the compressor. To first study the CO_2 emission levels, it is considered in this study that the combustion chamber is fed with H_2/CH_4 fuel blends of various compositions.

The mathematical modeling of the combustion process was performed based on the equations of the Law of Conservation of Energy and the 2nd Law of Thermodynamics for the steady-state operation of the adiabatic CC, assuming the combustion of H_2/CH_4 fuel mixtures with variable excess air (λ) in order to control and maintain constant the temperature of the combustion gases T_3 at the CC outlet. The formation, by dissociation, of the following chemical species was also considered: CO_2, CO, H_2O, OH, H_2, O_2, N_2, NO, NO_2.

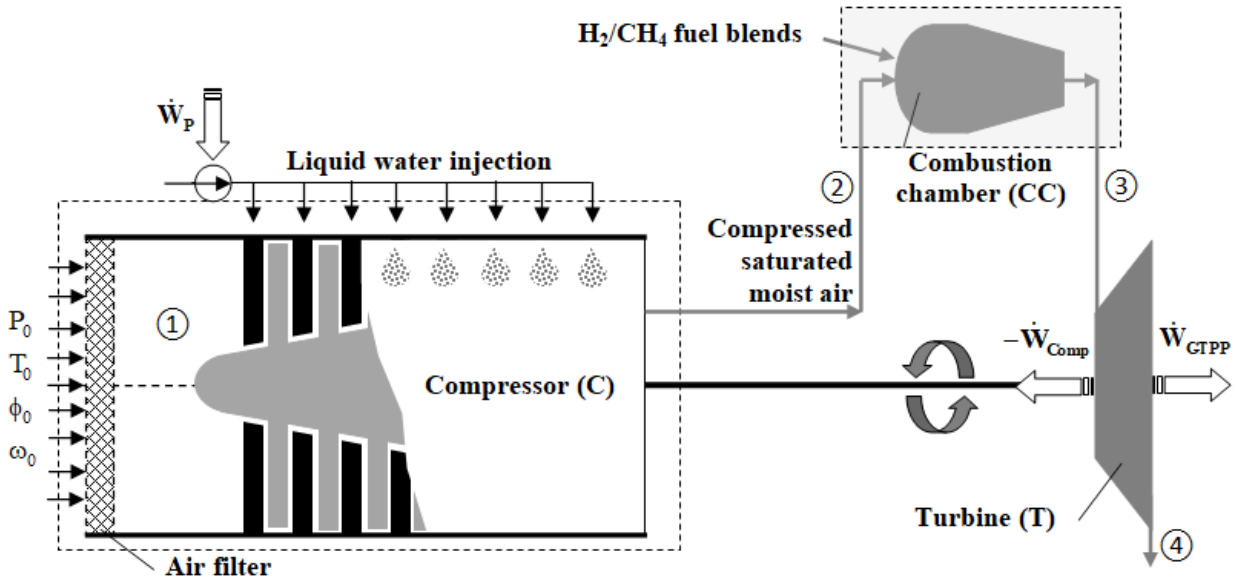

Fig. 1 – Physical configuration of a GTPP using H_2/CH_4 fuel blends, where the liquid water injection develops along the compressor permanently maintaining the relative humidity of the compressed moist air at its maximum possible value.

Table 1

Numerical values of the excess air λ and the chemical composition of the combustion gases

f_{H_2}	λ	y_CO_2 (%)	y_CO (ppm)	y_H_2O (%)	y_OH (ppm)	y_H_2 (ppm)	y_O_2 (%)	y_N_2 (%)	y_NO (ppm)	y_NO_2 (ppm)
0.0	2.02	4.94	0.159	9.88	33.406	0.131	10.053	75.048	680.64	7.572
0.1	2.04	4.77	0.146	10.06	32.934	0.128	10.115	74.982	672.89	7.576
0.3	2.08	4.33	0.118	10.51	31.727	0.120	10.277	74.810	653.54	7.585
0.5	2.13	3.72	0.087	11.15	30.238	0.111	10.511	74.551	629.30	7.607

Based on the mathematical model, the numerical values of the excess air and the chemical composition of combustion gases are calculated when the molar fraction of H_2 in the fuel mixture, f_{H2}, is known.

3. **RESULTS**

Results of the numerical simulation, performed with the CEA program developed by NASA Lewis Research Center [5], are presented in Table 1. The fuel mixture ratios, as well as the fuel/oxide mixture ratio, were defined by imposing the molar fractions of CH_4 and H_2, and O_2 and N_2, respectively, to maintain a maximum temperature of 1450 K under constant pressure at 0.7MPa. The main chemical species resulting from the dissociation processes during combustion are tracked as molar fractions and studied in relation to compliance with current emission standards. Based on the 2nd Law, the generation of entropy (exergy destruction) was also calculated. The numerical results obtained show a decrease of only 0.2% in the combustion chamber`s exergy efficiency when the fraction of hydrogen in the fuel blend increases to 50%.

4. **DISCUSSION AND CONCLUSIONS**

The first step in developing the new low-impact high-efficiency Brayton cycle concept was to investigate the limits and conditions in which the real axial compressor's design may evolve in order to make the gas compression as close as possible to an isothermal process. Based on the Constructal Theory the compressor`s physical modeling was carried out as an ensemble of adjacent elemental compressors that"...provides easier access to the imposed currents that flow through it". Compressed moist air temperature control within each of the elemental compressor is done based on the evaporative cooling principle. The results obtained based on the Constructal approach, with indirect evaporative cooling at the compressor aspiration and "inter-stage water spraying", show comparatively that during most of the compression process a temperature of the compressed moist air 45% lower. Providing a "globally easier flowing configuration", the Constructal approach with indirect evaporative cooling at the compressor aspiration and "inter-stage water spraying", shed some light on the potential of growth in the mechanical power delivered by the GTPP of 45.81% and a simultaneous reduction of 2.26% in the fuel specific consumption. Numerical results on the entropy generation due to the compressor functioning confirm the realism of the adopted assumptions and the adequacy of the mathematical formulation of the proposed model for numerical simulation purposes. Application of water injection in each compressor stages involves miniature holes drilled on stators and a sophisticated water injection system. The experiments regarding water injection through TV2-117A intake, reconfigured from kerosene to methane showed not only a power augmentation but also NO_x emissions reduction similar to the work presented in [6]. Thus the introduction of water into the gas turbine intake at idle generates a reduction of averaged turbine inlet temperature of about 5 ^{0}C and also NO_x emissions fall by approximately 4 ppm. The results also agree well in terms of variation of cross-sectional area, isentropic efficiency, maximum temperature and pressure, with the data available for the axial compressors of the following widely produced and "in service" gas turbine engines: TV2-117, TV3-117, RU19A-300 and AI20 [7]. The numerical results presented in this work compare well with those of other authors [8] and show advantages in terms of emission reduction when H_2/CH_4 fuel mixtures are fed into gas turbine power plants. Therefore, it is feasible to integrate the two components studied so far, compressor and combustion chamber, into a single low-impact, high-efficiency equipment. Next, this research will be continued following the principles of

finite-speed irreversible thermodynamics [9], focusing on the optimization of gas turbine blade geometry. Thus, minimizing the generation of entropy in order to maximize the mechanical power of the turbine, the expansion process of the gases passing through the turbine must be carried out as close as possible to an isentropic expansion.

ACKNOWLEDGEMENTS

This work was carried out through the framework Program-Nucleu within the National Research, Development, and Innovation Plan 2022–2027, conducted with the support of the Romanian Ministry of Research, Innovation, and Digitization (MCID), project number PN23.12.02.02.

REFERENCES

1. Barigozzi G. *et al*., Techno-economic analysis of gas turbine inlet air cooling for combined cycle power plant for different climatic conditions, *Applied Thermal Engineering*, **82***,* 57–67 (2015).
2. Ibrahim M. A., Varnham A., A review of inlet air-cooling technologies for enhancing the performance of combustion turbines in Saudi Arabia, *Applied Thermal Engineering*, **30**, 1879–1888 (2010).
3. Bhargava *et al*., Gas turbine compressor performance characteristics during wet compression – influence of polydisperse spray, *Proceedings of ASME Turbo Expo 2009: Power for Land, Sea and Air* (GT2009), June 8–12, 2009, Orlando, FL USA.
4. Stanescu G., Ene B., Vilag V., Andreescu T., Constructal approach on the feasibility of compressed air temperature control by evaporative cooling in gas turbine power plants, *Proceedings of the Romanian Academy, Series A*, Special Issue, 2018, pp. 201–206
5. Gordon S. and McBride B.J., *Computer Program for Calculation of Complex Chemical Equilibrium Compositions and Applications*, NASA Reference Publication, 1311, 1996.
6. Barbu E. *et al*., The influence of inlet air cooling and afterburning on gas turbine cogeneration groups performance, *Gas Turbines – Materials, Modeling and Performance*, Dr. Gurrappa Injeti (Ed.), InTech, 2015.
7. Stanescu G., Barbu E., Vilag V. and Vilag J., Achieving Temperature Control by Direct Injection of Liquid Water in Axial Compressors of "in-service" Gas Turbine Engines, *Proceedings of the 16th International Conference on Heat Transfer, Fluid Mechanics and Thermodynamics*, 2022.
8. Lopez-Ruiz G., Castresana-Larrauri J., Blanco Ilzarbe, J.M., Thermodynamic Analysis of a Regenerative Brayton Cycle Using H_2, CH_4 and H_2/CH_4 Blends as Fuel, *Energies*, *15*, p. 1508 (2022), https://doi.org/10.3390/en15041508
9. Petrescu S. *et al*., *Advanced Thermodynamics of Irreversible Processes with Finite Speed and Finite Dimensions*, Edit. AGIR, 2015.

CONSTRUCTAL LAW CONFERENCE – CLC2024
Design in Nature and Evolution
Romanian Academy, Bucharest, 10–11 October 2024

Proceedings of CLC2024
pp. 149–152

CONSTRUCTAL LAW LEADS TO DISCOVERY OF THE FUNDAMENTAL LAW IN ECONOMICS

MIRCEA SCURTU, ELMOR L. PETERSON

NCSU
mitch.scurtu@optimalglobalpricing.com, +1 336 380 3363

Fundamental Law of Economics (FLoE).

A finitely (not infinitely) converging algorithm addressing simultaneously the dual market variables price and quantity represents the mathematical formulation for the economic globalization of the planet.

The document discusses the application of the Constructal Law and the Fundamental Law of Economics in addressing resistance to flow in economic systems, leading to the globalization of the planet

Keywords: Economic equilibria; Duality in physics; Duality in economics; Duality in geometric programming.

1. INTRODUCTION

*Constructal Law:*For a finite economic system to persist in time must evolve with freedom such as to increase access to what flows.

Problem with economic systems is that they do not evolve with freedom. There is a resistance to flow. Therefore, we need a corollary to the Constructal Law.

*Corollary:*For an economic system to evolve with freedom the resistance to flow must be contained.

The document discusses the application of the Constructal Law and the Fundamental Law of Economics (FLoE) to address resistance to flow in economic systems, which is crucial for the economic globalization of the planet. Key points include:

Constructal Law in Economics: Economic systems must evolve with freedom to increase access to what flows. Resistance to flow, often caused by human actions like market arbitrage, must be contained. *Market Arbitrage*: Market arbitrage, which exploits global price differentials without producing value, is a significant issue, estimated to cause $150 trillion in global market distortions annually. *Entanglement in Economics*: The concept of entanglement from quantum physics is applied to economics, suggesting that dual variables like price and quantity are instantaneously complementary. This is demonstrated through market models showing how changes in quantity or price affect the other variable. *Finitely Converging Algorithm:* A finitely converging algorithm, derived from the equilibrium of electrical circuits, is proposed to address dual variables simultaneously, integrating physical sciences with economics. *Economic Equilibrium*: The algorithm can solve economic equilibrium problems efficiently, returning significant value to producers and consumers, and negating the need for parallel trade. *Globalization and Wealth Redistribution*: The FLoE aims to secure the globalization of the planet by economic cycles without the negative effects of recessions and depressions, redistributing wealth equitably upfront. *Integration of Physics and Economics*: The document emphasizes the ultimate integration of physics and economics, aligning with Adrian Bejan's "Physics of Life," and proposes that economic systems can evolve without the negative impacts of current business practices. The document concludes that the FLoE can contribute to the natural economic globalization of the planet by addressing resistance to flow and ensuring equitable wealth distribution.

2. EXPLAINING THE FUNDAMENTAL LAW OF ECONOMICS FLOE

The Fundamental Law of Economics (FLoE) is a concept that integrates principles from physics, specifically the Constructal Law, into economic systems. It posits that for an economic system to persist and evolve over time, it must increase access to what flows within the system, such as goods, services, science / technology and capital.

DOI: https://doi.org/10.59277/CLC/2024.38

The FLoE addresses the dual market variables of price and quantity simultaneously to achieve economic equilibrium and reduce resistance to flow, which is often caused by human actions like market arbitrage.

Key aspects of the FLoE include:

Simultaneous Addressing of Dual Variables: The FLoE involves a finitely converging algorithm that simultaneously addresses the dual variables of price and quantity, ensuring that changes in one variable are instantaneously reflected in the other.

Containment of Resistance to Flow: Resistance to flow, such as market arbitrage, must be contained to allow the economic system to evolve freely. This resistance is seen as a hindrance to the natural flow of economic activities.

Entanglement Principle: The FLoE applies the concept of entanglement from quantum physics to economics, suggesting that price and quantity are entangled variables that assume complementary statuses instantaneously in measurable time and space.

Economic Equilibrium: By using the finitely converging algorithm, the FLoE aims to achieve economic equilibrium efficiently, maximizing revenue and ensuring equitable distribution of wealth.

Globalization and Wealth Redistribution: The FLoE supports the natural economic globalization of the planet by promoting economic cycles that do not crash but transfer energy to new cycles, thus avoiding recessions and depressions and making wealth redistribution more effective.

Overall, the FLoE seeks to integrate physical laws with economic principles to create a more efficient, equitable, and sustainable global economic system.

2. **MATERIALS AND METHODS**

The dual market variables in economics are price and quantity. These variables are interdependent and play a crucial role in determining market equilibrium. When entangled these dual variables act in tandem.

Price: This is the amount of money required to purchase a good or service. It is influenced by factors such as supply, demand, production costs, and market competition.

Quantity: This refers to the amount of a good or service that is available for purchase or that consumers are willing to buy at a given price. It is influenced by factors such as consumer preferences, income levels, and the availability of substitutes.

In economic models, changes in one of these variables typically result in adjustments in the other to reach a new equilibrium. For example, an increase in the price of a good generally leads to a decrease in the quantity demanded, while a decrease in price usually results in an increase in the quantity demanded.

Example (Table 1): from our study of five medicines in seven European markets we have the medicines in the first column, sponsors in the second, recorded market arbitrage aka parallel trade next. Actual measured market arbitrage in the 4th column. Notice that the recorded market arbitrage is always underreported sometimes as much as 50%. This can be due to a couple of reasons: defective market statistics, but more likely intentional underreporting by parallel traders in an effort to justify the legality of parallel trade. Next two columns are the percentage returns of the resistance to flow after we resolve the economic equilibrium problem. Next column we have the annual sales of these five medicines as per market statistics.

Last two columns are the dollar returns of the resistance to the producers and consumers. $2 billion are returned to the five producers, $800 million to the consumers. This is a significant finding. It is challenging the reason for parallel trade to become legal. Parallel traders claim that they benefit consumers. From our study above it turns out the parallel trade is hurting consumers by $800 million. Return of resistance to producers and consumers will increase access to what flows. This is the way the FLoE is affecting the economic globalization of the planet.

From our study of five medicines in seven European markets, we have the medication in the first column, the sponsor in the second, and recorded market arbitrage, parallel trade next. Actual measured market arbitrage is in the 4^{th} column. Notice that the recorded market arbitrage is consistently underreported to legitimize the legality of market arbitrage. Applying optimal solutions that are optimal prices and optimal quantities (optimal trade flows) will return the flow resistance, aka market arbitrage, to the sponsors of the medicines and the global patient in the amount of about three billion dollars. $2 billion to the producers, $800 million to the consumers. This will increase access to what flows. This return of capital to the sponsor and consumer is productive capital, which will stimulate the economic globalization of the planet. This is about knowing the laws of physics and developing the instruments to affect globalization positively.

Table 1

Parallel trade earnings in seven European countries are to be returned to the pharma and global patients

Medicine	Pharma sponsor	Recorded Parallel Trade	Actual Parallel trade losses	return to pharma	welfare improvement global patient	Global Annual sales 2018	Pharma gains with optimal solution	Global patient gains with optimal solution
Adalimumab (Humira)	ABBVIE	8.48%	11.64	6.82%	1.65%	$20,358,000,000	$1,388,415,600	$335,907,000
Levothyroxine Sodium	Abbot	0.59%	18.38%	12.69%	6.13%	$2,600,000,000	$329,940,000	$159,380,000
Enbrel (Etanercept)	Amgen Pfizer	8.27%	15.42%	13.9%	1.76%	Not available; seven European countries sales 2017 $2,677,631,644	$372,190,798.52	$47,126,316.93
Infliximab (Remicade)(DRY INF VIAL 100MG 1)	Johnson & Johnson	13.83%	17.86%	8.93%	8.61%	$3,700,000,000	$330,410,000	$318,570,000
HYDROXYCHLOROQUINE (Plaquenil)	Mylan, Teva	4.54%	47.6%	13.11%	9.26%	Not available; seven European countries sales 2017 - $50,549,039	$6,626,979.01	$4,680,841.01
Average			22.18%					
Total revenue returned to pharma sponsor via optimal solution							$2,427,583,377.53	
Welfare gain to global patient								$865,664,157.94

OGP (Optimal Global Pricing) technology can measure size of global parallel trade markets from market statistics.

Calculations performed on IMS statistics 2017.

* Factoring in client statistics will likely drive up these numbers.

3. Results

Generalizing the FLoE. Economic systems are Man-Man systems.

For all Man-Man systems:

A finitely (not infinitely) converging algorithm addressing simultaneously the dual variables of the system represents the mathematical formulation for the globalization of the system.

Our finitely converging algorithm in economics has been the subject of my PhD. research under Elmor L. Peterson. The computer code activating this algorithm I developed in collaboration with a brilliant software engineer, Mihnea Galca from Politehnica Bucharest. Peterson has some other similar algorithms and invites collaboration in writing the computer code for them. For these algorithms the appropriate scientific laws, have been "digitized" by "meshing" and "discretization": Rush Hour Traffic (travel), Simulation of Heav3y-hydrogen Fusion (science), Cosmic Simulation (science), Climate Simulations and Weather Predictions (science).

4. **DISCUSSION AND CONCLUSIONS**

Fundamental Law of Economics (FLoE):

Integrates principles from physics, specifically the Constructal Law, into economic systems.

Aims to increase access to what flows within the system (goods, services, science, technology, capital) to ensure the system's persistence and evolution. Addresses dual market variables (price and quantity) simultaneously to achieve economic equilibrium and reduce resistance to flow.

Key Aspects of FLoE:

Simultaneous Addressing of Dual Variables: Uses a finitely converging algorithm to ensure changes in price and quantity are instantaneously reflected in each other. Containment of Resistance to Flow: Reduces resistance caused by market arbitrage to allow the economic system to evolve freely. Entanglement Principle: Applies the concept of entanglement from quantum physics, suggesting that price and quantity are interdependent and complementary. Economic Equilibrium: Achieves equilibrium efficiently, maximizing revenue and ensuring equitable wealth distribution. Globalization and Wealth Redistribution: Promotes natural economic globalization, avoiding recessions and depressions, and making wealth redistribution more effective.

Entanglement Principle:

Derived from quantum physics and applied to economics. Suggests that price and quantity are entangled, meaning changes in one variable are immediately reflected in the other. Helps achieve economic equilibrium more efficiently by quickly adapting to changes and maintaining balance between supply and demand.

Impact on Globalization:

Supports economic cycles that avoid the negative effects of recessions and depressions. Ensures equitable wealth distribution upfront, making traditional wealth redistribution methods obsolete. These insights could be valuable in the strategic planning and understanding of economic systems.

REFERENCES

1. Scurtu M., *An Empirical Study of Spatial Economic Equilibria Via Geometric Programming*, Doctoral Thesis, North Carolina University, Raleigh, USA, 1986.
2. Peterson E.L., An economic interpretation of duality in linear programming, *Jour. Math. Anal. Applications*, **30**, p. 172 (1970).
3. Peterson E.L., Symmetric duality for generalized unconstrained geometric programming, *SIAM Jour. Applied Math.*, **19**, p. 487 (1970).
4. Babayev D., *Computational algorithms in geometric programming,* Supplement I in the Russian translation of Geometric Programming, Mir of Moscow, 1972, p. 289.
5. Babayev D., *Algebraic programs treated by geometric and harmonic means*, Supplement II in the Russian translation of Geometric Programming, Mir of Moscow, 1972, p. 294.
6. Himmelblau D., Ed., *The decomposition of large (generalized) geometric programming problems by tearing, Decomposition of Large-scale Problems*, North-Holland, American Elsevier, 1973, p. 525.
7. Avriel M., Rijckaert M., Wilde D., Eds., *An introduction to mathematical programming, Optimization and Design*, Prentice-Hall, 1971, p. 6.
8. Avriel M., Rijckaert M., Wilde D., Eds., *Geometric programming and some of its extensions, Optimization and Design*, Prentice-Hall, 1973, p. 228.
9. Peterson E.L., Fenchel's hypothesis and the existence of recession directions in convex programming, Northwestern Univ. Center for Research in Mathematical Economics and Management Sciences, Discussion Paper No. 152, 1975.
10. Avriel M., Ed., Geometric programming, *SIAM Rev*., **19**, p. 1 (1976). Reprinted in *Advances in Geometric Programming*, Plenum Press, 1980, p. 31.
11. Peterson E.L., The conical duality and complementarity of price and quantity for multi-commodity spatial and temporal network allocation problems, Northwestern Univ. Center for Research in Mathematical Economics and Management Sciences, Discussion Paper No. 207, 1976.
12. Peterson E.L., Ordinary duality vis-à-vis geometric duality, Northwestern Univ. Center for Research in Mathematical Economics and Management Sciences, Discussion Paper No. 263, 1976.
13. Peterson E.L., The complementary unbounded-ness of dual feasible solution sets in convex programming, *Jour. Math. Programming*, **12**, p. 392 (1977).
14. Peterson E.L., The duality between sub-optimization and parameter deletion, *Math. Operations Res*., **2**, p. 311 (1977).
15. Peterson E.L., Geometric duality via Rockafellar duality, Northwestern Univ. Center for Research in Mathematical Economics and Management Sciences, Discussion Paper No. 270, 1977.
16. Avriel M. Ed., Optimality conditions in generalized geometric programming, *Jour. Opt. Th. Applications* (special issue on geometric programming), **26**, p. 3 (1978), Reprinted in *Advances in Geometric Programming*, Plenum Press, 1980, p. 95.
17. Avriel M. Ed., Saddle points and duality in generalized geometric programming, *Jour. Opt. Th. Applications* (special issue on geometric programming), **26**, p. 15 (1978). Reprinted in *Advances in Geometric Programming*, Plenum Press, 1980, p. 107.
18. Avriel M. Ed., Constrained duality via unconstrained duality in generalized geometric programming, *Jour. Opt. Th. Applications* (special issue on geometric programming), **26** (1978). Reprinted in *Advances in Geometric Programming*, Plenum Press, 1980, p. 117.
19. Avriel M. Ed., Fenchel's duality theorem in generalized geometric programming, *Jour. Opt. Th. Applications* (special issue on geometric programming), **26**, p. 51 (1978). Reprinted in *Advances in Geometric Programming*, Plenum Press, 1980, p. 143.
20. Moder J.J., Elmaghraby S., Eds., *Geometric Programming, Handbook of Operations Research*, Van Nostrand Reinhold, 1978, p. 207, A highly condensed version of 32.
21. Lucas W., Ed., Traffic equilibria on a roadway network, *Modules in Applied Mathematics, Discrete and Systems Models*, Vol. 3, Springer-Verlag, 1983, p. 155.

ADDENDUM: EXPLAINING THE ENTANGLEMENT PRINCIPLE IN THE CONTEXT OF THE FLOE

In the context of the Fundamental Law of Economics (FLoE), the entanglement principle is derived from quantum physics and applied to economics. It suggests that the dual market variables of price and quantity are entangled, meaning they are instantaneously complementary and interdependent. Changes in one variable (*e.g*., price) are immediately reflected in the other variable (*e.g*., quantity), and vice versa.

This principle implies that price and quantity are not independent but are closely linked in such a way that adjustments in one will directly and instantaneously affect the other. This entanglement helps in achieving economic equilibrium more efficiently, as the system can quickly adapt to changes and maintain balance between supply and demand. By addressing these dual variables simultaneously, the FLoE aims to reduce resistance to flow within the economic system, leading to more stable and equitable economic outcomes.

CONSTRUCTAL LAW CONFERENCE – CLC2024
Design in Nature and Evolution
Romanian Academy, Bucharest, 10–11 October 2024

Proceedings of CLC2024
pp. 153–156

FLUID MODES, DEEP LEARNING, AND CONSTRUCTAL LAW

PAUL CIZMAS

Department of Aerospace Engineering, Texas A&M University
cizmas@tamu.edu

The fluid modes generated using a proper orthogonal decomposition (POD) method were predicted for a fluidized bed and a power generation turbine. The POD-based reduced-order models were solved using either a Galerkin projection or a deep learning strategy. In both cases, as the number of the fluid modes increased, the modes appeared to fragment/bifurcate, indicating that these modes follow the constructal law.

Keywords: Reduced-order model; Proper orthogonal decomposition; Machine learning; Constructal law.

1. INTRODUCTION

Inspired by the structural modes identified in structural engineering, fluid mechanicians were able to determine the fluid modes of general transport phenomena [1]. Similarly to structural analysis, the fluid modes can be used to determine the flow solution if the weightings of the modes are known. Consequently, the solution $\mathbf{u}(\mathbf{x}, t_i)$ of the transport phenomena can be approximated as

$$\mathbf{u}(\mathbf{x}, t_i) = \sum_{k=1}^{M} a_k(t_i)\phi_k(\mathbf{x})\ i = 1, \dots, M,$$

where $\mathbf{u} \in \mathbb{R}^n$ is the state vector, $\phi_k \in \mathbb{R}^n$ is the k-th flow mode, $\mathbf{x} \in \mathbb{R}^d$ is the spatial coordinate, d is the spatial dimension $1 \leq d \leq 3, a_k \in \mathbb{R}$ is the time coefficient, the weighting of the flow mode, $t_i \in \mathbb{R}$ is time, and M is the number of snapshots. For compressible, non-reacting, three-dimensional flows $n = 5$.

2. METHODS

The minimization of the approximation error in (1) requires the minimization of the averaged least-square truncation error [2]

$$\epsilon_m = < \|\mathbf{u}(\mathbf{x}, t_i) - \sum_{k=1}^{m} a_k(t_i)\phi_k(\mathbf{x})\|^2 > \ i = 1, \dots, M,$$

where <> denotes the time average and $\|\|$ is the L^2-norm. The optimum condition (2) reduces to an eigenvalue problem, which for a discrete case is

$$\mathrm{R}(\mathrm{x}, \mathrm{y})\phi(\mathrm{x}) = \lambda\phi(\mathbf{x})\ \mathbf{x}, \mathbf{y} \in \mathbb{R}^d$$

where **R** is the autocorrelation matrix

$$\mathrm{R}(\mathrm{x}, \mathrm{y}) = \sum_{i=1}^{M} \mathbf{u}(\mathbf{x}, t_i)\mathbf{u}^T(\mathbf{y}, t_i)/M.$$

DOI: https://doi.org/10.59277/CLC/2024.39

The eigenvectors (or eigenfunctions) of the autocorrelation matrix (4) are the fluid modes, aka basis functions or proper orthogonal decomposition (POD) modes. The eigenvalues $\lambda_i, 1 \leq i \leq M$ of (3) determine how much relative energy is captured by the POD modes, where the relative energy is defined as $\lambda_i / \sum_{i=1}^{M} \lambda_i$.

The POD modes represent the skeleton of the solution. They can be calculated once snapshots of the solution are generated. Then the POD modes can be used to generate a reduced-order model (ROM) that allows us to predict the solution at any other time and flow conditions.

The following steps must be completed to generate a POD-based ROM: (a) generate database using a full-order model, (b) assemble autocorrelation matrix **R** and extract eigenmodes, (c) substitute approximation (1) in the governing equations and perform Galerkin projection using the POD modes, and (d) solve system of ordinary differential equations to obtain the time coefficients $a_k(t_i)$ and reconstruct the solution using (1).

Since the substitution and the Galerkin projection of step (c) are tedious, we are currently using deep learning to determine the time coefficients $a_k(t_i)$. Deep learning is a subset of machine learning methods based on neural networks, which uses multiple layers in the network. Machine learning is automated data analysis during which computer programs (or modules) are learned from data. The model (or computer program) describes the relationship between variables (or data) and properties of interest, such as the time coefficients a_k. The model is learned using training data, such as the flow snapshots, by using a learning algorithm that automatically adjusts the model's parameters to agree with the data. The cornerstones of machine learning are (i) data, (ii) model, and (iii) learning algorithm [3].

3. **RESULTS**

Whether the time coefficients are calculated using Galerkin projection or deep learning, the reconstructed solution uses the POD modes. The relative energy of the modes, which indicates the influence of the POD modes on the solution, typically decays rapidly, as shown in Fig. 1. This implies that only a reduced number of modes, m, needs to be kept in the approximation. Furthermore, often the energy of the modes vs. number of POD modes [4] comes in pairs, that is, modes i and $i+1$ have similar energy, while modes $i+2$ and $i+3$ have similar energy but significantly less than modes i and $i+1$.

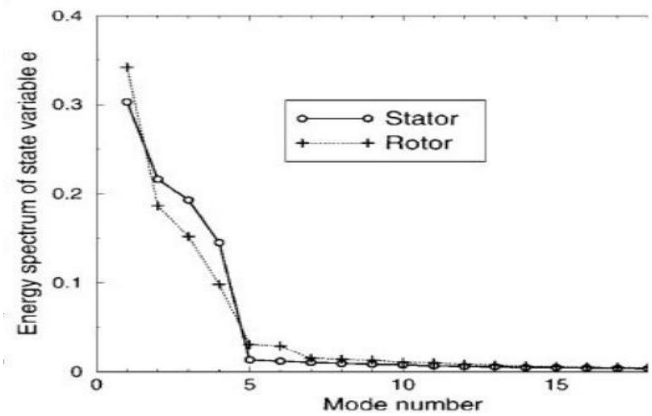

Fig. 1 – Cumulative energy (1) vs. number of modes [4].

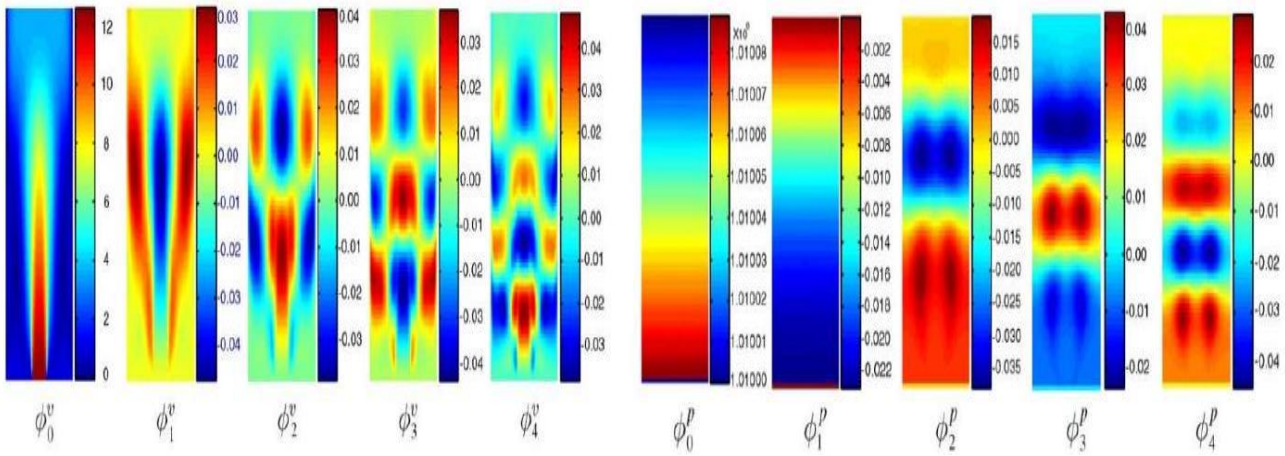

Fig. 2 – First five POD modes of v velocity (left) and pressure (right) [5].

Figure 2 shows the POD modes of the velocities and pressure in a fluidized bed [5]. It is apparent that as the mode number increases, the fragmentation of the contour plots increases. The vertical velocity shown in Fig. 2 is fragmented first in the x direction while shifting from mode ϕ_0^v to ϕ_1^v. Subsequently, the fragmentation happens in y direction while advancing from mode ϕ_1^v to ϕ_4^v.

A similar trend of fragmentation/bifurcation is evident in Fig. 3, which shows the POD modes of the unsteady flow generated by the rotor-stator interaction in a turbine. In this case, the fragmentation of the contour plots is more pronounced than that shown in Fig. 2, as multiple flow features are present in the turbine flow.

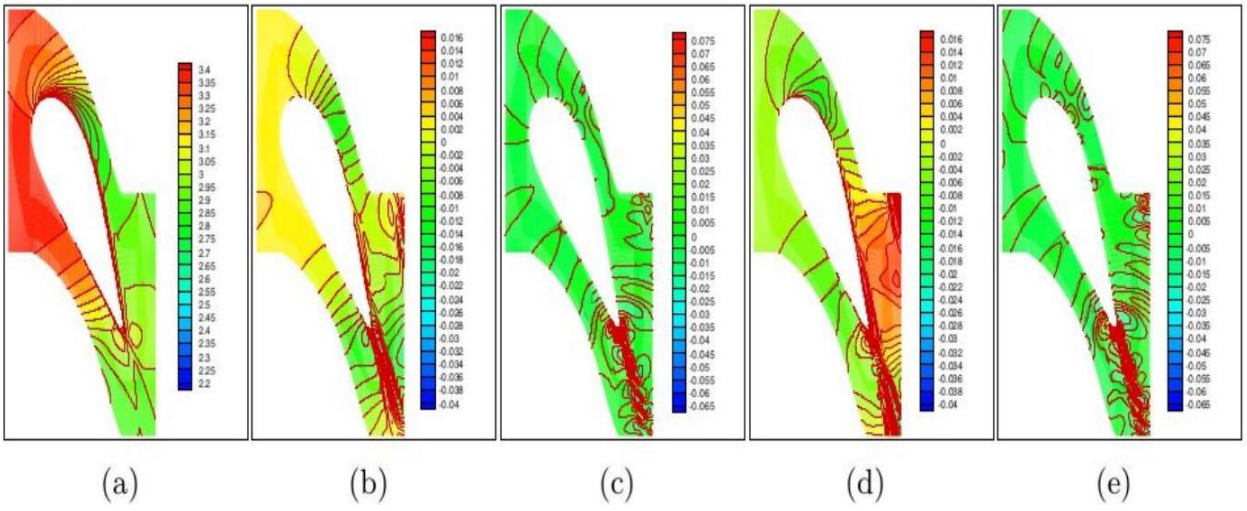

Fig. 3 – Five most relevant POD modes of energy [4].

3. **CONCLUSIONS**

The POD modes of transport phenomena equations are the building blocks for the solutions of these conservation equations. As the mode number increases, the modes appear to fragment/bifurcate, indicating that these modes follow the contructal law.

REFERENCES

1. Mahajan A.J., Dowell E.H., Bliss D.B., Eigenvalue Calculation Procedure for Euler/Navier-Stokes Solvers with Application to Flows over Airfoils, *Journal of Computational Physics*, **97**, pp. 398–413 (1991).
2. Holmes P., Lumley J.L., Berkooz G., *Turbulence, Coherent Structures, Dynamical Systems and Symmetry*, Cambridge University Press, 1996.
3. Lindholm A., Wahlstrom N., Lindsten F., Schon T.B., *Machine Learning: A First Course for Engineers and Scientists*, Cambridge University Press, 2022.
4. Cizmas P.G.A., Palacios A., Proper Orthogonal Decomposition of Turbine Rotor-Stator Interaction, *Journal of Propulsion and Power*, **19**, pp. 268–281 (2003).
5. Yuan T., Cizmas P.G., O'Brien T.A., Reduced-Order Model for a Bubbling Fluidized Bed based on Proper Orthogonal Decomposition, *Computers & Chemical Engineering*, **30**, pp. 243–259 (2005).

CONSTRUCTAL LAW CONFERENCE – CLC2024
Design in Nature and Evolution
Romanian Academy, Bucharest, 10–11 October 2024

Proceedings of CLC2024
pp. 157–160

UPGRADING ALONG THE VALUE CHAIN: CONFORMITY BETWEEN HELICES

ÇELIK KURTOĞLU

Evolution of the Value Chain, Istanbul, Türkiye Contact Information
ckurdoglu@gmail.com

Keywords: Value chain; Helices; Conformity.

1. VALUE CHAIN AND ITS DYNAMICS

Is our point of departure why the product cycle bends east while rising? Why does it not continue its rise?

The economist would define this rise as a fall in costs, a rise in net revenue, and a decline with diminishing returns, i.e., always a cost-based assessment. However, costs are not necessarily the only or most critical performance indicator in a competitive economy.

This is true mainly because of technological progress. Costs are accounting items and can be reduced independently of productivity. Pricing is essential and must be tackled, with the recognition that we are all predictably irrational. Homo economicus applies in theory but not in reality.

An increase in value-added may carry a cost element, but the value it adds via quality and better response to consumer demand contributes to a company's performance.

2. DOES ECONOMICS PROVIDE AN ANSWER?

Costs do not account for or consider the evolution of technology or consumer behavior/tastes. This effect is magnified when we consider intra- and/or inter-firm transactions. Furthermore, cost is a pricing concept and relates to buyers' budgets as much as what is offered.

The economic analysis considers production as the "production function," a relationship between output and the amount of capital and labor involved in its production. Elasticities of substitution between capital and labor add up to one and remain constant. This is what economic analysis commands.

Production in engineering involves material inputs and services, the technology of processing them according to an initial design and offering the output to a final user. Interdependencies between these "actors" continue, and the value chain evolves.

3. PROCUREMENT OR INTEGRATED PRODUCTION, THE PROBLEM REMAINS

The final user may be the consumer or another producer who combines this output with others to produce a final output. The entire process of "production," *i.e.*, the value chain, may be organized integrally, as was the

DOI: https://doi.org/10.59277/CLC/2024.40

case in Henry Ford's Model T or some Korean manufacturers today, or it may depend on a symbiosis of suppliers and final manufacturers, OEMs.

Globalization has moved to a stage where we talk of vertical trading networks. OEMs are in three centers: the USA, Japan (China, Korea), and Europe (Germany, France, UK), with suppliers in countries in the network. These suppliers need to meet the requirements of their customers, who may be OEMs or other component suppliers. It should be kept in mind that those requirements change according to the technical mutation of the OEM or the other component supplier.

Our question is how we might synchronize this symbiosis, which is important for supply chain organization.

4. **GENETICS OF MANUFACTURING**

Here, we encounter the helix concept. C. Fine uses a helix to explain the fruit fly's life cycle, drosophila. The same concept applies to Professor Bejan's constructal law. The evolution of a growth survives in symbiosis with other materials that may help or hinder its growth.

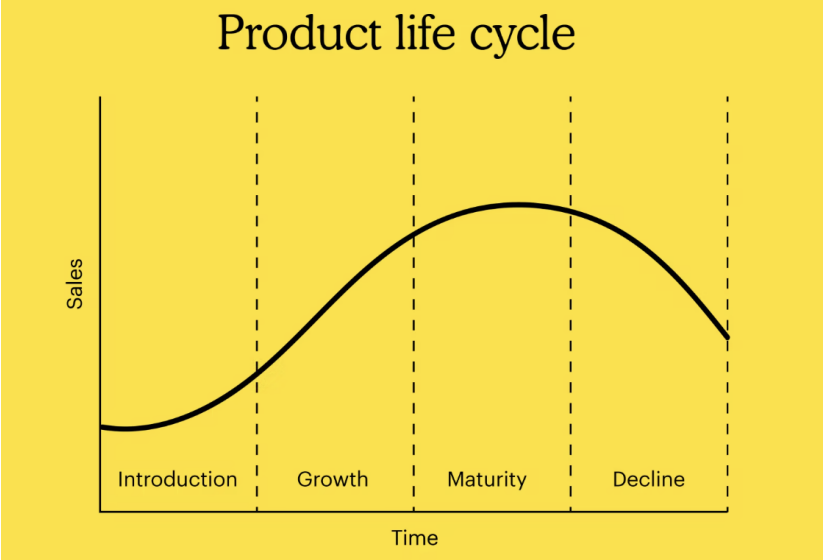

The product cycle hypothesis assumes that growth tapers off at a point as a consequence of diminishing returns. However, we are living through a period when this is not correct. Software has taken over during the last decade to exploit the ground provided by chip technology by creating new environments of "needs and solutions."

5. **A DIFFERENT HELIX BEHAVIOR**

For this reason, the product cycle does not bend east at an inflection point but continues its northward climb, in line with J.A. Schumpeter's "creative destruction" hypothesis. If this scenario fails, the company/industry in question will fall out of the marketplace because overall technology progresses, offering new avenues for growth.

The helix concept is also used to explain technological change. Under the triple helix, collaboration between universities, government, and industry is foreseen. The quadruple helix brings in the collaboration of media, art, and innovation. Finally, the quintuple helix introduces global warming and the environment as drivers for innovation.

We will stick to the helix explanation of endogenous growth, innovation, and technical progress in our effort to understand how the value chain with its contributing elements may upgrade and increase value-added and create new products. Electric cars, autonomous mobility, and other solutions in life sciences, daily life, space technology, and AI are examples of today.

6. **SYNCHRONIZATION OF DIFFERENT HELICES**

The question that brought me to this conference is whether and how we might identify, define, and measure the elements constituting the helix. The end purpose is to explore the synchronism of progress's evolution in each of these elements. When I mentioned this question to Adrian Bejan, this might be an exciting subject at the Bucharest Conference.

The analysis differs according to industry in question. In process industries, agriculture, and life sciences, helix in its original sense would apply, as constituting elements would have biological and chemical characteristics, hence definable like in the original explanation of the double helix, i.e., the relationship between sugar and phosphates in the evolution of the genome.

How can helices be defined in material sciences so that the evolution of, for example, an aluminum particle, graphite, or magnesium can be investigated and joint operation with a part made of steel or petrochemical products can be secured? In the end, similar to the growth of the genome into a human being, we want the product cycle to continue its climb so that technology progresses and the value chain upgrades via the development of innovations and new solutions.

7. **APPROACHES TO DEFINE THE HELICES**

Some research attempted to tackle the question using input-output methodology; however, that is based on fixed production coefficients, whereas we need to identify ever-changing routes and modes for A. Bejan's rivers and trees to proceed to advance and to grow or for pharmaceutical industries to develop solutions in the field of life sciences. The question applies to battery technologies today, which are the subject of research in the electric vehicle industry. If AI is to bring a solution, what and where will the data be used in the process? We return to the question, "How can respective resilience, sustainability, tolerance, and the like be measured, and concordance be secured?"

The Late Nobel laureate R. Solow questioned the impact of technical progress; lacking alternative measurement possibilities, the production function was the basis of analysis, where the "Solow residual" was interpreted as the output of technical progress, i.e., output rising beyond that made possible by the increase in labor and/or capital.

May QFD, quality function distribution, serve as an instrument to identify where technical specs of different "molecules" conform or conflict while the technology of the entire material world is changing and evolving and the helix is progressing? May we imagine a system where digital QFDs attached to constituting

parts of a helix talk to each other and offer solutions? Or am I being more far-fetched in my imagining exercise than Ray Kurzweil?

In other words, how can the dynamics of endogenous growth in production and the value chain be defined and measured?

Ecochain, a consultancy based in Amsterdam, develops tools for "life cycle assessments" across industries. While not stated on its website, Ecochain seems to deliver sustainability studies on demand, presumably to meet the demands of the EU rules.

What we seek includes sustainability in the economic sense but also involves the technological progress potential of every industry. Talking of progress potential, may AI help answer the question? Could I refer to ChatGPT instead of speaking to you?

If so, where would AI obtain the data? This question takes us back to the original question: how to define and measure the specs of numerous inputs in a value chain. We face this question at the design phase, all the way to the shop floor and marketing. I believe this question underlies the entire evolution process.

8. **EXPECTATION**

I end my presentation not with proof, as would be the case for a paper in engineering, but with a question. The question also concluded my book on the Evolution of the Value Chain, published recently in Turkish. The book also proposes a new look into economics, not constrained by diminishing returns. This offers a new paradigm for investors, company managers, and engineers by highlighting new opportunities. It also suggests governments adopt a new look into industrial policy.

CONSTRUCTAL LAW CONFERENCE – CLC2024
Design in Nature and Evolution
Romanian Academy, Bucharest, 10–11 October 2024

Proceedings of CLC2024
pp. 161–166

EVOLUTION OF MARITIME TECHNOLOGY: ADVANCEMENTS IN SHIP DESIGN

UMIT GUNES

Yildiz Technical University, Department of Naval Architecture and Marine Engineering,
Besiktas, Istanbul,34349, Türkiye
umitgunes87@gmail.com

The evolution of ships has occurred through significant improvements in their design, materials, propulsion systems, size, navigation, and military capabilities. Ships were first built using simple, flat wooden hulls and were only suited for traveling short distances. Hull designs gained sophistication over time, taking on curved lines and later being built from steel and other composite materials that would improve their durability and efficiency. As for ship propulsion systems, these were initially powered by humans or the wind before evolving to steam engines, diesel engines, gas turbines, and nuclear power, vastly increasing their speed, range, and reliability. Ship size has also drastically improved, with modern supertankers and container ships now capable of transporting enormous loads across oceans. Developments in navigation technology, including the invention of radar, sonar, and GPS, have greatly improved marine safety and positional accuracy. Meanwhile, modern naval vessels now possess advanced defense systems, electronic warfare capabilities, and missile technologies. The drive toward sustainable practices have led to the adoption of green technologies such as hybrid engines and renewable energy and the adoption of more environmentally friendly ships. Ongoing innovations regarding maritime technology are reflected in these advancements and are helping shape the future of global shipping.

Keywords: Maritime evolution; Ship design; Propulsion systems; Constructal law; Energy efficiency.

1. INTRODUCTION

Driven by the need for increased speed, stability, and efficiency, ship hull designs have significantly evolved throughout history. In early times, hulls were simple and flat, a suitable design for navigating rivers and coasts, but they needed to be better suited for sailing the open seas. In the Middle Ages, curved hulls began being developed, which improved ship stability and lowered water resistance, thus letting ships navigate rougher seas more effectively [1]. With the Age of Exploration (15^{th}–17^{th} centuries), light sailing ships and galleons began to be designed with more sophisticated hulls to endure long transoceanic journeys. Modern times have seen fluid dynamics and materials science advancements, resulting in streamlined hulls being developed and optimized for reducing drag and improving fuel efficiency [2].

Shipbuilding materials have also undergone impressive evolution. Ships were initially wooden vessels, as trees were readily available and easy to shape, but wood has certain limitations regarding durability and resistance to marine environments. The Industrial Revolution introduced iron and steel to shipbuilding, significantly improving ships' strength and size. Being lighter and more durable than iron, steel allowed much larger and more robust vessels to be constructed [3]. In the 20^{th} century, aluminum and composite materials such as fiberglass and carbon fiber further revolutionized shipbuilding by reducing overall weight and improving performance, particularly for high-performance and military vessels [4].

DOI: https://doi.org/10.59277/CLC/2024.41

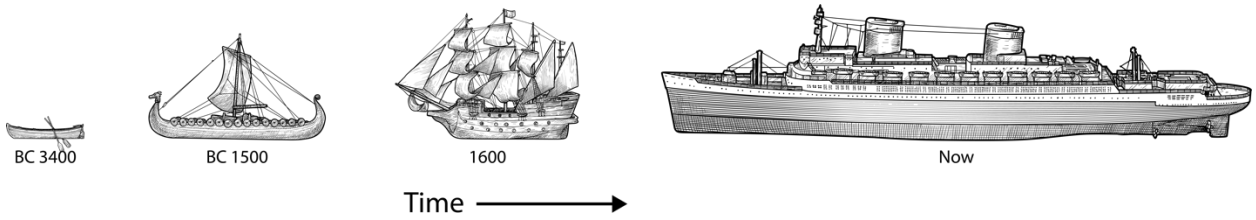

Fig. 1 – Evolution of ship design over time [5].

Sail and rigging systems have evolved to reflect the shift from wind-based to engine-powered vessels. Earlier ships relied on square sails hung from a single mast, which limited a ship's maneuverability and speed [6]. The Middle Ages saw more complex rigging systems being developed, such as multiple masts and sails. This allowed ships to harness wind from multiple directions [7]. Later, the steam engines of the 19th century marked a decline in sail-powered ships because steam power was more reliable and offered more powerful propulsion [8].

Many examples of evolution regarding ship design are found. For example, the bulbous bow is a specialized design feature found on many large vessels, particularly cargo ships and tankers. The purpose of this shape is to reduce wave resistance and improve hydrodynamic efficiency. This protruding structure is positioned just below the waterline to change the pattern of water flows around the hull. The shape creates a wave that offsets the bow wave generated by a ship's forward motion. This, in turn, reduces drag and increases fuel efficiency [9]. Studies have shown a bulbous bow can decrease fuel consumption significantly and increase speed, especially on ships operating at higher speeds over great distances [10]. Moreover, this specific design also improves ship stability by lowering its center of gravity, which helps inhibit pitching and rolling in turbulent seas. However, a bulbous bow is only effective when designed in line with the vessel's specific dimensions and operational conditions.

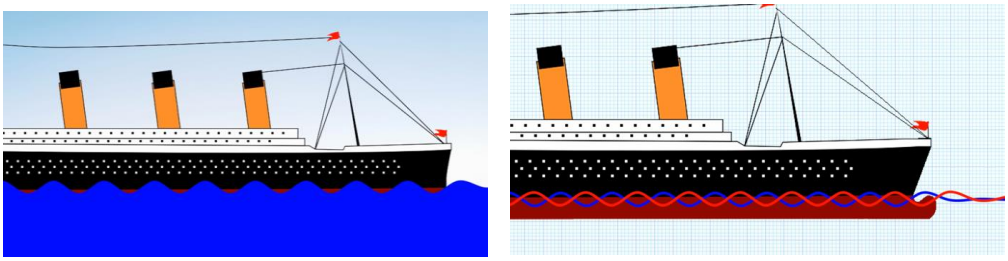

Fig. 2 – How a bulbous bow offsets wave resistance (credit: [11]).

2. PROPULSION AND POWER SYSTEMS

Ship propulsion first occurred through the power of human effort and wind. Rowing with oars was the common means of propulsion for smaller vessels, particularly in calm or inland waters. This method is labor-intensive, however, and has limited applications. Sails were first used to harness wind power. This became the primary means of propulsion for larger vessels and allowed ships to remain at sea longer. The drawback to this method, though, is that it greatly depends on wind conditions, and the predictability of winds could be better by nature.

The 19th century saw the introduction of steam power, which revolutionized maritime travel. Steam engines allowed ships to move independently of wind, greatly improving the reliability and speed of a journey. Early steamships mostly traveled on rivers and lakes, but not much time passed before technology advanced

to allow them to cross oceans. Steam-powered vessels could maintain consistent speeds regardless of weather conditions, marking a significant shift in how maritime commerce and warfare were conducted [12].

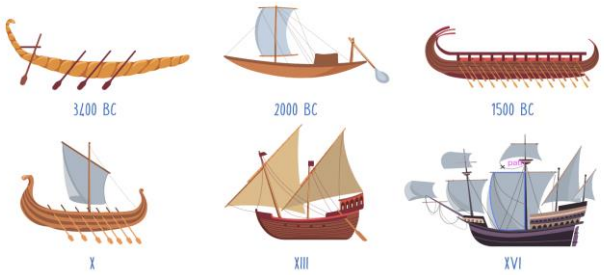

Fig. 3 – Ship designs up to the 16th century (credit: Shutterstock).

The 20th century witnessed further developments with the creation of diesel engines, which are more efficient, powerful, and reliable than steam engines. For this reason, diesel engines became the preference for most commercial and military vessels. Gas turbines were invented alongside diesel engines and are commonly used in military vessels that require higher speeds. Because of the greater power gas turbines offer, they consume more fuel than diesel engines. Thus, their usage is primarily limited to specialized applications [13].

The 1950s saw nuclear power emerge as a revolutionary propulsion technology for the navy, providing a unique edge for submarines and aircraft carriers. Nuclear power offers vessels virtually unlimited range and the ability to operate for extended periods without the need to refuel. This makes nuclear-powered vehicles strategically ideal for military applications. Nuclear propulsion has greatly improved modern naval fleets' operational capacities [14].

In more recent times, sustainability requirements have led to renewable energy sources being developed to power ships using wind, solar, and hybrid systems to combine traditional engines with electric motors. These novel developments aim to limit the impacts shipping has on the environment and to provide higher energy efficiency [15]. Hybrid systems have become ever more popular, particularly for short-distance shipping by sea and port operations, as these systems can operate on significantly less fuel and output fewer emissions.

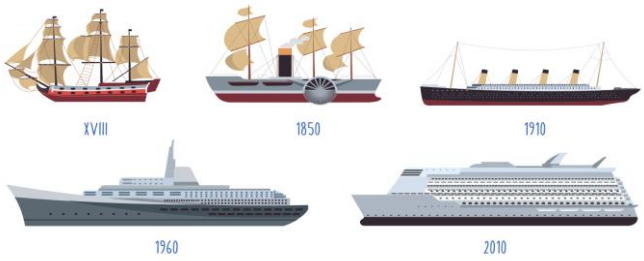

Fig. 4 – Ship designs from the 18th–21st centuries (credit: Shutterstock).

3. THE EVOLUTION OF SIZE AND CAPACITY

Ship size has increased greatly over the centuries. The first ships were relatively small, could only carry limited cargo, and were typically used for short-distance trade or navigating along coasts. Since the Age of

Exploration, incredible growth has been seen in ship size, with vessels now being able to carry tremendous volumes of cargo over the oceans. Since the Industrial Era, even larger steel-hulled vessels, such as modern supertankers and container ships, have been constructed. Some of these are over 400 meters long and able to transport tens of thousands of containers (one container can weigh 30 tons) or millions of barrels of oil (one barrel weighs 600 pounds) [16]. Currently, these giant ships of the sea have major roles in global trade.

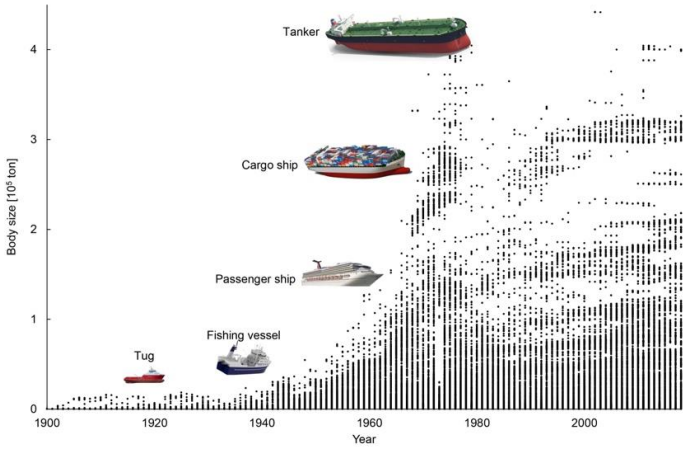

Fig. 5 – The emergence of ship models and sizes (1900–present) [18].

The evolution of passenger ships has seen small ferries and merchant ships that could only carry a few dozen people grow to modern cruise liners that can accommodate thousands of passengers. Steam-powered transatlantic liners became popular in the 19th century, offering reliable and relatively quick intercontinental voyages [17]. Luxury liners became more and more popular in the 20th century as ships were designed for comfort and entertainment rather than just transportation. Modern cruise ships are cities on the sea and have all the accompanying amenities of a city, such as theaters, swimming pools, and shopping centers. These vessels can accommodate up to 6,000 passengers.

4. **ENVIRONMENTAL AND ENERGY EFFICIENCY**

In the transition from sail- to steam- and then to diesel-powered ships, fuel efficiency has become more and more critical. Steam engines were first powered by coal, a heavy fuel that takes up considerable onboard storage, which in turn limits ships' operational range [19]. Diesel engines significantly improved fuel efficiency when they first appeared [20], and aerodynamic and hydrodynamic optimizations in modern times are employed to further reduce fuel consumption, providing ships with greater efficiency and lower environmental impacts.

In addition to fuel efficiency, the maritime industry has placed an extreme focus on reducing emissions. Ship engines produce harmful pollutants such as sulfur dioxide (SO_2) and carbon dioxide (CO_2) when burning fossil fuels, thus producing more air pollution and negatively affecting climate change. The International Maritime Organization (IMO) has tasked itself with addressing these issues and implementing strict regulations on emissions. This has helped technologies such as exhaust gas cleaning systems (scrubbers) to be adopted and low-sulfur fuels and liquefied natural gas (LNG) to be used. These regulations aim to reduce the large environmental impact of global shipping.

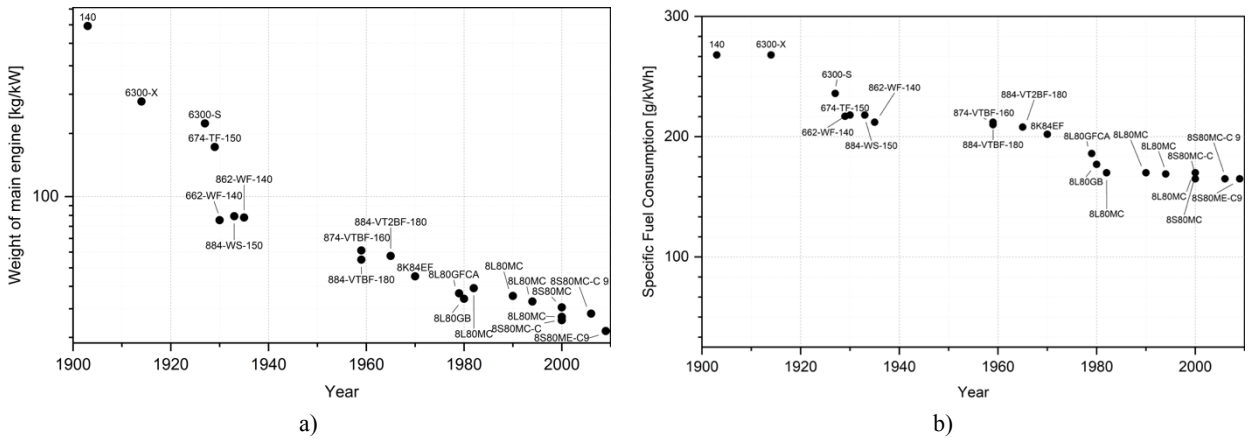

Fig. 6 – The evolution of a) marine engines' specific fuel oil consumption and b) main engine weight [5].

Figure 6 shows the installed main engine weights in kg per kW. For producing the same unit power, the main engine weight has decreased significantly since the 1900s. The reasons behind this include technological developments in such areas as materials and production. When examining the time-based change in terms of specific fuel consumption per unit of main engine power, fuel consumption is seen to have also decreased significantly due to the development of technologies and systems that make movement easier. Figure 6b shows the specific fuel consumption for installed main engines. The specific fuel consumption required per kW of power has decreased over time. When considering how specific fuel consumption is inversely proportional to efficiency, a decrease in specific fuel consumption clearly results in greater engine efficiency.

5. **CONCLUSION**

Maritime technology has gone through major evolutions, a dynamic journey of continuous advancements regarding ship design, propulsion systems, and materials. All these developments have aimed to improve efficiency, safety, and environmental sustainability. Since the first days of simple wooden hulls operating under human power and the wind up to the modern era and its sophisticated vessels operating under nuclear power and renewable energy sources, the maritime industry continues to adapt to provide what global trade and exploration demand. The invention and implementation of advanced materials such as steel, aluminum, and composite materials have improved the durability of ships per unit weight while also allowing ship size to increase and ship performance and capabilities to undergo revolutionary changes.

In line with this, the evolution of propulsion systems has gone from less efficient hand-operated and wind-based mechanisms to much more efficient diesel engines, gas turbines, and nuclear reactors. This has significantly expanded ships' range and speed. Furthermore, the newer interest in sustainability has inspired green technologies such as hybrid engines to be adopted and alternative fuels to be used, further reducing the negative environmental impacts of shipping. As a response to the global environmental challenges the world is experiencing, these continuous innovations testify to the maritime industry and its commitment to increasing the energy efficiency of ships and reducing their emissions.

REFERENCES

1. Papanikolaou A., *Ship design: Methodologies of Preliminary Design*, New York, Springer, 2014.
2. Birk L., *Fundamentals of ship hydrodynamics: fluid mechanics, ship resistance and propulsion*, 1st ed., Wiley, 2019.
3. Smith T., *The Handbook of Iron Shipbuilding*, Legare Street Press, 2023.
4. Shenoi R.A., Wellicome J.F., *Composite Materials in Maritime Structures*, Volume 1: *Fundamental Aspects*, Cambridge University Press, 1993.
5. Gunes U., Çetkin E., Şahin B., Gemi sevk gücü ve isı transferinin yapısal gelişim teorisi ile ilişkisi, *Gemi ve Deniz Teknolojisi*, *222*, pp. 138–152 (2023).
6. Holmes S.G.C.V., *Ancient and Modern Ships*, Anboco, 2016.
7. Bejan A., Ferber L., Lorente S., Convergent Evolution of Boats with Sails, *Scientific Reports*, **10**, *1*, Art. no. 1 (2020).
8. Souza D.J., *The Persistence of Sail in the Age of Steam: Underwater Archaeological Evidence from the Dry Tortugas*, Springer Science & Business Media, 2013.
9. Molland A.F., *The Maritime Engineering Reference Book: A Guide to Ship Design, Construction and Operation*, Elsevier, 2011.
10. Molland A.F., Turnock S.R., Hudson D.A., *Ship resistance and propulsion: practical estimation of ship propulsive power*, 2nd ed. Cambridge, Cambridge University Press, 2017.
11. Casual Navigation, *What is the BULBOUS BOW for?* (May 11, 2018). Accessed: Aug. 18, 2024. [Online Video]. Available: https://www.youtube.com/watch?v=6FrCusDG41U
12. Darwin J., *Unlocking the World: Port Cities and Globalization in the Age of Steam*, *1830–1930*, Penguin UK, 2020.
13. Grove E., *The Future of Sea Power*, Taylor & Francis, 2021.
14. Schank J.F., *Sustaining U.S. Nuclear Submarine Design Capabilities*, Rand Corporation, 2007.
15. Ölçer A.I., Kitada M., Dalaklis D., and Ballini F., *Trends and Challenges in Maritime Energy Management*, Springer, 2018.
16. R. Barker, *The Rise of an Early Modern Shipping Industry: Whitby's Golden Fleet, 1600–1750*, Boydell Press, 2011.
17. Anonymous, *An Account of The Great Eastern, the Largest Steamship in the World [microform]: Belonging to the Eastern Steam Navigation Company,* Creative Media Partners, LLC, 2023.
18. A. Bejan, U. Gunes, B. Sahin, The evolution of air and maritime transport, *Applied Physics Reviews*, **6**, *2*, p. 021319 (2019).
19. *Improving the energy efficiency of ships*. Accessed: Aug. 18, 2024. [Online]. Available: https://www.imo.org/en/OurWork/Environment/Pages/Improving%20the%20energy%20efficiency%20of%20ships.aspx
20. Jimenez V.J., Kim H., Munim Z.H., A review of ship energy efficiency research and directions towards emission reduction in the maritime industry, *Journal of Cleaner Production*, **366**, p. 132888 (2022).

CONSTRUCTAL LAW CONFERENCE – CLC2024
Design in Nature and Evolution
Romanian Academy, Bucharest, 10–11 October 2024

Proceedings of CLC2024
pp. 167–170

FLUX-FLOW INTERACTION IN ELECTROMAGNETIC BIOIMPEDANCE

ALIN A. DOBRE[a], ANDREEA MITROFAN[b,c], ALEXANDRU M. MOREGA[a,b,d]

[a]The National University of Science and Technology Politehnica Bucharest, Faculty of Electrical Engineering, 313 Splaiul Independenței, District 6, 06004, Bucharest, Romania.
[b]The National University of Science and Technology Politehnica Bucharest, Doctoral School of Electrical Engineering, 313 Splaiul Independenței, District 6, 06004, Bucharest, Romania.
[c]The National University of Science and Technology Politehnica Bucharest, Faculty of Medical Engineering, 1-7 Gheorghe Polizu, District 1, 011061, Bucharest, Romania.
[d]"Gheorghe Mihoc-Caius Iacob" Institute of Mathematical Statistics and Applied Mathematics, The Romanian Academy, 13 Calea 13 Septembrie, District 5, 050711, Bucharest, Romania
alin.dobre@upb.ro, andreea_mitrofan@yahoo.com, amm@iem.pub.ro.

The electromagnetic field's morphing in interaction with blood flow may be used to propose a novel bioimpedance technique aimed at the non-invasive detection and mapping of large cerebral vascular networks, such as the dural venous sinuses, which collect the venous deoxygenated blood from the brain region and returns it to the heart through the internal jugular vein and the superior vena cava. In this impedance method, the position of the electrodes on the skull leads the incident flux (the electric current density) to outline the vascular flow and spot the venous sinuses noninvasively. It is crucial for some neurosurgical interventions that the venous sinuses are not accidentally damaged during the procedure since hemorrhage at this level is often fatal.

Keywords: Electromagnetic bioimpedance; Vascular flow; Electric current flow; Flux-flow interaction.

1. INTRODUCTION

The electrical impedance of a biological media (*e.g.*, cell cultures, living tissues) depends on the frequency of an electrical excitation signal (typically, a low-amplitude, high-frequency electrical current) applied from external sources to evaluate it. The response given by the electrical impedance variation provides information about physiological or pathological aspects of the investigated biological environments. A series of classical clinical investigation techniques based on electrical bioimpedance [1], such as electrical cardiometry (ECM) and impedance cardiography (ICG), used for evaluating the hemodynamic parameters of the heart, complement the information provided by the electrocardiogram and outline a global picture of the electrical activity of the myocardium. An incident electromagnetic field (EMF) is used to unveil lower impedance paths (*e.g.*, blood vessels) inside the body to gain helpful information on the body's rhythms and composition that vessel trees "echo".

EMF – blood flow morphing is used here to detect and map cerebral vascular networks. The dural venous sinuses [2–7] are blood vessels in the head's skull region that act as venous blood collectors, returning the deoxygenated blood to the heart through the internal jugular vein and the superior vena cava. Additionally, the superior sagittal sinus ensures the circulation of the cerebrospinal fluid. This bioimpedance method may be of interest in neurosurgery for high-precision detection of large blood vessels requiring brain surgery (tumor removal, aneurysm embolization, strokes).

DOI: https://doi.org/10.59277/CLC/2024.42

2. MATERIALS AND METHODS

A harmless electric current $O(10^2)$ mA with an $O(10)$ kHz frequency is applied as an excitation signal using a pair of electrodes conveniently fixed on the scalp. In contrast, another pair of electrodes measures the electrical impedance of the investigated anatomical region as a response (Fig. 1, left side). Since the largest blood vessels in the head region are the venous sinuses and the blood has a higher electrical conductivity value than the nearby tissue, these will become a preferential closing path for the electrical excitation current, signaling their presence and position. No such investigative techniques have been reported in the literature for morphological analysis of the cranial circulatory system.

The mathematical model of the electric field is:

$$\nabla \cdot (\sigma \mathbf{E}) = \nabla \cdot [-\sigma(\nabla V)] = -\sigma[\nabla \cdot (\nabla V)] = -\sigma \Delta V = 0, \quad (1)$$

where σ [S/m] is the electrical conductivity of the tissue, $\mathbf{E}$ [V/m] is the electric field strength, and V [V] is the electric potential. The boundary conditions that close the model consist of injecting a continuous electric current of 400 μA at one excitation electrode, a ground condition at the other, and floating electric potentials for the measurement electrodes. The exterior boundaries are electrical insulation, while the interfaces between different tissues are set as continuity.

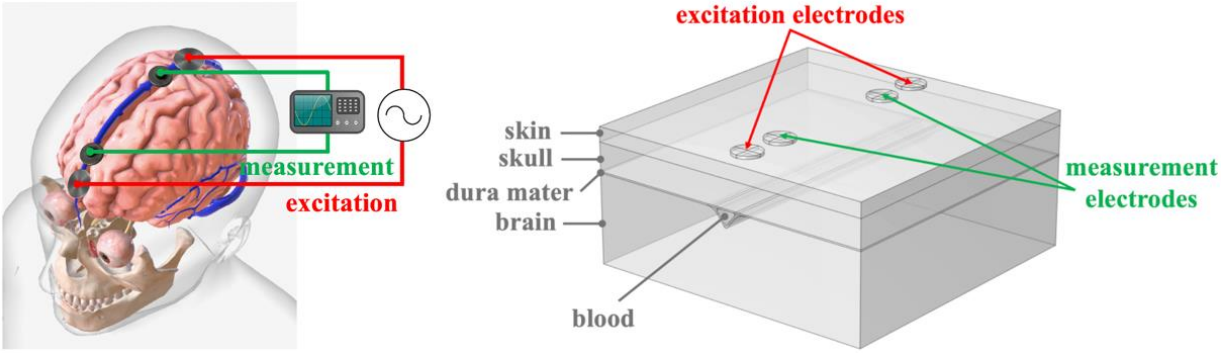

Fig. 1 – Principle of the electromagnetic bioimpedance technique (left side) and the idealized computational domain (right side).

3. RESULTS AND DISCUSSION

ICG and ECM, an incident electromagnetic field (EMF), are used to unveil lower impedance paths inside the body to unveil helpful information on the body's rhythms and composition that vessel trees reverberate. Here, the EMF is presented through a stationary electrical conduction problem governed by the mathematical model described in eq. (1), which was integrated numerically using the finite element method [8].

Figure 2 presents the electrical current density and the venous blood flow for several electrode positions on the scalp. Blood is a relatively good electroconductive medium compared to the surrounding biological media, so the electric current path is mainly through the vessel. Several electrode positions are used to adjust (morph) the EMF flux through the blood flow, and the minimum impedance position is found here by trial and error. More accurate methods can be easily defined.

The electrical bioimpedance was calculated by integrating the resulting electric potential at each measurement electrode. The values are presented in Table 1.

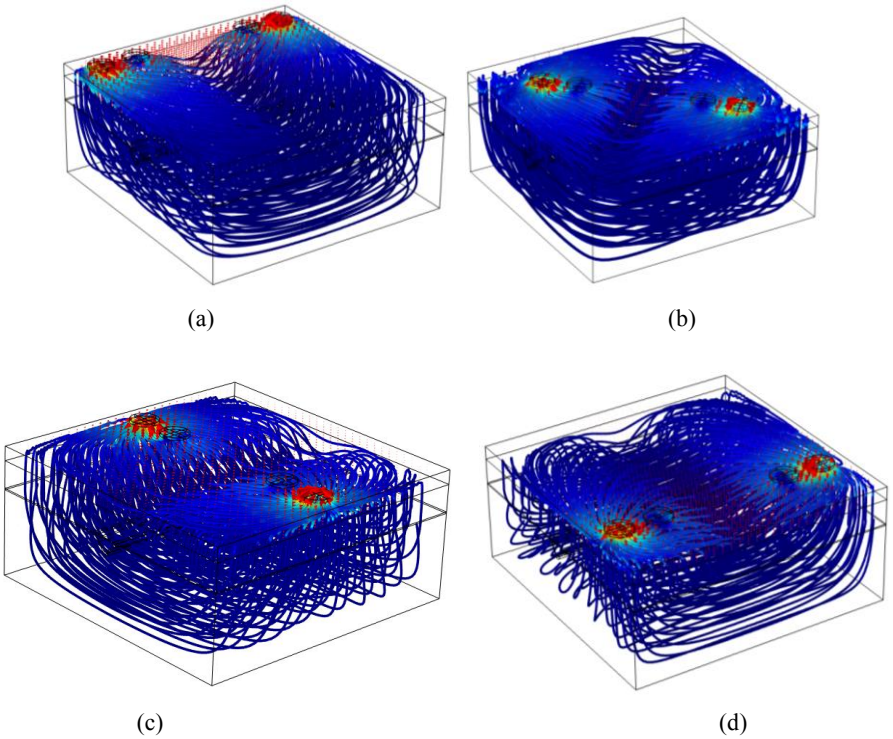

(a) (b)

(c) (d)

Fig. 2 – Flux-flow interaction for different electrode placement.

Table 1

Electrical bioimpedance evaluated for each setup

Electrode placement on the scalp [case]	Electrical bioimpedance value [Ω]
(a) – 4 cm distance from the superior sagittal sinus	423.25
(b) – electrodes are rotated 45° with respect to the superior sagittal sinus	279.10
(c) – electrodes are rotated 90° with respect to the superior sagittal sinus	278.99
(d) – 2.5 cm distance from the superior sagittal sinus	320.80

There is a close relation between the electrical bioimpedance values and the electrodes' placement: the presence of the blood vessels can be predicted regardless of the four electrodes' alignment to the vein (cases (c), (e), and (f) reveal similar low electrical bioimpedance value) if these are close enough to the low impedance path (the blood vessel).

Thus, the proposed method is suitable for the non-invasive detection of more prominent veins in the head region.

In our future work, we will also study a more realistic computational domain generated using medical image-based reconstruction techniques, which respects the anatomical morphology of the investigated area.

ACKNOWLEDGMENTS

This work was conducted in the Laboratory for Electrical Engineering in Medicine at Politehnica Bucharest. The first author acknowledges the support offered by the grant from the National Program for Research of the National Association of Technical Universities – GNAC ARUT 2023.

REFERENCES

1. Morega A.M., Morega M., Dobre A.A., *Computational Modeling in Biomedical Engineering and Medical Physics*, Chapter 5 – Bioimpedance Methods, Academic Press, Elsevier, 2021, pp. 142–166.
2. Stranding S. (Ed.), *Gray's Anatomy*: *The Anatomical Basis of Clinical Practice*, 42nd Edition, Elsevier, 2021.
3. Bayot M.L., Reddy V., Zabel M.K., *Neuroanatomy: Dural Venous Sinuses*, National Library of Medicine, National Center for Biotechnology Information, StatPearls Publishing LLC, 2023.
4. Ge S., Wen J., Kei P.L., Cerebral Venous Thrombosis: A Spectrum of Imaging Findings, *Singapore Med. J.*, **62**, *12*, pp. 630–635 (2021).
5. Koyfman A., Long B., *Vascular Disasters, an Issue of Emergency Medicine Clinics of North America*, 1st Edition, Elsevier, 2017.
6. Mankad K. *et al*., Venous Pathologies in Paediatric Neuroradiology: from Foetal to Adolescent Life, *Neuroradiology*, **62**, pp. 15–37 (2020).
7. Johns Hopkins Medicine, *Health – Conditions and Diseases, Cerebral Venous Sinus Thrombosis* (CVST), https://www.hopkinsmedicine.org/health/conditions-and-diseases/cerebral-venous-sinus-thrombosis
8. Comsol Multiphysics v.6.2, Comsol A.B., Sweden, 2024.

CONSTRUCTAL LAW CONFERENCE – CLC2024
Design in Nature and Evolution
Romanian Academy, Bucharest, 10–11 October 2024

Proceedings of CLC2024
pp. 171–174

CONSTRUCTAL DESIGN OF LATENT HEAT STORAGE SYSTEMS

SIVA ZIAEI

Microsoft
shivaziaei@gmail.com

1. INTRODUCTION

The project applies constructal theory to enhance the design of heat-flow paths in latent heat storage systems, aiming to minimize the time required for complete melting of the material. Constructal theory suggests that optimal flow configurations, which can be achieved by allowing more degrees of freedom in the design, facilitate better flow access.

2. OBJECTIVES

The main goal is to find effective 2D and 3D heat-flow architectures that lead to the fastest melting process. Starting with a simple structure where a single line acts as the heat source, the design evolves by allowing the heat source to change shape. Numerical simulations are used to identify geometric features that result in the fastest melting process.

3. METHODS

The study uses numerical simulations to explore the layout of invading lines that minimize melting time. By increasing the freedom to morph the flow architecture, a steeper S-shaped melting fraction curve is achieved. Parameters such as the number of bifurcation levels, stem length, bifurcation angle, and Peclet number are varied to optimize the melting fraction curve.

4. RESULTS

The results show that increasing the complexity and degrees of freedom of the structure enhances the heat transfer rate density. The angles between heat invasion lines have a minor effect compared to other factors like the number of branching levels, stem length, and branch lengths. The impact of natural convection in the melt zone is also documented.

5. CONCLUSION

The Constructal Law provides valuable insights into optimizing flow systems across various disciplines. The studies and numerical simulations demonstrate the versatility and significance of this principle in driving innovation and improving system efficiency.

6. ADDITIONAL INSIGHTS

- The study identifies two phases in the melting process: "invasion" (heat diffuses along the line) and "consolidation" (heat diffuses perpendicularly).
- The evolution of the melt layer is analyzed in both 2D and 3D contexts, with the amount of melted material following an S-shaped curve.

DOI: https://doi.org/10.59277/CLC/2024.43

- Faster diffusion occurs with more complex designs, steepening the S-curve.
- The article reviews traditional designs and introduces tree-shaped surfaces for volumetric heating and cooling.
- The challenge is to configure the heating paths to accelerate the energy storage process.

6.1. **Tree Invasion**

The natural tendency of flow systems that are free to morph is to develop configurations that provide greater access to the currents that flow. In the case of storage by melting, the flow is of heat from the invading plate to the rest of the domain, which is solid at the melting temperature. The invading plate is given the freedom to change its shape as it grows, leading to tree-shaped paths with more levels of bifurcation.

6.2. **3D Configuration**

In a three-dimensional geometry, the invading line of higher temperature is a thin needle. Melting occurs around the needle as it invades the solid. The scales of the S-history change if the spreading is from one point to a volume, instead of from one point to an area.

This summary encapsulates the essence of the project, highlighting the application of constructal theory to optimize heat-flow paths for efficient energy storage through melting. The detailed exploration of various parameters and the introduction of tree-shaped paths underscore the innovative approach taken in this study.

6.3. **Constructal Law and Flow Systems**

The constructal law describes how systems evolve to improve flow access, often resulting in tree-like structures that enhance the movement of currents. This principle is applied to energy storage systems to optimize heat transfer during the melting process of PCM.

6.4. **Melting Process in PCM**

The study examines the melting of PCM within a square domain, heated by an invading line at a higher temperature. The amount of melted material follows an S-shaped curve over time. Unlike previous studies with fixed heating patterns, this study allows the pattern to change freely, leading to the discovery of tree-like designs that improve heat spread and melting efficiency.

6.5. **Numerical Simulations and Results**

- The domain is a square filled with PCM solid at 303 K, with an adiabatic outer surface.
- Heat is introduced through an invading line at 353 K, which can branch out and advance.
- The heat conduction in the liquid PCM follows the energy equation, and the properties are assumed to be the same in liquid and solid states.
- The study finds that the melt layer thickness during invasion has a parabolic shape in time, and the instantaneous enclosed area is proportional to time.
- The growth of melted material during consolidation is slower than during invasion, explaining the inflexion of the S-curve.
- Numerical simulations validate the theoretical results, showing that tree-shaped invading lines accelerate the approach to complete melting along a steeper S-curve.

6.6. **Effect of Complexity and Stem Length**

- The effect of complexity (number of bifurcation levels) on the evolution of the average temperature is assessed.
- Trees with greater levels of complexity accelerate the arrival of equilibrium.

- The optimal stem length is found to be around 0.6 times the length of the domain.
- The study explores whether the melting process can be further accelerated by varying the stem length and bifurcation angle.

6.7. **Optimal Configuration**

- The simulations aim to find the optimal configuration for the shortest melting duration.
- The results show that a bifurcation angle of 150 degrees and a minimum stem length of 0.1 times the domain length yield the shortest melting duration.
- Freely varying bifurcation angles accelerate the melting process.

6.8. **Peclet Number and Melting Process**

- The rate of melting depends on the Peclet number, which is the ratio of the time of thermal diffusion perpendicular to the invading line divided by the time of line invasion.
- Higher Peclet numbers and optimal branching designs accelerate the melting process.
- The study compares one-line invasion at high Peclet numbers with optimized Y-shaped invasion at lower Peclet numbers, showing that morphing the design can significantly speed up the melting process.

6.9. **Conclusions**

The paper investigates the numerical process of phase-change energy storage, focusing on how the layout of higher temperature lines, which can morph freely, affects the melting process. The results show that allowing more freedom for the flow architecture to morph results in a steeper S curve, indicating faster melting. Key parameters like the number of bifurcation levels, stem length, bifurcation angle, and Peclet number were analyzed, with the conclusion that more design flexibility leads to better performance.

This summary encapsulates the key findings and methodologies of the study, highlighting the application of constructal theory to optimize heat-flow paths for efficient energy storage through melting. The detailed exploration of various parameters and the introduction of tree-shaped paths underscore the innovative approach taken in this research.

The study describes a two-dimensional square domain filled with a solid at its melting temperature (Tm). At time t = 0, a plate at a higher temperature (Tm+ΔT) starts growing along the centerline from x = 0 to x = L at a constant speed (V). Liquid layers of thickness δ(x) form on both sides of the advancing line. The thickness δ is determined by balancing the conduction heat flux (q'') into the melting front and the rate of melting at the front.

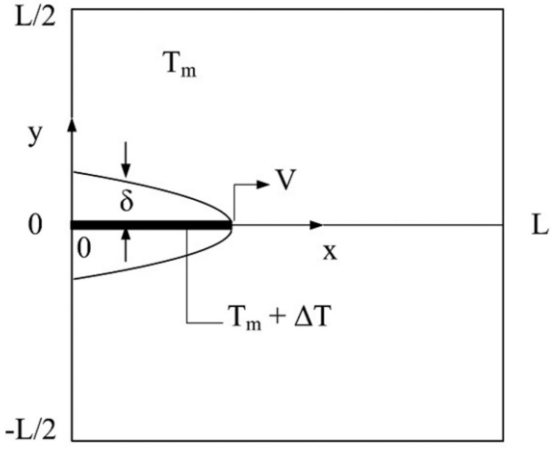

Fig. 1 – Square shaped construct containing the line-shaped invasion advancing.

Tree Invasion. The natural tendency of all flow systems that are free to morph is to develop configurations that provide greater access to the currents that flow. In the case of storage by melting, the flow is of heat, from the invading plate to the rest of the domain, which is solid at T_m. In this section, we endow the invading plate with freedom to change its shape as it grows. The change is from the single line

to the tree-shaped paths. More freedom means more levels of bifurcation (n) in the invading tree of plates. Relative to Fig. 2, the single-plate invasion scenario of Fig. 1 is the tree with one stem and no branches (n = 0).

For analytical ease, consider the limit where the invading finger of melt is slender enough so that the melt generated during invasion is small in comparison with the melt generated during consolidation. This is the limit of slender melt layers on both sides of the invading plate, which is represented by $\left(\frac{a}{LV}\right) \ll 1$,

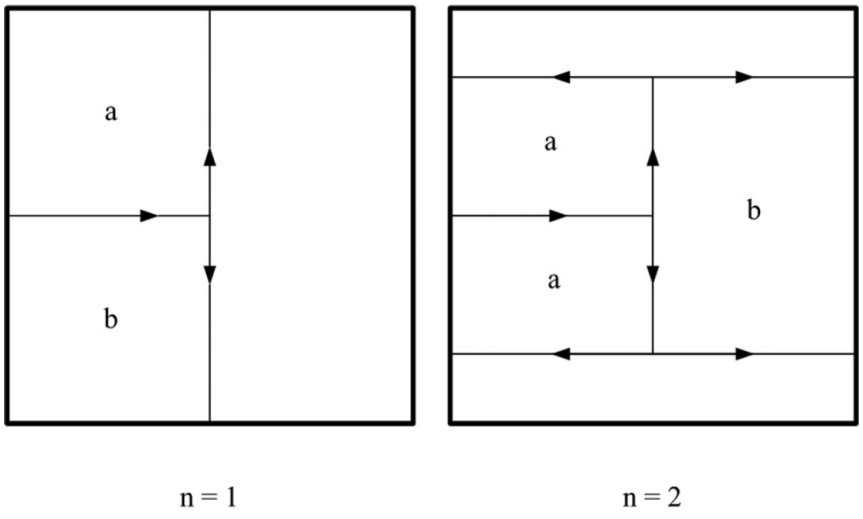

Fig. 2 – Two-dimensional model of a tree-shaped line invasion of a conducting domain for one and two levels of bifurcation.

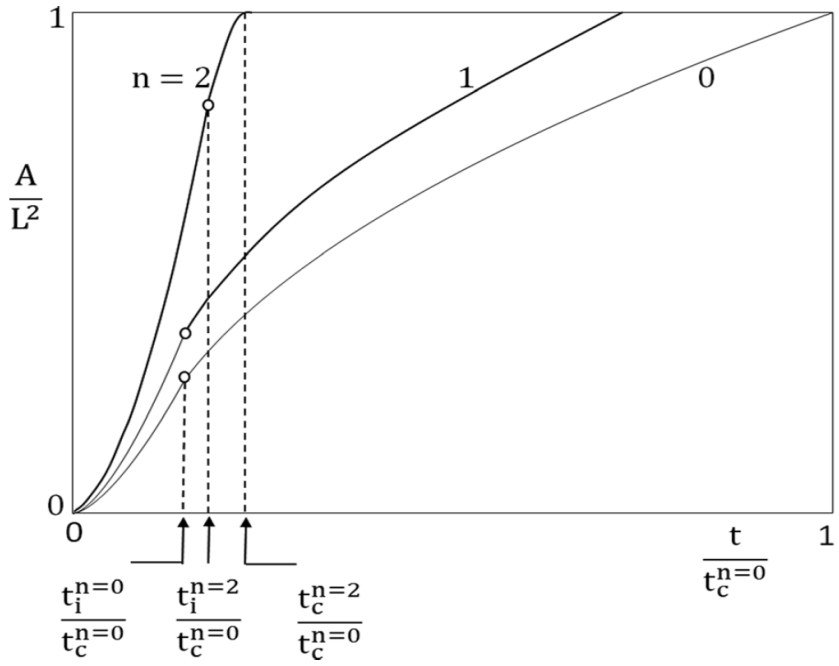

Fig. 3 – The effect of the number of the bifurcation levels on the shape of the S-curve.

CONSTRUCTAL LAW CONFERENCE – CLC2024
Design in Nature and Evolution
Romanian Academy, Bucharest, 10–11 October 2024

Proceedings of CLC2024
pp. 175–178

INTERACTION OF ULTRASONIC AND HEAT FLOW IN ESSENTIAL OIL EXTRACTION – A CONSTRUCTAL GLIMPSE

YELDA VELI[a,*], FLORIN SĂFTOIU[b], ALEXANDRU M. MOREGA[a,c]

[a] National University of Science and Technology POLITEHNICA Bucharest, Faculty of Electrical Engineering, yelda.veli@upb.ro [a]
[b] National University of Science and Technology POLITEHNICA Bucharest, Doctoral School of Electrical Engineering, florinsaftoiu@gmail.com
[c] 'Gheorghe Mihoc-Caius Iacob' Institute of Statistical Mathematics and Applied Mathematics, Romanian Academy, amm@iem.pub.ro
*Correspondence: yelda.veli@upb.ro; Tel. +40728049500.

Micro-cavitation processes through ultrasonic transducers are an unconventional way to extract essential oil rapidly. This paper numerically studies the interaction between the fluid and the heat flow from a constructal perspective. The ultrasound source is the pressure the piezoelectric transducer gives, which sources the flow–heat transfer interaction in the working pot. The three flows (the US, the working fluid flow, and the heat produced) interact and morph in response to the mechanical stress created by its source, a sonotrode.

Keywords: Constructal; Ultrasonic; Transducer; Piezoelectric; Micro-cavitation; Heat flow.

1. INTRODUCTION

Ultrasonic (US) machines are used in a variety of applications, ranging from industrial [1] (cleaning, welding, detecting, *etc*.) to medical [2] and biological [3] (medical diagnosis, cell disruption, *etc*.). For membrane disruption and essential oil extraction, the piezoelectric (PZE) US transducer is used in the frequency range of 20 kHz – 40 kHz, with higher values providing qualitative in-depth processing since the cavitation effect is more pronounced, but at the cost of increasing the extraction time, lower values causing a coarse extraction in a much shorter time, but with unwanted thermal effects [3].

This paper analyses the effects of a PZE US transducer on the essential oil extraction process of lavender leaves and the subsequential heat flow generation inside the work vessel (liquid medium – water with solvent and solid medium). The most straightforward setup used in extraction is the PZE source, US transducer, and vessel. An amplifying case and a sonotrode enhance and focus on the US wave. The Constructal law states that a given finite volume changes its structure over time to facilitate the flow of different currents and fluxes. The model is solved using acoustic-piezoelectric, pressure-acoustics, laminar flow, and heat transfer. Two fluxes – mass flux and heat flux – are interacting and changing their configuration continuously.

2. PHYSICS

For the acoustic-piezoelectric problem, the transducer is considered without a vessel; for the pressure-acoustic and heat transfer problem, only the vessel is considered, and the laminar flow considers the fluid as a homogenized medium.

DOI: https://doi.org/10.59277/CLC/2024.44

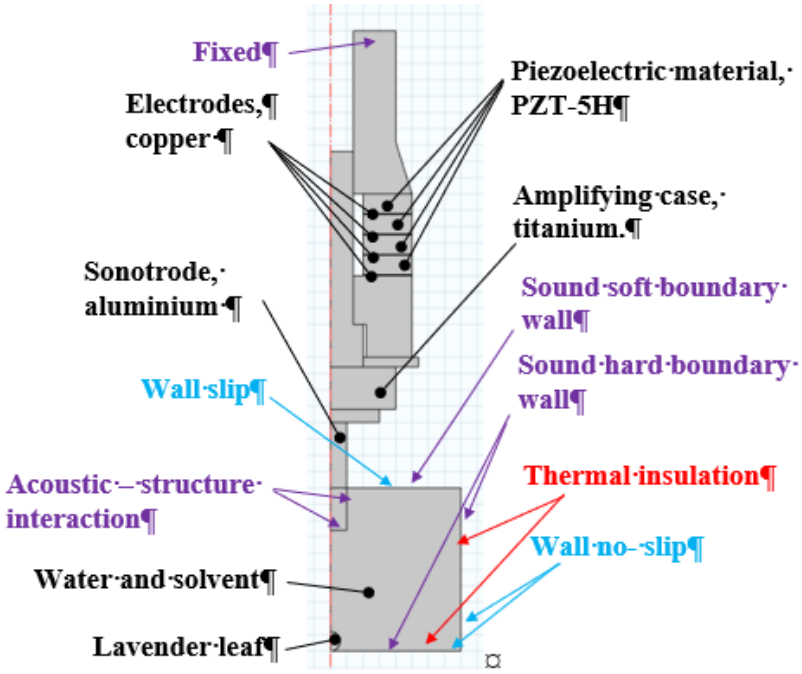

Fig. 1 – The model and the BCs for the acoustic-piezoelectric interaction problem (violet), the laminar flow (blue), and the heat transfer problem (red) – the sonotrode and the work vessel.

3. MATHEMATICAL MODEL

The equation of the sound wave represents the mathematical model for the acoustic problem:

$$\nabla \cdot \left(-\frac{1}{\rho_0} (\nabla p) \right) - \frac{\omega^2 p}{\rho_0 c_s^2} = 0, \tag{1}$$

where p [Pa] is the sound pressure, c_s [m/s] is the US velocity, ρ_0 [kg/m^3] is the mass density. The laminar flow of the water and the solvent inside the vessel is modeled by:

$$\rho_0 (\mathbf{u} \cdot \nabla)\mathbf{u} = -\nabla p + \mu \nabla^2 \mathbf{u} + \rho_0 \mathbf{f}, \tag{2}$$

$$\nabla \cdot \mathbf{u} = 0, \tag{3}$$

where $\mathbf{u}$ [m/s] is the velocity, and μ [1/s] is the dynamic viscosity. The volumetric force $\mathbf{f}$ [N/m^3] of the liquid is given by:

$$\mathbf{f} = \frac{2\alpha}{c_s} \mathbf{I}, \tag{4}$$

where α [Np/m] is the attenuation coefficient and $\mathbf{I}$ [W/m^2] is the sound intensity.

The equation for the time-dependent heat transfer problem is given by:

$$\rho_0 C_p \frac{\partial T}{\partial t} = k \nabla^2 \mathrm{T} - \rho_0 C_p (\mathbf{u} \cdot \nabla) T + \dot{Q}, \tag{5}$$

where C_p [J/kg·K] is the specific heat, k [W/m·K] is the thermal conductivity, and $\dot{Q}$ [W/m^3] is the heat source, which is obtained by computing the acoustic-piezoelectric interaction and the pressure-acoustic physics.

4. NUMERICAL SIMULATION RESULTS

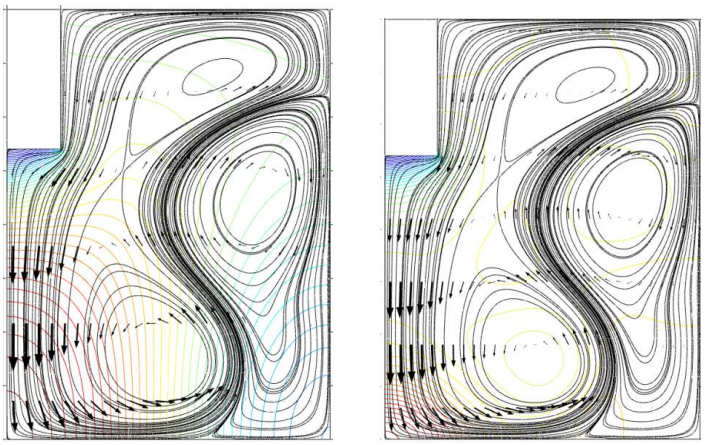

(a) Isobars and flow. (b) Isobars and flow.

Fig. 2 – The lines of the input pressure (applied as BC), and the pressure established in the work vessel, along with the velocity streamline and arrows (black).

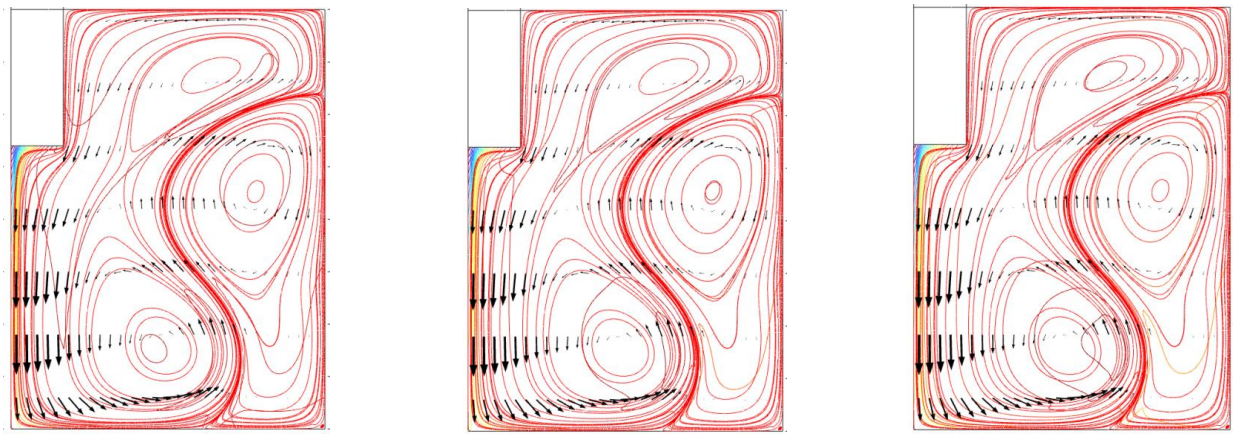

(a) Isotherms, heat flux (red) and flow, $t = 10$ s.

(b) Isotherms, heat flux (red) and flow, $t = 100$ s.

(c) Isotherms, heat flux (red) and flow, $t = 900$ s.

Fig. 3 – The temperature contour lines and the streamlines of the heat flux (red) and fluid flow (black) for three different moments, at $t = 10$ s, $t = 100$ s, and $t = 900$ s.

5. CONCLUSIONS

The temperature distributes from the tip of the sonotrode along the fluid flow, reaching an isothermal uniform distribution. The heat flux is in the same direction as the fluid flux, with which it interacts, and the temperature uniformly distributes along the lines.

The extraction process in this paper is not accounted for, as the fluid is considered a homogenized medium with lavender leaf suspension. Here, a 20% lavender leaf suspension is considered. The pressure-acoustic and thermal material property values are a mean value considering the percentage of each constitutive part of the mix inside the working vessel.

ACKNOWLEDGMENTS

The research was conducted in the Laboratory of Energy Conversion and Sources at the Faculty of Electrical Engineering at the National University of Science and Technology POLITEHNICA Bucharest. The first author acknowledges the support of the grant from the National Program for Research of the National Association of Technical Universities – GNAC ARUT 2023.

REFERENCES

1. Guo S., Chen S., Zhang L., Chen Y.F., Mirshekarloo M.S., Yao K., Design and fabrication of direct-write piezoelectric ultrasonic transducers for determining yielding of aluminum alloy, *NDT & E International*, **98**, pp. 186–194 (2018).
2. Vranić E., Sonophoresis-mechanisms and application, *Bosn. J. Basic Med. Sci*., **4**, *2*, pp. 25–32 (2004).
3. Struckas A., Vasiljev P., Bareikis R., Borodinas S., Kasperoviciene J., Ultrasonic zeppelin-shape transducer for algae oil extraction, *Sensors and Actuators A: Physical*, **263**, pp. 754–761 (2017).
4. Veli Y., Saftoiu F., Morega A.M., Numerical analysis of a piezoelectric ultrasound transducer (in Romanian), *Electrical Machines, Materials and Drives — Present and Trends*, **19**, *1*, pp. 52–57 (2023).

CONSTRUCTAL LAW CONFERENCE – CLC2024
Design in Nature and Evolution
Romanian Academy, Bucharest, 10–11 October 2024

Proceedings of CLC2024
pp. 179–180

THE LUNGS OF PLEASURE ARE FULL OF DEATH OXYGEN

MOHAMMAD OLFATI[a*], AMIR NEKOUNAM[b]

[a] Engineering Faculty, Razi University, Kermanshah, Iran, m_olfati@yahoo.com
[b] Economics faculty, Allameh Tabataba'i University, Tehran, Iran,
*Correspondence: m_olfati@yahoo.com;+989398394261.

The pleasure naturally diminishes over time due to its existence. This study delves into this idea and connects it to the Constructal Law, which suggests that to maintain sustained pleasure in our lives, we must continuously adapt and evolve to keep the flow of pleasure alive. It explores the profound significance of pleasure as a motivating factor in our lives. It provides valuable insights into how we can ensure its continuous evolution for our overall well-being.

Keywords: Constructal law; Pleasure; Economics; Evolution; Utility; Welfare.

1. INTRODUCTION

Have you ever wondered why our enjoyment of pleasurable experiences seems to fade over time? The initial excitement and pleasure we get from something gradually diminishes, and it becomes just another normal part of our lives. As children, many of us have fond memories of how we used to love certain toys like bikes or dolls. We would ask our parents to buy these toys for us, and the longer it took for them to do so, the more excited we would become. When we finally received the toy, we experienced maximum pleasure in the first moments. However, over time, this pleasure decreased and eventually faded away. Sometimes, we tried to revive the initial joy by changing the toy, such as installing a different horn on the bike or dressing up the doll in new clothes. While these modifications temporarily brought back some of the lost pleasure, the overall trend gradually faded. This feature is not specific to childhood and is not only about obtaining an object; enjoyable situations also exhibit this feature. Becoming the champion of a sports competition, winning a top scientific title, etc., are all pleasant experiences. However, over time, the pleasure derived from being in a pleasurable situation becomes normal. If we delve deeper into this issue, we will realize that all pleasures start to fade after they are acquired; it's as if pleasure is on the path of fading away (death) as it continues. It's as if pleasure is a creature that moves closer to its demise with each breath (continuation). In the words of Iranian poet Sohrab Sepehri, "the lungs of pleasure are full of the death oxygen.[1]" This is a great fact of life that makes the flow of life not static (dead) but constantly changing (alive). Change is needed for progress. Human development is due to this feature [2].

Consider a river stream that flows down a hill and stops (dies) after hitting an obstacle. For the river to continue (survive), it must change course, bypass the obstacle, and flow again (survive). Just as pleasure must change and evolve to last (installing a different horn on a bicycle, dressing a doll in new clothes, gaining a higher sports position, gaining a higher scientific position, *etc*.). In fact, the desire for more pleasure (more welfare, more access) serves as a driving force that propels a living system to move, survive, and progress. We get pleasure from accomplishing and succeeding in sports or academics and attaining wealth (more access). It reminds us of the constructal law: “For a finite-size flow system (not infinitesimal, one particle, or sub-particle) to persist in time (to live), it must evolve with freedom such that it provides easier and greater access to what flows [3].” This fundamental principle, known as the Constructal Law, seems to apply in all universe dimensions, including the perception of pleasure – the live flow systems like to evolve.

2. TOTAL UTILITY AND MARGINAL UTILITY IN ECONOMICS

This feature is also true in microeconomics. In microeconomics, the utility function expresses the consumer's behavior regarding the desire to buy a good or service. For this reason, consumers demand a product that gives them satisfaction or utility (pleasure). Utility refers to the satisfaction or happiness of consumers who consume goods. When a new product or service enters the market, it will have high utility if designed correctly and based on current needs. As the consumption of goods and services increases, its utility decreases over time.

DOI: https://doi.org/10.59277/CLC/2024.45

This results in the total utility rising at a decreasing rate until it reaches its maximum point. Beyond this point, the total utility decreases (see Fig. 1).

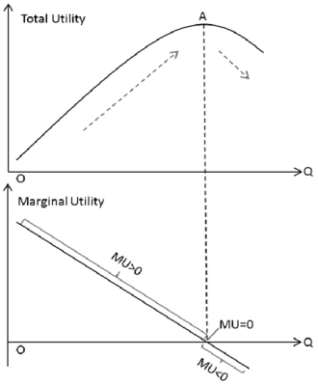

Fig. 1 – Total and marginal utility functions.

Marginal utility is a consumer's satisfaction or pleasure from the last unit of a good or service consumed. As consumption increases, the satisfaction gained from each additional unit of goods decreases. For example, the first glass of water may provide high utility, but subsequent glasses offer less. This is the law of diminishing marginal utility, where the marginal utility decreases as consumption increases (see Figure 1) [4].

In a way, the utility (pleasure) of a product or service decreases with the increase (continuation) of its use. (The lungs of pleasure are full of death oxygen). That is why innovation and change (evolution) are essential for the success and sustainability (survival) of companies producing goods or services (flow system). Successful and dynamic commercial companies, according to the feedback they receive from their customers, discover the features that make more utility and improve (evolve) their goods or services in the same way. These improvements are to make more welfare and pleasure (more access). This human trait is responsible for the advancements in producing flat, concave televisions, smartphones, etc. Nokia's descent into the mobile market is a story that resonates with many technology enthusiasts. One of the primary factors contributing to this decline was the company's sluggish response to the burgeoning smartphone revolution that took off with the groundbreaking launch of the iPhone in 2007 (evolution). At that pivotal moment, the Symbian operating system, which had been Nokia's pride, quickly became irrelevant. Unlike its competitors, iOS and Android, Symbian struggled to foster a vibrant and robust app ecosystem, leaving it unable to meet the evolving demands of consumers. As a result, Nokia became increasingly marginalized in a fast-paced industry, shifting towards innovative and user-friendly smartphone solutions. The story of Nokia clearly illustrates that a product or service's utility (pleasure) tends to diminish with increased usage. This phenomenon underscores the critical need for continuous innovation and adaptation within companies that manufacture goods or deliver services. To thrive and maintain relevance in a competitive marketplace, these businesses must embrace change and evolve to meet their customers' shifting preferences and expectations.

In today's fast-paced business environment, companies that fail to adapt and embrace new product or service developments risk falling behind their competitors and facing the possibility of going out of business (death of flow system).

3. **CONCLUSION**

Pleasure must change and evolve to last. The desire for more pleasure drives progress, as the constructal law states. In economics, the utility function represents satisfaction and happiness from purchasing goods or services. As consumption increases, the satisfaction from each additional unit decreases (law of diminishing marginal utility). Innovation and change are essential for companies' success and sustainability. Failure to adapt and embrace new developments can lead companies to fall behind competitors and even leave business.

REFERENCES

1. Sepehri S., Emami K., Water's footsteps: a poem, *Iranian Studies*, **15**, *1–4*, pp. 97–116 (1982).
2. Bejan A., *The physics of life: the evolution of everything*, St. Martin's Press, 2016.
3. Bejan A., The Physics of the Urge to Have Freedom, *BioSystems*, **243**, p. 105277 (2024).
4. Nekounam A., *Principles of Economics 1: Microeconomics*, Farsiran, 2010.

CONSTRUCTAL LAW CONFERENCE – CLC2024
Design in Nature and Evolution
Romanian Academy, Bucharest, 10–11 October 2024

Proceedings of CLC2024
pp. 181–182

CONSTRUCTAL LAW AND FREE ECONOMIC MARKET

AMIR NEKOUNAM[a], MOHAMMAD OLFATI[b*]

[a] Allameh Tabataba'i University, Tehran, Iran,
[b] Engineering faculty, Razi university, Kermanshah, Iran, m_olfati@yahoo.com
*Correspondence: m_olfati@yahoo.com;+989398394261.

Constructal law is a rapidly expanding field in physics, biology, technology, economics, and social sciences. It states that everything that flows and moves does so with an evolutionary design. Flow configurations, patterns, and rhythms change over time to provide greater access to their streams, allowing for easier flow. The rule of law and government describe movement "with design" on Earth. In a free market system, each person freely follows their interests, ultimately maximizing the interests of society as a whole. This means that free people can choose and trade, leading to increased growth in the country. In other words, in a free market system, individual freedom is a crucial principle for the country's progress; as the Constructal law states, " for a flow system to survive over time, it must evolve freely." In this paper, we will illustrate that when economic freedom increases, the per capita production of countries rises. In other words, economic freedom leads to welfare in society.

Keywords: Constructal law; Economics; Evolutionary design; Free market; Welfare.

1. INTRODUCTION

Constructal law was first formulated at Duke University by Bejan in 1996. Since then, it has spread worldwide. Thousands of researchers have written about the constructal law, and many more have heard about it. The Constructal law is a law of physics that explains the natural tendency of all flow systems to evolve into configurations that offer progressively greater flow access over time [1]. The statement is that “for a flow system to persist in time, it must evolve in such a way that it provides easier access to its currents” [2]. The constructal law, also known as the law of configuration generation or the law of design, is a rapidly expanding field in physics, biology, technology, and social sciences [3].

The Constructal law is not about optimization, maximization, minimization, or any specific end design. Instead, it describes the direction of evolution over time, emphasizing that the design phenomenon is dynamic and constantly changing. It's important to note this as many ad hoc proposals of optimality are emerging in this regard [4].

2. CONSTRUCTAL LAW OF DESIGN AND EVOLUTION IN NATURE

Constructal law applies to a universal concept: Whenever something flows or moves, it does so with an evolutionary design. This involves changing flow patterns and rhythms that naturally adapt over time to allow for easier movement. The rule of law and government essentially describe organized movements on earth. For example, traffic signs in the city demonstrate this principle [1]. Another example is the free market. They all “happen,” and their evolution toward easier flow over time happens.

Flow generates better flow. A society that flows more is wealthier. It has a greater tendency to reconfigure itself to flow even more and to become even richer over time. There is no end to this evolving design. There is just the time direction of the evolutionary changes and the rate at which changes are occurring. Good is a government that facilitates the movement, reach, and staying power of the whole society, which includes mobility, participation, access, health, and life expectancy. A government becomes better when it opens the channels, *i.e.*, access. This means that we need a government that creates free flow. A more open government is good for better-flowing business streams and vice versa. Their evolution is the large-scale manifestation of every individual’s urge to be free, make choices, vote, and make changes to live better [1]. Therefore, according to the constructal law, capitalism causes progress and development. The constructal law emphasizes decentralized decision-making. Systems evolve spontaneously, adapting to optimize flow and access.

DOI: https://doi.org/10.59277/CLC/2024.46

3. CAPITALISM AND INDIVIDUAL FREEDOM

In a capitalist economy or a free market system, each person freely follows his interests, ultimately maximizing the interests of the whole society. Adam Smith first stated this idea [5] and interpreted it as the market's invisible hand. Hayek [6] believed there is a spontaneous order in the free market system, which is not based on a human plan but on human action. It means that free people can choose and trade, which increases the country's growth. In centralized planning, people's freedom is ignored, and since the government does not know everything, the centralized planning system will fail.

On the other hand, Mises [7] considered time a key issue in his analysis and believed that people's preferences may change at different times, so centralized planning is ineffective. In other words, in the free market system, individual freedom is a key principle for the country's progress; as the constructal law states, "for a flow system to survive over time, it must evolve freely."

The idea of spontaneous order is Hayek's best-known contribution to contemporary social science. However, as several chapters demonstrate, it is also very relevant to the natural sciences. In Hayek's view, spontaneous order—the emergence of complex order as the unintended consequence of individual actions that have no such end in view—is both the origin of the Great Society and its underlying principle. Hayek means, by the Great Society, a social and political order that has emerged spontaneously through the interaction of individuals going about their everyday business and sustains itself through the exact mechanism. In this sense, the idea of the Great Society and spontaneous order stand or fall together [8].

The economic freedom of countries can be calculated. Some sources have rated the economic freedom of countries with assumptions. Also, the per capita production obtained by dividing the gross domestic product by the population can be achieved. Figure 1 illustrates economic freedom on the X-axis and per capita production on the Y-axis, where almost a direct relationship between these two variables is visible. In other words, as economic freedom increases, the per capita production of countries rises.

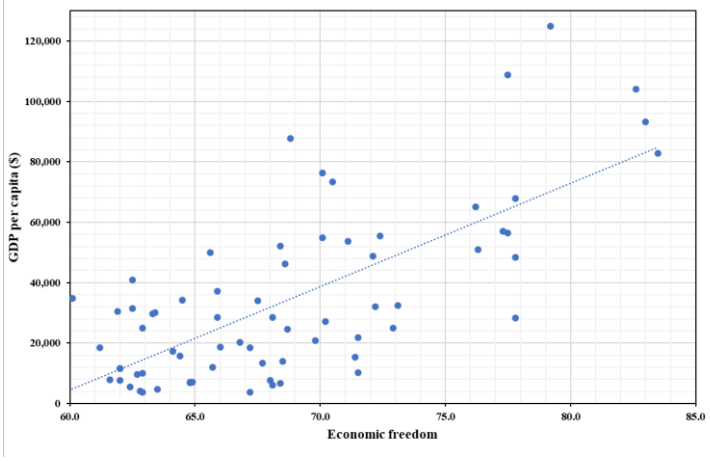

Fig. 1 – GDP per capita *versus* Economic freedom.

REFERENCES

1. Bejan A., Lorente S., Constructal law of design and evolution: Physics, biology, technology, and society, *Journal of Applied Physics*, **113**, *15* (2013).
2. Bejan A., The constructal law of organization in nature: tree-shaped flows and body size, *Journal of Experimental Biology*, **208**, *9*, pp. 1677–1686 (2005).
3. Bejan A., Lorente S., Constructal theory of generation of configuration in nature and engineering, *Journal of Applied Physics*, **100**, *4* (2006).
4. Bejan A., Lorente S., The constructal law and the evolution of design in nature, *Physics of Life Reviews*, **8**, *3*, pp. 209–240 (2011).
5. Smith A., *The Wealth of Nations* [1776], na, 1937.
6. Hayek F. A., *Individualism and Economic Order*, University of Chicago Press, 1980.
7. Mises L. v., *Human Action*, Ludwig von Mises Institute, 1949.
8. McNamara P., Hunt L., *Liberalism, Conservatism, and Hayek's Idea of Spontaneous Order*, Springer, 2007.

INDEX AUTHORS

L

M

N

O

P

R

S

T

U

V

Y

Z

The 14° edition of the Constructal Law Conference explored diverse instances that evidence the causal relationship between freedom, the imagined (perfection), the observed design in nature (diversity), and the engineered and societal human design.

Diverse phenomena of gravity, sound, turbulence, fish swimming, animal and human migrations, plants, and chemical processes, are manifestations of Constructal Law in physics, biology, and engineering.

The evolutionary design of artifacts (machines) led to the human & machine era of human evolution. When the time arrow of evolution is recognized, humans are enabled to predict their future and surroundings, and improve their lives.

Constructal Law underpins predictive theories of evolution, bio, and non-bio. Its core concepts are interwoven: freedom, organization, motion, shape, structure morphing, hierarchy, and arborescence.

The articles in this volume illustrate perfection and diversity over space and time: the configurations and rhythms of moving and changing designs of people, animals, athletes, technologies, universities, and science itself: divergent evolution hand-in-glove with convergent evolution.

The Constructal Law states: "For a finite-size flow system (not infinitesimal, one particle, or subparticle) to persist in time (to live), it must evolve with the freedom to provide easier and greater access to what flows."

DOI: https://doi.org/10.59277/CLC/2024

9 789732 739198